Quelques problèmes liés à la description de systèmes en interaction forte

Lukas Theussl

UNIVERSITE JOSEPH FOURIER - GRENOBLE I

THESE

pour obtenir le titre de

DOCTEUR

DE L'UNIVERSITE JOSEPH FOURIER - GRENOBLE I

Discipline: **Physique Nucléaire Théorique**

présentée et soutenue publiquement

par

Lukas THEUSSL

le 15 juin 2001

QUELQUES PROBLEMES LIES A LA DESCRIPTION DE SYSTEMES EN INTERACTION FORTE

Directeur de thèse:
Bertrand Desplanques

JURY

J.-M. Richard	Président
Fl. Stancu	Rapporteur
J.-F. Mathiot	Rapporteur
D. Rebreyend	
B. Desplanques	

Acknowledgements

I would like to start this section by generally expressing my thanks to all my friends and collegues, who have contributed to my scientific education by numerous discussions, helpful advices and even more numerous criticisms. It is from them that I have profited the most and I apologize not to mention all their names explicitly here.

It is a very special pleasure to express my gratitude towards my supervisor, Bertrand Desplanques for both his personal as well as scientific values. It is hard to estimate what a chance I had being able to work with him.

I thank all the members of the theory group at the ISN for the stimulating scientific atmosphere and the joyful time that we had together.

Special thanks go to Robert 'up the irons' Wagenbrunn. Without his expertise and help I would have had much less to write in this thesis.

I would also like to mention the students who did their training courses in the theory group of the ISN. I hope they have profited at least a part of the amount that I have profited from the interaction with them.

I thank C. Tur for her kind help on bibliographical matters, A.-M. Guglielmini for help on burocratic matters and C. Mazzola for help on administrative matters.

Special acknowledgements go to Christine Gondrand, whose expertise, efficiency and availability form an exceptional ensemble in the group 'Service d'Informatique' of the ISN.

It is a pleasure to thank my dear friend and collegue Raphaël Bonnaz for all the usefull advices, interesting discussions and the healthy atmosphere of competition all along those long three years. Special thanks to him for having brought me in contact with that group of crazy role players, Titel (qui ?), Seb (un petit squash tranquille), Fred (je serais là à l'heure), David (ne touchez pas à mon adversaire !), as well as Steph and Céline, and for the happy hours we spent together.

Last, but not least at all, I send the most tender expressions of gratitude to my family, my parents in particular, and all the friends I left back behind in Austria, for their warm support, explicit or implicit, which always reminded me of the fact that there is not only these crazy french people in this world.

Table of Contents

Chapter 1

Introduction

Wertlos ist ein Denken, das logisch oder wissenschaftlich heißen will, aber nicht vermag, die in der Wirklichkeit selbst vorhandenen Widersprüche in sich aufzunehmen und zu verarbeiten, in ihnen die höhere Einheit zu finden – denn nur so kann das Denken dem lebendigen Fluß der Entwicklung gerecht werden.

G.W.F. Hegel, Wissenschaft der Logik

De nos jours il est généralement accepté que la dynamique des mésons et des baryons est décrite par la théorie des quarks et des gluons, c'est à dire la Chromodynamique Quantique (Quantum Chromodynamics, QCD) [MP78]. Le but ultime de l'étude des phénomènes hadroniques est de les comprendre à partir de cette théorie. Pour des processus de très haute énergie, telle que la diffusion profondément inélastique des leptons sur des hadrons, ce programme a connu un succès remarquable, ce qui est dû à la nature asymptotiquement libre de la QCD: la théorie des perturbations est applicable dans le régime des hautes énergies. Cependant, aux énergies faibles, comme par exemple dans le domaine de la spectroscopie hadronique, la QCD montre un comportement non perturbatif, comme le confinement des quarks et des gluons, ou la brisure spontanée de la symétrie chirale [Pag75]. Ces effets rendent difficile, voire inapproprié, un traitement précis de la QCD en utilisant ses propres degrés de liberté des quarks et des gluons. Par conséquent, plusieurs modèles des états liés hadroniques, plus ou moins phénoménologiques, ont été développés.

Parmi ceux-ci on trouve les modèles de sac [CJ+74] où les quarks circulent librement à l'intérieur d'une région de confinement (le sac) qui est entourée par un nuage de mésons. Cette image de la structure hadronique est peut-être la plus proche de celle tirée de la QCD.

Cependant, plusieurs difficultés rendent ces modèles techniquement complexes et on peut se demander s'il ne serait pas possible de construire un modèle non-relativiste équivalent, en ce qui concerne la description à basse énergie. Sans doute, les extensions et élaborations du modèle naïf des quarks constituants pour la structure hadronique sont des avancées dans cette direction. La conséquence immédiate de ceci est que les quarks perdent la connexion directe avec les champs du lagrangien de la QCD, ainsi ils représentent des degrés de liberté effectifs [Wei79].

L'interaction entre ces quarks constituants doit être construite à l'aide de certaines propriétés de symétries et une bonne part d'intuition. L'approche traditionnelle repose sur l'analogie avec les degrés de liberté d'origine de la QCD, les quarks courants, qui interagissent par l'échange de gluons. Après une réduction non relativiste et perturbative de l'interaction, on arrive au scénario familier où les quarks constituants interagissent par échange d'un seul gluon. Ce modèle peut être justifié partiellement si l'on présume qu'il existe une seule échelle relevante dans la région d'énergie considérée, celle qui caractérise le confinement (Λ_{QCD}). Cependant, nous savons qu'il y a au moins une deuxième échelle d'énergie qui est importante pour la physique hadronique à basse énergie: celle où la symétrie chirale du lagrangien de la QCD est brisée spontanément. Si l'on suppose que l'échelle pour la brisure spontanée de la symétrie chirale est supérieure à celle du confinement, on obtient l'image d'un baryon constitué de trois quarks confinés et massifs, qui interagissent par échange de bosons de Goldstone, provenant de la brisure spontanée de la symétrie chirale.

Malheureusement, il n'est pas possible pour l'instant de préciser beaucoup plus cette image qualitative

de la structure hadronique à partir de la QCD à cause de l'absence d'une méthode adéquate et pratique de décrire des états liés et des résonances dans le cadre d'une théorie des champs, et à cause de difficultés liées au caractère non perturbatif de l'interaction en dessous de Λ_{QCD}. Les calculs sur réseau, qui constituent probablement l'approche la plus fondamentale de tels problèmes non perturbatifs, ne sont pas encore suffisamment au point pour donner une idée claire de la physique.

Le travail présenté ici sera divisé en deux parties, la première traitant les modèles non relativistes des résonances nucléoniques. Quelques aspects relevant d'un point vue théorique mais aussi expérimental seront discutés, et les propriétés principales de quelques modèles, avantages et défauts, seront explicités. Nous nous concentreront sur la description des processus de désintégration des résonances baryoniques, une problematique qui ne permet pas d'ignorer son caractère non perturbatif. Nous allons en particulier essayer d'identifier les raisons exactes des défauts de certains modèles, et ainsi faire ressortir les ingrédients essentiels à une description réaliste de ces processus.

La seconde partie de ce travail est quelque peu plus ambitieuse d'un point vue théorique. Nous allons considérer sur un niveau plus formel la description des états liés basée sur la théorie des champs, dans le cadre de l'équation de Bethe-Salpeter. La différence principale avec la première partie est que nous nous contenterons de systèmes à deux particules seulement, ce qui permet de donner un aperçu de la physique sans trop se perdre dans des détails techniques pour résoudre une équation.

Plus précisément, nous allons nous occuper des échanges de bosons croisés, dont l'absence est habituellement tenue pour responsable de certains défauts de l'équation de Bethe-Salpeter dans l'approximation en échelle, comme par exemple le fait que l'on ne reproduit pas le spectre de l'atome d'hydrogène dans la limite où une des particules constituantes devient infiniment massive. Nous allons ensuite nous occuper de la question d'obtenir une équation à trois dimensions qui est équivalente à l'équation de Bethe-Salpeter. Cela nous amènera à l'étude des potentiels effectifs et leurs principales caractéristiques. La recherche sur de bonnes approximations de l'équation de Bethe-Salpeter a une longue histoire et continue encore de nos jours. Nous contribuerons à cette ligne de recherche en mettant l'accent sur l'importance dynamique de la dépendance en énergie du potentiel découlant d'un tel schéma de réduction. Pour donner une belle illustration, nous allons démontrer à l'aide d'un exemple explicite que des solutions anormales, c'est à dire, des solutions sans analogues non relativistes, apparaissent également dans un formalisme à trois dimensions, ce qui est possible seulement si l'on prend proprement en compte la dépendance en énergie du potentiel.

Part I

Non-Relativistic Models of the Nucleon

Chapter 2

Quark Models and Baryon Spectroscopy

Nature, for her part, seemed resolved to be no party to my penance,
but to be imperturbably bent on shedding mild ridicule over my wrongs.

E. Childers, The Riddle of the Sands

In this chapter we shall discuss some relevant issues in theoretical baryon spectroscopy. The first three sections will be devoted to recall some general basic results, both from a theoretical and from an experimental point of view. Some emphasize will be laid on the question of how resonance properties are actually extracted from experimental data and what are the most appropriate means to describe them in a theoretical framework. In the last two sections, we shall discuss two explicit constituent quark models, whose relevance for a proper account of baryonic properties is currently under heavy discussion. These models will then be tested in the following chapter by their predictions of strong decay widths.

2.1 A Brief History of Baryon Spectroscopy

The whole story started in 1952 when Fermi and coworkers [1] discovered the first baryon resonance - the $\Delta(1232)$. Since then, hundreds of resonances have been identified and the proliferation of "elementary" particles has led physicists to look for more fundamental theories, culminating in the advent of the quark model. Baryon spectroscopy was crucial in the early 1960's in pointing the way to SU(3). The algebraic concept was introduced by Gell-Mann [2, 3] and Zweig [4]. The discovery of the Ω^- and the establishment of the 56 baryon multiplet also started the SU(6) [5,6] scheme with spin 1/2 quarks. The fact that free quarks were never experimentally observed (see ref. [7] for a recent attempt) led to the important concept of confinement, whereas the apparent success of deep inelastic scattering calculations suggested the asymptotic freedom of quarks.

Major steps in the history of baryon spectroscopy are the introduction of the parton model [8,9] and the subsequent discovery that these partons carry the quantum numbers of the quarks, the introduction of the concept of color [10,11], and finally the discovery of the standard model of electro-weak interactions [12–14], and of QCD [15].

The complicated nature of QCD has led to a veritable industry of model building for hadron structure, the most prominent of QCD inspired models being the Bag model [16–18] and various kinds of potential models. The latter ones were pioneered by Dalitz [19], Greenberg [10] and Faiman and Hendry [20, 21], and experienced a major breakthrough by the introduction of spin-dependent forces [22] that led to the advent of very sophisticated potentials [23, 24].

The rapid development of baryon spectroscopy very soon triggered the study of transitions within the quark model. This was initiated by Becchi and Morpurgo [25], Mitra and Ross [26], and Faiman and Hendry [20, 21], but a conceptually crucial step in the formulation of explicit quark models for decays

was the development of the quark-pair-creation model, first by Micu [27], and extensively applied by Le Yaouanc et al. [28,29].

The ideas of quarks and a hidden color degree of freedom have to be considered as the most significant achievements of baryon spectroscopy, comparable to the role that atomic spectroscopy played for the development of quantum mechanics, leading to the Bohr model of the hydrogen atom.

A general introduction to the quark model is given in the books by Kokkedee [30], Close [31], Flamm and Schöberl [32], for a discussion of hadron transitions in particular, see the book by Le Yaouanc et al. [33].

2.2 Strong Interaction of Quarks

This section is devoted to a brief introduction of the fundamental theory of strong interactions, QCD, and the development and motivation of the approximations that are usually employed in actual calculations.

2.2.1 QCD

Quantum Chromodynamics (QCD) is a non-Abelian gauge field theory based on the gauge group $SU(3)_c$, where c stands for color. It is defined in terms of the Lagrange density:

$$\mathcal{L}_{\rm QCD} \;=\; \mathcal{L}_{\rm inv} \;+\; \mathcal{L}_{\rm gauge} \;+\; \mathcal{L}_{\rm ghost}, \tag{2.2-1}$$

where $\mathcal{L}_{\rm inv}$ is the classical Lagrangian, invariant under local gauge transformations of the $SU(3)_c$ group:

$$\mathcal{L}_{\rm inv} \;=\; \bar{\psi}_{i,f}(i\gamma^\mu D_\mu - m_f)_{ij}\psi_{j,f} \;-\; \frac{1}{4}F^a_{\mu\nu}F^{\mu\nu\ a}. \tag{2.2-2}$$

The quark fields $\psi_{i,f}$ carry a flavor ($f = u, d, s, \ldots$, with masses m_f) and a color index $i = 1, 2, 3$. The covariant derivative is $D_\mu = \partial_\mu - igT^aA^a_\mu$, where g is the QCD coupling constant and T^a are the generators of the $SU(3)_c$ group, with $a = 1, ..., 8$. In terms of the gluon field A^a_μ the gluon field strength tensor is $F^a_{\mu\nu} = \partial_\mu A^a_\nu - \partial_\nu A^a_\mu + gf^{abc}A^b_\mu A^c_\nu$, with f^{abc} the SU(3) structure constants. The major difference between QCD and Quantum Electrodynamics (QED) is the appearance, due to the non-Abelian structure of the theory, of gluon self-couplings in the $F \cdot F$ term. This gives rise to 3- and 4-point gluon interactions which make the theory highly non-linear.

The additional term, $\mathcal{L}_{\rm gauge}$, which fixes a specific gauge, is introduced in order to avoid some difficulties when quantizing the theory. In the Lorentz (covariant) gauge, one has $\mathcal{L}_{\rm gauge} = -(1/2\alpha)(\partial^\mu A^a_\mu)^2$, where α is an arbitrary parameter. Of course observables cannot depend on the choice of α, and some common choices are $\alpha = 1$ (Feynman gauge) and $\alpha \to 0$ (Landau gauge). Other, non-covariant, choices are the Coulomb gauge ($\partial_i A^a_i = 0$), the axial gauge ($A^a_3 = 0$), and the temporal gauge ($A^a_0 = 0$).

The Faddeev-Popov ghost density, $\mathcal{L}_{\rm ghost} = (\partial_\mu \bar{\chi}^a)(\delta^{ab}\partial_\mu - gf^{abc}A^c_\mu)\chi^c$, where χ^a and $\bar{\chi}^a$ are scalar anti-commuting ghost fields, ensures that the gauge fixing does not spoil the unitarity of the S-matrix; see refs. [34,35] for a further discussion of the gauge fixing problem.

In renormalizable field theories such as QCD the strength of the interaction depends on the energy scale. A property almost unique to QCD is that the renormalized coupling constant decreases with energy — known as asymptotic freedom. The running of the QCD coupling with energy allows one to compute cross sections for any quark–gluon process using a perturbative expansion if the coupling is small. Writing the full QCD Lagrangian as $\mathcal{L}_{\rm QCD} = \mathcal{L}_0 + \mathcal{L}_{\rm I}$, where

$$\mathcal{L}_0 = \bar{\psi}(i\gamma^\mu\partial_\mu - m)\psi - \frac{1}{4}(\partial_\mu A^a_\nu - \partial_\nu A^a_\mu)(\partial^\mu A^{a\nu} - \partial^\nu A^{a\mu}) - \frac{1}{2\alpha}(\partial^\mu A^a_\mu)^2 + (\partial^\mu \bar{\chi}^a)(\partial_\mu \chi^a) \tag{2.2-3}$$

is the free Lagrangian, and

$$\mathcal{L}_{\rm I} = g\,\bar{\psi}\gamma^\mu T^a \psi A^a_\mu - \frac{g}{2}f^{abc}(\partial_\mu A^a_\nu - \partial_\nu A^a_\mu)A^{b\mu}A^{c\nu} - \frac{g^2}{4}f^{abe}f^{cde}A^a_\mu A^b_\nu A^{c\mu}A^{b\nu} - gf^{abc}(\partial^\mu \bar{\chi}^a)\chi^b A^c_\mu \tag{2.2-4}$$

the interaction part, one can derive from $\mathcal{L}_{\rm I}$ a complete set of Feynman rules for computing any scattering amplitude involving quarks and gluons.

Perturbative QCD (PQCD) has been enormously successful in calculating processes in high energy lepton-lepton, lepton-hadron and hadron-hadron scattering. However, even at high energies, one is always confronted with the problem that the physical (asymptotically free) states are hadrons, not quarks or gluons, which are the fundamental quantities in QCD. This means that one always encounters soft scales in any strongly interacting system. While operator product expansions (OPE) usually allow one to factorize the short and long distance dynamics, understanding the complete physical process necessarily requires going beyond perturbation theory.

Several methods have been developed to deal with the problem of non-perturbative QCD. The most direct way is to solve the QCD equations of motion numerically on a discretized space-time lattice [36]. Recent advances in lattice gauge field theory and computing power has made quantitative comparison of full lattice QCD calculations with observables within reach.

Alternative methods of tackling non-perturbative QCD involve the building of soluble, low-energy, QCD-inspired models, which incorporate some, but not all, of the elements of QCD. Phenomenological input is then used to constrain the model parameters, and identify circumstances where various approximations may be appropriate. These approaches often exploit specific symmetries of QCD, which for some observables may bring out the relevant aspects of the physics independent of the approximations used elsewhere. A good example of this, which has had extensive applications in low energy physics, is chiral symmetry. Its consequences and implications will be discussed more thoroughly in sec. 2.3.2.

2.2.2 The Non-Relativistic Approximation

The most fundamental framework for the description of bound states within relativistic quantum field theories is the Bethe–Salpeter formalism. This will be introduced and discussed in the second part of this work, where it will become clear that this approach presents difficulties not only on the practical, but also on the fundamental level. Even if one is willing to put up with the complexity of the Bethe–Salpeter formalism, it is hard to obtain information from it.

The alternative which comes closest to one's physical intuition is the description of bound states with the help of the Schrödinger equation

$$H\,\psi = E\,\psi, \tag{2.2-5}$$

where the non-relativistic Hamiltonian for a quantum system consisting of two particles with masses m_1 and m_2, respectively, which interact via some potential $V(\vec{x})$, is given in the center-of-momentum frame by

$$H = m_1 + m_2 + \frac{\vec{p}^{\,2}}{2\,\mu} + V(\vec{x}), \tag{2.2-6}$$

where μ denotes the reduced mass:

$$\mu \equiv \frac{m_1\,m_2}{m_1 + m_2}. \tag{2.2-7}$$

The only problem is to find the potential $V(\vec{x})$ which describes the interaction of the two particles constituting the bound state under consideration. By investigating the corresponding scattering problem of the involved bound-state constituents, the perturbatively accessible part of this potential may be derived according to the well-known rules of S-matrix theory. One starts by computing the scattering amplitude T_{fi}, which is defined in terms of the S-matrix element $S_{\mathrm{fi}} \equiv \langle \mathrm{f}, \mathrm{out} \mid \mathrm{i}, \mathrm{in} \rangle$ by the decomposition $S_{\mathrm{fi}} = \delta_{\mathrm{fi}} - i\,(2\pi)^4\,\delta^{(4)}(P_{\mathrm{f}} - P_{\mathrm{i}})\,T_{\mathrm{fi}}$, for the elastic scattering process $\mathrm{i} \to \mathrm{f}$ in lowest non-trivial order of perturbation theory, the so-called "first Born approximation." After performing the non-relativistic limit one obtains the configuration-space interaction potential $V(\vec{x})$ as the Fourier transform of the scattering amplitude T_{fi}:

$$V(\vec{x}) = -(2\pi)^3 \int d^3k\, e^{-i\,\vec{q}\cdot\vec{x}}\, T_{\mathrm{fi}}(\vec{q}). \tag{2.2-8}$$

Applying this prescription to the QCD Lagrangian, eq. (2.2-1), one could for instance obtain the short-range part of the quark–quark potential (which is of perturbative origin), but no insight is gained whatsoever on the shape of its long-range, confining part, which is of non-perturbative origin!

In order to improve the non-relativistic formalism one has to take into account relativistic corrections. This is usually done perturbatively up to order $v^2 \simeq \vec{p}^{\,2}/m^2$. Furthermore, only the spin-dependent

contributions to these relativistic corrections are usually considered, because they control the fine- and hyperfine level splittings of the bound-state spectra. The spin-independent corrections may be obtained along similar lines.

The main correction along this prescription is the expansion of the relativistic kinetic energy $E_p = \sqrt{\vec{p}^2 + m^2}$ beyond its lowest-order term $E_p \simeq m$ in the normalization factors of the Dirac spinors $u_s(p)$ and $v_s(p)$, (see eq. (A.1-5)) and in the T-matrix element $T_{\rm fi}$. It must be stressed that these kind of corrections are purely kinematical ones, and do not incorporate any relativistic effects in the dynamics. Furthermore, the series in $\vec{p}^2/m^2$ formally diverges, so that it appears questionable in practical calculations, to stop the expansion at any finite order.

2.2.3 The "Naive" Constituent Quark Model

The quark model historically preceded QCD and the idea of gluons, but nowadays it gets more and more justified in the context of this underlying theory. The basic hypothesis of the quark model is that, once the gluon fields have been integrated out from the QCD action, one obtains a satisfactory description of hadrons by using an effective Hamiltonian in terms of (effective) quarks only. These quarks come in 6 different flavors, with different masses, and three colors, a classification scheme that explains a variety of symmetry patterns observed in hadron spectroscopy. The most drastic simplification is the one adopted in the non-relativistic quark model where the equation of motion is assumed to be the Schrödinger equation for particles interacting via a two-body potential. Even if it is used in a relativized form, it is an essential feature of the Schrödinger equation that the number of particles is fixed, and hadron states can be constructed with a definite number of quarks. Such a model is then called a constituent quark model (CQM), whose quanta, the constituent quarks, are not simply related to the quanta of the original QCD Lagrangian: the current quarks. This is due to the fact that the potential of the non-relativistic description and the constituent quark masses must effectively account for two essential, non-perturbative effects present in QCD: confinement and dynamical breaking of chiral symmetry. It is a serious drawback of the constituent quark model that it does not reflect in an explicit way the presence of Goldstone bosons as a consequence of the dynamically broken chiral symmetry. Thus, in principle, one expects troubles whenever processes are considered that involve pions, which do not play the role of Goldstone bosons in constituent quark models. Unfortunately, the processes of immediate relevance for hadron spectroscopy are mostly the ones where pions are involved.

We shall outline in a bit more detail the theoretical basics that are relevant for a proper understanding of the problematics in the next sections, before we present some explicit quark model calculations.

2.3 Symmetries

Symmetries have been an essential guide to the theory of QCD. Interestingly enough, they have been most useful in circumstances where they are not exact, but broken by some dynamical properties. This is particularly true for hadronic physics, where the breaking of chiral symmetry is one of the very foundations of the standard model. We shall therefore discuss in the following the two symmetries that are the most crucial ones in strong interaction physics: flavor- and chiral symmetry.

2.3.1 General Considerations

One of the big advantages of the Lagrangian formulation is that symmetries of the Lagrangian lead to conserved quantities (currents). In classical mechanics we know that symmetries of the Lagrange function imply conserved quantities. If we assume that $\mathcal{L}$ is invariant under a transformation of the fields $\Phi \longrightarrow \Phi + \delta\Phi$ (which means that $\mathcal{L}(\Phi + \delta\Phi) - \mathcal{L}(\Phi) = 0$), then we find that the quantity

$$J_\mu = \frac{\partial \mathcal{L}}{\partial(\partial_\mu \Phi)} \delta\Phi \tag{2.3-1}$$

is a conserved current, called a Noether current[1]. Its conservation, $\partial^\mu J_\mu = 0$, leads of course to a conserved charge

$$Q = \int d^3x J_0(x), \qquad \frac{d}{dt}Q = 0. \tag{2.3-2}$$

If we add a small symmetry breaking term to the Lagrangian $\mathcal{L} = \mathcal{L}_0 + \mathcal{L}_1$, where $\mathcal{L}_0$ is symmetric with respect to a given symmetry transformation of the fields and $\mathcal{L}_1$ breaks this symmetry, then the variation of the Lagrangian $\mathcal{L}$ does not vanish as before but is given by $\delta\mathcal{L} = \delta\mathcal{L}_1$. The variation of the Lagrangian can still be expressed as the divergence of a current, which is given by eq. (2.3-1), so that we have

$$\delta\mathcal{L} = \delta\mathcal{L}_1 = \partial^\mu J_\mu \tag{2.3-3}$$

Since $\delta\mathcal{L}_1 \neq 0$ the current J_μ is not conserved. The relation (2.3-3) nicely shows how the symmetry breaking term of the Lagrangian is related to the non-conservation of the current. It will also prove very useful when we later on introduce the slight breaking of chiral symmetry due to the finite quark masses.

2.3.2 Chiral Symmetry

To give an important example of a Noether current, consider the Lagrangian of two flavors of massless fermions. Since we will only discuss transformations on the fermions, the results will be directly applicable to massless QCD.

Massless fermions

The Lagrangian in this case is simply given by

$$\mathcal{L} = i\bar{\psi}_j \partial\!\!\!/ \psi_j \tag{2.3-4}$$

where the index 'j' refers to the two different flavors, let's say 'up' and 'down', and $\partial\!\!\!/$ is the usual shorthand for $\partial_\mu\gamma^\mu$.

Consider the following transformations

$$\Lambda_V: \quad \psi \longrightarrow e^{-i\frac{\vec{\tau}}{2}\vec{\Theta}}\psi \qquad \bar{\psi} \longrightarrow e^{+i\frac{\vec{\tau}}{2}\vec{\Theta}}\bar{\psi} \tag{2.3-5}$$

$$\Lambda_A: \quad \psi \longrightarrow e^{-i\gamma_5\frac{\vec{\tau}}{2}\vec{\Theta}}\psi \qquad \bar{\psi} \longrightarrow e^{-i\gamma_5\frac{\vec{\tau}}{2}\vec{\Theta}}\bar{\psi} \tag{2.3-6}$$

where $\vec{\tau}$ refers to the Pauli - (iso)spin matrices, and where we have switched to a iso-spinor notation for the fermions, $\psi = (u, d)$. It follows that the Lagrangian (2.3-4) is invariant both under Λ_V and Λ_A. The associated conserved currents are

$$V^a_\mu = \bar{\psi}\gamma_\mu\frac{\tau^a}{2}\psi \tag{2.3-7}$$

$$A^a_\mu = \bar{\psi}\gamma_\mu\gamma_5\frac{\tau}{2}\psi \tag{2.3-8}$$

often referred to as the 'vector current' and 'axial - vector' current, respectively.

The Lagrangian of massless fermions, and hence massless QCD, is invariant under both transformations, Λ_V and Λ_A.[2] This symmetry is what is meant by chiral symmetry (Often, people talk about 'chiral' symmetry but actually only refer to the axial transformation Λ_A. This is due to its special role is plays,

[1] Some Noether currents may not be conserved on the quantum-level, which means that not every symmetry of the classical field theory has a quantum analog. In this case one speaks of anomalies.

[2] Note, that the above Lagrangian is also invariant under the operations $\psi \to exp(-i\Theta)\psi$ and $\psi \to exp(-i\gamma_5\Theta)\psi$. The first operation is related to the conservation of the baryon number while the second symmetry is broken on the quantum level. This is referred to as the U(1) axial anomaly, which is a real breaking of the symmetry in contrast to the spontaneous breaking discussed below.

since it is spontaneously broken in the ground state, see sec. 2.3.3). The chiral symmetry is often referred to by its group structure as the $SU(2)_V \times SU(2)_A$ symmetry.

Now let us see, what happens if we introduce a mass term.

$$\delta\mathcal{L} = -m\,(\bar{\psi}\psi) \tag{2.3-9}$$

From the above, $\delta\mathcal{L}$ is obviously invariant under the vector transformations Λ_V but not under Λ_A

$$\Lambda_A: \; m\,(\bar{\psi}\psi) \longrightarrow m\bar{\psi}\psi - 2im\vec{\Theta}\left(\bar{\psi}\frac{\vec{\tau}}{2}\gamma_5\psi\right) \tag{2.3-10}$$

Thus, Λ_A is not a good symmetry, if the fermions (quarks) have a finite mass. But as long as the masses are small compared to the relevant scale of the theory one may treat Λ_A as an approximate symmetry, in the sense, that predictions based under the assumption of the symmetry should be reasonably close to the actual results.

In case of QCD we know that light quarks have current masses of about $5-10$ MeV whereas the relevant energy scale given by $\Lambda_{QCD} \simeq 200$ MeV is considerably larger. We, therefore, expect that Λ_A should be an approximate symmetry and that the axial current should be approximately (partially) conserved. The slight symmetry breaking due to the quark masses is the basis of the so called Partial Conserved Axial Current hypothesis (PCAC), that will be discussed in more detail later on. Furthermore, as long as the symmetry breaking is small, one would also expect, that its effect can be described in a perturbative approach. This is carried out in a systematic fashion in the framework of chiral perturbation theory [37, 38].

Another important consequence of chiral symmetry is the occurrence of parity doublets.

Consider the classical quark Lagrange density in eq. (2.2-2) in the limit where the masses of the quarks are zero:

$$\mathcal{L}^q_{\text{inv}} \;=\; \overline{\psi} i\gamma^\mu D_\mu \psi \;=\; \overline{\psi}_L i\gamma^\mu D_\mu \psi_L \;+\; \overline{\psi}_R i\gamma^\mu D_\mu \psi_R \;, \tag{2.3-11}$$

where (suppressing color and flavor indices) $\psi_{L,R} = (1/2)(1\pm\gamma_5)\psi$ are left- and right-handed projections of the Dirac fields. Under independent global left- and right-handed rotations $\mathcal{L}^q_{\text{inv}}$ remains unchanged. For N_f massless quarks, the classical QCD Lagrangian is then said to have a chiral $\mathrm{SU}(N_f)_L \otimes \mathrm{SU}(N_f)_R$ symmetry. Of course non-zero quark masses break this symmetry explicitly by mixing left- and right-handed quark fields, however, for the u and d quarks, and to some extent the s quark, the masses are small enough for the chiral symmetry to be approximately valid.

If chiral symmetry were exact, a natural consequence would be parity doubling. The nucleon would have a negative-parity partner with the same mass, just as the pseudo-scalar pion would have an equal-mass positive-parity partner. In nature, the lightest negative-parity spin-1/2 baryon is the S_{11} resonance, which is several hundred MeV heavier than the nucleon. Moreover, the pion has an exceptionally small mass, while the lightest candidate for a scalar meson is several times heavier than the pion, so that chiral symmetry in nature is clearly broken. The above arguments suggest however, that it should be at least approximately conserved. The resolution to this problem will be the spontaneous breakdown of the axial symmetry. Before we discuss what is meant by that, let us first advance further arguments that the axial vector current is indeed conserved to a good approximation, so that the axial symmetry must be present somehow.

PCAC

Taking the divergence of the matrix element of the axial current between the vacuum and the pion, one obtains the relation

$$\left\langle 0\middle|\partial^\mu A^a_\mu(x)\middle|\pi^b(q)\right\rangle = -f_\pi q^2 \delta^{ab} e^{-iq\cdot x} = -f_\pi m_\pi^2 \delta^{ab} e^{-iq\cdot x}. \tag{2.3-12}$$

To the extent that the pion mass is small compared to hadronic scales, the axial current is approximately conserved. In other words, the smallness of the pion mass is directly related to the partial conservation of the axial current, i.e. to the fact that the axial transformation is an approximate symmetry of QCD. The relation (2.3-12) is often referred to as the PCAC relation.

Goldberger-Treiman relation

Even more evidence for the conservation of the axial current is supplied by the Goldberger-Treiman relation [39], which relates the strong-interaction pion-nucleon coupling constant with quantities extracted from the weak interaction, in remarkable close agreement with experimental data. Of course, the reason why this works is that there is some symmetry, namely chiral symmetry, at play, which allows to connect seemingly different pieces of physics.

2.3.3 Spontaneous Breaking of Chiral Symmetry

From the results of the last section there seems to be a contradiction:

- On the one hand the meson mass spectrum does not reflect the axial-vector symmetry (because the a_1 is heavier than the ρ and probably the σ much heavier than the π), neither does the baryon spectrum (because the nucleon has no negative parity partner).
- On the other hand, the weak pion decay is consistent with a (partially) conserved axial-vector current, see eq. (2.3-12). Also the success of the Goldberger-Treiman relation indicates that the axial-vector current is conserved and, hence, that the axial transformation Λ_A is a symmetry of the strong interactions.

The solution to this puzzle is, that the axial-vector symmetry is spontaneously broken. One speaks of a spontaneously broken symmetry, if a symmetry of the Hamiltonian is not realized in the ground state of the theory.

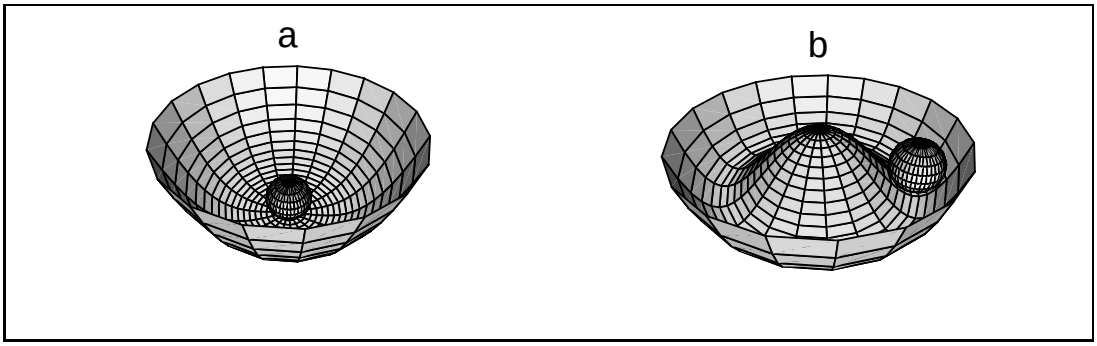

Figure 2.1: Effective potentials without (a) and with spontaneous breaking of symmetry (b).

This is usually illustrated in a classical-mechanics analogue. In fig. 2.1 we have two rotationally invariant potentials ('interactions'). In (a) the ground state is right in the middle, and the potential plus ground state are both invariant under rotations. In this case one speaks of the 'Wigner-Weyl mode' of symmetry realization. In (b), on the other hand, the ground state is at a finite distance away from the center. The point at the center is a local maximum of the potential and thus unstable. By picking one point in the valley as the ground state, the rotational symmetry is obviously broken. Potential plus ground-state are not symmetric anymore and one speaks of the 'Nambu-Goldstone mode' of symmetry realization. The symmetry has been broken spontaneously by choosing a certain direction to be the ground-state. However, effects of the symmetry are still present. Moving around in the valley (rotational excitations) does not cost any energy, whereas radial excitations do cost energy.

Let us now use this mechanics analogy in order to understand what the spontaneous breakdown of the axial-vector symmetry of the strong interaction means. Assume, that the effective QCD-Hamiltonian at zero temperature has a form similar to that depicted in fig. 2.1(b), where the (x,y)-coordinates are replaced by $(\sigma, \vec{\pi})$-fields. The spatial rotations are then the mechanics analog of the axial-vector rotation Λ_A, which rotates $\vec{\pi}$ into σ. Since the ground state is not at the center but at some finite distance away from it, one of the fields will have a finite expectation value. This is usually chosen to be the σ-field, because it carries the quantum numbers of the vacuum. In the quark language, this means we expect to have a finite scalar quark condensate $\langle \bar{q}q \rangle \neq 0$. In this picture, pionic excitations correspond to small

'rotations' away from the ground-state along the valley, which do not cost any energy. Consequently the mass of the pion should be zero. In other words, due to the spontaneous breakdown of chiral symmetry, we predict a vanishing pion mass. Excitations in the σ-direction correspond to radial excitations and therefore are massive. Generally, according to Goldstone's theorem, a consequence of a spontaneously broken chiral symmetry is the appearance of massless pseudo-scalar bosons. For $N_f = 2$ (namely, for u and d flavors), these correspond to the pseudo-scalar pions; for $N_f = 3$ (counting the strange quark as light), these include in addition the kaons and the η meson.

This scenario is in perfect agreement with what we have found above. The spontaneous breakdown of the axial-vector symmetry leads to different masses of the pion and sigma. However, since the interaction itself is still symmetric, pions become massless, which is exactly what we find from the PCAC relation, provided that the axial current is perfectly conserved. Thus the mesonic mass spectrum as well as the PCAC– and the Goldberger-Treiman relation are consistent with a spontaneous breakdown of the axial-vector symmetry Λ_A. The pion appears as a massless mode (Goldstone boson) as a result of the symmetry of the interaction.

The fact that the physical pion mass is not exactly zero is due to the still finite values of the current quark masses; it is only in the chiral limit that the pseudo-scalar mesons become massless. This is most clearly illustrated by the Gell-Mann–Oakes–Renner relations [40] that relate the pseudo-scalar meson masses to the quark condensates.

One expects, that at high temperature and/or density the finite expectation value of the scalar quark condensate diminues, so that chiral symmetry will be restored[1]. In this chirally restored phase, the pion and σ as well as the ρ and a_1, if they exist[2], should be degenerate and the pion looses its identity as a Goldstone boson, i.e. it will become massive. Furthermore the baryon spectra would reveal a parity doubling [41]. The effective interaction in this phase would then have a shape similar to fig. 2.1(a). It is one of the major goals of the ultra-relativistic heavy ion program to create and identify a macroscopic sample of this phase in the laboratory.

2.3.4 Flavor Symmetry

We saw in the last section that the Lagrangian for a fermion stays invariant under vector transformations Λ_V if a mass term is introduced. This means that the QCD Lagrangian, eq. (2.2-2), is also invariant under Λ_V, provided the different quark flavors carry the same mass. Since at least for light quarks, the differences are not very large, $m_d - m_u \sim 3\text{MeV}$, $m_s - m_{u,d} \sim 150\text{MeV}$, the strong interactions have an approximate global flavor symmetry $\text{SU}(3)_f$. This symmetry between u, d and s quarks is indeed well supported by the data and it was a major indication on the way to the quark model. From the QCD Lagrangian, eq. (2.2-2), we see that not only does the quark-quark-gluon interaction conserve flavor, but its strength is actually flavor independent. The only dependence on flavor in QCD is through the quark masses.

In summary we note that for equal quark masses we have exact flavor symmetry, whereas for chiral symmetry to hold, the quark masses have to vanish. In addition, because of the small values of the u and d quark masses, QCD preserves both flavor and chiral symmetry to a better approximation in the light- than in the heavy-quark sector.

2.4 The Baryon Spectrum

We shall give in this section a brief introduction to both experimental and theoretical basics of baryon spectroscopy. In the experimental part, some emphasis is laid on the question of how resonance properties are extracted from the data and how one should interpret them. The theoretical part then presents some concepts of how to describe the empirical data within constituent quark models, based on and inspired by the general results discussed in the last sections.

[1] In the classical mechanics analogue of fig. 2.1, this would mean that the little ball obtains such a large energy that the dip at the bottom of the potential (b) is effectively not seen anymore.

[2] If de-confinement and chiral restoration occur at the same temperature, it may become meaningless to talk about mesons above the critical temperature.

The following paragraphs are meant as a reminder of some basic results of quantum scattering theory which are most relevant for the understanding of the problematics. For a more detailed treatment, we refer to standard text books [42].

2.4.1 Scattering Theory

The theory of scattering of hadrons on nuclei at low and intermediate energies is generally formulated on the basis of potential scattering theory. Even though some results obtained from non-relativistic wave mechanics can be generalized to the case of relativistic wave equations (Klein-Gordon and Dirac equations), a fully relativistic treatment of multiple scattering of hadrons on composite targets is not available. Such treatments can be generalized to take into account relativistic kinematics but its dynamical basis is essentially non-relativistic. This has to be kept in mind if one tries to understand the way, how properties of physical particles are extracted from experiment.

The Breit-Wigner resonance formula

Various cross sections are usually described in terms of the parameters η_l and δ_l, where $2\delta_l$ denotes the change of phase of the lth partial wave and η_l its amplitude. They set bounds on cross sections imposed by the conservation of probability (often called the unitarity condition). The quantity

$$f(l) = \frac{\eta_l e^{2i\delta_l} - 1}{2i} \tag{2.4-1}$$

is the elastic scattering amplitude for the l^{th} partial wave from which one obtains the total elastic cross section, integrated over angles, as

$$\sigma_{el} = \frac{4\pi}{k^2} \sum_l (2l+1) \mid f(l) \mid^2 . \tag{2.4-2}$$

If one plots f as a vector in the complex plane, one obtains a so-called Argand diagram. These ones are extremely useful for analyzing hadron scattering data. For $\eta_l = 1$ the end of the vector describes a circle of radius $1/2$ and center $i/2$ as the phase shift varies from 0 to $\pi/2$. When $\delta = \pi/2$, f is purely imaginary. If $\eta_l < 1$, the end of the vector lies within the unitarity circle, a constraint imposed by the conservation of probability.

For the sake of illustration and simplicity, let the particles be spin-less in the following. If, in a given Argand diagram, the elastic scattering amplitude $f(l)$ passes through a maximum for a particular value of l and a particular CMS (center of mass system) wavenumber k, the two particles are said to resonate. The resonant state (the resonance) is then characterized by a unique angular momentum or spin $l = J$, a unique parity and isospin, and a mass corresponding to the total CMS energy of the two particles. A criterion of resonance is that the phase shift δ_l of the l^{th} partial wave should pass through $\pi/2$.

Apart from its mass, the most important dynamical property of the resonance is its total width Γ or lifetime τ. It may be extracted from the cross section data in the following way: setting $\eta_l = 1$ in eq. (2.4-1), i.e. assuming an elastic scattering process, we may rewrite f in the form

$$f = \frac{e^{i\delta_l}(e^{i\delta_l} - e^{-i\delta_l})}{2i} = e^{i\delta} \sin\delta = \frac{1}{\cot\delta - i}. \tag{2.4-3}$$

Near resonance we have $\delta \sim \pi/2$, so that $\cot\delta \sim 0$. If E is the total energy of the two-particle state in the CMS, and E_R is the value of E at resonance ($\delta = \pi/2$), then, expanding in a Taylor series,

$$\cot\delta(E) = \cot\delta(E_R) + (E - E_R)\left[\frac{d}{dE}\cot\delta(E)\right]_{E=E_R} + ... \sim -(E - E_R)\frac{2}{\Gamma}, \tag{2.4-4}$$

where we have defined $2/\Gamma = -[d(\cot\delta(E))/dE]_{E=E_R}$. Neglecting further terms in the series is justified provided $|E - E_R| \sim \Gamma \ll E_R$. Then from eq. (2.4-3),

$$f(E) = \frac{1}{\cot\delta - i} = \frac{\Gamma/2}{(E_R - E) - i\Gamma/2}. \tag{2.4-5}$$

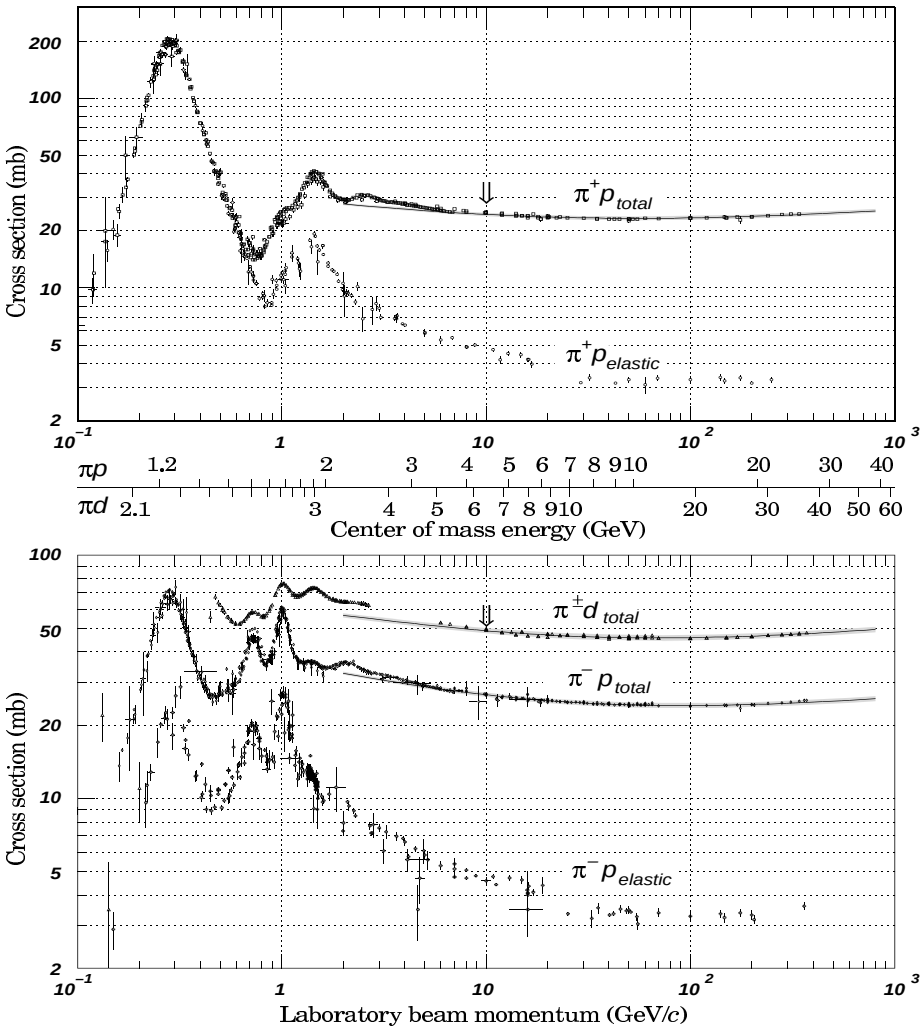

Figure 2.2: πN cross sections (from ref. [43]).

From eqs. (2.4-2) and (2.4-1), we obtain for the elastic scattering cross section

$$\sigma_{el}(E) = \frac{4\pi}{k^2}(2l+1)\frac{\Gamma^2/4}{(E-E_R)^2+\Gamma^2/4}. \tag{2.4-6}$$

This is known as the Breit-Wigner formula. We see that the width Γ is defined in such a way that the elastic cross section σ_{el} falls by a factor 2 from the peak value when $|E-E_R| = \Gamma/2$.

For a spin-less projectile hitting a spin-less target, the orbital angular momentum equals the total angular momentum of the resonant state, $l = J$. For spin-0 particles (eg. pions, kaons) incident on nucleons (spin 1/2), the factor $(2J+1)$ still applies, except that now only half the target spin states can contribute. For a resonance of angular momentum J formed from a nucleon target by a spin-less incident particle, eq. (2.4-6) becomes

$$\sigma_{el}(E) = \frac{\pi}{2k^2}(2J+1)\frac{\Gamma^2}{(E-E_R)^2+\Gamma^2/4}. \tag{2.4-7}$$

Figure 2.2, (taken from ref. [43]), shows the $\pi^+ p$ and $\pi^- p$ total cross sections as a function of the kinetic energy of the incident pion. There is a very obvious $I = 3/2$ resonance at $T_\pi = 195$ MeV, corresponding to a pion-proton mass of 1232 MeV. It is designated $P_{33}(1232)$, meaning that it is a P-wave ($l = 1$) pion-nucleon resonance, with $I = 3/2$ and $J = 3/2$. Obviously, one can distinguish other peaks in σ_{tot}. For example, in the $I = 1/2$ channel one can see evidence for the states $D_{13}(1520)$ and $F_{15}(1680)$ as peaks in

$\sigma(\pi^- p)$, and $F_{37}(1950)$ as a peak in $\sigma(\pi^+ p)$. For the $\Delta(1232)$ resonance, the amplitude is almost purely elastic because of the low mass, so that the tails of higher-lying resonances may be neglected. From eq. (2.4-7) we expect $\sigma_{el} = 2\pi/k^2(2J+1)$ at the peak. The limiting value for $J = 3/2$, $\sigma_{el} = 8\pi/k^2$ clearly proves that the $\Delta(1232)$ is a P-wave resonance of spin-parity $J^\pi = (3/2)^+$.

When analyzing the experimental data, one finds that resonances are almost never completely symmetrical, as it can already be guessed from fig. 2.2. The reason for this effect will be discussed later. Let us just note that, in order to take this asymmetry into account, formula (2.4-7) is multiplied by a new, energy dependent variable, x, called the elasticity.

It turns out, furthermore, that there are many overlapping pion-nucleon resonances, with at least 20 states of $M < 2200$ MeV. A mere inspection of the total cross section is therefore misleading. It is necessary to make a sophisticated phase shift analysis of the pion-nucleon elastic-scattering data, based on the behavior of the various polynomial coefficients required to fit the angular distributions, as a function of bombarding energy. The best values for the masses, widths and elasticities of resonant states are fitted to the data by an iterative procedure. Different analyses give somewhat different solutions. In particular, the masses and widths of resonant states depend upon the shape of the resonance form that is used to fit the data. This is of course an important issue, especially in the context of the calculations that we are going to present in subsequent sections, where theoretical predictions have to be compared with experimental data.

2.4.2 Experimental Overview

Since the first discovery of the Δ resonance [1], there were many formation and production experiments carried out to study the excited states of the nucleon. The masses, widths and elasticities of the N and Δ resonances come almost entirely from partial wave analyses (PWA's) of πN total, elastic and charge exchange scattering data.

However, it is not possible to extract a unique set of partial waves from the data alone, even if all measurable scattering data were known with high accuracy. It is essential to add the theoretical constraints of unitarity, isospin invariance and analyticity. Usually, dispersion relation techniques are used to extract the real part of the amplitude, but the exact procedure is not unique and different groups use different conventions. Another practical point is, that there are always a few higher partial waves that are too large to be neglected, but too small to be determined accurately from the data.

To extract the resonance parameters, usually generalized Breit-Wigner formulas, like eq. (2.4-6), are fitted to the amplitudes. In addition to statistical errors, there are also systematic errors inherent in this procedure. They depend on the assumptions that go into the parameterization of background terms and the energy dependence of partial widths.

Plots of the energy dependence of the amplitudes show that the resonances are almost never symmetrical. The reason is that angular-momentum penetration-barrier and phase-space factors usually increase rapidly with energy. This is taken into account by using Breit-Wigner formulas with energy dependent widths $\Gamma(E)$. The quantity that is called the "width" Γ is the value of $\Gamma(E)$ at the resonance energy $E = M$. Thus it depends on the model used for the energy dependence and on the definition of M. The same goes for elasticities and partial widths.

This short survey should give us a feeling of the difficulties, that partial wave analysts usually encounter (in practice, of course, there are still many more, see the article by Workman, ref. [43, p.696] for a short overview and a relevant list of references), and make understandable the fact, that different groups mostly quote quite different resonance parameters. In fact, lots of different partial wave analyses are not consistent with each other.

A theorist working in this field is therefore necessarily confronted with the problem of finding out which data is the most reliable or appropriate one to compare with his theoretical predictions. The standard reference in this case is the compilation of the Particle Data Group (PDG) which is updated every two years and which contains a collection of all the data available at that time. However, as recommendations for particle properties, the PDG usually takes into account only a part of the available data and, furthermore, no systematic procedure is defined how these properties are in fact extracted. Concerning decay widths, it is explicitly stated, that *"The following branching fractions are our estimates, not fits or averages"*. Most irritating in this context is the fact that results of the most recent partial

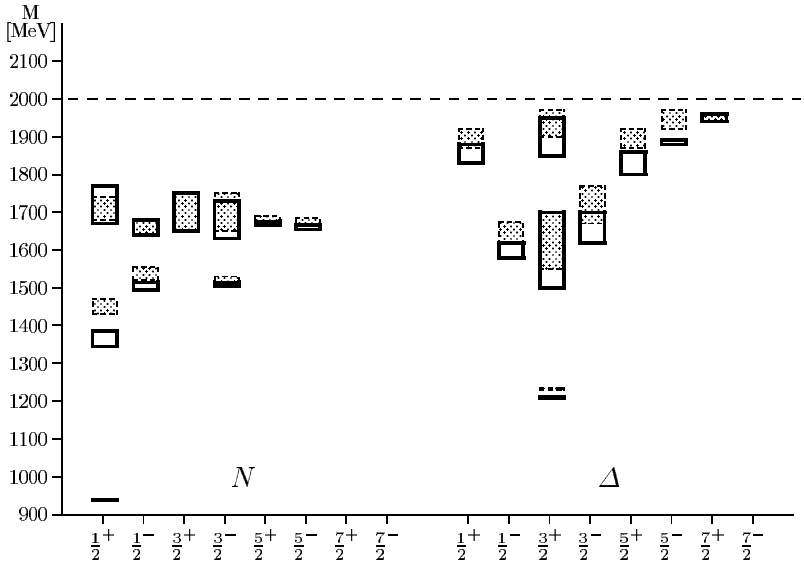

Figure 2.3: Experimental masses of light baryon resonances up to 2 GeV. The shaded areas give the Breit-Wigner masses, the thick solid boxes give the pole positions (from ref. [43]).

wave analyses are usually ignored in these estimates.

The references that are mainly used by the PDG are the early works by Cutkosky et al. [44] and Höhler [45], as well as the PWA of Manley and Saleski [46], which is probably the one with the largest underlying data set. In the last issue of the PDG [43], also the work of Green and Wycech [47] has been partially taken into consideration.

The most important works that are usually ignored by the PDG are the ones by Arndt and coworkers, who successively updated their NN phase-shift analyses from 2.1 GeV [48] to 2.5 GeV [49] and 3.0 GeV [50], and also studied the pion photo-production [51]; as well as the one by the Zagreb group [52].

Another ambiguity arises from the fact that the PDG actually quotes two values for both the mass and the width of every resonance. The first corresponds to values obtained by a Breit-Wigner fit to the cross sections, the second to the pole positions of the scattering amplitude in the complex energy plane. These values are not always compatible, as it may be seen from fig. 2.3, the largest discrepancy occuring for the Roper resonance (the first positive-parity excitation of the nucleon), whose pole mass lies almost 100 MeV below its Breit-Wigner value. Also the Δ resonance, whose nominal mass is 1232 MeV, has a pole mass of only 1210 MeV. The issue of pole vs. Breit-Wigner description of resonances has been raised recently by Workman [53], who found that more satisfactory fits to experimental masses may be obtained using the pole values instead of the Breit-Wigner ones.

In spite of numerous "pole-emics" by Höhler in various issues of the Particle Data Group (see ref. [43, p. 696]), the 'conventional' values, i.e. the ones that are commonly used and regarded as the physical ones by both theorists and experimentalists, are the Breit-Wigner ones. Höhler puts forward two main objectives to this:

- Contrary to conventional parameters, pole positions have a well defined relation to S-matrix theory,
- the model dependence of procedures to fit Breit-Wigner parameters is much larger than the determination of pole parameters.

An overview of current efforts in theoretical as well as experimental baryon spectroscopy, as evidenced by the recent formation of the "Baryon Resonance Analysis Group" [54], may be found in proceedings of recent conferences and workshops, see for instance ref. [55].

The $N\eta$ channel

We shall lay some emphasize on the description of hadronic decays of baryon resonances in this work, the most important processes with this respect being the ones with pions in the final state. However, $N\eta$, ΛK and ΣK branching fractions have also been extracted by partial wave analyses, even if the sets of data are much smaller in this case.

Contrary to the π-decays, the decays into η have some unusual properties. Due to the large η mass, the phase-space for a decay of a certain resonance into $N\eta$ is much smaller than the one for a decay into $N\pi$. Therefore, one expects the η decays to be suppressed as compared to the corresponding π decays[1].

The experimental situation is to a large extent unclear. The 1992 PDG compilation [56] gave systematic small but finite widths for all resonances with the exceptions of the N_{1535} and N_{1710}. The 1994 PDG compilation [57] deleted all η widths except the N_{1535}. This situation persists in the following PDG compilations, refs. [58, 59], until the latest one [43], where only the N_{1650} is now assigned a small but non-zero $N\eta$ width. However, generally all the η decay widths can be considered small ($\sim 1\,\mathrm{MeV}$) with the exception of the N_{1535} which has a partial width of $\sim 60\,\mathrm{MeV}$ [60]. The pole positions of the two S_{11} resonances N_{1535} and N_{1650} have been explicitly determined in ref. [61], there is however evidence that there might be a third S_{11} resonance around 1700 MeV [62] which would clearly contradict the quark model prediction. This resonance, if it exists, could possibly be interpreted as a quasi-bound $K\Sigma$ or $K\Lambda$ state [63]. Studies of the η coupling constant in effective Lagrangian approaches [64, 65] have only given very vague results, whereas a determination of photo-production amplitudes in a quark model [66] has given a rather satisfactory description.

2.4.3 Baryon Wave Functions

After this short experimental overview, let us now start the discussion of theoretical descriptions of baryon spectra. This will be done exclusively in the framework of constituent quark models. We note however, that there exist different models of the nucleon that emphasize different aspects of its properties, like bag models or soliton models, see ref. [67] for an overview. For some basic formulas concerning the quark shell-model, see ref. [68], for general discussions the books by Close [31], Le Yaouanc et. al [33] and Flamm and Schöberl [32]. For references on group theory applied to physical problems the books by Barut and Raczka [69] and Stancu [70] may be consulted.

Obviously, the **56** multiplet gives a good description of the ground state baryons, as it contains exactly a spin $\frac{1}{2}$ octet and a spin $\frac{3}{2}$ decuplet - as it is observed in nature. However, quarks being fermions, they obey the Fermi-Dirac statistics, which means that the total baryon wave function has to be antisymmetric with respect to the exchange of any two quarks. Therefore, one would have to combine the symmetric spin-flavor wave-function of the **56** multiplet with an antisymmetric spatial wave-function - which is very unlikely for the ground state. This paradox was the first indication of a new degree of freedom - color. Postulating the color singlet nature of all physical observables, one may write the general wave function of a baryon as

$$\underbrace{|\psi\rangle}_{\text{antisymmetric}} = \underbrace{|\phi\rangle_{space}\,|\chi\rangle_{spin}\,|\varphi\rangle_{flavor}}_{\text{symmetric}} \underbrace{|\eta\rangle_{color}}_{\text{antisymmetric}}. \tag{2.4-8}$$

The baryons are therefore viewed as color-singlet qqq states with a wave-function totally antisymmetric with respect to all degrees of freedom. We shall concentrate on baryons made up of u, d and s quarks that span the $SU(6) \times O(3)$ group in the approximation where all quarks have the same mass. It is possible to extend these considerations to the unequal-mass case by properly taking into account the flavor mass differences.

The construction of appropriate wave functions with definite permutation symmetry is well known, we collect all the formulas relevant for this work in Appendix C. In order to make a connection with physical states, one has to specify which symmetries are ascribed to which state. The usual prescriptions are collected in table 2.1, where we use the notation of the translationally invariant shell model (TISM) [71]. The eigenstates of a specific Hamiltonian will be denoted by $|N(\lambda\mu)L[f]_X[f]_{FS}[f]_F[f]_S\rangle$. The Elliott

[1] The spin-flavor part is approximately the same for $N\pi$ and $N\eta$ since π and η are in the same SU(3) multiplet.

Table 2.1: The structure of all the N and Δ resonances in the $N = 0, 1, 2$ bands. The notation in the second column is $[N^{J^\pi}]_n\,(N^*)$, with J the total angular momentum, π the parity, and N^* the physical resonance, where known. The index n enumerates the states for later identification.

$\lvert N(\lambda\mu)L[f]_X[f]_{FS}[f]_F[f]_S\rangle$	$[N^{J^\pi}]_n\,N^*$
$\lvert 0(00)0[3]_X[3]_{FS}[21]_F[21]_S\rangle$	$[N^{\frac{1}{2}^+}]_1\,N_{939}$
$\lvert 0(00)0[3]_X[3]_{FS}[3]_F[3]_S\rangle$	$[\Delta^{\frac{3}{2}^+}]_1\,\Delta_{1232}$
$\lvert 1(10)1[21]_X[21]_{FS}[21]_F[21]_S\rangle$	$[N^{\frac{3}{2}^-}]_1\,N_{1520};\ [N^{\frac{1}{2}^-}]_1\,N_{1535}$
$\lvert 1(10)1[21]_X[21]_{FS}[21]_F[3]_S\rangle$	$[N^{\frac{1}{2}^-}]_2\,N_{1650};\ [N^{\frac{5}{2}^-}]_1\,N_{1675};\ [N^{\frac{3}{2}^-}]_2\,N_{1700}$
$\lvert 1(10)1[21]_X[21]_{FS}[3]_F[21]_S\rangle$	$[\Delta^{\frac{1}{2}^-}]_1\,\Delta_{1620};\ [\Delta^{\frac{3}{2}^-}]_1\,\Delta_{1700}$
$\lvert 2(20)0[3]_X[3]_{FS}[21]_F[21]_S\rangle$	$[N^{\frac{1}{2}^+}]_2\,N_{1440}$
$\lvert 2(20)0[21]_X[21]_{FS}[21]_F[21]_S\rangle$	$[N^{\frac{1}{2}^+}]_3\,N_{1710}$
$\lvert 2(20)2[3]_X[3]_{FS}[21]_F[21]_S\rangle$	$[N^{\frac{3}{2}^+}]_1\,N_{1720};\ [N^{\frac{5}{2}^+}]_1\,N_{1680}$
$\lvert 2(20)0[3]_X[3]_{FS}[3]_F[3]_S\rangle$	$[\Delta^{\frac{3}{2}^+}]_2\,\Delta_{1600}$
$\lvert 2(20)2[3]_X[3]_{FS}[3]_F[3]_S\rangle$	$[\Delta^{\frac{1}{2}^+}]_2;[\Delta^{\frac{3}{2}^+}]_3\,\Delta_{1920};\ [\Delta^{\frac{5}{2}^+}]_1\,\Delta_{1905};\ [\Delta^{\frac{7}{2}^+}]_1$
$\lvert 2(20)0[21]_X[21]_{FS}[21]_F[3]_S\rangle$	$[N^{\frac{3}{2}^+}]_2$
$\lvert 2(20)2[21]_X[21]_{FS}[21]_F[21]_S\rangle$	$[N^{\frac{3}{2}^+}]_3;\ [N^{\frac{5}{2}^+}]_2$
$\lvert 2(20)2[21]_X[21]_{FS}[21]_F[3]_S\rangle$	$[N^{\frac{1}{2}^+}]_4;\ [N^{\frac{3}{2}^+}]_4;\ [N^{\frac{5}{2}^+}]_3;\ [N^{\frac{7}{2}^+}]_1$
$\lvert 2(20)0[21]_X[21]_{FS}[3]_F[21]_S\rangle$	$[\Delta^{\frac{1}{2}^+}]_1\,\Delta_{1910}$
$\lvert 2(20)2[21]_X[21]_{FS}[3]_F[21]_S\rangle$	$[\Delta^{\frac{3}{2}^+}]_4;\ [\Delta^{\frac{5}{2}^+}]_2$
$\lvert 2(01)1[111]_X[111]_{FS}[21]_F[21]_S\rangle$	$[N^{\frac{1}{2}^+}]_5;\ [N^{\frac{3}{2}^+}]_5$

symbol $(\lambda\mu)$ determines the SU(3) harmonic-oscillator multiplet, N is the total number of excitation quanta and L is the total orbital angular momentum. The allowed values of L that are compatible with a given Elliott symbol $(\lambda\mu)$ are given by the Elliott formula [71–73]. The spatial permutation symmetry of the state is indicated by the Young pattern $[f]_X$. The $[f]_F, [f]_S$, and $[f]_{FS}$ Young patterns denote the flavor, spin and combined flavor-spin permutation symmetries, respectively. The totally antisymmetric color state $[111]_C$, which is common to all the states, will be suppressed in the notation. For more complete treatments, the assignments of table 2.1 apply to the main components of the wave functions only, since symmetry breaking terms in the Hamiltonian may lead to configuration mixing.

2.5 The One-Gluon Exchange Interaction

So far we have not considered any dynamical model for baryonic structure. The quark-quark interaction of the harmonic-oscillator type, as outlined in Appendix C, corresponds only to the simplest shell-model picture of baryon structure, with the quarks moving in a mean confining field. However, one expects some residual interaction to be present, which is also necessary to break the degeneracy of the naïve model. The most conventional approach, motivated by QCD, is based on a perturbative gluon-exchange.

2.5.1 Theoretic Foundations

Inspired by QCD, one usually starts with the non-relativistic reduction of the one-gluon exchange (OGE) diagram shown in fig. 2.4.

According to the discussion in sec. 2.2.2, we obtain the non-relativistic potential from the corresponding T-matrix element

$$T_{\rm fi} = -\frac{1}{(2\pi)^6}\frac{m^2}{\sqrt{E_{p_1}E_{p_2}E_{q_1}E_{q_2}}}\frac{\epsilon_{ijm}}{\sqrt{3}}\frac{\epsilon_{kln}}{\sqrt{3}}\,\delta_{mn}\,\frac{g^2}{(p_1-q_1)^2}\frac{\lambda^a_{ki}}{2}\frac{\lambda^a_{jl}}{2}\,\bar{u}(q_1)\gamma_\mu u(p_1)\,\bar{u}(q_2)\gamma^\mu u(p_2). \qquad (2.5\text{-}1)$$

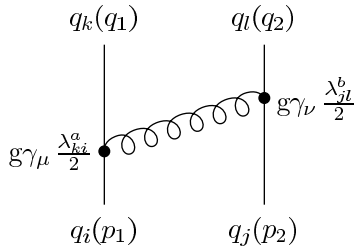

Figure 2.4: Picture of two quarks exchanging a gluon.

Here we have included the baryon color wave-function, which allows us to calculate immediately the color factor

$$\frac{\epsilon_{ijm}}{\sqrt{3}}\frac{\epsilon_{kln}}{\sqrt{3}}\,\delta_{mn}\,\frac{\lambda^a_{ki}}{2}\frac{\lambda^a_{jl}}{2} = \frac{1}{24}\Big\{(\mathrm{Tr}\lambda^a)^2 - \mathrm{Tr}\big[(\lambda^a)^2\big]\Big\} = -\frac{2}{3}, \tag{2.5-2}$$

which is the same for all baryons. Defining the strong coupling constant in the usual way

$$\alpha_{\rm s} = \frac{g^2}{4\pi}, \tag{2.5-3}$$

we find that the one-gluon exchange potential between two equal-mass quarks is given by

$$\begin{aligned} V_{\rm OGE}\,(\vec{r}) \;\; = \;\; & -\frac{2}{3}\alpha_{\rm s}\left[\frac{1}{r} - \frac{\pi}{m^2}\delta(\vec{r}) - \frac{1}{4m^2r^3}S_{12} - \frac{2\pi}{3m^2}\vec{\sigma}_1\cdot\vec{\sigma}_2\delta(\vec{r})\right] \\ & -\frac{1}{4m^2r^3}\Big[\,(\vec{\sigma}_1+2\vec{\sigma}_2)\cdot(\vec{r}\times\vec{p}_1) - (\vec{\sigma}_2+2\vec{\sigma}_1)\cdot(\vec{r}\times\vec{p}_2)\,\Big]. \end{aligned} \tag{2.5-4}$$

The first three terms inside the square bracket of the first line can be thought of as the Coulomb, Darwin and tensor ($S_{12} = 3\,\vec{\sigma}_1\cdot\hat{r}\,\vec{\sigma}_2\cdot\hat{r} - \vec{\sigma}_1\cdot\vec{\sigma}_2$) terms respectively, while the last term is a spin-spin hyperfine interaction, called the color-magnetic term. The second line contains the spin-orbit interaction.

The Hamiltonian containing all spin-dependent relativistic corrections up to order $v^2 = \vec{p}^{\,2}/m^2$ is called the generalized Breit–Fermi Hamiltonian:

$$H = m_1 + m_2 + \frac{\vec{p}^{\,2}}{2\,\mu} + V_{\rm NR}(r) + H_{\rm SS} + H_{\rm T} + H_{\rm LS}, \tag{2.5-5}$$

where the different spin-components of the interaction have been explicitly indicated.

2.5.2 Explicit Quark Models Based on OGE

We shall consider in the following the most prominent examples of specific quark models that are motivated from OGE. Basically they all start from the Breit interaction and differ only by the degree of simplification via the neglect of various terms.

The model of de Rújula, Georgi and Glashow

The paper of de Rújula, Georgi and Glashow [22] was an attempt to interpret the familiar non-relativistic quark model within the framework of the quark dynamics described by Quantum Chromodynamics. The essential new feature was the inclusion of the non-relativistic one-gluon exchange interaction as an additional short range potential. The justification for keeping only the lowest order terms at short distances is rather hand-waving: it is argued that at typical hadron masses – say ~ 1 GeV – the effective quark - gluon coupling is small because of asymptotic freedom. With the assumption of non-relativistic quark dynamics, they are able to motivate the appearance of the familiar Breit interaction between quarks i and j. The Hamiltonian for three quarks in a baryon is then written as

$$H = \sum_i \left(m_i + \frac{\vec{p}_i^{\,2}}{2m_i} + ...\right) + V_{conf}(\vec{r}_1,\vec{r}_2,\vec{r}_3) - \frac{2}{3}\alpha_s\sum_{i>j}V_{ij}. \tag{2.5-6}$$

Here V_{conf} is the color confining interaction and V_{ij} is the above mentioned Breit interaction,

$$\begin{aligned} V_{ij} = \; & \frac{1}{r} - \frac{1}{2m_i m_j}\left(\frac{\vec{p}_i\cdot\vec{p}_j}{r} + \frac{\vec{r}\cdot(\vec{r}\cdot\vec{p}_i)\vec{p}_j}{r^3}\right) && \text{(Coulomb term + corrections)} \\ & -\frac{\pi}{2}\,\delta^3(\vec{r})\Big(\frac{1}{m_i^2}+\frac{1}{m_j^2}\Big) && \text{(Darwin term)} \\ & -\frac{1}{m_i m_j}\Big(\frac{8\pi}{3}\vec{s}_i\cdot\vec{s}_j\,\delta^3(\vec{r}) + \frac{1}{r^3}\big[3\,(\vec{s}_i\cdot\hat{r})(\vec{s}_j\cdot\hat{r}) - \vec{s}_i\cdot\vec{s}_j\big]\Big) && \text{(spin}-\text{spin + tensor)} \\ & -\frac{1}{2r^3}\Big(\frac{1}{m_i^2}\,\vec{r}\times\vec{p}_i\cdot\vec{s}_i - \frac{1}{m_j^2}\,\vec{r}\times\vec{p}_j\cdot\vec{s}_j + \\ & \qquad \frac{2}{m_i m_j}\big[\vec{r}\times\vec{p}_i\cdot\vec{s}_j - \vec{r}\times\vec{p}_j\cdot\vec{s}_i\big]\Big), && \text{(spin-orbit)} \end{aligned}$$

where all relativistic corrections (including spin-independent) have been consistently taken into account up to order $\vec{p}^2/m^2$. This interaction is in fact just the generalization of eq. (2.5-4) to the case of different quark masses.

Technically, the problem was then solved by a perturbation expansion around the zeroth-order Hamiltonian H_0:

$$H_0 = \sum_i \left(m_i + \frac{\vec{p}_i^{\,2}}{2m_i}\right) + V_{conf}(\vec{r}_1,\vec{r}_2,\vec{r}_3), \tag{2.5-7}$$

with the perturbing potential V defined by $H = H_0 + V$. To first order in V, a number of SU(3) and SU(6) relations were recovered, such as the Gell-Mann–Okubo mass formula.

The Isgur-Karl model

Isgur and Karl applied a very specific Hamiltonian to a large amount of resonance data [23, 24, 74]. The calculation is based on a perturbation around a harmonic oscillator Hamiltonian H_0 (as given by eq. (C.1-11)), where the perturbation includes both an arbitrary an-harmonic term U and a hyperfine correction H_{hyp}:

$$H = H_0 + U + H_{hyp}. \tag{2.5-8}$$

The key point of the model is the neglect of the spin-orbit forces in the Breit interaction but the retention of all the spin-spin and tensor components, so that

$$H_{hyp} = \frac{2\alpha_s}{3m_i m_j}\Big(\frac{8\pi}{3}\vec{s}_i\cdot\vec{s}_j\delta^3(\vec{r}) + \frac{1}{r^3}[3(\vec{s}_i\cdot\hat{r})(\vec{s}_j\cdot\hat{r}) - \vec{s}_i\cdot\vec{s}_j]\Big). \tag{2.5-9}$$

With this rather simple and plausible (apart from the question of spin-orbit forces) Hamiltonian, Isgur and Karl are able to describe the whole spectra of light and strange baryons. Subsequent calculations of decay widths (strong and electromagnetic, see ref. [75]) seemed to indicate that the problems of mixing angles and missing states have been solved. To quote Koniuk and Isgur, *"the tables argue convincingly that at least the main features of baryon physics have been captured by the structure and decay models described here: the sign and magnitude of almost every measured baryon decay amplitude has been correctly predicted"*. While this is certainly an overstatement (as formulated in ref. [76]), the overall success of such a simple non-relativistic model is indeed impressive.

The model of Isgur and Godfrey

This is a relativized version of the IK model, first introduced in ref. [77] and further refined and adapted to baryons in ref. [78]. It is especially important in that the wave-functions from this model were used by Capstick and Roberts to calculate a wealth of decay processes (see ref. [79] for a recent review). We briefly outline the model here in the form as it was presented in ref. [80].

The Hamiltonian of this model contains a kinetic-energy term in semi-relativistic form:

$$H = \sum_i \sqrt{\vec{p}_i^{\,2} + m_i^2} + V, \tag{2.5-10}$$

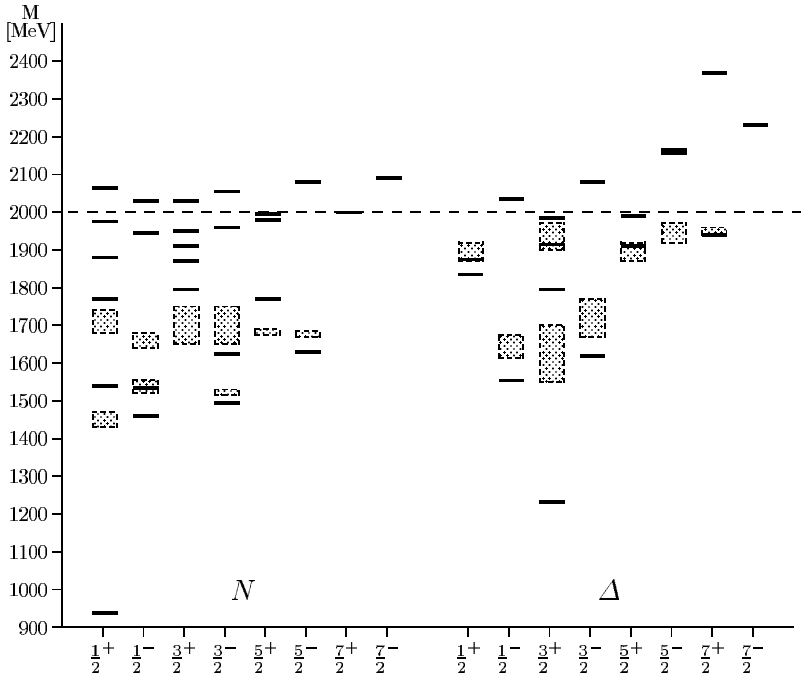

Figure 2.5: Spectrum of the model of Isgur and Godfrey, which was used by Capstick and Roberts for their calculations of decay widths. The shaded boxes give the experimental Breit-Wigner masses (compare fig. 2.3).

where V is a relative position- and momentum-dependent potential, which tends in the non-relativistic limit (not taken in their work) to

$$V \to V_{string} + V_{Coul} + V_{hyp} + V_{so(cm)} + V_{so(Tp)}. \tag{2.5-11}$$

Here, V_{string} is a confining potential, taken in linear form. The Coulomb and hyperfine potentials, V_{Coul} and V_{hyp} are taken as in the IK model, except that the inter-quark coordinates r_{ij} are smeared out over mass-dependent distances, and the momentum dependence away from the $p \to 0$ limit is parameterized. Finally, $V_{so(cm)}$ and $V_{so(Tp)}$ are the color-magnetic spin-orbit and the Thomas precession spin-orbit potentials, respectively.

The smearing mentioned above is brought about by convoluting the potentials with a function

$$\rho(r_{ij}) = \frac{\sigma_{ij}^3}{\pi^{3/2}} \exp\left(-\sigma_{ij}^2 r_{ij}^2\right), \tag{2.5-12}$$

where the σ_{ij} are chosen to smear the inter-quark coordinates over a distance of 0.1 fm for light quarks. The potentials are made momentum-dependent by introducing factors that replace m_i by E_i. For example, the contact part of V_{hyp} becomes

$$V_{cont} = \sum_{i<j} \left(\frac{m_i\, m_j}{E_i\, E_j}\right)^{\epsilon+1/2} \frac{16\pi}{9} \alpha_s(r_{ij}) \frac{\vec{S}_i \cdot \vec{S}_j}{m_i\, m_j} \frac{\sigma_{ij}^3}{\pi^{3/2}} \exp\left(-\sigma_{ij}^2 r_{ij}^2\right), \tag{2.5-13}$$

where ϵ is a constant parameter and $\alpha_s(r_{ij})$ is a running coupling constant inspired by the lowest order QCD formula.

The problem is then solved again by expanding in a harmonic oscillator basis in the form of eqs. (C.1-14) and (C.1-15), extending the basis to $N = 6$ for positive-parity states, and to $N = 7$ for negative-parity states. Energies are then minimized by a variation of the oscillator size parameter b, eq. (C.1-16). This minimization is done state by state, however, Capstick and Roberts, for the calculation of decay widths, take in all their wave functions the same numerical value of b in order to ensure orthogonality.

The resulting spectroscopy of the model is claimed to be comparable to the one of the IK model (see fig. 2.5). This is largely a consequence of the assumption that the two spin-orbit contributions in eq. (2.5-11), the one from the Breit interaction and the one from the Thomas precession, cancel each other. Note however, that the negative-parity states in this model tend to lie too low, while the positive-parity states are rather too high. This is obviously a consequence of the attempt to minimize the error due to the wrong parity ordering that occurs in all OGE models (see the discussion in the next section).

A very similar model, with corresponding similar results, was discussed by Stancu and coworkers [81–83], who also calculated a number of decay widths in the related flux-tube breaking decay model.

The model of Bhaduri, Cohler and Nogami

For the purpose of comparison we shall investigate a simplified version of a OGE CQM. Specifically, it is the model following Bhaduri, Cohler, and Nogami (BCN) [84,85]. In this case the total potential has the form

$$V_{ij} = V_0 + Cr_{ij} - \frac{2b}{3r_{ij}} + \frac{\alpha_s}{9m_i m_j}\Lambda^2 \frac{e^{-\Lambda r_{ij}}}{r_{ij}} \vec{\sigma}_i \cdot \vec{\sigma}_j, \tag{2.5-14}$$

i.e., it contains a short-range Coulomb term, a linear confinement, and a flavor-independent spin-spin interaction. Results from this model will point out the essential differences when neglecting spin-orbit and/or tensor forces in the interaction. The parameter values for the original BCN potential were determined from a fit to the meson spectra, and they were also used in a previous study [86]. We have re-determined the model parameters from a fit to the baryon spectra. In addition, we shall investigate the influence of the kinetic energy operator. Mostly this one is taken in a non-relativistic (NR) form

$$H_0^{NR} = \sum_{i=1}^{3} \left(\frac{\vec{p}_i^{\,2}}{2m_i} + m_i \right). \tag{2.5-15}$$

This choice leads to the theoretical shortcoming that the average velocity of a quark inside a hadron is larger than the velocity of light, $(v/c)^2 > 1$, so that people were led to use a kinetic energy operator in semi-relativistic (SR) form:

$$H_0^{SR} = \sum_{i=1}^{3} \sqrt{\vec{p}_i^{\,2} + m_i^2}. \tag{2.5-16}$$

The parameter values for the BCN potential in different parameterizations are summarized in table 2.2, from where it can be seen that they differ from the parameter set used in ref. [85], specifically in the NR case.

Table 2.2: Parameters of the OGE CQM after BCN [84, 85] for the semi-relativistic (SR) and non-relativistic (NR) parameterizations. The quark masses are set to $m_u = m_d = 337$ MeV.

	b	α_s	Λ [fm^{-1}]	C [fm^{-2}]	V_0 [MeV]
SR	0.57	0.57	2.7	3.12	-409
NR	0.825	0.825	5.0	2.26	-366

The spectra are produced in quite a similar manner by both the SR and NR versions, see fig. 2.6. Again, the typical difficulties of OGE CQMs appear, e.g., with respect to the relative orderings of the lowest positive- and negative-parity excitations. Note however, that the semi-relativistic kinematics helps a lot in reducing the discrepancy, an effect that will be discussed in a later section.

2.5.3 Inherent Problems of the OGE

It has been argued [87,88] that in spite of all the crude approximations, from non-relativistic dynamics until perturbative gluon-exchange, the interaction suggested by the naive quark potential model may

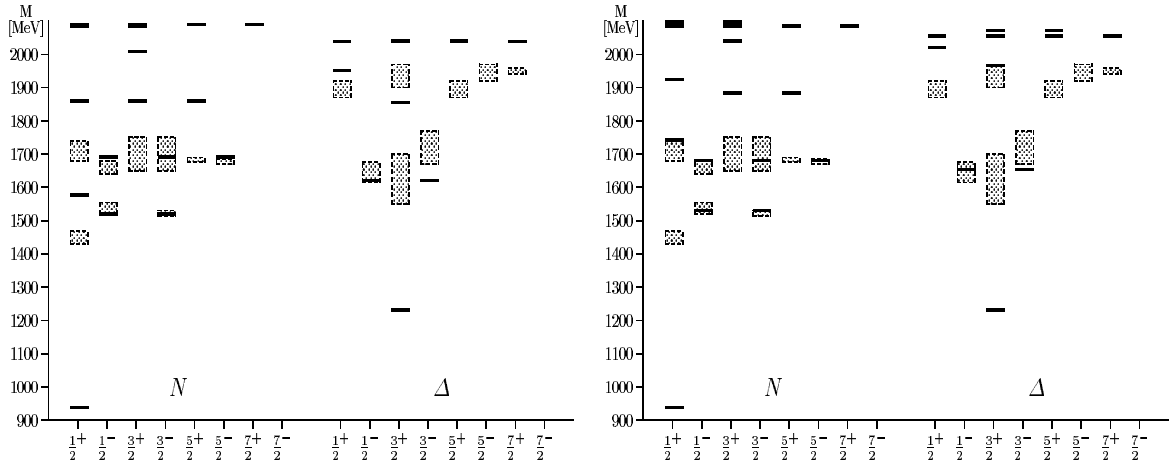

Figure 2.6: Spectrum of the BCN model in the semi-relativistic (left) and non-relativistic (right) versions.

not be completely unreasonable. This claim was mainly based on the observation that for light quarks, because of their practically vanishing mass, the only relevant scale in the problem is Λ_{QCD}. This viewpoint completely ignores the fact that there is still an important scale present in QCD, that must become important in particular at low energies: the scale of chiral symmetry breaking. The consequences of the latter effect will be discussed in the next chapter, for the OGE one has to stress that it is its huge empirical success that provides the main part of its justification. There are, however, also problems inherent in this approach.

The most prominent shortcoming of all models based on OGE is the prediction of a wrong ordering of positive- and negative-parity states as compared to the experimental data. This is evident by inspecting as representative examples figs. 2.5 and 2.6, where one always finds the Roper resonance N_{1440} and its analog in the Δ sector, the Δ_{1600}, above the lowest negative-parity doublets, the $N_{1520} - N_{1535}$ and the $\Delta_{1620} - \Delta_{1700}$, respectively. It must be stressed that this is a principle shortcoming, that may not be arranged by a specific parameterization of the interaction, as it may be seen from the following argument.

The most important component of the OGE interaction is the so-called color-magnetic term in the Breit-Fermi interaction, see eq. (2.5-4):

$$V_{cm} = -\alpha_s \sum_{i<j} \frac{\pi}{6 m_i m_j} \vec{\lambda}_i^C \cdot \vec{\lambda}_j^C \vec{\sigma}_i \cdot \vec{\sigma}_j \delta(\vec{r}_{ij}), \tag{2.5-17}$$

where the $\vec{\lambda}_i^C$ are color SU(3) Gell-Mann matrices. The matrix elements of this term between two-quark states with definite color-spin symmetry are given by

$$\left\langle [f]_C \times [f]_S : [f]_{CS} \middle| \vec{\lambda}_i^C \cdot \vec{\lambda}_j^C \, \vec{\sigma}_i \cdot \vec{\sigma}_j \middle| [f]_C \times [f]_S : [f]_{CS} \right\rangle = \begin{cases} 8 & [11]_C \times [11]_S : [2]_{CS} \\ -\frac{8}{3} & [11]_C \times [2]_S : [11]_{CS}. \end{cases} \tag{2.5-18}$$

Hence the color-magnetic contribution to the Δ state ($[111]_{CS}$) is repulsive, while it is attractive for the nucleon ($[21]_{CS}$), so the Δ becomes heavier than the N. However, the contribution is the same for the positive-parity state N_{1440} and the negative-parity state N_{1520}, which have both the same mixed ($[21]_{CS}$) color-spin symmetry. But since the N_{1440} belongs to the $N = 2$ band in a harmonic oscillator basis, it should lie about $\hbar\omega$ above the N_{1520}. The situation is even worse in the Δ sector. The Δ_{1600} positive-parity state has a completely antisymmetric color-spin symmetry ($[111]_{CS}$), while the negative-parity state Δ_{1700} has a mixed one. Thus the color-magnetic interaction provides repulsion for the Δ_{1600} and attraction for the Δ_{1700}. In addition, the Δ_{1600} is in the $N = 2$ band. This shows that the wrong parity ordering in OGE models is a direct consequence of the symmetry of the interaction.

We note that the Roper problem may be solved by the inclusion of three-body forces [89], which affect mainly the nucleon and its radial excitations while producing essentially no effect on states with mixed symmetry. For other works dealing with the problem of the Roper resonance, see refs. [90, 91].

The second problem with OGE is the presence of large spin-orbit forces. The phenomenological success of the IK-model seems to indicate that spin-orbit forces are not important in the baryon spectra. The Breit interaction, however, manifestly contains such forces, see eq. (2.5-4). Where have they gone? The argument that is usually given is based on the observation that in addition to the spin-orbit forces from OGE, there are also spin-orbit forces from the (assumed Lorentz-scalar) confining interaction, via the Thomas precession. Even though it has been shown in phenomenological studies that these different contributions tend to cancel each other, the situation is not so clear (see ref. [76] for a discussion and a list of references). Also the question why this subtle cancellation should be so exact remains unanswered, so that the dropping of the spin-orbit forces in the OGE potentials has to be considered an ad-hoc procedure.

2.6 The Goldstone-Boson Exchange Interaction

We have mentioned already earlier that in approaches based on the one-gluon exchange interaction one completely ignores the presence of the second relevant scale in QCD: the one where the chiral symmetry of the QCD Lagangian gets spontaneously broken. We shall discuss now in a more detailed way the consequences of this effect and deal with a model for hadronic structure inspired by it.

2.6.1 Introduction

The importance of the constraints posed by chiral symmetry on baryon models was recognized rather rapidly [92]. In the bag or bag-like models [93], the massless current quarks within the bag were assumed to interact not only by perturbative gluon exchange, but also through chiral meson-field exchange. In these models the chiral field is used as an auxiliary field only and the breaking of chiral symmetry arises from confinement.

This contrasts with the point of view of Manohar and Georgi [94], who pointed out that there should be two different scales in QCD:

- one scale which characterizes the occurrence of spontaneous symmetry breaking, given roughly by $\Lambda_\chi \simeq 4\pi f_\pi \simeq 1$ GeV,
- the other one that characterizes confinement, $\Lambda_{QCD} \simeq 100$ MeV.

Between these two scales, the effective Lagrangian should contain gluon fields that provide confinement, as well as constituent quark and pseudo-scalar meson fields, that are responsible for the hyperfine interaction[1].

It is commonly accepted today that at low temperature and density, the approximate chiral symmetry of QCD is realized in the Nambu-Goldstone mode (see sec. 2.3.3). This hidden mode of chiral symmetry is revealed by the existence of the low-mass pseudo-scalar mesons, which represent the associated approximate Goldstone bosons. The second consequence of the spontaneous breaking of chiral symmetry is that the current quarks acquire their dynamical, or constituent, mass. The chiral symmetry breaking and its consequences are probably best illustrated by the Nambu and Jona-Lasinio model [97,98], which in its original form however, does not have a confining interaction.

Inspired by the principal inability of the OGE to describe the baryon spectra, in particular as regarding the problem of level ordering of positive and negative-parity states, as discussed at the end of the last section, Glozman and Riska [99] took the above viewpoint to the extreme by neglecting completely the hyperfine interaction stemming from one-gluon exchange and taking into account its effect only through the presence of a phenomenological confinement interaction. The resulting Goldstone boson exchange (GBE) model was then shown to provide a more satisfactory fit to the baryon spectra than the OGE.

This may be easily understood by looking at the flavor-spin structure of the interaction that follows from the pseudo-scalar octet exchange. The main component is given by $-V(\vec{r}_{ij})\,\vec{\lambda}_i^F \cdot \vec{\lambda}_j^F\,\vec{\sigma}_i \cdot \vec{\sigma}_j$ (note the

[1] This viewpoint complements rather nicely the one that stems from the instanton liquid picture of QCD, see refs. [95,96]. Here too, it was argued that at low momenta, QCD should be approximated by an effective Langrangian of the σ-model type which contains valence quarks with effective (constituent) masses and meson fields.

crucial difference with the color-magnetic interaction of eq. (2.5-17): the λ's here are flavor matrices), and its matrix elements between two-quark states are readily determined to be

$$\left\langle [f]_F \times [f]_S : [f]_{FS} \middle| -V(\vec{r}_{ij})\, \vec{\lambda}_i^F \cdot \vec{\lambda}_j^F\, \vec{\sigma}_i \cdot \vec{\sigma}_j \middle| [f]_F \times [f]_S : [f]_{FS} \right\rangle$$
$$= \begin{cases} -\frac{4}{3}V(\vec{r}_{ij}); & [2]_F \times [2]_S : [2]_{FS} \\ -8V(\vec{r}_{ij}); & [11]_F \times [11]_S : [2]_{FS} \\ 4V(\vec{r}_{ij}); & [2]_F \times [11]_S : [11]_{FS} \\ \frac{8}{3}V(\vec{r}_{ij}); & [11]_F \times [2]_S : [11]_{FS}. \end{cases} \qquad (2.6\text{-}1)$$

One can deduce the following important properties (assuming $V(\vec{r}_{ij})$ to be positive, which is true at short distances where the hyperfine interaction is dominant):

- the chiral interaction is attractive in symmetrical flavor-spin pairs and repulsive in anti-symmetrical ones,
- among the flavor-spin symmetrical pairs, the flavor anti-symmetrical ones experience a much larger attraction (by a factor 6) than the flavor symmetrical ones.

Thus, from table 2.1 we deduce that the states N_{1440} and Δ_{1600} from the $N = 2$ harmonic oscillator band will be lowered in mass relative to the states N_{1520} and Δ_{1700}, respectively. This effect will be larger in the N sector than in the Δ one. It can be concluded therefore, that the chiral interaction that follows from pseudo-scalar boson exchange, favors exactly the symmetry properties that are required to describe correctly the observed spectra.

Regarding the physical interpretation of the model, there is a rather nice analogy with solid state physics, where one describes the electric and thermo-dynamic properties of metals in terms of heavy, dynamical electrons, phonons (the Goldstone bosons of the spontaneously broken translational symmetry of the ion-lattice), and electron-phonon interactions. The corresponding quantities in baryon physics would be constituent quarks, pseudo-scalar mesons and the interaction between them[1]. No one would seriously try to describe a solid with the original degrees of freedom (electrons, positive lattice ions and a photon exchange that gives rise to a Coulomb potential between them), even though it would in principle be possible.

It should also be emphasized that this new approach with effective degrees of freedom does not deny the existence of the original, and more fundamental ones. It simply means that the calculation of physical observables is most facilitated by the use of those degrees of freedom that are most appropriate for the problem considered. With this respect, the critique sometimes put forward in the literature, that the GBE model denies the existence of gluons is plain nonsense.

A point that is scarcely noted (see refs. [100,101], however for applications in the chiral soliton model) is that the QCD inspired one-gluon exchange interaction of eq. (2.5-1) effectively incorporates components

[1]The one-gluon exchange interaction between constituent quarks would correspond to the Coulomb interaction between heavy, effective electrons in the lattice, which is known to be completely inessential for physical observables.

of exchanges of different Dirac structure via a Fierz transformation.

Consider the five Lorentz scalars

$$\begin{aligned} s(4,2;3,1) &= \bar{u}(4)u(2)\bar{u}(3)u(1) \\ v(4,2;3,1) &= \bar{u}(4)\gamma^\mu u(2)\bar{u}(3)\gamma_\mu u(1) \\ t(4,2;3,1) &= \tfrac{1}{2}\bar{u}(4)\sigma^{\mu\nu} u(2)\bar{u}(3)\sigma_{\mu\nu} u(1) \\ a(4,2;3,1) &= \bar{u}(4)\gamma^5\gamma^\mu u(2)\bar{u}(3)\gamma_\mu\gamma^5 u(1) \\ p(4,2;3,1) &= \bar{u}(4)\gamma^5 u(2)\bar{u}(3)\gamma^5 u(1). \end{aligned} \tag{2.6-2}$$

Here $u(1)$ denotes $u(p_1, s_1)$, the spinor with momentum p_1 and polarization s_1, and the symbol $(4,2;3,1)$ denotes the way how the Dirac indices are contracted. The theorem of Fierz states that there exists a numerical 5×5 matrix that relates the quantities of eq. (2.6-2) to those where 4 is contracted with 1 and 3 with 2 (the transformation matrix here corresponds to the one given in ref. [102], the one in ref. [103] is incorrect):

$$\begin{pmatrix} s \\ v \\ t \\ a \\ p \end{pmatrix} (4,2;3,1) = \frac{1}{4} \begin{bmatrix} 1 & 1 & 1 & -1 & -1 \\ 4 & -2 & 0 & -2 & 4 \\ 6 & 0 & -2 & 0 & -6 \\ -4 & -2 & 0 & -2 & -4 \\ -1 & 1 & -1 & -1 & 1 \end{bmatrix} \begin{pmatrix} s \\ v \\ t \\ a \\ p \end{pmatrix} (4,1;3,2). \tag{2.6-3}$$

It follows that the one-gluon exchange interaction of eq. (2.5-1) may be expressed as

$$\bar{u}(4)\gamma^\mu u(2)\bar{u}(3)\gamma_\mu u(1) = v(4,2;3,1) = \left[s - \frac{1}{2}v - \frac{1}{2}a + p \right] (4,1;3,2). \tag{2.6-4}$$

The approach by Glozman and Riska may therefore just be based on the assumption that the pseudo-scalar part of the form (2.6-4) is the dominant or at least the most important one in the low-energy regime. The Fierz transformation also nicely illustrates that one should have scalar, vector and axial-vector exchanges between constituent quarks, too. These ones have been included in recent versions of the GBE potential [104, 105] but they will be neglected throughout the present work.

2.6.2 Specific Parameterizations

As outlined above, the model originates from the viewpoint that beyond the scale of spontaneous breaking of chiral symmetry (SBχS) the effective degrees of freedom in light and strange baryons are furnished by constituent quarks and Goldstone bosons [94]. Thus one has to consider these particular degrees of freedom rather than the original ones – current quarks and gluons. The effective interaction Lagrangian is to be constructed from the coupling of constituent-quark fields ψ and chiral meson fields $\vec{\phi}$. The latter include the octet of the (pseudo-)Goldstone bosons π, K, and η, as well as the η' meson, which decouples from the original nonet because of the axial anomaly[1].

The simplest ansatz for a chiral interaction Lagrangian is:

$$\mathcal{L} \sim i g_{PS} \bar{\psi}\gamma_5 \vec{\lambda}^F \cdot \vec{\phi}\psi. \tag{2.6-5}$$

Here, g_{PS} is the pseudo-scalar coupling constant and $\vec{\lambda}^F$ are the Gell-Mann flavor matrices. To lowest order in a non-relativistic reduction, this Lagrangian produces a spin- and flavor-dependent interaction potential between constituent quarks i and j, which contains a spin-spin and a tensor part:

$$V_\chi^{octet}(\vec{r}_{ij}) = \vec{\lambda}_i^F \cdot \vec{\lambda}_j^F \left\{ V^S(\vec{r}_{ij})\, \vec{\sigma}_i \cdot \vec{\sigma}_j + V^T(\vec{r}_{ij})\, \hat{S}_{12} \right\}. \tag{2.6-6}$$

Note in particular that the GBE interaction to lowest order does not lead to any spin-orbit forces, in contrast to the OGE interaction (see eq. (2.5-4)). We know that in reality $SU(3)_F$ is broken by the

[1] In the large N_c limit, where the axial anomaly becomes suppressed, the η' would become the ninth Goldstone boson.

quark- and meson-mass differences and maybe also because of flavor dependent coupling constants, so the flavor-dependent parts of the potentials are split up according to

$$\vec{\lambda}_i^F \cdot \vec{\lambda}_j^F \, V^{S,T}(\vec{r}_{ij}) \Rightarrow \left\{ \sum_{a=1}^{3} V_\pi^{S,T}(\vec{r}_{ij}) \lambda_i^a \lambda_j^a + \sum_{a=4}^{7} V_K^{S,T}(\vec{r}_{ij}) \lambda_i^a \lambda_j^a + V_\eta^{S,T}(\vec{r}_{ij}) \lambda_i^8 \lambda_j^8 \right\}. \tag{2.6-7}$$

The pseudo-scalar singlet-exchange potential takes the same form

$$V_\chi^{singlet}(\vec{r}_{ij}) = \frac{2}{3} \left\{ V_{\eta'}^S(\vec{r}_{ij}) \vec{\sigma}_i \cdot \vec{\sigma}_j + V_{\eta'}^T(\vec{r}_{ij}) \hat{S}_{12} \right\}, \tag{2.6-8}$$

where the factor $\frac{2}{3}$ comes from the flavor matrix element. To lowest order in a non-relativistic reduction, a coupling in the form of eq. (2.6-5) will give rise to a Yukawa interaction between constituent quarks, so that the meson-exchange potentials in eqs. (2.6-6) and (2.6-8) assume the spatial dependence

$$V_\gamma^S(\vec{r}_{ij}) = \frac{g_\gamma^2}{4\pi} \frac{1}{12 m_i m_j} \left\{ \mu_\gamma^2 \frac{e^{-\mu_\gamma r_{ij}}}{r_{ij}} - 4\pi\delta(\vec{r}_{ij}) \right\}, \tag{2.6-9}$$

$$V_\gamma^T(\vec{r}_{ij}) = \frac{g_\gamma^2}{4\pi} \frac{1}{12 m_i m_j} \mu_\gamma^2 \left\{ \frac{3}{(\mu_\gamma r_{ij})^2} + \frac{3}{\mu_\gamma r_{ij}} + 1 \right\} e^{-\mu_\gamma r_{ij}}, \tag{2.6-10}$$

with $\gamma = \pi, K, \eta, \eta'$ and quark and meson masses m_i and μ_γ, respectively.

We shall first investigate the model in a parameterization neglecting the tensor component in the interaction [99, 106]. This is motivated by the observation that the mass splittings in empirical $L-S$ multiplets in the baryon spectra are rather small (of the order ~ 100 MeV on a total mass scale of ~ 2 GeV)[1]. It is furthermore a convenient simplification that permits to grasp the essential features of the model in a first approximation. Finally it will be useful to compare results with those stemming from OGE dynamics, in particular the BCN model (see page 28), where tensor forces were also neglected.

The total quark-quark potential in the chiral constituent-quark model thus consists of the sum of the octet- and singlet-chiral interactions, eqs. (2.6-7) and (2.6-8), as well as a linear confinement [106]:

$$V^{tot}(\vec{r}_{ij}) = V_\chi^{octet}(\vec{r}_{ij}) + V_\chi^{singlet}(\vec{r}_{ij}) + C r_{ij}. \tag{2.6-11}$$

The potentials (2.6-9) and (2.6-10) are strictly applicable only for point-like particles. Since one deals with structured particles (constituent quarks and pseudo-scalar mesons) of finite extension, one must regularize the short-range interaction. The parameterization of the meson-exchange potential (2.6-9) with a certain representation of the δ-function must have the property of a vanishing volume integral of the chiral potential.

To show this we have to come back to the interaction Lagrangian, eq. (2.6-5) and write its non-relativistic reduction in momentum space,

$$V(\vec{q}) \sim \vec{\sigma}_i \cdot \vec{q} \vec{\sigma}_j \cdot \vec{q} \vec{\lambda}_i^F \cdot \vec{\lambda}_j^F \, D(q^2) F(q^2), \tag{2.6-12}$$

where $D(q^2)$ is the dressed Green's function for the chiral field and $F(q^2)$ is a meson-quark form factor that takes into account the internal structure of the quasi-particles. For large distances ($q^2 \to 0$) one has $D^{-1}(q^2) \to D_0^{-1}(\vec{q}^2) = -(\vec{q}^2 + \mu^2) \neq 0$ and $F(q^2) \to 1$. It then follows from eq. (2.6-12) that $V(\vec{q}=0) = 0$, which implies that the volume integral of the Goldstone boson exchange interaction in configuration space should vanish[2]:

$$\int d\vec{r} V(\vec{r}) = 0. \tag{2.6-13}$$

In order to design a parameterization that meets this requirement one makes use of the common Yukawa-type smearing of the δ-function, which just corresponds to a Pauli-Villars regularization. This leads to a meson-exchange potential with the spatial dependence

$$V_\gamma(\vec{r}_{ij}) = \frac{g_\gamma^2}{4\pi} \frac{1}{3} \frac{1}{4 m_i m_j} \left\{ \mu_\gamma^2 \frac{e^{-\mu_\gamma r_{ij}}}{r_{ij}} - \Lambda_\gamma^2 \frac{e^{-\Lambda_\gamma r_{ij}}}{r_{ij}} \right\}, \qquad (\gamma = \pi, K, \eta, \eta'). \tag{2.6-14}$$

[1] There is one exception in the strange spectra, namely the $\Lambda(1405) - \Lambda(1520)$ multiplet. It is known however, that tensor forces cannot explain this exceptionally large splitting and in spite of numerous suggestions of solutions, the situation for the $\Lambda(1405)$ remains unclear.

[2] The argument leading to eq. (2.6-13) is not valid in the chiral limit, where $\mu = 0$ and therefore $D_0^{-1}(\vec{q}^2 = 0) = 0$

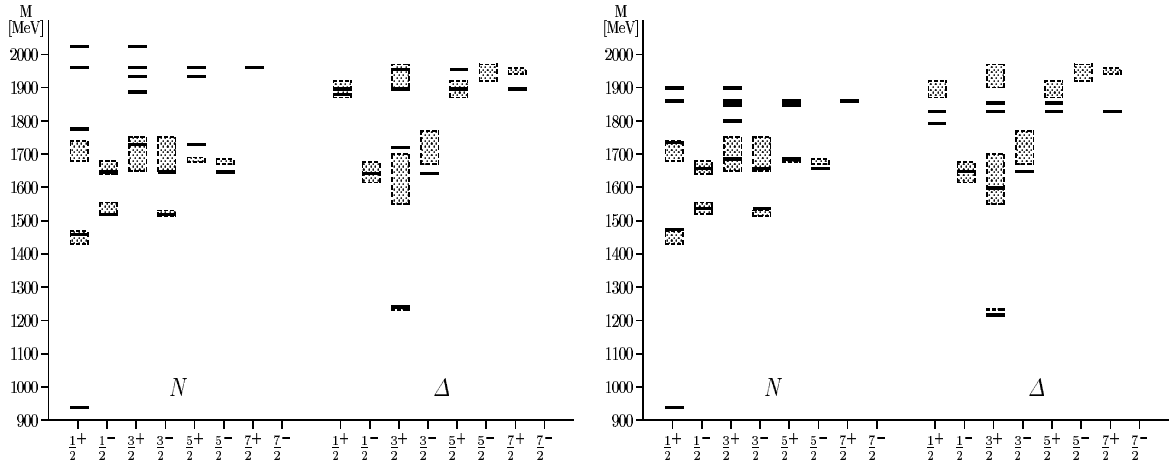

Figure 2.7: Spectrum of the GBE model in semi-relativistic (left) and non-relativistic (right) versions.

Here Λ_γ represents the cut-off parameter for each individual meson exchange. Clearly, if the phenomenological values for the different meson masses μ_γ are employed, also the cut-off parameters Λ_γ must be different (otherwise the chiral interaction (2.6-14) could receive wrong contributions from particular meson-exchange terms). The dependence of the cut-offs Λ_γ on the meson masses is parameterized through the scaling prescription

$$\Lambda_\gamma = \Lambda_0 + \kappa\mu_\gamma, \tag{2.6-15}$$

which involves the two free parameters Λ_0 and κ.

Table 2.3: Parameters of the GBE CQM for the semi-relativistic (SR) and non-relativistic (NR) parameterizations without tensor force. The predetermined parameter values (parameters that were not varied during the fit) are the quark masses ($m_u = m_d = 340$ MeV) and the pseudo-scalar meson masses ($\mu_\pi = 139$ MeV, $\mu_\eta = 547$ MeV and $\mu_{\eta'} = 958$ MeV).

	$\frac{g_8^2}{4\pi}$	$(g_0/g_8)^2$	Λ_0 [fm^{-1}]	κ	C [fm^{-2}]	V_0 [MeV]
SR	0.67	1.34	2.87	0.81	2.33	-416
NR	1.24	2.23	5.82	1.34	0.77	-112

The parameters that were determined by a fit to the spectra are summarized in table 2.3, where it should be noticed that in the non-relativistic case, a slightly higher value for the octet coupling constant was employed. With the parameterization of the type (2.6-14) the phenomenological baryon spectra can be reproduced with satisfactory quality both with non-relativistic and with semi-relativistic kinematics (see eqs. (2.5-15),(2.5-16)). The spectra of all the states up to the $N = 2$ band in a harmonic oscillator basis (that is, all the states displayed in table 2.1) are shown in fig. 2.7. We note in particular the right level ordering of the Roper resonance and the first negative-parity states in the N spectrum in both cases.

However, in the Δ spectrum, the GBE SR parameterization predicts the Δ_{1600} to be heavier than the negative-parity states, contrary to the GBE NR parameterization, where the ordering is correct also in this case. This is the only qualitative difference between spectra employing non-relativistic and semi-relativistic kinematics.

The reason for this may be understood with the help of the matrix elements of the chiral interaction, eq. (2.6-1) and the numerical values of the parameters, table 2.3. The matrix element for the totally symmetrical Δ_{1600} is smaller by a factor 6 than the corresponding matrix element for the Roper resonance, which contains $[11]_F \times [11]_S : [2]_{FS}$ components. In addition, the confinement in the GBE SR case is much larger than the confinement in the GBE NR, which means that the hyperfine interaction is more suppressed for the Δ_{1600}, which has a larger spatial extension than the Roper. On the other side, the

small value of the confinement strength in the GBE NR parameterization is not consistent with the values commonly accepted for the QCD string constant (which would require $C \simeq 2.5$ fm^{-2} [107]).

It should be noted that simultaneously the strange spectra can be reproduced with a comparable quality in the GBE, see refs. [108,109].

A first test of the wave functions stemming from the solution of the three-quark problem is their mean square radius. In the context of the present work this quantity is also useful for understanding some general characteristics of the results for decay widths that will be presented later on. In table 2.4 we therefore quote mean square radii of the N and Δ ground-state wave functions for the CQMs considered. The values refer to the case with point-like constituent quarks. They should therefore not be compared to experimental values but are useful to obtain insight into the relative extensions of the wave functions from each CQM.

Table 2.4: Mean square radii of N and Δ from the various CQMs, assuming point-like constituent quarks.

	GBE SR	GBE NR	OGE SR	OGE NR	exp.
$\langle r_N^2 \rangle$ [fm^2]	0.092	0.134	0.076	0.219	0.74
$\langle r_\Delta^2 \rangle$ [fm^2]	0.152	0.172	0.115	0.288	

Obviously, the values of the mean square radii are all rather small. Within each type of CQM, GBE or OGE, they are smaller in the semi-relativistic cases, as it was already observed in refs. [107,110]. This may be viewed as a consequence of the stronger confinement generally needed in the semi-relativistic CQMs. Inspection of the absolute magnitudes of the relevant quantities in tables 2.3, 2.2, and 2.4 shows, however, that confinement cannot be the only factor determining the mean square radii of the wave functions (note that the differences in confining strengths are much larger for the GBE parameterizations). A smaller extension of the baryon wave functions evidently implies even larger values for internal momenta (in the semi-relativistic CQMs). This will help to explain certain results for decay widths involving high momenta in the next chapter.

2.6.3 The Role of the Scalar Meson Exchange

In the last section it has been shown that a properly parameterized interaction based on Goldstone-boson exchange provides good baryon spectra with a correct order of positive and negative-parity levels, both in a non-relativistic [106] and in a semi-relativistic [108] treatment. In both parameterizations, the pseudo-scalar meson exchange interaction has two distinct parts: a long-range Yukawa potential tail and a short-range part having the opposite sign as compared to the Yukawa part. It is the latter which plays a major role in describing the baryon spectra in the framework of Goldstone-boson exchange (GBE) models.

The underlying symmetry of the GBE model is related to the flavor–spin $\mathrm{SU}_F(3) \times \mathrm{SU}_S(2)$ group combined with the S_3 permutation symmetry required for a system of three identical quarks. A thorough independent analysis of this model, recently performed for $L = 1$ baryons, has shown [111] that within the chiral picture, one can obtain more satisfactory fits to the observed spectrum than with one-gluon exchange (OGE) models. Also the operator set deduced in ref. [112] from a large-N_c analyses of the baryon spectra suggested a single pion exchange between quark lines.

Although the models of refs. [106, 108] are thought to be a consequence of the spontaneous chiral symmetry breaking, the chiral partner of the pion, the σ-meson, is not considered explicitly. One can think of having mocked up its contribution in the parameters of the Hamiltonian, e.g., in the regularization parameter of the short-range spin–spin term. The price which could have been paid is the large role played by the η' meson exchange which comes into the interaction with a strength $g_0^2/(4\pi)$ about equal [108] or larger [106] than the strength $g_8^2/(4\pi)$ associated with the pseudo-scalar octet (π, K, η), (see values in table 2.3).

Meson exchange potentials including σ-exchange have been considered in the so-called "hybrid" models where both meson and gluon exchanges contribute to the quark–quark interaction. However these studies

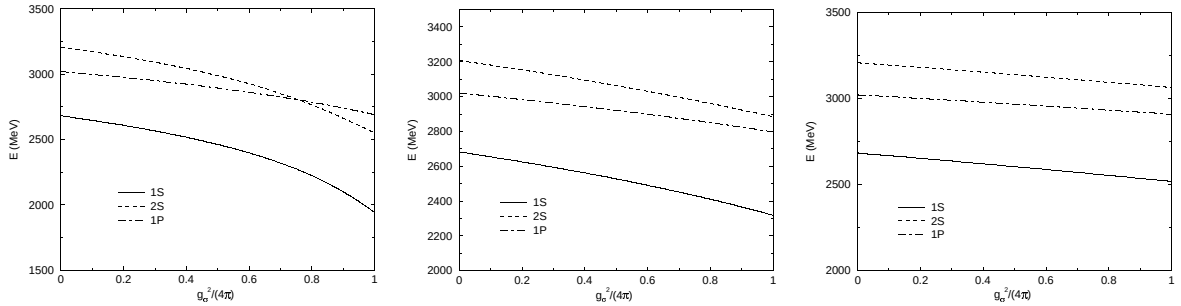

Figure 2.8: Energies of the first three eigenvalues of the Hamiltonian (2.6-16) for increasing values of the coupling constant $g_\sigma^2/(4\pi)$ in the limit $\Lambda \to \infty$(left), for $\Lambda = 2$ GeV (center) and for $\Lambda = 1$ GeV (right).

were mainly devoted to the baryon–baryon interaction [113,114] and little conclusion has been explicitly drawn about the role of the σ-exchange in the baryon spectrum. Moreover these models are all non-relativistic.

In ref. [115] the explicit role of a σ-exchange interaction has been studied by considering the following semi-relativistic Hamiltonian:

$$H_0 = \sum_i \left(m_i^2 + p_i^2\right)^{1/2} + \frac{1}{2}\sqrt{\sigma}\sum_{i<j} r_{ij} - \frac{g_\sigma^2}{4\pi}\sum_{i<j}\left[\frac{\exp(-\mu_\sigma r_{ij})}{r_{ij}} - \frac{\exp(-\Lambda r_{ij})}{r_{ij}}\right] + V_0, \qquad (2.6\text{-}16)$$

where $m_i = 340$ MeV and $r_{ij} = |\vec{r}_{ij}| = |\vec{r}_i - \vec{r}_j|$. The second term is the confinement potential with a string tension [107]

$$\sqrt{\sigma} = 1 \text{ GeV fm}^{-1}. \qquad (2.6\text{-}17)$$

Note that this value gives a confinement strength comparable to the one used in the GBE SR parameterization (see table 2.3) since $\frac{1}{2}\sqrt{\sigma} = 2.534$ fm^{-2}. The third term is the σ-exchange interaction, the form of which corresponds to the Pauli–Villars regularization (compare eq. (2.6-14)). In this term the σ-meson mass was fixed to $\mu_\sigma = 600$ MeV. The coupling constant $g_\sigma^2/(4\pi)$ and the regularization parameter Λ were taken as variable parameters. Note that the interaction of eq. (2.6-16) is attractive whenever $\mu_\sigma < \Lambda$.

From the pion–nucleon coupling constant $g_{\pi NN}^2/(4\pi) \simeq 14$, one obtains a pion–quark coupling constant $g_{\pi qq}^2/(4\pi) = 0.67$ which has been used in refs. [106,108]. Assuming a σ–nucleon coupling $g_{\sigma NN}^2/(4\pi) \simeq 8$ [116] one obtains, by naive scaling, $g_{\sigma qq}^2/(4\pi) \simeq 0.4$. Larger values are however obtained [113,114] if $g_{\sigma qq}$ is linked to $g_{\pi qq}$ by chiral-symmetry considerations. A recent evaluation [117] of the σ–quark coupling constant from the two-pion exchange interaction between constituent quarks leads to $g_{\sigma qq}^2/(4\pi) \simeq 1$. In ref. [115] the role of the σ-meson exchange for a range of $g_{\sigma qq}^2/(4\pi)$ between 0 and 1 was investigated.

It is instructive to discuss the limit $\Lambda \to \infty$ first. In this case the second term in the σ-exchange interaction vanishes. The dependence of the first three expectation values E_{1s}, E_{1p} and E_{2s} of the Hamiltonian (2.6-16) on the coupling constant is displayed on the left graph of fig. 2.8. One can see that the energy difference between the first radially excited state E_{2s} and the negative-parity state E_{1p} is positive up to a coupling constant value of about 0.75. Note also that the difference between the radially excited state and the ground state remains practically constant as a function of the coupling constant, while the mass difference between the orbitally excited state and the ground state increases with $g_\sigma^2/(4\pi)$. The reason for this is that at $g_\sigma^2/(4\pi) \neq 0$, every s state is lowered with respect to the p states. The wave function of the latter is small around the origin, so that it is less sensitive to the short-range attraction due to the Yukawa-type term.

The results show that the mass difference $E_{2s} - E_{1p}$ becomes negative for $g_\sigma^2/(4\pi) \gtrsim 0.75$. This is precisely the desired behavior for reproducing the correct order of the experimental spectrum, as it was achieved with the GBE interaction model with the help of an explicitly flavor-spin dependent interaction. These calculations indicate that a model incorporating a potential whose Laplacian is negative in a region around the origin, can yield the right ordering of the lowest positive and negative-parity states. For the

potential of eq. (2.6-16) such a situation is achieved for suitable values of the coupling constant $g_\sigma^2/(4\pi)$. Indeed the sign of the Laplacian governs the relative magnitude of radial vs. orbital excitations, as shown rigorously in the two-body case [118, 119] and approximately in the three-body case [120].

Realistically, one expects Λ to be finite. This was illustrated first by taking $\Lambda = 2$ GeV, typical for the cut-off used in the Bonn nucleon–nucleon potential [116]. The graph in the middle of fig. 2.8 shows that the expectation value of the $L = 1$ state decreases slightly slower than that of the first radially excited state. The latter remains practically parallel to the expectation value of the ground state. No crossing of levels ($E_{2s} = E_{1p}$) is observed for reasonable values of the strength $g_\sigma^2/(4\pi)$.

Current quark models [113] use still lower values of the cut-off. Repeating the calculation with $\Lambda = 1$ GeV it was found that the effect practically disappeared. The cancellation between the attractive Yukawa-type term and the regularizing counter-term is now more effective in the σ-exchange potential of the Hamiltonian (2.6-16). Accordingly this interaction is less beneficial for an enhanced level bending of S states. Indeed, as shown in the right graph of fig. 2.8, the level spacings are much less sensitive to the strength of the coupling constant $g_\sigma^2/(4\pi)$ in this case. The wave functions remain, however, influenced by the regularized scalar exchange. For instance, the averaged square radius of the ground state goes down from 0.549 fm^2 to 0.444 fm^2 i.e. it drops by about 20% when the coupling constant $g_\sigma^2/(4\pi)$ rises from 0 to 1.

It is important to understand the effects incorporated in the Hamiltonian (2.6-16). Introducing the quantity

$$R = (E_{1p} - E_{1s})/(E_{2s} - E_{1s}) \ , \tag{2.6-18}$$

where E_{1s}, E_{1p} and E_{2s} are the expectation values for the ground state, the first negative-parity- and the first radially excited state, respectively, it is clear that for $R \gtrsim 1$, the desired order is obtained. It is well known that the "naive" potentials of harmonic oscillator type have $R < 1$ (see e.g. [121]), and no tuning could improve the situation. It is also known that the addition of the OGE interaction with a reasonable strength does not improve the situation either, the Roper resonance always appearing above the first negative-parity states, in contradiction to the experimental situation. The fact that $R < 1$ for "naive" potentials is not surprising, at least for the 2-body problem. There are general theorems stating that R is smaller than unity if $\triangle V \geq 0$ [118, 119]. This happens for most empirical potentials and in particular for the celebrated Coulomb + linear potential of heavy quarkonia. Although there do not exist rigorous theorems in the 3-body case, within the approximation of the lowest hyper-spherical partial wave, one can also show that $R < 1$ if $\triangle V \geq 0$ [120].

Actually, in ref. [115] several distinct effects were studied that contribute to the level ordering:

- In the potential components with $\triangle V < 0$ were introduced through the Yukawa-type potential. This is the case for the results on the left hand side of fig. 2.8. When a regularizing term with a finite Λ is subtracted from the Yukawa type potential it is not surprising that R decreases because the regularization term leads to a $\triangle V \geq 0$ contribution at small values of r.

- A relativistic kinematics was adopted. Looking first at the two-body case, results were compared with the ones following from non-relativistic (NR) kinematics. The Schrödinger and the Herbst equation were then solved for the potential

$$V = \lambda r - g \exp(-\mu r)/r \ . \tag{2.6-19}$$

  Values of the parameters λ, g and μ, taken in units of the quark mass m, are given in table 2.5. The results obtained for R are indicated in the same table. One can see that with or without the Yukawa-type potential, the ratio R is systematically larger in the semi-relativistic (SR) than in the non-relativistic case. The case $\lambda = 0.01$ tests that relativistic effects disappear in the weak-coupling limit.

- The effects of the many-body character were investigated by looking comparatively at the two- and three-body cases, both solved for the potential (2.6-19) to see if there are differences in the value of R. In the NR case it was shown [120] that R is very similar for the two-body and the three-body problem for potentials of type $V \propto r^\beta$ with $\beta \geq -1$. It occurs however that R might be larger in the three-body case than in the two-body one when the potential V is such that $\triangle V < 0$. In the present case, this is more delicate. In eq. (2.6-19) there is a linear term with a positive Laplacian,

and a Yukawa term with a negative Laplacian. The latter being however of short-range, it is less easily felt by baryons which, in a first approximation, obey a two-body dynamics with an effective angular momentum $J = 3/2$ [120]. For instance, for the non-relativistic version of the Hamiltonian (2.6-16) with $m_i = 1$, $\sqrt{\sigma} = 2$, $g_\sigma^2/(4\pi) = 0.2$, $\mu_\sigma = 1$ and $\Lambda = \infty$, the ratio R is found equal to $R \simeq 0.67$ for the three-body case, to be compared to $R \simeq 0.60$ for the two-body case.

Table 2.5: Values of R, eq. (2.6-18), for the non-relativistic (NR) and the semi-relativistic (SR) 2-body equation with the potential (4). The parameters λ, g and μ are dimensionless, as explained in the text

λ	g	μ	NR	SR
0.01	0	-	0.585	0.588
0.865	0	-	0.585	0.628
2.0	0	-	0.585	0.644
0.865	0.2	1.765	0.597	0.655

This detailed study shows that the three effects above, $\triangle V < 0$, the relativistic kinematics and the 3-body effect cumulate and together lead to the results shown in fig. 2.8 and table 2.5.

A correct level ordering of the first positive-parity- and the first orbitally excited states has been achieved by the GBE model of refs. [106, 108], as discussed in the last section. Even though the main effect comes from the spin-flavor dependent terms in the GBE interaction, it is evident that the above mentioned effects should play a certain role, too. In particular, the GBE model includes Yukawa terms with negative Laplacian and a semi-relativistic kinetic energy operator in the GBE SR parameterization.

Once the meson-exchange picture (GBE interaction) is accepted one should also consider multiple meson exchange. In Ref. [117] it was found that the two-pion exchange plays also a significant role in the quark-quark interaction. The obtained interaction has a spin independent central component, which, averaged over the isospin part of the nucleon wave function, gives rise to an attractive spin independent interaction. The σ-meson exchange represents in fact a good approximation of such a central interaction.

It is rather natural to include the chiral partner of pseudo-scalar mesons in models based on Goldstone-boson exchanges. Scalar exchange gives a contribution with a negative Laplacian to the spin-independent interaction and this helps to restore the proper order of positive-parity and negative-parity excitations. However, when a low cut-off ($\Lambda \sim 1$ GeV) is applied, although the same trend remains, the effect becomes quite marginal, leading essentially to an overall shift of the spectrum. In that case, a proper order of levels would be nearly entirely due to the pseudo-scalar meson exchange, possibly supplemented by conventional chromo-magnetic terms.

There is no definite prescription for choosing a cut-off parameter Λ of the σ-meson exchange potential. Existing models fit this parameter in conjunction with the baryon-baryon problem [113, 114]. However, the wave functions and the sizes of the three-quark system are influenced by the σ-meson exchange. The baryon wave functions can be tested, for example, in strong decay calculations, once the hyperfine interaction is included. With this idea in mind ref. [115] concluded that the σ-meson exchange should also be incorporated within the three-quark systems describing the interacting baryons.

2.6.4 The Tensor Interaction

The pseudo-scalar exchange interaction following from the Lagrangian of eq. (2.6-5) also contains a tensor component that has been neglected until now. In analogy with the smearing of the contact interaction of the spin-spin component (the δ-functions in eq. (2.6-9)), we use the same type of regularization for the tensor component, i.e. corresponding to a Pauli–Villars regularization:

$$V_\gamma^T(r_{ij}) = \frac{g_\gamma^2}{4\pi}\frac{1}{12 m_i m_j}\left\{\mu_\gamma^2\left[\frac{3}{(\mu_\gamma r_{ij})^2}+\frac{3}{\mu_\gamma r_{ij}}+1\right]\frac{e^{-\mu_\gamma r_{ij}}}{r_{ij}}\right.$$

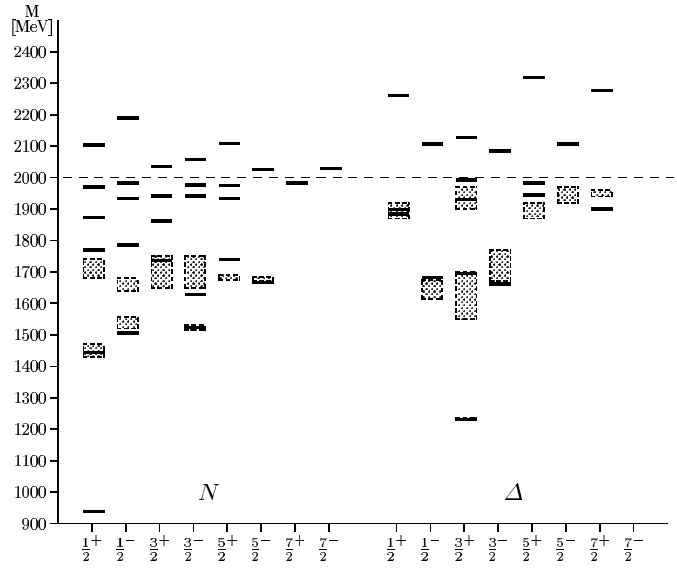

Figure 2.9: Spectrum of the chiral potential model including tensor force.

$$-\Lambda_\gamma^2 \left[\frac{3}{(\Lambda_\gamma r_{ij})^2} + \frac{3}{\Lambda_\gamma r_{ij}} + 1 \right] \frac{e^{-\Lambda_\gamma r_{ij}}}{r_{ij}} \Bigg\}, \qquad \text{(2.6-20)}$$

where $\gamma = \pi, K, \eta, \eta'$. Note that with this type of regularization, the r^{-3} singularity at the origin is reduced to r^{-1}.

The parameter set that has been determined in ref. [122] by a fit to the phenomenological spectrum is given in table 2.6, leading to the spectrum displayed in fig. 2.9.

Table 2.6: Numerical values of free parameters in the GBE SR model including tensor force.

$C = 2.15$ fm^{-2}	$g_8^2/4\pi = 0.67$	$(g_0/g_8)^2 = 1.0$
$\Lambda_0 = 2.3$ fm^{-1}	$\kappa = 0.78$	$V_0 = -349$ MeV

It can be seen that the description of the spectra is of the same quality as for the GBE models without tensor force. In particular, the Roper resonance is still the lightest excitation of the nucleon, so the right parity ordering is preserved. The Δ_{1600} lies only slightly above the negative-parity doublet $\Delta_{1620} - \Delta_{1700}$, a feature that may be explained again by the arguments drawn from and discussed after eq. (2.6-1) together with the strong confinement.

We note here the presence of one experimental state that is obviously missed by any constituent quark model (compare also fig. 2.5 for predictions of the OGE): the $D_{35}(1930)$ ($\Delta^{\frac{5}{2}-}$) is overestimated by ~ 200 MeV, as pointed out in ref. [82]. In any constituent quark model, the first state with the corresponding quantum numbers comes in the $N = 3$ band in a harmonic oscillator basis, so it is clear that its mass will lie about $\hbar\omega$ above the surrounding positive-parity states in the $N = 2$ band.

The most important feature of the tensor interaction is the fact that states that belong to one $L - S$ multiplet are not degenerate anymore, and that there is configuration mixing between states with the same total angular momentum J that belong to different $L - S$ multiplets. From table 2.7 we see that the $N_{1535} - N_{1650}$ states get mixed by about 15% (the sign of this mixing remains undetermined from these numbers) and the $N_{1520} - N_{1700}$ states by about 10%. All the rest of the observed resonances is effected only on the % level by the tensor interaction[1]. The Δ wave functions as a whole remain rather

[1]I am grateful to R.F. Wagenbrunn for providing the data of tables 2.7 and 2.8.

Table 2.7: Symmetry components of N^* wave functions from the GBE SR potential with tensor component. Only those states are given whose masses lie below 2 GeV (see fig. 2.9), except for the 6$^{\text{th}}$ P_{11} resonance $[N^{\frac{1}{2}^+}]_6$, which will be discussed later on.

			$S=1/2$					$S=3/2$				
$[N^{J^\pi}]_n$	Mass [MeV]	N^*	L=0	L=1	L=2	L=3	L=4	L=0	L=1	L=2	L=3	L=4
$[N^{\frac{1}{2}^+}]_1$	939	N_{939}	98.7							1.3		
$[N^{\frac{1}{2}^+}]_2$	1443	N_{1440}	98.9							1.1		
$[N^{\frac{1}{2}^+}]_3$	1770	N_{1710}	96.9							3.1		
$[N^{\frac{1}{2}^+}]_4$	1874		98.5	0.1						1.4		
$[N^{\frac{1}{2}^+}]_5$	1970		2.9	43.3					0.1	53.7		
$[N^{\frac{1}{2}^+}]_6$	2104	N_{2100}	1.8	54.7					0.8	42.7		
$[N^{\frac{1}{2}^-}]_1$	1506	N_{1535}		87.0					13.0			
$[N^{\frac{1}{2}^-}]_2$	1786	N_{1650}		14.7					85.3			
$[N^{\frac{1}{2}^-}]_3$	1933			87.3					12.7			
$[N^{\frac{1}{2}^-}]_4$	1982			97.8					2.2			
$[N^{\frac{3}{2}^+}]_1$	1737	N_{1720}			97.3			1.1		1.6		
$[N^{\frac{3}{2}^+}]_2$	1862				4.4			82.3		13.3		
$[N^{\frac{3}{2}^+}]_3$	1941				74.3			0.2		25.5		
$[N^{\frac{3}{2}^-}]_1$	1523	N_{1520}		89.1					9.8		1.1	
$[N^{\frac{3}{2}^-}]_2$	1629	N_{1700}		9.6					89.9		0.5	
$[N^{\frac{3}{2}^-}]_3$	1941			94.2					4.9		0.9	
$[N^{\frac{3}{2}^-}]_4$	1977			95.0					4.1		0.9	
$[N^{\frac{5}{2}^+}]_1$	1739	N_{1680}			99.1					0.5		0.4
$[N^{\frac{5}{2}^+}]_2$	1934				51.3					48.0		0.7
$[N^{\frac{5}{2}^+}]_3$	1975				48.8					50.3		0.9
$[N^{\frac{5}{2}^-}]_1$	1667	N_{1675}				3.6			95.7		0.7	
$[N^{\frac{7}{2}^+}]_1$	1982						1.3			97.1		1.6

unmixed, as shown in table 2.8, even though the Δ_{1232} receives a relatively large component of $\sim 3\%$ in the $L=2, S=\frac{3}{2}$ channel.

While the lowest negative-parity excitations of both the nucleon and the Δ (the $N_{1520}-N_{1535}$ and the $\Delta_{1620}-\Delta_{1700}$) remain almost unsplit by the tensor interaction, the effect goes in the wrong direction in both cases. There is however a strong effect in the $L-S$ triplet $N_{1650}-N_{1675}-N_{1700}$. In particular, the N_{1650} lies much too high, and the relative ordering of these states is not correct either. While this large splitting was shown to be avoided by the inclusion of vector-meson exchanges [104,105], the influence on wave functions by this component is not clear.

The most important effect regarding configuration mixing is probably the one between the N_{1535} and the N_{1650}. Both of them are S_{11} waves in the pion-nucleon system, but the former has the particularity of decaying most strongly into $N\eta$, rather than into $N\pi$, despite its phase space suppression. By writing the two mass eigenstates N_{1535} and N_{1650} as mixtures of states with spin 1/2 and spin 3/2, parameterized by a mixing angle θ_1,

$$\begin{bmatrix} N_{1535} \\ N_{1650} \end{bmatrix} = \begin{bmatrix} \cos\theta_1 & \sin\theta_1 \\ -\sin\theta_1 & \cos\theta_1 \end{bmatrix} \begin{bmatrix} N_{11} \\ N_{31} \end{bmatrix}. \tag{2.6-21}$$

Isgur and Karl, in their model, succeeded in making the parameter free prediction that $\theta_1 = \arctan(\frac{\sqrt{5}-1}{2}) \simeq -32^\circ$, a value that is allegedly consistent with phenomenology (it is not discussed which model assumptions go into the determination of these parameters). Note that, contrary to the GBE,

Table 2.8: Symmetry components of Δ^* wave functions from the GBE SR potential with tensor component. Only those states are given whose masses lie below 2 GeV (see fig. 2.9).

			$S=1/2$					$S=3/2$				
$[\Delta^{J^\pi}]_n$	Mass [MeV]	Δ^*	L=0	L=1	L=2	L=3	L=4	L=0	L=1	L=2	L=3	L=4
$[\Delta^{\frac{1}{2}^+}]_1$	1889	Δ_{1910}	97.8							2.2		
$[\Delta^{\frac{1}{2}^+}]_2$	1894		0.7							99.3		
$[\Delta^{\frac{1}{2}^-}]_1$	1682	Δ_{1620}		99.1					0.9			
$[\Delta^{\frac{3}{2}^+}]_1$	1232	Δ_{1232}			1.6			95.7		2.7		
$[\Delta^{\frac{3}{2}^+}]_2$	1695	Δ_{1600}			1.4			96.0		2.6		
$[\Delta^{\frac{3}{2}^+}]_3$	1931	Δ_{1920}			6.3			1.5		92.2		
$[\Delta^{\frac{3}{2}^+}]_4$	1991				92.4			0.6		7.0		
$[\Delta^{\frac{3}{2}^-}]_1$	1662	Δ_{1700}		97.7					0.1		2.2	
$[\Delta^{\frac{5}{2}^+}]_1$	1945	Δ_{1905}			3.0					96.5		0.5
$[\Delta^{\frac{5}{2}^+}]_2$	1982				96.4					2.9		0.7

in the model of Godfrey and Isgur, the N_{1650} lies much lower than its LS partners, see fig. 2.5, which confirms a mixing angle of different sign as compared to the GBE case. This was one of the arguments used recently by Isgur to criticize the GBE model in general [123], claiming that in this model the wrong size of the mixing angle is predicted. Stating that the internal structure of the baryon wave functions is wrong, he concluded that the GBE is in principle not able to describe the decay properties of the N_{1535} and the N_{1650} resonances.

This issue will be taken up again in the next chapter, where strong decays of baryon resonances will be studied. Let us note for the moment that Glozman, in his reply to Isgur's critique [124] argues that in addition to the tensor force of the π exchange, there should be a tensor component stemming from the ρ exchange, once the vector-meson exchange is taken into account in the GBE interaction. Both of these exchanges supply a spin-spin force with the same sign, while the tensor components have the opposite sign, and will tend to cancel each other. It has been shown that the two-pion exchange interaction (which is often parameterized by ρ exchange in analogy with the NN interaction) is stronger and of opposite sign than that the one-pion exchange [117].

Furthermore, it turned out that the inclusion of vector-meson exchange in the interaction [104, 105] also tends to cancel the large effect in the mass splitting of the $N_{1650} - N_{1675} - N_{1700}$ multiplet [125].

2.6.5 Problems and Open Questions

General discussions about theoretical foundations and phenomenological implications of the GBE interaction may be found in refs. [126–128], in particular the question about the parity restoration phase has been discussed in ref. [41]. Isgur has recently compiled a list of what he regards to be the most serious arguments against the validity of the Goldstone-boson exchange models [123], which has provoked an immediate rejection [124].

One of the drawbacks of the GBE models is the fact that mesons cannot be described in a satisfactory manner in this framework. Even though the overall description of spectra is quite correct, the low pion mass is completely missed [129, 130]. On the one hand, this may not be a complete disaster (as claimed in ref. [123]), since describing the interaction between quarks and anti-quarks, which are bound to give a pseudo-scalar meson, by the exchange of pseudo-scalar mesons, represents a conceptual paradox (resembling the old bootstrap ideas) that would at least lead to a double counting problem. On the other hand, it is certainly a pity that the unified description of mesons and baryons, one of the strong points of the OGE, is lost in this model.

Another serious point raised by Isgur is the claim that the spin-orbit problem has not been solved

by the GBE model. Indeed, as mentioned earlier, the GBE interaction to lowest order does not provide any spin-orbit forces, contrary to the OGE models. Since spin-orbit forces seem to be absent from the phenomenological spectra, this was put forward as a supporting argument in favor of the GBE model. However, as pointed out by Isgur, the zeroth order confining potential will produce very strong spin-orbit forces through Thomas precession, a purely kinematical effect. The true problem of spin-orbit forces is therefore to arrange a sufficiently precise cancellation between dynamically generated and kinematical spin-orbit forces. This was the fundamental assumption in the IK-model but in the GBE model, the absence of the spin-orbit forces from the Goldstone-boson exchange dynamics would lead to inverted spin-orbit multiplets with splittings of hundreds of MeV.

The counter-argument, apart from the fact that there will also arise spin-orbit forces in the GBE from vector- and scalar-meson exchanges, is based on the qualitative observation that the Thomas precession should be suppressed for light-quark systems. The conclusion, that it is incorrect to identify the linear confining interaction between two heavy, static sources, which is indeed established, with the effective confining interaction between quasi-particles in the light-quark systems, keeps a hand-waving character, however.

The GBE model has also been applied to the NN interaction [131–133], and multi-quark systems, such as tetra-quark [134], penta-quark [135, 136], and hexa-quark [137] systems, see ref. [138] for an overview. The question about the 'H'-particle (i.e. a di-baryon of $uuddss$ structure with $J^\pi = 0^+$, $I = 0$) has been discussed in [139], where it was pointed out that the the GBE leads to different predictions as to its existence than models based on OGE. Magnetic moments of the nucleon have been studied in refs. [140, 141] and electromagnetic form factors in refs. [142] and [143]. The latter reference presented results obtained in the so-called point form of relativistic quantum mechanics and provides an almost perfect prediction of electromagnetic form factors of the proton and the neutron. However, the fact that important physical ingredients were left out in this calculation have led people to doubt the relevance of these results and a detailed examination of the point form approach for calculating form factors has indeed led to the conclusion that results presented in ref. [143] may be misleading. This will be discussed in more detail in a later section.

The question of the 'correct' dynamics to describe baryon spectra has also led to the issue of accurately solving the few-body (in this context in particular the three-body) problem. The standard tools in this area are expansions in harmonic oscillator functions (as employed in refs. [75, 80]) or hyperspherical harmonics [86], direct solutions of Faddeev-equations (see ref. [144], recently this method was also adapted to deal with semi-relativistic kinetic-energy operators, see ref. [145]) or numerical integrations using Monte-Carlo methods [146]. The stochastic variational method (SVM, see App. B) employed in this work seems to be superior as regarding the numerical accuracy as well as the handiness of the obtained wave functions (see ref. [147] for a recent application). The discussion about the proper solution of the Schrödinger equation has also led to some nasty argumentations [148–150] that, if any, had only the effect of hiding the physics issues and confusing the conclusions.

We have introduced and discussed in this chapter different kind of dynamical models to describe the spectroscopic properties of non-strange baryon resonances. The next step is to test the wave functions stemming from different models in order to gain further insight into the 'true' nature of the underlying quark-quark dynamics.

Chapter 3

Strong Decays of Baryon Resonances

I have no data yet. It is a capital mistake to theorize before one has data.
Insensibly one begins to twist facts to suit theories instead of theories to suit facts.

Sherlock Holmes

This chapter will be devoted to testing the different constituent quark models discussed previously by their predictions of strong decay widths of baryon resonances. Again, there will be a general outline of basic results first, before we introduce some specific approaches to model the decay process. Numerical results will then be presented and discussed. In particular, it will be argued, that it is not the wave functions stemming from a constituent quark model, that are mainly responsible for the gross decay properties, but rather the symmetry structure of the resonances and the decay operator. This sets some limitations on the prospect of discriminating different constituent quark models by their predictions of dynamical properties.

3.1 General Theoretical Results

The theoretical treatment of strong decays is much less developed than the one for electromagnetic or weak decay processes, mainly since the emitted meson is not an elementary field quantum, but, by itself, made up of constituent particles. The explicit form of the decay operator is not definitely known and several alternative forms have been suggested, mainly based on simple symmetry arguments and general requirements, such as covariance and compositeness of the emitted meson.

Hadronic decay widths are typically of a magnitude of ~ 100 MeV (except in a few cases when only a very small phase space is available). Thus Γ/M is of the order of 10%, rather than of the order of 1% or less, as for most weak and electromagnetic decay processes. Consequently, the strong-decay widths cannot be calculated perturbatively and one has to rely on effective models.

Starting from the old $\vec{\sigma} \cdot \vec{k}$ coupling [25], one has derived more refined treatments, such as including the recoil term $\vec{\sigma} \cdot \vec{p}$ [26], or the - to some extend equivalent - Feynman-Kislinger-Ravndal model [151]. In general, one faces the problem of reducing a relativistic description to a non-relativistic one, with the aim to describe the emission process in terms of effective operators between non-relativistic wave functions.

We shall recall first some general theoretical results that are relevant for the study of decay processes before we introduce and discuss the two most popular models to describe hadronic transitions: the elementary emission model and the $^3P_0$ quark-pair creation model.

3.1.1 Kinematics

From perturbation theory we know, that we can calculate the S-matrix quite generally in terms of the Hamiltonian of the system by

$$S = T \exp\left\{-i \int dt H(t)\right\}. \tag{3.1-1}$$

Here T denotes the time ordering symbol and the exponential is defined by its power series expansion. To lowest order in perturbation theory we can forget the time ordering and write

$$S = 1 - i \int dt H(t) = 1 - 2\pi i\, \delta(E_i - E_f) \int d^3x\, \mathcal{H}(\vec{x}), \tag{3.1-2}$$

where in the last step we have assumed that the time dependence of the Hamiltonian is just a simple exponential.

The matrix elements for a scattering or decay process are written in terms of the scattering reaction matrix $-i\mathcal{T}$ which is related to the S-matrix by

$$\langle f|S-1|i\rangle = -i(2\pi)^4 \delta^4(P_i - P_f)\mathcal{T}. \tag{3.1-3}$$

We use a (non-covariant) state normalization

$$\langle p \mid p'\rangle = (2\pi)^3 \delta^3(\vec{p} - \vec{p}\,') \tag{3.1-4}$$

for bosons and for fermions. In the latter case one has to include a Kronecker delta for the spin indices in eq. (3.1-4). The partial decay rate of a particle of mass M^* decaying into n bodies in its rest frame is then given by:

$$d\Gamma = (2\pi)^4 \prod_{i=1}^{n} (2E_i) \mid \mathcal{T} \mid^2 d\Phi_n(P, p_1, ...p_n), \tag{3.1-5}$$

where $d\Phi_n$ is an element of the n-body phase space, which is a Lorentz invariant quantity:

$$d\Phi_n(P, p_1, ..., p_n) = \delta^4(P - \sum_{i=1}^{n} p_i) \prod_{i=1}^{n} \frac{d^3p_i}{(2\pi)^3 2E_i}. \tag{3.1-6}$$

We are just interested in decays with two bodies in the final state. Let us therefore calculate $d\Phi_2$. In the final formula for the decay width, we have to integrate over those final momenta in eq. (3.1-5) that are not observed. We can therefore cancel in our calculation integration variables with corresponding delta functions, if we remember the kinematical constraints that are imposed by these operations.

$$\begin{aligned} d\Phi_2(P, p_1, p_2) &= \delta^4(P - p_1 - p_2) \frac{d^3p_1}{(2\pi)^3 2E_1} \frac{d^3p_2}{(2\pi)^3 2E_2} \\ &= \delta(M^* - E_1 - E_2)\delta^3(\vec{p}_1 + \vec{p}_2) \frac{d^3p_1}{(2\pi)^3 2E_1} \frac{d^3p_2}{(2\pi)^3 2E_2} \\ &= \delta(M^* - E_1 - E_2) \frac{1}{(2\pi)^3 2E_2} \frac{d^3p_1}{(2\pi)^3 2E_1}. \end{aligned} \tag{3.1-7}$$

Here we have assumed that we work in the rest frame of the decaying resonance, so that $P = (M^*, \vec{0})$, and by virtue of the delta function we have $|\vec{p}_1| = |\vec{p}_2|$. Writing short just $\vec{q}$ for the remaining momentum integration variable, we change from Cartesian to spherical coordinates by writing $d^3q = q^2 dq\, d\Omega$, where $d\Omega$ is the solid angle of particle 1. In order to proceed we make a change of variable by setting $E = E_1 + E_2$. Observing that $qdq = (E_1 E_2)/E\, dE$, the phase space element simplifies to

$$d\Phi_2(P, p_1, p_2) = \delta(M^* - E) \frac{1}{4(2\pi)^6} \frac{q}{E} dE d\Omega = \frac{1}{4(2\pi)^6} \frac{q}{M^*} d\Omega. \tag{3.1-8}$$

With this result, the partial decay width of eq. (3.1-5) for a decay with two particles in the final state is reduced to

$$d\Gamma = \frac{1}{4\pi^2} \frac{q\, E\, \omega}{M^*} \mid \mathcal{T} \mid^2 d\Omega. \tag{3.1-9}$$

Here the quantities E and ω are the energies of the particles in the final state, q the magnitude of their momentum, and M^* the mass of the decaying particle. If the latter one is unpolarized or spin-less, the matrix element is isotropic and we can also integrate over the solid angle in eq. (3.1-9). To obtain the total decay width, we finally have to sum over all final and average over all initial spin-isospin channels and polarization states. We then end up with

$$\Gamma = \frac{1}{\pi} \frac{q\, E\, \omega}{M^*} \mid \mathcal{T} \mid^2. \tag{3.1-10}$$

For clarity we have not included in eq. (3.1-10) the sum over final and the average over initial spins and isospins. This has to be done additionally, if the emitted meson carries isospin (like for decays into pions, for instance).

Let us collect the kinematical constraints imposed by the above phase space calculation. We see that in every decay process with two particles in the final state, all kinematic magnitudes are fixed by the masses of the involved particles. For a process $B^* \to BM$, where B^* is a baryon resonance with mass M^*, B a baryon with mass M and M a meson with mass μ, the following relations hold:

$$q = \frac{\sqrt{\left(M^{*2} - (M+\mu)^2\right)\left(M^{*2} - (M-\mu)^2\right)}}{2M^*}, \tag{3.1-11}$$

$$\omega = \frac{M^{*2} - M^2 + \mu^2}{2M^*}, \tag{3.1-12}$$

$$E = \frac{M^{*2} + M^2 - \mu^2}{2M^*}, \tag{3.1-13}$$

where E and ω are the energies of the final state baryon and meson, respectively.

We shall briefly discuss the question of "proper" phase space to be used in practical calculations of decay widths, because this is an issue that has frequently been raised in the literature [152, 153]. The fully relativistic phase space for a process $A \to BC$, as applied in eq. (3.1-10), is often referred to as a 'semi-relativistic' choice:

$$\Phi(ABC) = 2\pi \frac{E_B(q) E_C(q)}{M_A} q, \tag{3.1-14}$$

because it is usually employed together with a matrix element calculated in a non-relativistic, or semi-relativistic framework. In the former case, a completely non-relativistic phase space would be the most appropriate choice:

$$\Phi(ABC) = 2\pi \frac{M_B M_C}{M_A} q. \tag{3.1-15}$$

A third choice that deserves to be discussed in more detail is the one by Kokoski and Isgur [154], whose essence basically lies in replacing all the energy factors in eq. (3.1-14) by "effective" constants:

$$\Phi(ABC) = 2\pi \frac{\tilde{M}_B \tilde{M}_C}{\tilde{M}_A} q. \tag{3.1-16}$$

This prescription is claimed to be valid in the weak binding limit where the pion and the ρ are degenerate. The phase space of eq. (3.1-16) was also used by Capstick and Roberts in their calculation of decay widths of baryon resonances [80, 155], see ref. [79] for a recent overview. For the numerical values of effective masses in eq. (3.1-16) for a decay process $R \to N\pi$ they take $\tilde{M}_N = 1.1$ GeV, $\tilde{M}_\pi = 0.72$ GeV and $\tilde{M}_R = M_R$. We note the crudest approximation in this prescription: the pion effectively obtains a mass 5.2 times larger than its physical value! The implications of this prescription will be further discussed when we present our results.

3.1.2 Formalism

It is most convenient to work in the language of second quantization. Thus, baryonic and mesonic states with total momentum $\vec{P}$, respectively, are written as

$$|B\rangle = \frac{1}{\sqrt{6}} \frac{\epsilon_{ijk}}{\sqrt{6}} \int d\vec{p}_1 \, d\vec{p}_2 \, d\vec{p}_3 \; \psi^{\vec{P}}_{i_1 i_2 i_3}(\vec{p}_1, \vec{p}_2, \vec{p}_3) b^\dagger_{i,i_1}(\vec{p}_1) \, b^\dagger_{j,i_2}(\vec{p}_2) b^\dagger_{k,i_3}(\vec{p}_3) \, |0\rangle \tag{3.1-17}$$

$$|M\rangle = \frac{\delta_{ij}}{\sqrt{3}} \int d\vec{p}_1 \, d\vec{p}_2 \; \psi^{\vec{P}}_{i_1 i_2}(\vec{p}_1, \vec{p}_2) b^\dagger_{i,i_1}(\vec{p}_1) \, d^\dagger_{j,i_2}(\vec{p}_2) \, |0\rangle \tag{3.1-18}$$

where we have separated out the color wave function explicitly and the indices i_1, i_2, i_3 denote discrete quantum numbers of the quarks, like spin, isospin, etc.

The operators $b_i^\dagger$ and $d_j^\dagger$ create a quark or antiquark with quantum numbers i or j, respectively. These creation operators together with their corresponding destruction operators b_i, d_j obey the canonical anti-commutation rules

$$\begin{aligned}\{b_i, b_j\} = \ \{b_i^\dagger, b_j^\dagger\} = \{b_i^\dagger, d_j^\dagger\} = \{d_i, d_j\} = \ \{d_i^\dagger, d_j^\dagger\} = \{b_i, d_j\} = 0 \\ \{b_i(\vec{p}_i), b_j^\dagger(\vec{p}_j)\} = \{d_i(\vec{p}_i), d_j^\dagger(\vec{p}_j)\} = \delta_{ij}\ \delta(\vec{p}_i - \vec{p}_j).\end{aligned} \tag{3.1-19}$$

Finally, the state $|0\rangle$ is the vacuum state, defined by $b_i\,|0\rangle = d_i\,|0\rangle = 0, \forall i$.

The states (3.1-17) and (3.1-18) are properly normalized according to eq. (3.1-4) if we assume that the internal wave functions ψ, which include spin, flavor and spatial wave functions, fulfil

$$\int d\vec{p}_1\ d\vec{p}_2\ d\vec{p}_3 \psi^{\vec{P}}_{i_1 i_2 i_3}(\vec{p}_1, \vec{p}_2, \vec{p}_3)^* \psi^{\vec{P}'}_{i_1 i_2 i_3}(\vec{p}_1, \vec{p}_2, \vec{p}_3) = (2\pi)^3\, \delta(\vec{P} - \vec{P}') \tag{3.1-20}$$

for baryons and

$$\int d\vec{p}_1\ d\vec{p}_2\ \psi^{\vec{P}}_{i_1 i_2}(\vec{p}_1, \vec{p}_2)^* \psi^{\vec{P}'}_{i_1 i_2}(\vec{p}_1, \vec{p}_2) = (2\pi)^3 \delta(\vec{P} - \vec{P}') \tag{3.1-21}$$

for mesons. When we shall deal with quark-pair creation models, we will also have to consider two-particle final states, where both particles are expressed in terms of their constituent quark fields. These states will need further anti-symmetrization in identical particles, and have to be normalized separately. We write such a state (we shall only consider one baryon - one meson final states) as

$$\begin{aligned}|\, BM\rangle \ &= \ \frac{\mathcal{N}_{BM}}{\sqrt{6}} \frac{\epsilon_{ijk}}{\sqrt{6}} \frac{\delta_{lm}}{\sqrt{3}} \int \prod_{i=1}^{5} d\vec{p}_i \\ &\psi_B(\vec{p}_1, \vec{p}_2, \vec{p}_3) \psi_M(\vec{p}_4, \vec{p}_5) b_i^\dagger(\vec{p}_1)\, b_j^\dagger(\vec{p}_2) b_k^\dagger(\vec{p}_3)\, b_l^\dagger(\vec{p}_4)\, d_m^\dagger(\vec{p}_5)\, |0\rangle\,.\end{aligned} \tag{3.1-22}$$

Calculating the norm of this state we find

$$\begin{aligned}\langle BM \mid B'M'\rangle \ &= \ \mathcal{N}_{BM}^2 \Big\{ (2\pi)^6 - \int \prod_{i=1}^{5} d\vec{p}_i \\ &\psi_B^*(\vec{p}_1, \vec{p}_2, \vec{p}_3)\, \psi_{B'}(\vec{p}_4, \vec{p}_2, \vec{p}_3) \psi_M^*(\vec{p}_4, \vec{p}_5)\, \psi_{M'}(\vec{p}_1, \vec{p}_5) \Big\},\end{aligned} \tag{3.1-23}$$

where the first factor comes from the direct overlap of eqs. (3.1-20) and (3.1-21). The second integral is hard to calculate. We assume however that the normalization takes place after free evolution of the final states, i.e. when they are asymptotically far away from each other. In this limit the integral of eq. (3.1-23) will vanish because the baryon B and the Meson M are traveling away from each other. We can therefore set $\mathcal{N}_{BM}^2 = 1$ in order to satisfy eq. (3.1-4).

3.1.3 Quasi Two-Body Decays

In our previous treatment of two-body decays $A \to BC$, the decay widths were obtained from the amplitudes by using

$$\Gamma = \frac{1}{\pi} \int dq q^2 \mid \mathcal{T}(q) \mid^2 \delta(M_a - E_b(q) - E_c(q)), \tag{3.1-24}$$

where q is the momentum of the daughter hadrons in the rest frame of the decaying particle, and $\mathcal{T}(k)$ is the transition amplitude calculated within a certain decay model. This eventually led us to eq. (3.1-10) for the final formula of the decay width.

We now turn our attention to the quasi-two-body decays of baryons, i.e., the decays of the type $A \to BM_1$, with the subsequent decay of the daughter baryon $B \to CM_2$, see fig. 3.1. One could use the prescription described above which would amount to a narrow-width treatment of both daughter hadrons. This may however be inaccurate in some circumstances, especially for states that lie close to a threshold.

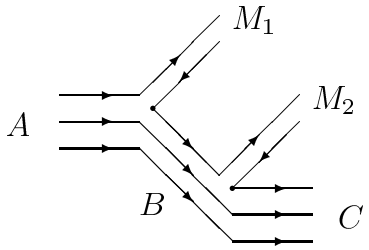

Figure 3.1: Feynman diagram for quasi-2-body decays.

Capstick and Roberts [80, 155] therefore suggested to take the finite width of the daughter hadron into account by replacing the Dirac δ-function in eq. (3.1-24). They regard the δ-function as arising from the narrow-width limit of the energy denominator

$$\frac{1}{M_a - E_b - \omega_1 - i\epsilon} = \frac{\mathcal{P}}{M_a - E_b - \omega_1} + i\pi\delta(M_a - E_b - \omega_1), \tag{3.1-25}$$

where M_a is the mass of the decaying baryon A, E_b the energy of the final-state baryon B, which is itself unstable, and ω_1 is the energy of meson M_1. Furthermore, $\mathcal{P}$ means principal part and ϵ is related to the total width of the unstable final state. For daughter hadrons that are broad, the energy denominator can be written as

$$\frac{1}{M_a - E_b - \omega_1 - i\frac{\Gamma_b}{2}} = \frac{M_a - E_b - \omega_1 + i\frac{\Gamma_b}{2}}{(M_a - E_b - \omega_1)^2 + \frac{\Gamma_b^2}{4}}, \tag{3.1-26}$$

suggesting the replacement

$$\delta(M_a - E_b - \omega_1) \rightarrow \frac{\frac{\Gamma_b}{2}}{\pi(M_a - E_b - \omega_1)^2 + \frac{\Gamma_b^2}{4}}. \tag{3.1-27}$$

The decay rate for $A \rightarrow (CM_2)_B M_1$ therefore generalizes to

$$\Gamma = \frac{1}{\pi}\int_0^{q_{max}} dq \frac{q^2 \mid \mathcal{T}(q) \mid^2 \Gamma_b(q)}{(M_a - E_b - \omega_1)^2 + \frac{\Gamma_b^2}{4}}. \tag{3.1-28}$$

The momentum integration in eq. (3.1-28) is limited by kinematic constraints, and the maximum value q_{max} is given by (compare eq. (3.1-11)):

$$q_{max} = \frac{\sqrt{(M_a^2 - (\mu_1 + \mu_2 + M_c)^2)(M_a^2 - (\mu_1 + \mu_2 - M_c)^2)}}{2M_a}, \tag{3.1-29}$$

where μ_1 and μ_2 are the masses of the final state mesons. The value of eq. (3.1-29) corresponds to the situation where the two emitted mesons have the same vector velocity in the rest frame of the decaying particle and are thus moving anti-parallel to the final state baryon. In addition, since the mass of the final state baryon is in general larger than the mass of any meson considered here, we have the relation $\mid \vec{p} \mid_{max} > \mid \vec{q}_1 \mid_{max}, \mid \vec{q}_2 \mid_{max}$, where $\vec{p}$, $\vec{q}_1$ and $\vec{q}_2$ are the momenta of the final state baryon and mesons, respectively.

The prescription of eq. (3.1-28) can be compared to the one given by Cutkosky et. al [156], which was used by Stassart and Stancu in their calculations of $N\rho$ [157], $N\omega$ [158] and $\Delta\pi$ [159] decays of baryon resonances. Its essence lies in the inclusion of a relativistic Breit-Wigner mass distribution σ and in integrating over the mass of the broad resonance. For instance, for a process $R \rightarrow N\rho$, the width is

$$\Gamma = \int_{4m_\pi^2}^{(M_R - M_N)^2} \sigma(m_\rho^2)\Gamma_{R\rightarrow N\rho}(m_\rho^2) dm_\rho^2. \tag{3.1-30}$$

In ref. [155] it was claimed that this prescription gives qualitative similar results as the one of eq. (3.1-28).

Two theoretical shortcomings have to be mentioned when applying eq. (3.1-28):

- The quantity $\Gamma_b(q)$ is the partial width of the resonance in the intermediate state. This one is usually calculated in its own rest-frame, but in eq. (3.1-28) it is needed in a moving frame. The appropriate boost that should be performed, is neglected in refs. [80, 155].
- The quantity q in $\Gamma_b(q)$ is the momentum of the resonance in the intermediate state. However, in refs. [80, 155], $\Gamma_b(q)$ was obtained by applying the usual rules for a one-body decay, where q is the momentum of the final state hadrons.

In view of these difficulties, we chose to investigate only decay modes with narrow resonances in the final state. It must be kept in mind, however, that the problem of two-body decays is an important one, especially if one intends to investigate higher lying resonances. Here, decay modes like $N^* \to N\pi\pi$ become dominant and it is an essential requirement to enable reliable predictions on decay channels, in particular in view of the problem of missing states.

3.2 The Elementary Emission Model

The elementary emission model (EEM) follows quite the simplest approach to strong interaction transitions. The decay takes place through the emission of a point-like meson by one of the quarks of the baryon (see fig. 3.2). The baryons are therefore considered as composite objects, whereas the meson is treated as a point-like particle that couples to the quark current. As a consequence, the interaction potential between quarks intervenes only through the baryon wave functions in the initial and final states. The asymmetric treatment of final state hadrons leads to some conceptual problems if the model is applied to decays with two identical particles in the final state, like the decay $\rho \to \pi\pi$, where one of the pions is treated as point-like while the other as being composite. This problem does not arise if we consider decays of baryon resonances, however, as we shall see, the basic model assumption of a point-like meson naturally implies the general limitations of the model.

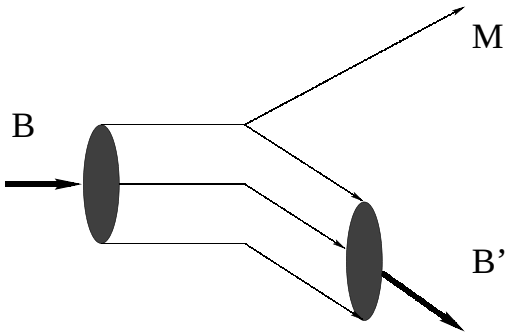

Figure 3.2: Decay of a baryon B by the emission of a point-like meson M.

Historically, pioneered by the work of Faiman and Hendry [20, 21], the EEM was the first one to be applied for the calculation of strong decay processes [160, 161] (see ref. [162] for an early review), and in fact, the main motivation came from its simplicity.

It has been used by Koniuk and Isgur [75] for predicting a huge and impressive amount of strong end electromagnetic decay processes; other works that used the EEM in one form or the other include the one by Forsyth and Cutkosky [163], Bijker et al. [164] and Sartor and Stancu [165]. It was applied to wave functions from the BCN model to compare predictions with special forms of quark-pair creation models [86, 166], that will be discussed in a later section.

3.2.1 Derivation of the Decay Operator

The matrix element for the process $B \to B' + M$ takes the general form $\langle B'M|H|B\rangle$. Let us denote by $\vec{\Phi}(\vec{x})$ the (elementary) meson field, which in the language of second quantization takes the form

$$\vec{\Phi}(\vec{x}) = \int d\vec{q} \frac{1}{\sqrt{2\omega}} \left[\vec{a}(\vec{q}) e^{i\vec{q}\cdot\vec{x}} + \vec{a}^{\,\dagger}(\vec{q}) e^{-i\vec{q}\cdot\vec{x}}\right], \tag{3.2-1}$$

where $\vec{a}(\vec{q})$ and $\vec{a}^{\,\dagger}(\vec{q})$ are the creation and annihilation operators of a meson with three-momentum $\vec{q}$, and the vector indicates possible isospin components. We also express the quark current in terms of elementary quark fields:

$$\vec{j}(\vec{x}) = \bar{q}(\vec{x})\,\vec{\Gamma}\,q(\vec{x}), \tag{3.2-2}$$

where the explicit form of $\vec{\Gamma}$ depends on the quark-quark-meson coupling applied in the calculation. We shall adopt here the axial-vector coupling Lagrangian:

$$\mathcal{L}_{int} \sim ig\overline{\Psi}\gamma_\mu\gamma_5\vec{\lambda}^F \cdot \left(\partial_\mu\vec{\Phi}\right)\Psi, \tag{3.2-3}$$

where $\vec{\lambda}^F$ are the Gell-Mann flavor matrices. This choice of interaction Lagrangian differs from the one that was adopted to derive the interaction in the GBE model, see eq. (2.6-5), however, as far as decay processes are concerned, it is to some extend equivalent to the pseudo-scalar Lagrangian, as we shall see later on. At this point, the axial-vector Lagrangian is the better choice because it is more consistent with chiral symmetry (due to the derivative-coupling, any amplitude calculated from (3.2-3) will automatically tend to zero for vanishing four-momentum of the meson). We have to take matrix elements of the Hamiltonian H, but since this Lagrangian contains the derivative of the meson fields, we can not immediately set $H = -L$. It can be shown however [33], that L differs from $-H$ only by a four Fermi contact term, which is quadratic in the coupling constant. Since terms of this order will be neglected anyway in a systematic non-relativistic expansion, we can still set

$$H_{QQM} = \frac{g_{QQM}}{2m} \int d\vec{x} : \bar{q}(\vec{x})\gamma^\mu\gamma_5 q(\vec{x})\vec{\lambda}^F \cdot \left(\partial_\mu\vec{\Phi}(\vec{x})\right) :, \tag{3.2-4}$$

where : : is the normal ordering symbol and g_{QQM} the coupling constant between constituent quarks and mesons. Expanding also the quark fields

$$q(\vec{x}) = \int d\vec{p}\sqrt{\frac{m}{E}} \sum_s \left[u_s(\vec{p}) b_s(\vec{p}) e^{i\vec{p}\cdot\vec{x}} + v_s(\vec{p}) d_s^\dagger(\vec{p}) e^{-i\vec{p}\cdot\vec{x}}\right], \tag{3.2-5}$$

we can write the elementary quantum-emission component of the Hamiltonian (3.2-4) as

$$\begin{aligned} H_{QQM} \;=\; & (2\pi)^3 \frac{g_{QQM}}{2m} \int d\vec{p}\, d\vec{p}\,'\, d\vec{q}\,' \sum_{s,s'} \\ & \sqrt{\frac{m^2}{E_1 E_2}} \frac{1}{\sqrt{2\omega}} q'_\mu \delta^3(\vec{p} - \vec{p}\,' - \vec{q}\,') \bar{u}_{s'}(\vec{p}\,')\,\gamma^\mu\gamma_5\, u_s(\vec{p})\,\vec{\lambda}^F \cdot \vec{a}^{\,\dagger}(\vec{q}\,')\, b_s(\vec{p})\, b_{s'}^\dagger(\vec{p}\,'). \end{aligned} \tag{3.2-6}$$

Sandwiching this between baryon wave functions in the form of eq. (3.1-17), we have to evaluate the vacuum expectation value of

$$\begin{aligned} & \left\langle 0\middle| a_\alpha(\vec{q}) b_{s'_1}(\vec{p}_1\,') b_{s'_2}(\vec{p}_2\,') b_{s'_3}(\vec{p}_3\,') a^\dagger(\vec{q}\,') b_s(\vec{p}) b_{s'}^\dagger(\vec{p}\,') b_{s_1}^\dagger(\vec{p}_1) b_{s_2}^\dagger(\vec{p}_2) b_{s_3}^\dagger(\vec{p}_3)\middle|0\right\rangle = \\ & \quad 18\,\delta_{\alpha\beta}\,\delta^3(\vec{q} - \vec{q}\,')\,\delta_{s_1,s'_1}\,\delta^3(\vec{p}_1 - \vec{p}_1\,')\,\delta_{s_2,s'_2}\,\delta^3(\vec{p}_2 - \vec{p}_2\,')\,\delta_{s_3,s}\,\delta^3(\vec{p}_3 - \vec{p})\,\delta_{s'_3,s'}\,\delta^3(\vec{p}_3\,' - \vec{p}\,') \end{aligned} \tag{3.2-7}$$

Taking into account the normalization factors for baryons, this is usually written as

$$\langle B'|H|B\rangle = \sum_{i=1}^{3} \langle B'|H(i)|B\rangle = 3\,\langle B'|H(3)|B\rangle, \tag{3.2-8}$$

which is just the first-quantization analogue of the total symmetry of the baryon wave function.

In our case this means, that we just have to take matrix elements of the Hamiltonian eq. (3.2-6) between one quark states in order to obtain the operator that acts directly between baryon wave

functions. One easily finds

$$\langle Q(\vec{p})M(\vec{q})\big|H\big|Q(\vec{p}\,')\rangle = (2\pi)^3 \frac{g_{QQM}}{2m}\sqrt{\frac{m^2}{EE'}}\frac{1}{\sqrt{2\omega}}\vec{\lambda}^F\,\delta^3(\vec{p}-\vec{p}\,'-\vec{q})\bar{u}_{s'}(\vec{p}\,')\,\gamma^\mu\gamma_5\,u_s(\vec{p})\,q_\mu \qquad (3.2\text{-}9)$$

With the usual representations of the γ matrices and Dirac spinors (see App. A.1), one determines

$$\begin{aligned}\bar{u}_{s'}(\vec{p}\,')\,\gamma^\mu\gamma_5\,u_s(\vec{p})\,q_\mu = \\ \sqrt{\frac{E+m}{2m}}\sqrt{\frac{E'+m}{2m}}\left\{\omega\left(\frac{\vec{\sigma}\cdot\vec{p}}{E+m}+\frac{\vec{\sigma}\cdot\vec{p}\,'}{E'+m}\right)-\vec{\sigma}\cdot\vec{q}-\frac{\vec{\sigma}\cdot\vec{p}\,'\,\vec{\sigma}\cdot\vec{q}\,\vec{\sigma}\cdot\vec{p}}{(E'+m)(E+m)}\right\}\simeq \\ \sqrt{1+\frac{\omega}{2m}}\Bigg\{-\left[1+\frac{\omega}{2m}-\frac{1}{4m^2}\frac{\vec{p}^{\,2}}{1+\frac{\omega}{2m}}\right]\vec{\sigma}\cdot\vec{q} \\ +\frac{1}{4m^2}\frac{1}{1+\frac{\omega}{2m}}\left[4m\omega(1+\frac{\omega}{2m})-2\vec{p}\cdot\vec{q}-\mu^2\right]\vec{\sigma}\cdot\vec{p}\Bigg\}\end{aligned} \qquad (3.2\text{-}10)$$

In the last step we have set $E = E' + \omega$ and $E' \simeq m$. Neglecting contributions of order $(p/m)^2$ and $(\omega/m)^2$, as well as the normalization factor, one finds the the well known structure of the elementary emission operator

$$\hat{O} = \frac{g_{QQM}}{2m}\vec{\lambda}^F e^{-i\vec{q}\cdot\vec{r}}\left[\left(1+\frac{\omega}{2m}\right)\vec{\sigma}\cdot\vec{q}\,-\frac{\omega}{m}\vec{\sigma}\cdot\vec{p}\right], \qquad (3.2\text{-}11)$$

where ω and $\vec{q}$ are the energy and the momentum of the outgoing meson, $\vec{r}$, $\vec{p}$ and m the quark coordinate, momentum, and mass, respectively, and $\vec{\sigma}$ the Pauli spin matrices. If the constituent quark - meson coupling constant g_{QQM} is taken in an SU(3) invariant manner, it assumes the same numerical value for π and η decays.

We shall refer to the $\vec{\sigma}\cdot\vec{q}$ term in eq. (3.2-11) as the direct term and to the $\vec{\sigma}\cdot\vec{p}$ term as the recoil term, even though this differs somehow from the conventional notation, since the recoil term is usually proportional to $(\vec{p}-\vec{q})$, i.e. the momentum of the recoiling final-state quark. Also with this convention, the direct term incorporates part of effects of higher order in ω/m.

The operator $\hat{O}$ in the form of eq. (3.2-11) was derived from the axial-vector-coupling Lagrangian of eq. (3.2-3) in lowest order non-relativistic reduction. It differs from the form obtained by a similar reduction of an interaction Lagrangian with pseudo-scalar coupling as in eq. (2.6-5). The latter one does not provide the term proportional to $\vec{p}$ (it only gives the $\vec{\sigma}\cdot\vec{q}$ term). In order to recover this term in the pseudo-scalar coupling case one has to go beyond the lowest order in the non-relativistic reduction. At the order p/m one obtains exactly the second term of eq. (3.2-11) and the results become identical to the case of axial-vector coupling. However, beyond the order p/m a systematic difference appears between the two types of coupling. Though an expansion in p/m appears questionable anyway, in view of the large value this quantity can take, it has become customary to keep only the first-order term of the expansion and to work with the form (3.2-11) of the decay operator. In practice this choice is necessary because the recoil term provides appreciable decay widths for certain resonances that have only a small phase space available [26]. It also has the advantage that one uses a Galilean-invariant form which would not be the case if higher order terms were included. In fact, as it has been noted before [167], one cannot expect a priori that terms of higher relativistic order satisfy Galilean invariance. It is important to realize however that leaving out higher-order relativistic terms may not be justified as they become large in the p/m expansion. This was explicitly studied in ref. [86], and has led the authors to consider an expansion

in p/E rather than p/m [166].

We remark that the form (3.2-11) for the transition operator could also be obtained from a pseudo-scalar Lagrangian if one employs what in nuclear physics is called the angle transformation [168], i.e. transforming the meson-nucleon amplitude from the meson-nucleon to the meson-nucleus CMS. The values of the momenta in eq. (3.2-11) are those in the meson-quark CMS (M-Q CMS), whereas in the final formula for the decay width the values in the meson-nucleon CMS (M-N CMS) have to be used. If $\vec{k}$ is the meson momentum in the M-N CMS and $\vec{p}_N$ the quark momentum in that system, the transformation is

$$\vec{q} = \frac{m\vec{k} - \omega\vec{p}_N}{m+\omega}, \tag{3.2-12}$$

where $\vec{p}_N$ can further be decomposed into the intrinsic momentum $\vec{p}$ (the distribution of which is given by the quark wave function) and a recoil momentum, according to $\vec{p}_N = \vec{p} - \vec{k}/3$. Even though one arrives at the same form of the transition operator as in the derivative-coupling case, this transformation is of purely kinematical origin and it does not suffer from theoretical ambiguities like the recoil correction. If one starts out from the operator in the form of eq. (3.2-11), which is already Galilean invariant to order p/m, the transformation (3.2-12) has no effect and is thus superfluous.

In order to evaluate the matrix elements of $\hat{O}$ the wave function of a baryon of total angular momentum $\vec{J}$ and z-component M_J is factorized as a plane wave of momentum $\vec{P}_B$ (the baryon momentum) for the center of mass (CMS) motion, and an intrinsic wave function:

$$|B\rangle = \frac{1}{(2\pi)^{3/2}} e^{i\vec{P}_B\cdot\vec{R}} \big[\Psi_B(\vec{r}_{12},\vec{\rho})\Phi_B(S,M_S;T,M_T),\big]_{J,M_J}, \tag{3.2-13}$$

where Φ_B stands for the spin-isospin part and Ψ_B is the spatial wave function in terms of the Jacobi coordinates $\vec{r}_{12}$ and $\vec{\rho}$. The latter ones are defined as in eq. (B.2-7) for equal-mass constituent quarks. Performing the integration over the CMS coordinate we can write the decay amplitude as

$$\left\langle B' \middle| \hat{O} \middle| B \right\rangle = (2\pi)^3\, \delta\left(\vec{P}_B - \vec{P}_{B'} - \vec{q}\right)\, A_\lambda, \tag{3.2-14}$$

where

$$A_\lambda = \frac{3i}{\sqrt{2\omega}} \int d\vec{r}_{12}\, d\vec{\rho}\, \left[\Psi_{B'}(\vec{r}_{12},\,\vec{\rho})\Phi_{B'}(S',M'_S;I',M'_I)\right]^*_{J',M_{J'}}\, \hat{O}\, \left[\Psi_B(\vec{r}_{12},\,\vec{\rho})\Phi_B(S,M_S;T,M_T)\right]_{J,M_J}, \tag{3.2-15}$$

with $M_{J'} = M_J = \lambda$. For technical simplicity we choose quark 3 to be the emitting particle in the calculations. We recover the factor 3 due to the overall symmetry of the baryon wave function, and the factor i is necessary to ensure hermeticity. We also express $\hat{O}$ in terms of the Jacobi coordinates:

$$\hat{O} = \frac{g_{QQM}}{2m}\vec{\lambda}^F e^{i\frac{2}{3}\vec{q}\cdot\vec{\rho}} \left[\left(1+\frac{\omega}{2m}\right)\vec{\sigma}\cdot\vec{q} - \frac{\omega}{m}\vec{\sigma}\cdot(-\vec{p}_\rho + \frac{1}{3}\vec{P}_B)\right] \tag{3.2-16}$$

The occurrence of $\vec{P}_B$ may suggest a dependence of the amplitudes on the frame of reference. However, the corresponding term in eq. (3.2-16) combines with the first term proportional to $\vec{q}$ to produce a term proportional to $\vec{q} - \frac{\omega}{3m}\vec{P}_B$, which reduces to $\vec{q} - \mu\frac{\vec{P}_B}{M_B}$ in the non-relativistic limit and therefore allows to recover the Galilean invariance of the amplitude at the lowest order in $\frac{\omega}{M_B}$, as discussed earlier. This invariance of the amplitude at the quark level was introduced by Mitra and Ross [26] to get some ω-dependent term in the transition operator but this procedure still leaves some ambiguity [169,170]. We shall work in the rest frame of the decaying resonance ($\vec{P}_B = 0$), but it is important to realize that the amplitudes remain explicitly frame dependent after this step.

3.2.2 Some Analytic Properties

It is instructive to study some of the most prominent properties of the EEM in the harmonic oscillator model, where results may be obtained in closed form. We shall see later on, that calculations with more realistic wave functions still show the basic features of this simple model, which will provide an interpretation for certain results.

Table 3.1: Analytic expressions for the decay widths of $N^* \to N\pi$, and $N^* \to N\eta$ in the harmonic-oscillator model for the lowest N and Δ resonances. The full widths are obtained by multiplying the factors A (which are the same for π and η decays) and B by $(1/4\pi)\,(g/2m)^2\,q^3\,(E/M)\,exp(-\frac{1}{3}b^2q^2)$. The numerical results in the column of set 2 were obtained by a χ^2 fitting procedure of the parameters b and g to the 13 $N\pi$ widths, keeping the constituent quark mass fixed at $m = 340$ MeV. The values obtained are $b = 1.25$ fm and $g^2/4\pi = 1.7$, giving $\chi^2 = 95$. For set 1, the value of b was fixed to $b = 0.4$ fm and only g was fitted to the $\Delta \to N\pi$ width to give $g^2/4\pi = 0.956$ with a $\chi^2 = 328$. Experimental data are from ref. [43]; for the quoted uncertainties refer to the text. All decay widths in MeV.

N^*		$N^* \to N\pi$				$N^* \to N\eta$			
	A	B	set 1	set 2	exp.	B	set 1	set 2	exp.
N_{1440}	P_0'	$\frac{25}{162}\,(bq)^4$	33	81	$(227 \pm 18)^{+70}_{-59}$				
N_{1710}	P_0'	$\frac{4}{81}\,(bq)^4$	24	49	$(15 \pm 5)^{+30}_{-5}$	$\frac{1}{81}\,(bq)^4$	8	5	
N_{1535}	S	$\frac{16}{27}\,(bq)^2$	716	40	$(67 \pm 15)^{+55}_{-17}$	$\frac{4}{27}\,(bq)^2$	199	11	$(64 \pm 19)^{+76}_{-15}$
N_{1650}	S	$\frac{4}{27}\,(bq)^2$	207	10	$(109 \pm 26)^{+36}_{-3}$	$\frac{4}{27}\,(bq)^2$	342	0	$(10 \pm 5)^{+4}_{-1}$
N_{1720}	P	$\frac{5}{81}\,(bq)^4$	533	24	$(23 \pm 8)^{+9}_{-5}$	$\frac{1}{405}\,(bq)^4$	15	0	
N_{1520}	D	$\frac{16}{27}\,(bq)^2$	78	112	$(66 \pm 6)^{+9}_{-5}$	$\frac{4}{27}\,(bq)^2$	0	1	
N_{1700}	D	$\frac{2}{135}\,(bq)^2$	6	2	$(10 \pm 5)^{+3}_{-3}$	$\frac{2}{135}\,(bq)^2$	1	3	
N_{1680}	F	$\frac{5}{81}\,(bq)^4$	28	101	$(85 \pm 7)^{+6}_{-6}$	$\frac{1}{405}\,(bq)^4$	9	3	
N_{1675}	D	$\frac{4}{45}\,(bq)^2$	30	12	$(68 \pm 8)^{+14}_{-4}$	$\frac{4}{45}\,(bq)^2$	5	16	
Δ_{1620}	S	$\frac{2}{27}\,(bq)^2$	101	5	$(38 \pm 8)^{+8}_{-6}$				
Δ_{1232}	P_0	$\frac{16}{3}$	120	115	$(119 \pm 1)^{+5}_{-5}$				
Δ_{1600}	P_0'	$\frac{4}{81}\,(bq)^4$	20	50	$(61 \pm 26)^{+26}_{-10}$				
Δ_{1700}	D	$\frac{2}{27}\,(bq)^2$	28	9	$(45 \pm 15)^{+20}_{-10}$				

$$P_0 = D = F = \left(1 + \tfrac{\omega}{6m}\right)^2$$

$$P_0' = \left[1 + \tfrac{\omega}{6m}\left(1 - \tfrac{12}{b^2q^2}\right)\right]^2 \qquad P = \left[1 + \tfrac{\omega}{6m}\left(1 - \tfrac{30}{b^2q^2}\right)\right]^2 \qquad S = \left[1 + \tfrac{\omega}{6m}\left(1 - \tfrac{18}{b^2q^2}\right)\right]^2$$

Direct and Recoil Term

For the decay of a resonance with quark orbital angular momentum L' into the baryon ground state ($L = 0$) only the partial waves $l = L' \pm 1$ are allowed. It can be shown in general [33], that the upper partial wave $l = L' + 1$ is essentially given by the direct term and receives only a small correction from the recoil term, while the lower partial wave $l = L' - 1$ receives its essential contribution from the recoil term. Since the direct term merely contributes the average overlap of the two involved wave functions, the corresponding decay amplitude is not very sensitive to the detailed form of the wave functions or the model parameters, whereas the recoil term includes derivatives and therefore probes more sensibly the structure of the wave function. In the first case, one speaks of structure-independent amplitudes, following the terminology of ref. [75], whereas the second case leads to structure-dependent ones.

In order to illustrate this, it is useful to investigate the predictions of the EEM using harmonic oscillator functions, see eqs. (C.1-14) and (C.1-15). The relevant matrix elements are collected in tables C.1 and C.2 in Appendix C. Table 3.1 gives the results for the lowest N and Δ resonances in such a form that the full widths are obtained by multiplying the factors in columns A and B for each resonance by $(1/4\pi)\,(g/2m)^2\,q^3\,(E/M)\,\exp(-\frac{1}{3}b^2q^2)$. Here, as usual, q is the momentum of the emitted meson, E the energy of the final state baryon and M the mass of the decaying resonance. The harmonic oscillator parameter b is defined in eq. (C.1-16).

The separation of the factors A and B was made to distinguish the effect of the direct and the recoil term in eq. (3.2-11). Leaving out the factor A would lead to decay widths when employing the direct term only (without the factor $1 + \frac{\omega}{2m}$, which would just be a multiplicative constant), the corresponding results were first given by Faiman and Hendry [20, 21].

The factor A entirely contains the contribution of the recoil term and one sees that all the amplitudes fall into different classes according to the form of their recoil contributions. First are the ones whose factor A is labeled by P_0, D, or F; these are the structure-independent ones where the amplitudes just get multiplied by a factor A similar in magnitude for all corresponding states. The rest are structure-dependent ones, where the values of A depend very sensitively on the meson momentum q as well as on the oscillator parameter b.

As an example of this classification we mention the $N_{1520} - N_{1535}$ multiplet, the former producing a D-wave (structure-independent), the latter an S-wave (structure-dependent) in the meson-nucleon system.

In table 3.1 we also give two samples of numerical results that may be compared to the experimental data as compiled by the PDG [43]. For the latter there arise two kinds of uncertainties: First, the total decay width of each resonance is given by a central value and a lower and upper bound. Second, the partial decay width has its own uncertainty. In table 3.1 we quote the value for the π decay widths deduced from the central value of the total width and first add the uncertainty from the partial decay width itself (numbers inside the parentheses). Then we indicate also the range of the total decay width by an upper and lower bound. We understand that the total uncertainty in a partial decay width must be estimated by combining both types of uncertainties (inherent separately in the total and partial widths).

The first set of theoretic predictions in table 3.1 (set 1) was obtained by fixing the oscillator parameter to the value $b = 0.4$ fm and by fitting the coupling constant to the $\Delta \to N\pi$ width to give $g^2/4\pi = 0.956$. This is done for the purpose of illustration because this value of b gives a mean squared radius for the nucleon wave function of $\langle r^2 \rangle = 0.16$ fm^2, a value that corresponds approximately to the sizes of the nucleon wave functions in the parameterizations of the GBE and OGE models in table 2.4. The numerical results for this case will be discussed later when we also give results for the more elaborate wave functions of the OGE and GBE type, let us note for the moment only the exceedingly large values for the widths of $N_{1535} \to N\pi, \eta$, $N_{1650} \to N\pi, \eta$ and $N_{1720} \to N\pi$.

The second set (set 2) was obtained by a χ^2 fitting procedure of the parameters b and g to the 13 $N\pi$ widths, keeping the constituent quark mass fixed at $m = 340$ MeV. The values obtained are $b = 1.25$ fm and $g^2/4\pi = 1.7$, giving $\chi^2 = 95$. The latter is defined by

$$\chi^2 = \sum \left[\frac{\sqrt{\Gamma_{exp}} - \sqrt{\Gamma_{th}}}{\Delta\sqrt{\Gamma_{exp}}} \right]^2 , \tag{3.2-17}$$

where Δ means the experimental error (only the value for the partial width uncertainty is taken here) and the sum is over all the 13 widths in the $N^* \to N\pi$ channel.

We note that the fitted values for b and g are larger than what is commonly expected from physical arguments. Fitting for instance the value of b to the N-Roper mass difference would give $b = 0.67$ fm, from the nucleon charge radius one would expect $b = 0.86$ fm, leading to an even smaller value if one relates b to the matter radius of the nucleon. Also the coupling constant g is found to be too large, since from SU(3) considerations (linking g to the pion - nucleon coupling constant) one would expect $g^2/4\pi = 0.67$. The larger value obtained by the fit is however just a consequence of the larger value of b because of the exponential $\exp(-b^2q^2/3)$, that multiplies the decay width.

The fact that the fit to decay widths gives larger values for b may indicate the need for more extended wave functions, in particular if one takes into account that usual constituent quark models lead to wave functions that are much more compact (see for instance table 2.4).

However, the unphysical parameters following from the rigorous fit lead to some very welcome features in the decay amplitudes. As it will be discussed later in more detail, there are basically three amplitudes that generally pose problems in constituent quark model calculations: the $N_{1650} \to N\eta$ and the $N_{1720} \to N\pi$ amplitudes, that are generally predicted to be too large, as well as the $N_{1440} \to N\pi$ amplitude, that is too small, as compared to the experimental data (for the latter one we note that this is a specific feature of the EEM as discussed in the next subsection). Requiring that the factor S for the $N_{1650} \to N\eta$ amplitude in table 3.1 is small, one obtains a value of $b \simeq 1.2$ fm, the corresponding requirement for the factor P of the $N_{1720} \to N\pi$ amplitude would give $b \simeq 0.87$ fm, whereas for the factor P_0' (multiplying the $N_{1440} \to N\pi$ amplitude) to be large, one needs $b \gg 0.71$ fm. This indicates that with more extended wave functions (larger values of b) one solves with one strike all the problems mentioned above.

However, there persist some severe discrepancies, in particular the $N_{1650} \to N\pi$ width remains far

too small, but one has to take into account that in a more realistic model there will occur configuration mixing, for instance through the influence of tensor forces. Parameterizing this mixing like in eq. (2.6-21), Faiman and Hendry [20] derived the corresponding decay width depending on the phenomenological mixing angle θ_1. We will see a bit later on, when we discuss the mixing induced by the tensor force in the GBE, that a small mixing angle leads to an enhanced $N_{1650} \to N\pi$ as relative to the $N_{1535} \to N\pi$, an effect that is just desired in table 3.1. In addition, one has to bear in mind that these are structure-dependent resonances, so that in more realistic quark models, with more open parameters, one might hope for a better description. The problem in this respect is of course, that parameters in the quark-quark potential are never fitted to decay amplitudes, but rather to the spectra, which is not a unique procedure. The examples above show very clearly however, that the structure-dependent amplitudes may serve as a very stringent test of wave functions stemming from different quark-quark dynamics, as long as one agrees to work in the framework of a certain decay model.

In ref. [75] the factors A corresponding to the recoil term were replaced by four constants, called the 'reduced partial widths'. However, as evidenced by the previous discussion, in every explicit quark-model approach, these factors are far from being constants. It is even so that certain decay widths can get almost arbitrarily large or small if the parameter values are chosen within a physically meaningful range. Note especially the factors S and P, which can become very large for small (bq) or show some cancellation effect.

One may only hope that higher-order terms in the non-relativistic expansion of the interaction Lagrangian will wash out this sensitivity on model parameters, as argued by Koniuk and Isgur [75], but this remains to be shown.

Radial Excitations

It has become clear from various works (see ref. [33] for an exhaustive discussion), that the EEM finds one of its fundamental limitations in the decays of radial excitations, a feature that can be illustrated again in a most transparent way by the harmonic oscillator model.

Indeed, it can be shown [33, p. 238] that for transitions between $L = 0$ states the operator (3.2-11) may effectively be reduced to a very simple form (dropping the coupling constant and the isospin operator to simplify the notation):

$$\hat{O} \to -\frac{1}{2}\, q^2\, \sigma_0\, (q - q_0)\, z^2. \tag{3.2-18}$$

Here z denotes the longitudinal component of the Jacobi coordinate $\vec{\rho}$, q is the meson momentum and q_0 is the theoretical energy difference of the decaying resonance and the ground state. The latter one follows from a Schrödinger equation employing a non-relativistic kinetic energy operator, so that the following argument is not valid for the so called relativized, or semi-relativistic, quark models. Eq. (3.2-18) clearly shows that there is a zero in the decay amplitude as a function of meson momentum q at $q = q_0$. As a consequence we expect the decay width as a function of q to behave like

$$\Gamma \sim q^5 (q - q_0)^2 \tag{3.2-19}$$

for decays of radial excitations into their ground states. This becomes evident from fig. 3.3, where we have calculated the $N\pi$ decay width of the Roper resonance with wave functions stemming from the models GBE NR, GBE SR and GBE with tensor force, as a function of the pion momentum q. The physical value of q (that is the value for which energy and momentum are conserved) for the Roper resonance is $q = 397$ MeV if one takes its nominal mass $M = 1440$ MeV. The GBE models give masses very close to this nominal (Breit-Wigner) value (in fact, all the GBE parameterizations were fitted to reproduce the Roper mass), so the value of q in these models is somewhere ~ 400 MeV.

We see from fig. 3.3 that the GBE NR model gives the zero just at the physical value of $q \sim 400$ MeV, which leads to a practically vanishing decay width in this case. The experimental value for the Roper resonance decaying into $N\pi$ being of the order ~ 200 MeV, this is a serious and fundamental shortcoming. We see also that employing a semi-relativistic kinetic energy operator and including the tensor force in the interaction pushes the zero to larger values of q, however, the resulting width of ~ 10

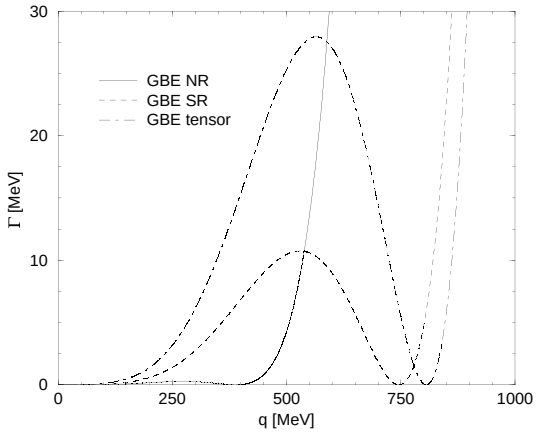

Figure 3.3: π-decay widths of the radial excitation N_{1440} as a function of meson momentum q for the models GBE NR, GBE SR and GBE with tensor force.

MeV at $q = 400$ MeV is still an order of magnitude too small as compared to the experimental value.

Even in the simple non-relativistic model, the positions of the zeros in our calculations do not correspond exactly to the energy difference of the decaying and ground states because in the derivation of the form (3.2-18) from the operator (3.2-11) two approximations were made:

1. The exponential factor is expanded in a power series up to second order in the direct term and up to first order in the recoil term.
2. The meson energy ω is replaced by its momentum q.

Altogether, this shows that the small widths for radial excitations are entirely a property of the operator and not of the wave functions or the CQM employed.

It is evident, that the vanishing widths of radial excitations are a direct consequence of the form of the decay operator in the EEM. Radial decays lie therefore outside the validity range of the EEM, even though one should bear in mind that this one works rather well for orbital excitations. A model independent analyses of decays of radial excitations has been carried out in ref. [171]. In particular, it has been shown that the introduction of a finite pion size indeed heals the problem [172], and we shall see later on, that quark-pair creation models, where the emitted meson naturally obtains a finite size, do not present the same shortcoming.

3.2.3 Numerical Results

It is interesting to notice that the relative strengths of the experimental $N^* \to N\pi$ decay widths seem to be mainly governed by $SU(6) \times O(3)$ symmetry [6]. To illustrate this, let us calculate the ratios of decay widths of all the states within one LS-multiplet in the $L = 1$ region neglecting the spatial part of the overlap. This approximation is not so bad, since within one LS-multiplet the masses and therefore all kinematic magnitudes are very similar. This is also the case for the phase-space factors, that will cancel in the ratios. The relative widths for these cases will therefore mainly be governed by the spin-isospin matrix elements. If one considers the ratios of the squared spin-isospin matrix elements and compares them with the corresponding experimental ratios (taken from ref. [43]), one finds the following:

$$\begin{aligned} \Gamma(N_{1650}) : \Gamma(N_{1675}) : \Gamma(N_{1700}) = &\quad \tfrac{4}{9} : \tfrac{4}{15} : \tfrac{2}{45} &&\simeq 109 \pm 26 : 68 \pm 8 : 10 \pm 5 \\ \Gamma(N_{1520}) : \Gamma(N_{1535}) = &\quad \tfrac{16}{9} : \tfrac{16}{9} &&\simeq 66 \pm 6 : 67 \pm 15 \\ \Gamma(\Delta_{1620}) : \Gamma(\Delta_{1700}) = &\quad \tfrac{2}{9} : \tfrac{2}{9} &&\simeq 38 \pm 8 : 45 \pm 15. \end{aligned} \tag{3.2-20}$$

This approximation, however, clearly fails in the case of $L = 2$ orbital excitations:

$$\Gamma(N_{1680}) : \Gamma(N_{1720}) = \quad \tfrac{5}{3} : \tfrac{5}{3} \quad \not\approx 85 \pm 7 : 23 \pm 8. \tag{3.2-21}$$

For the latter we note first some experimental ambiguity about the N_{1720} [48] and second the possibility of a wrong symmetry assignment, as discussed in ref. [173].

This reasonable prediction of decay ratios is entirely due to $SU(6) \times O(3)$ symmetry. It is still approximately observed even with the spatial part of the transition matrix element taken into account, if one employs only the direct term in the decay operator (i.e. the term proportional to $\vec{\sigma} \cdot \vec{q}$ in eq. (3.2-11)). Within any dynamical model this contributes merely the average overlaps of the spatial wave functions, which are constants within one LS-multiplet. However, the recoil term $\vec{\sigma} \cdot \vec{p}$ as well as a possible mixing of states destroys this general feature, in particular for the structure-dependent amplitudes. It is also not observed neither in $N^* \to N\eta$ nor in $N^* \to \Delta\pi$ decays [174].

Results for $N^* \to N\pi$ and $N^* \to N\eta$ decays employing different CQM wave functions (without tensor force) are given in table 3.2 and 3.3. We remark the following points:

1. In all calculations we use the theoretical values of the resonance masses, as they follow from the solution of the corresponding Schrödinger equation. This differs from what is usually done in this field, where the experimental masses (nominal Breit-Wigner masses from the PDG compilation) are employed. The latter procedure minimizes uncertitudes due to our lack of knowledge of the exact quark-quark interaction with the assumption that wave functions are still a good approximation to what would follow from a more complete approach. On the other hand, it introduces practically a free parameter for each transition and leaves the question open of how to treat resonances that were not observed yet experimentally. Historically, the use of experimental masses was of course necessitated by the fact that the harmonic oscillator, extensively employed in all kind of calculations, predicts a large part of resonances to be degenerate, but with the use of more sophisticated inter-quark potentials, this is not an argument anymore. Furthermore, using experimental masses immediately raises the question of which masses are actually to be used, Breit-Wigner or pole masses. Using theoretical masses, these problems are circumvented, and predictions for decay widths may be viewed as genuine of the particular CQM under consideration.

2. For $N\pi$ decays, the pseudo-scalar coupling constant was fitted to give the correct decay width of the Δ resonance. It is seen from table 3.2, that the values obtained for $g^2/(4\pi)$ are very similar for all the CQM's considered, but they differ from what is obtained from the pion-nucleon coupling constant, which would imply a value of $g^2/(4\pi) = 0.67$. Renormalizing the coupling constant to this value would give a width of ~ 90 MeV for the Δ, a result that is typical for the EEM [20, 25, 174].

3. For $N\eta$ decays, the same coupling constant was used as for the corresponding $N\pi$ decays.

4. Numerical values for decay widths have been rounded to the nearest integer (in MeV). This may sometimes hide the fact that for some resonances the width is almost exactly zero (of the order $\sim 10^{-5}$ as for decays of radial excitations or decays of states corresponding to an antisymmetric wave function), whereas for others it is only practically zero.

Inspecting the results some general features can be extracted that are observed in all the calculations. The $N\pi$ widths of the Roper resonance N_{1440} is practically zero for both NR parameterizations, while the SR results are finite but still an order of magnitude too small as compared to the experimental value. This is readily understood on the basis of the discussion in the last section.

A most prominent feature is the prediction of exceedingly large decay widths in some cases for the resonances N_{1535}, N_{1650} and N_{1720}. The results also differ appreciably from one model to the other, a fact that is explained by the observation that all theses resonances are structure dependent. In contrast, the widths of the N_{1520}, N_{1700}, N_{1680} and also N_{1675} are structure independent, a prediction that is confirmed by the numerical results.

The above peculiarities inevitably recall the results that were obtained in the harmonic oscillator model in the case where the size parameter b was fixed to give a value for the root mean square radius of the nucleon wave function comparable to the one of the models considered here, and the coupling constant g was fixed to reproduce the $\Delta \to N\pi$ width (see table 3.1). Comparison with the corresponding results

Table 3.2: $N^* \to N\pi$ decay widths of baryon resonances for the GBE and OGE constituent quark models both in non-relativistic and semi-relativistic parameterizations. Experimental data are from ref. [43].

$[N^{J^\pi}]_n$	N^*	$\Gamma(N^* \to N\pi)$ [MeV]				
		GBE SR	GBE NR	OGE SR	OGE NR	exp.
$[N^{\frac{1}{2}^+}]_2$	N_{1440}	7	0	34	0	$(227 \pm 18)^{+70}_{-59}$
$[N^{\frac{1}{2}^+}]_3$	N_{1710}	10	4	7	61	$(15 \pm 5)^{+30}_{-5}$
$[N^{\frac{1}{2}^+}]_4$		39	2	101	32	
$[N^{\frac{1}{2}^+}]_5$		0	0	0	0	
$[N^{\frac{1}{2}^-}]_1$	N_{1535}	757	103	1710	282	$(67 \pm 15)^{+55}_{-17}$
$[N^{\frac{1}{2}^-}]_2$	N_{1650}	210	19	509	57	$(109 \pm 26)^{+36}_{-3}$
$[N^{\frac{3}{2}^+}]_1$	N_{1720}	464	55	1204	417	$(23 \pm 8)^{+9}_{-5}$
$[N^{\frac{3}{2}^+}]_2$		9	19	19	0	
$[N^{\frac{3}{2}^+}]_3$		2	1	3	0	
$[N^{\frac{3}{2}^+}]_4$		20	1	50	16	
$[N^{\frac{3}{2}^+}]_5$		0	0	0	0	
$[N^{\frac{3}{2}^-}]_1$	N_{1520}	50	43	52	111	$(66 \pm 6)^{+9}_{-5}$
$[N^{\frac{3}{2}^-}]_2$	N_{1700}	3	2	4	7	$(10 \pm 5)^{+3}_{-3}$
$[N^{\frac{5}{2}^+}]_1$	N_{1680}	25	19	47	162	$(85 \pm 7)^{+6}_{-6}$
$[N^{\frac{5}{2}^+}]_2$		0	1	0	3	
$[N^{\frac{5}{2}^+}]_3$		0	0	0	1	
$[N^{\frac{5}{2}^-}]_1$	N_{1675}	17	12	23	41	$(68 \pm 8)^{+14}_{-4}$
$[N^{\frac{7}{2}^+}]_1$		1	0	2	4	
$[\Delta^{\frac{1}{2}^+}]_1$	Δ_{1910}	9	3	17	30	$(56 \pm 19)^{+6}_{-9}$
$[\Delta^{\frac{1}{2}^+}]_2$		302	22	741	199	
$[\Delta^{\frac{1}{2}^-}]_1$	Δ_{1620}	102	11	256	32	$(38 \pm 8)^{+8}_{-6}$
$[\Delta^{\frac{3}{2}^+}]_1$	Δ_{1232}	120	120	120	120	$(119 \pm 1)^{+5}_{-5}$
$[\Delta^{\frac{3}{2}^+}]_2$	Δ_{1600}	124	20	121	181	$(61 \pm 26)^{+26}_{-10}$
$[\Delta^{\frac{3}{2}^+}]_3$	Δ_{1920}	151	11	371	100	$(25 \pm 15)^{+20}_{-3}$
$[\Delta^{\frac{3}{2}^+}]_4$		19	1	53	16	
$[\Delta^{\frac{3}{2}^-}]_1$	Δ_{1700}	14	10	13	30	$(45 \pm 15)^{+20}_{-10}$
$[\Delta^{\frac{5}{2}^+}]_1$	Δ_{1905}	4	2	7	18	$(35 \pm 18)^{+13}_{-3}$
$[\Delta^{\frac{5}{2}^+}]_2$		1	0	1	3	
$[\Delta^{\frac{7}{2}^+}]_1$		18	8	32	82	
$\frac{g^2}{4\pi}$		0.886	0.969	0.938	0.957	

of tables 3.2 and 3.3 shows a remarkable similarity, the most striking one being the fact that we obtain almost the same value for the coupling constant ($\frac{g^2}{4\pi} = 0.956$ in the harmonic oscillator case). This indicates that the main features of decay properties obtained in rather sophisticated CQM's are already captured in the rather simple harmonic oscillator model. This comparison also provides us with a simple explanation of the main shortcomings evidenced by the present results, indicating that the most important reason for the bad description of decay amplitudes is due to the small sizes of wave functions obtained in any realistic quark model.

The only difference between results presented in table 3.2 and the harmonic oscillator model is evidenced by the pion decay width of the Roper resonance, which comes out almost reasonably large in table 3.1. This is simply due to the fact that we used experimental values for resonance masses in the

Table 3.3: $N^* \to N\eta$ decay widths of baryon resonances for the GBE and OGE constituent quark models both in non-relativistic and semi-relativistic parameterizations. Experimental data are from ref. [43].

$[N^{J^\pi}]_n$	N^*	$\Gamma(N^* \to N\eta)$ [MeV]				
		GBE SR	GBE NR	OGE SR	OGE NR	exp.
$[N^{\frac{1}{2}^+}]_2$	N_{1440}			1	2	
$[N^{\frac{1}{2}^+}]_3$	N_{1710}	4	0	13	2	
$[N^{\frac{1}{2}^+}]_4$		45	4	125	50	
$[N^{\frac{1}{2}^+}]_5$		0	0	2	2	
$[N^{\frac{1}{2}^-}]_1$	N_{1535}	171	52	339	145	$(64 \pm 19)^{+76}_{-15}$
$[N^{\frac{1}{2}^-}]_2$	N_{1650}	380	72	890	277	$(10 \pm 5)^{+4}_{-1}$
$[N^{\frac{3}{2}^+}]_1$	N_{1720}	22	5	74	45	
$[N^{\frac{3}{2}^+}]_2$		3	2	10	0	
$[N^{\frac{3}{2}^+}]_3$		16	0	37	11	
$[N^{\frac{3}{2}^+}]_4$		23	2	63	25	
$[N^{\frac{3}{2}^+}]_5$		0	0	1	1	
$[N^{\frac{3}{2}^-}]_1$	N_{1520}	0	0	0	0	
$[N^{\frac{3}{2}^-}]_2$	N_{1700}	0	0	0	1	
$[N^{\frac{5}{2}^+}]_1$	N_{1680}	0	0	1	5	
$[N^{\frac{5}{2}^+}]_2$		0	0	1	2	
$[N^{\frac{5}{2}^+}]_3$		0	0	0	1	
$[N^{\frac{5}{2}^-}]_1$	N_{1675}	1	1	3	5	
$[N^{\frac{7}{2}^+}]_1$		1	0	2	6	
$\frac{q^2}{4\pi}$		0.886	0.969	0.938	0.957	

determination of kinematical quantities for the calculation of widths in the harmonic oscillator model; had we used the theoretical values (which are completely unreasonable, especially for the Roper resonance in this case), we would have found a decay width compatible with zero, as discussed in the last section.

As for the resonances that have not been observed so far (which means: have not been rated three- or four-star by the PDG), one sees that most of them are predicted to decay very weakly into $N\pi$. This fact was actually used to explain why these states have not been seen in any PWA yet [175]. The only resonances that might be an exception in this case are the $[N^{\frac{1}{2}^+}]_4$, $[N^{\frac{3}{2}^+}]_4$, the $[\Delta^{\frac{1}{2}^+}]_2$ and the $[N^{\frac{7}{2}^+}]_1$, however, predictions from different models are not always consistent. In addition, in view of the fact that some well determined decay widths are already predicted far too large by these models, this prediction has to be taken with a grain of salt.

The results for η decays show a familiar pattern: the only resonances with appreciable width are the N_{1535} and the N_{1650}, both due to their structure dependence. However, the relative ordering is wrong in all cases: the width of the N_{1650} is always larger than the one of the N_{1535}, a fact that has been called the "$N\eta$" problem. A possible explanation has been suggested in the framework of the GBE interaction [176], however, explicit calculations like the ones presented here, did not confirm the argument. The $N\eta$ problem rather hints to a strong mixing effect due to tensor forces. Also the fact that the N_{1535} lies rather close to the $N\eta$ threshold (~ 50 MeV above) is very often forgotten or ignored in decay calculations (like the present one). As for π decays, there are some undiscovered resonances that are predicted to have a rather large $N\eta$ branching fraction, in particular the $[N^{\frac{1}{2}^+}]_4$ and some of the $[N^{\frac{3}{2}^+}]$ states.

Again, comparison with the results from the harmonic oscillator model show a very similar pattern. Most interesting here is the fact that with the larger value of the oscillator parameter b we obtain the right ordering of the N_{1535} and the N_{1650} decay widths into $N\eta$. This hints again to the need of more extended wave functions and leaves the question open whether the above arguments are really the solution of the

Table 3.4: Decay widths of N^* resonances from the GBE SR potential with tensor force in the EEM. Experimental data are from ref. [43].

$[N^{J^\pi}]_n$	N^*	$\Gamma(N^* \to N\pi)$	exp.	$\Gamma(N^* \to N\eta)$	exp.
$[N^{\frac{1}{2}^+}]_2$	N_{1440}	15	$(227 \pm 18)^{+70}_{-59}$		
$[N^{\frac{1}{2}^+}]_3$	N_{1710}	18	$(15 \pm 5)^{+30}_{-5}$	2	
$[N^{\frac{1}{2}^+}]_4$		31		0	
$[N^{\frac{1}{2}^+}]_5$					
$[N^{\frac{1}{2}^-}]_1$	N_{1535}	508	$(67 \pm 15)^{+55}_{-17}$	298	$(64 \pm 19)^{+76}_{-15}$
$[N^{\frac{1}{2}^-}]_2$	N_{1650}	501	$(109 \pm 26)^{+36}_{-3}$	220	$(10 \pm 5)^{+4}_{-1}$
$[N^{\frac{1}{2}^-}]_3$		1022		920	
$[N^{\frac{1}{2}^-}]_4$		61		5	
$[N^{\frac{3}{2}^+}]_1$	N_{1720}	574	$(23 \pm 8)^{+9}_{-5}$	39	
$[N^{\frac{3}{2}^+}]_2$		4		11	
$[N^{\frac{3}{2}^+}]_3$		31		26	
$[N^{\frac{3}{2}^-}]_1$	N_{1520}	54	$(66 \pm 6)^{+9}_{-5}$	0	
$[N^{\frac{3}{2}^-}]_2$	N_{1700}	27	$(10 \pm 5)^{+3}_{-3}$	0	
$[N^{\frac{3}{2}^-}]_3$		35		1	
$[N^{\frac{3}{2}^-}]_4$		15		1	
$[N^{\frac{5}{2}^+}]_1$	N_{1680}	33	$(85 \pm 7)^{+6}_{-6}$	0	
$[N^{\frac{5}{2}^+}]_2$		1		1	
$[N^{\frac{5}{2}^+}]_3$		0		0	
$[N^{\frac{5}{2}^-}]_1$	N_{1675}	32	$(68 \pm 8)^{+14}_{-4}$	2	
$[N^{\frac{7}{2}^+}]_1$		3		1	
$[\Delta^{\frac{1}{2}^+}]_1$	Δ_{1910}	412	$(56 \pm 19)^{+6}_{-9}$		
$[\Delta^{\frac{1}{2}^+}]_2$		382			
$[\Delta^{\frac{1}{2}^-}]_1$	Δ_{1620}	112	$(38 \pm 8)^{+8}_{-6}$		
$[\Delta^{\frac{3}{2}^+}]_1$	Δ_{1232}	120	$(119 \pm 1)^{+5}_{-5}$		
$[\Delta^{\frac{3}{2}^+}]_2$	Δ_{1600}	86	$(61 \pm 26)^{+26}_{-10}$		
$[\Delta^{\frac{3}{2}^+}]_3$	Δ_{1920}	347	$(25 \pm 15)^{+20}_{-3}$		
$[\Delta^{\frac{3}{2}^+}]_4$		42			
$[\Delta^{\frac{3}{2}^-}]_1$	Δ_{1700}	22	$(45 \pm 15)^{+20}_{-10}$		
$[\Delta^{\frac{5}{2}^+}]_1$	Δ_{1905}	4	$(35 \pm 18)^{+13}_{-3}$		
$[\Delta^{\frac{5}{2}^+}]_2$		2			
	$\frac{g^2}{4\pi}$	0.799		0.799	

"$N\eta$" puzzle.

First results for strong decay widths using wave functions from the GBE have been given in ref. [177] and extensions to describe strong decays of strange baryon resonances were considered in refs. [178,179]. In all these works, the contribution of the tensor component to the quark-quark interaction was neglected. In table 3.4 we present results for decay widths predicted by the EEM for wave functions from the GBE SR potential with tensor force.

It is not necessary to discuss these results in detail, the qualitative features as compared to the results without tensor force remain largely unchanged. The only exceptions are the cases where there occurs a noticeable mixing between states with the same total angular momentum J. Apart from the N_{1535} - N_{1650} mixing as parameterized in eq. (2.6-21), we have a corresponding mixing for the D-waves N_{1520} -

N_{1700}:

$$\begin{bmatrix} N_{1520} \\ N_{1700} \end{bmatrix} = \begin{bmatrix} \cos\theta_2 & \sin\theta_2 \\ -\sin\theta_2 & \cos\theta_2 \end{bmatrix} \begin{bmatrix} N_{13} \\ N_{33} \end{bmatrix} . \tag{3.2-22}$$

Once again it is highly instructive to look at the predictions of the harmonic oscillator model when these mixing angles are taken into account. The decay widths of the above mentioned four resonances get multiplied by the following factors [20]:

$$\begin{array}{lcrcr} \Gamma(N_{1535} \to N\pi) & : & \left[\cos\theta_1 - \frac{1}{2}\sin\theta_1\right]^2 & \simeq & 0.59 \\ \Gamma(N_{1650} \to N\pi) & : & \left[\cos\theta_1 + 2\sin\theta_1\right]^2 & \simeq & 2.6 \\ \Gamma(N_{1520} \to N\pi) & : & \left[\cos\theta_2 - \frac{1}{2\sqrt{10}}\sin\theta_2\right]^2 & \simeq & 0.78 \\ \Gamma(N_{1700} \to N\pi) & : & \left[\cos\theta_2 + 2\sqrt{10}\sin\theta_2\right]^2 & \simeq & 10 \quad , \end{array} \tag{3.2-23}$$

where the numbers on the right are obtained for values of the mixing angles of $\theta_1 = \theta_2 = +20°$, a value that is consistent with the mixing pattern deduced from the symmetry components given in table 2.7. The corresponding modifications of the $N^* \to N\eta$ widths are given by

$$\begin{array}{lcrcr} \Gamma(N_{1535} \to N\eta) & : & \left[\cos\theta_1 + \sin\theta_1\right]^2 & \simeq & 1.6 \\ \Gamma(N_{1650} \to N\eta) & : & \left[\cos\theta_1 - \sin\theta_1\right]^2 & \simeq & 0.36 \\ \Gamma(N_{1520} \to N\eta) & : & \left[\cos\theta_2 + \frac{1}{\sqrt{10}}\sin\theta_2\right]^2 & \simeq & 1.1 \\ \Gamma(N_{1700} \to N\eta) & : & \left[\cos\theta_2 - \sqrt{10}\sin\theta_2\right]^2 & \simeq & 0.02 \quad . \end{array} \tag{3.2-24}$$

With the help of these numbers we can naturally explain the results of decay widths of table 3.4, in particular the strong enhancement of the $N_{1700} \to N\pi$ width (about a factor 10 as compared to the results of the SR parameterizations of table 3.2). Furthermore the π decay width of the N_{1650} is enhanced relative to the one of the N_{1535}, whereas in the η channel it is suppressed. This has the particularly welcome consequence that the $N_{1650} \to N\eta$ decay width becomes smaller than the one of the N_{1535}.

These findings have to be contrasted with the arguments given by Isgur in his "Critique of a pion exchange model for inter-quark forces" [123]. He argues for a rejection of constituent quark models based on Goldstone boson exchange, one of the main arguments being the alleged wrong internal baryon wave functions that follow from the tensor interaction in the GBE. From numbers cited in ref. [99] he deduces mixing angles of $\theta_1 = \pm 13°$ and $\theta_2 = \pm 8°$, the sign being undetermined in this procedure. Such small values of mixing angles, even if they would have the correct sign, would have almost no impact on the prediction of decay widths.

However, the values that are obtained in our realistic (non-perturbative) calculations turn out to be larger, and even though the mixing angle between $J = \frac{1}{2}$ states is not as large as the one predicted by the IK model ($\theta_1 = -32°$), it seems to be sufficient to reverse the order of η decay widths of the two resonances N_{1535} and N_{1650}. In addition to the arguments given in ref. [124], it has also been noted that configuration mixing of states may not be enough to solve the η problem [62]. One has to bear in mind however the wrong effect of such a mixing angle on the mass splitting of these two resonances, see fig. 2.9.

Summing up, it is clear from the tables that the performance of the EEM in describing strong decays of non-strange baryon resonances is far from being excellent. Particularly, the exceedingly large values of some widths in the $N\pi$ and the $N\eta$ channel give rise to serious doubts whether the decay formalism and/or the wave functions used in the calculations are really appropriate. Observing the fact that the EEM seems to work rather well for heavy quark systems [180], one could be tempted to ascribe the remaining discrepancies to the fact that we are only working with light quarks here. On the other hand, also the harmonic oscillator results showed some very large widths in the case where the wave functions were not extended enough (see results under set 1 in table 3.1). This indicates the need for more extended wave functions which would necessitate a complete revision of the quark-quark dynamics. Note in particular, that normalization factors of Dirac spinors, like the factors $\sqrt{\frac{m_i m_j}{E_i E_j}}$ included in the model of Godfrey and Isgur (see eq. (2.5-13)), are omitted in all the models considered here. These factors evidently cut off some high momentum components and would lead to larger baryon wave functions.

We shall first investigate the influence of the most important model assumption of the EEM: the point-like nature of the emitted meson. The case of radial decays has shown that this may lead to

principal shortcomings, it remains to be seen therefore, how a model that incorporates the finite size of the meson performs for the whole of decay amplitudes.

3.3 The $^3P_0$

The central assumption of the EEM is the elementary nature of the emitted meson. This is based on the analogy with electromagnetism and nuclear physics; in the first case we know that the photon is indeed an elementary particle, in the latter one, the meson can be treated as point-like in practice. However, in sub-nuclear strong-interaction physics, in particular with light quark flavors, the extended size of any hadron should not be negligible. Decay models that describe the transition process by the creation of an additional quark-antiquark pair are generally referred to as quark-pair creation models (QPCM's). The guiding idea is based on the fundamental property of additivity. Inspired by the EEM, where the quantum is emitted from one of the quarks while the others remain spectators, one postulates that in a given process, only a minimum number of quarks is active. In the simplest version, one assumes that all the quarks in the initial hadron are spectators, so that the $q\bar{q}$–pair is necessarily created from the vacuum. The corresponding quantum numbers have given the name to the simplest and most popular model of hadronic transitions: the $^3P_0$ model.

3.3.1 Presentation of the Model

There exist different versions of quark-pair creation models in the literature and the choice between one of them comes mainly motivated by simplicity. In this sense the $^3P_0$ QPCM is manageable and comparable in the limit of a point-like meson to the EEM. Schematically the process is pictured in fig. 3.4a.

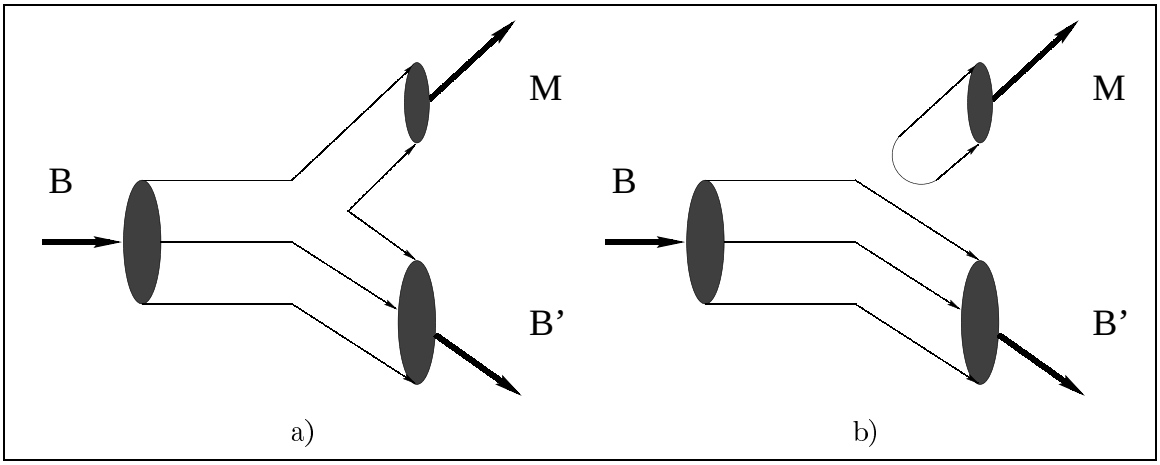

Figure 3.4: Decay of a baryon B by emission of a composite meson M (a) and OZI forbidden decay (b).

The $q\bar{q}$–pair created has the quantum numbers of the vacuum: flavor and color singlet, zero momentum and total angular momentum $J^{PC} = 0^{++}$ ($\Rightarrow L = 1, S = 1$). This translates into a transition operator:

$$\mathcal{T} = \gamma \sum_{i,j} \int d\vec{p}_q \, d\vec{p}_{\bar{q}} \, \delta(\vec{p}_q + \vec{p}_{\bar{q}}) \sum_m \left[C^{00}_{1m1-m} \mathcal{Y}^m_1(\vec{p}_q - \vec{p}_{\bar{q}}) (\chi_1^{-m} \phi_0)_{i,j} \right] b^\dagger_i(\vec{p}_q) \, d^\dagger_j(\vec{p}_{\bar{q}}), \tag{3.3-1}$$

where $\mathcal{Y}^M_L(\vec{p}) = p^L Y^M_L(\hat{p})$ is a solid harmonic function, representing the orbital structure of the $q\bar{q}$–pair wave function and ϕ_0 is the flavor singlet wave function of the pair:

$$\phi_0 = -\frac{1}{\sqrt{3}}(u\bar{u} + d\bar{d} + s\bar{s}). \tag{3.3-2}$$

Finally, χ_1^{-m} is a spin triplet wave function and γ is a dimensionless constant which represents the probability for a $q\bar{q}$–pair creation out of the vacuum. In the $^3P_0$, this probability does not depend on the

position of the three quarks, but is constant over the whole space. It is the only adjustable parameter of the model (apart from factors entering an eventual parameterization of the meson wave function). Note that in eq. (3.3-1) we have omitted a factor 3 in front of the decay constant which is frequently used to cancel a factor 1/3 coming from the matrix element of color wave functions, which are not written out explicitly here.

Note that so called OZI - forbidden diagrams (see fig. 3.4b) are in principle also present in quark-pair creation models. These do not contribute in the $^3P_0$ however, since here the created $q\bar{q}$–pair is restricted to have zero total momentum while by kinematics the emitted meson must carry a non-zero momentum which is given by eq. (3.1-11).

The matrix element for the process $B \to B'M$ is then written as:

$$\langle B'M|\mathcal{T}|B\rangle \equiv \langle B'M|H|B\rangle = 3\gamma \sum_m C^{00}_{1m1-m}\, \mathcal{I}_m(B;B'M) =: \delta(\vec{P}-\vec{P}'-\vec{q})\mathcal{A}. \tag{3.3-3}$$

Here, the factor 3 comes from the different possibilities of rearranging the quarks in the initial and final state, taking into account the symmetry of the wave functions. The momentum integral of eq. (3.3-3) takes the form

$$\begin{aligned}\mathcal{I}_m(B;B'M) \;=\; & \int d\vec{p}_1\, d\vec{p}_2\, d\vec{p}_3\, d\vec{p}_4\, d\vec{p}_5\, \mathcal{Y}^m_1(\vec{p}_4-\vec{p}_5)\; \delta(\vec{p}_4+\vec{p}_5)\; \Phi^{-m}_{pair} \\ & [\Psi_{B'}(\vec{p}_1,\vec{p}_2,\vec{p}_4)\,\Phi_{B'}]^*\,[\Psi_M(\vec{p}_3,\vec{p}_5)\,\Phi_M]^*\,[\Psi_B(\vec{p}_1,\vec{p}_2,\vec{p}_3)\,\Phi_B]\,. \end{aligned}\tag{3.3-4}$$

Here, $\vec{p}_1, \vec{p}_2, \vec{p}_3$ are the individual quark momenta of the initial baryon B that sum up to a total momentum $\vec{P} = \sum_{i=1}^3 \vec{p}_i = 0$ in the rest frame of B. The meson carries away the momentum $\vec{q} = \vec{p}_3 + \vec{p}_5$, and the residual baryon B' has momentum $\vec{P}' = \vec{p}_1 + \vec{p}_2 + \vec{p}_4 = -\vec{q}$, due to momentum conservation in the decay process. Finally, we denoted the combined spin-isospin wave functions for all resonances by Φ.

In a next step, one separates the center-of-mass and relative motions in all hadron wave functions, which allows to carry out some of the integrations in eq. (3.3-4):

$$\begin{aligned}\mathcal{I}_m \;=\; & \delta(\vec{P}-\vec{P}'-\vec{q}) \int d\vec{p}_x\, d\vec{p}_y\, \mathcal{Y}^m_1(2\vec{q}+2\vec{p}_y)\; \Phi^{-m}_{pair} \\ & \left[\Psi_{B'}(\vec{p}_x, \frac{2}{3}\vec{q}+\vec{p}_y)\,\Phi_{B'}\right]^* \left[\Psi_M(-\frac{1}{2}\vec{q}-\vec{p}_y)\,\Phi_M\right]^* [\Psi_B(\vec{p}_x,\vec{p}_y)\,\Phi_B]\,, \end{aligned}\tag{3.3-5}$$

where $\vec{p}_x = \frac{1}{2}(\vec{p}_1 - \vec{p}_2)$ and $\vec{p}_y = \frac{1}{3}(2\vec{p}_3 - \vec{p}_1 - \vec{p}_2)$ are the momenta conjugate to the Jacobi coordinates $\vec{x} = \vec{r}_{12}$ and $\vec{y} = \vec{\rho}$, as defined in eq. (B.2-7). For the meson wave function in configuration space we first adopt a simple parameterization of Gaussian type:

$$\Psi_G(\vec{r}) = \frac{1}{(\pi R^2)^{3/4}} \exp\left(-\frac{r^2}{2R^2}\right), \tag{3.3-6}$$

where the parameter R^2 is related to the relative distance of the constituent quark and anti-quark of the meson by $\langle r^2\rangle = \frac{3}{2}R^2$. The partial decay width is then obtained by

$$\Gamma = \frac{1}{\pi}\,\frac{q\,E\,\omega}{M_B}\,|\,\mathcal{A}\,|^2, \tag{3.3-7}$$

where M_B is the mass of the decaying resonance, E the energy of the final state baryon, and $\mathcal{A}$ is defined by eq. (3.3-3). In eq. (3.3-7) one still has to sum over final and to average over initial spin-isospin channels.

In order to compare the operational structure of the EEM with that of the $^3P_0$, it is most convenient to write the matrix elements in momentum space:

$$\begin{aligned}\langle B'|H|B\rangle_{EEM} = & \frac{1}{\sqrt{2\omega}}\frac{3}{(2\pi)^{3/2}}\,\frac{g}{2m}\delta^3(\vec{P}_B - \vec{P}_{B'} - \vec{q}) \\ & \int d\vec{p}_x\, d\vec{p}_y\; [\Psi_{B'}(\vec{p}_x,\vec{p}_y')\,\Phi_{B'}]^*\,\vec{\lambda}^F \left[(1+\frac{\omega}{2m})\vec{\sigma}\cdot\vec{q} + \frac{\omega}{m}\,\vec{\sigma}\cdot\vec{p}_y\right][\Psi_B(\vec{p}_x,\vec{p}_y)\,\Phi_B]\,, \end{aligned}\tag{3.3-8}$$

$$\begin{aligned}\langle B'M|H|B\rangle_{^3P_0} = & \frac{\gamma}{2\sqrt{2}}\sqrt{\frac{3}{4\pi}}\,\delta^3(\vec{P}_B - \vec{P}_{B'} - \vec{q}) \\ & \int d\vec{p}_x\, d\vec{p}_y\; [\Psi_{B'}(\vec{p}_x,\vec{p}_y')\,\Phi_{B'}]^*\,[\Psi_M(\vec{p}_y+\vec{q}/2)]^*\,\vec{\lambda}^F\vec{\sigma}\cdot(2\vec{q}+2\vec{p}_y)\,[\Psi_B(\vec{p}_x,\vec{p}_y)\,\Phi_B]\,, \end{aligned}\tag{3.3-9}$$

where $\vec{p}_y' = \vec{p}_y + \frac{2}{3}\vec{q}$ and where we also have rewritten the inner product of all the spin-isospin wave functions involved in the decay process like

$$\left(\Phi^*_{B'}\Phi^*_M\Phi^{-m}_{pair}\Phi_B\right) = \Phi^*_{B'}\frac{1}{\sqrt{6}}\,\tau^\dagger\,\frac{1}{2}\,\sigma_{-m}\,\Phi_B. \tag{3.3-10}$$

One finds that we obviously reproduce the EEM amplitudes by making the replacements:

$$\vec{\sigma}\cdot(2\vec{q}+2\vec{p}_y) \quad\longrightarrow\quad \left(1+\frac{\omega}{2m}\right)\vec{\sigma}\cdot\vec{q}+\frac{\omega}{m}\,\vec{\sigma}\cdot\vec{p}_y, \tag{3.3-11}$$

$$\gamma\frac{\sqrt{3}}{2}\,\pi \quad\longrightarrow\quad \frac{3i}{(2\omega)^{1/2}}\frac{g}{2m}, \tag{3.3-12}$$

provided the meson wave function is normalized such that $\Psi_M = 1$ in the point-like limit. These considerations have led to the introduction of a modified $^3P_0$ (M^3P_0) in ref. [86], which in addition to the replacement (3.3-11) modifies the pair-creation constant by

$$\gamma \longrightarrow \gamma\sqrt{\frac{\mu}{\omega}}. \tag{3.3-13}$$

Here μ and ω are the mass and energy of the emitted meson, respectively. Note that the factor $\sqrt{\mu/\omega}$ in eq. (3.3-13), which was motivated by a relativistic boost effect, will cancel a factor ω in the phase space element, see eq. (3.1-10), just as it was the case in the EEM. The first replacement (3.3-11) is obviously equivalent to the requirement $\frac{\omega}{2m} = 1$, which is indeed approximately fulfilled for physical decay processes, so that it does not represent a severe modification. However, the second one, eq. (3.3-13), implies a serious change in the decay constant γ, in particular, due to the small pion mass, when it comes to comparing results of $N\pi$ with $N\eta$ decay widths. This will be discussed in more detail when we present the numerical results.

The $^3P_0$ model was first introduced by Micu [27] but most extensively investigated and applied by the Orsay group [28,29,181], see also refs. [182,183]. Extensive numerical calculations for meson decays have been carried out in refs. [153,184], for a formal development of general calculations, see ref. [185].

3.3.2 Results

We first present results that are obtained within the M^3P_0 using wave functions from the different SR and NR parameterizations of the OGE and GBE dynamics, as they were partially presented in ref. [186]. These results are therefore directly comparable to the ones obtained in the EEM, see tables 3.2 and 3.3.

π decays

The results for the partial widths of the π decay modes of the N and Δ resonances are shown in table 3.5. All values have been calculated with the Gaussian-type parameterization of the meson wave function of eq. (3.3-6). For the baryons, the theoretical masses have been used as predicted by the different CQM's. In each case the strength parameter γ introduced into the decay operator has been adjusted so as to reproduce the $\Delta_{1232} \to N\pi$ decay width. All the other decay widths can then be considered as genuine predictions of the CQM's along the modified $^3P_0$ model.

Let us now examine the theoretical results in detail. For the $N_{1440}\ \frac{1}{2}^+$ resonance the SR GBE prediction is obviously too large, whereas the pertinent NR result lies within the experimental error bars. The SR OGE result overshoots the experiment by far, its NR version is also much smaller than the SR one and lies just at the lower end of the experimental error bar. The results for the next $\frac{1}{2}^+$ excitation of the nucleon, the N_{1710}, show a similar relative pattern as the ones for the Roper resonance, though all the values are smaller by about an order of magnitude. The fact that for each case, N_{1440} and N_{1710}, the predictions of the SR parameterizations of both the OGE and GBE models exceed by far their NR counterparts can be readily understood observing the higher momentum components present in the SR parameterizations, as compared to the NR ones or equivalently the smaller size of the baryon wave functions. In case of the OGE SR this effect is enhanced by a phase space that is much too large (due to the bad prediction of the resonance energy).

Table 3.5: $N^* \to N\pi$ decay widths of baryon resonances for the GBE and OGE constituent quark models both in non-relativistic and semi-relativistic parameterizations. A Gaussian-type meson wave function with $r_\pi = 0.565$ fm was used along with a modified $^3P_0$ decay model. Experimental data are from ref. [43].

$[N^{J^\pi}]_n$	N^*	$\Gamma(N^* \to N\pi)$ [MeV]				
		GBE SR	GBE NR	OGE SR	OGE NR	exp.
$[N\frac{1}{2}^+]_2$	N_{1440}	517	258	1064	161	$(227 \pm 18)^{+70}_{-59}$
$[N\frac{1}{2}^+]_3$	N_{1710}	54	14	202	8	$(15 \pm 5)^{+30}_{-5}$
$[N\frac{1}{2}^+]_4$		43	5	76	22	
$[N\frac{1}{2}^+]_5$		0	0	0	0	
$[N\frac{1}{2}^-]_1$	N_{1535}	336	75	462	109	$(67 \pm 15)^{+55}_{-17}$
$[N\frac{1}{2}^-]_2$	N_{1650}	53	5	87	8	$(109 \pm 26)^{+36}_{-3}$
$[N\frac{3}{2}^+]_1$	N_{1720}	377	100	689	238	$(23 \pm 8)^{+9}_{-5}$
$[N\frac{3}{2}^+]_2$		17	2	42	0	
$[N\frac{3}{2}^+]_3$		9	0	2	0	
$[N\frac{3}{2}^+]_4$		21	3	38	11	
$[N\frac{3}{2}^+]_5$		0	0	0	0	
$[N\frac{3}{2}^-]_1$	N_{1520}	131	161	108	168	$(66 \pm 6)^{+9}_{-5}$
$[N\frac{3}{2}^-]_2$	N_{1700}	6	6	7	9	$(10 \pm 5)^{+3}_{-3}$
$[N\frac{5}{2}^+]_1$	N_{1680}	85	85	149	313	$(85 \pm 7)^{+6}_{-6}$
$[N\frac{5}{2}^+]_2$		2	2	0	4	
$[N\frac{5}{2}^+]_3$		2	1	3	3	
$[N\frac{5}{2}^-]_1$	N_{1675}	34	35	40	52	$(68 \pm 8)^{+14}_{-4}$
$[N\frac{7}{2}^+]_1$		7	3	12	12	
$[\Delta\frac{1}{2}^+]_1$	Δ_{1910}	17	0	40	1	$(56 \pm 19)^{+6}_{-9}$
$[\Delta\frac{1}{2}^+]_2$		229	32	420	91	
$[\Delta\frac{1}{2}^-]_1$	Δ_{1620}	26	3	41	5	$(38 \pm 8)^{+8}_{-6}$
$[\Delta\frac{3}{2}^+]_1$	Δ_{1232}	120	120	120	120	$(119 \pm 1)^{+5}_{-5}$
$[\Delta\frac{3}{2}^+]_2$	Δ_{1600}	43	34	174	14	$(61 \pm 26)^{+26}_{-10}$
$[\Delta\frac{3}{2}^+]_3$	Δ_{1920}	115	16	210	45	$(25 \pm 15)^{+20}_{-3}$
$[\Delta\frac{3}{2}^+]_4$		21	3	34	11	
$[\Delta\frac{3}{2}^-]_1$	Δ_{1700}	28	29	20	38	$(45 \pm 15)^{+20}_{-10}$
$[\Delta\frac{5}{2}^+]_1$	Δ_{1905}	13	8	23	35	$(35 \pm 18)^{+13}_{-3}$
$[\Delta\frac{5}{2}^+]_2$		6	2	7	9	
$[\Delta\frac{7}{2}^+]_1$		59	37	104	160	
γ		15.365	14.635	18.015	11.868	

For the $N_{1720}\ \frac{3}{2}^+$ resonance the results again have similar characteristics, with the SR cases drastically overshooting the experimental data. Here, however, none of the NR versions can come close to the rather small experimental width. This problem was already encountered in similar analyses [80, 146] and may hint to a wrong symmetry assignment (or a strong mixing) of this state. Only for the $N_{1680}\ \frac{5}{2}^+$ resonance the GBE CQM produces correct results, both in its SR and NR versions. In this case the results from both variants of the OGE CQM are again too high.

For the negative-parity $N_{1535}\ \frac{1}{2}^-$ resonance the SR results are also much too high, whereas the predictions from the NR versions agree with experiment. For the $N_{1650}\ \frac{1}{2}^-$ the situation is just reversed. Most remarkably, in all instances the widths of the N_{1535} resonance are larger than the ones of N_{1650},

Table 3.6: $N^* \to N\eta$ decay widths of baryon resonances for the GBE and OGE constituent quark models both in non-relativistic and semi-relativistic parameterizations. A Gaussian-type meson wave function with $r_\eta = 0.565$ fm was used along with a modified $^3P_0$ decay model. Experimental data are from ref. [43].

$[N^{J^\pi}]_n$	N^*	$\Gamma(N^* \to N\eta)$ [MeV]				
		GBE SR	GBE NR	OGE SR	OGE NR	exp.
$[N\frac{1}{2}^+]_2$	N_{1440}			6	10	
$[N\frac{1}{2}^+]_3$	N_{1710}	26	4	50	10	
$[N\frac{1}{2}^+]_4$		28	8	41	19	
$[N\frac{1}{2}^+]_5$		0	0	0	1	
$[N\frac{1}{2}^-]_1$	N_{1535}	64	64	64	64	$(64 \pm 19)^{+76}_{-15}$
$[N\frac{1}{2}^-]_2$	N_{1650}	113	68	140	94	$(10 \pm 5)^{+4}_{-1}$
$[N\frac{3}{2}^+]_1$	N_{1720}	15	11	30	25	
$[N\frac{3}{2}^+]_2$		22	39	39	0	
$[N\frac{3}{2}^+]_3$		11	2	12	4	
$[N\frac{3}{2}^+]_4$		14	4	20	10	
$[N\frac{3}{2}^+]_5$		0	0	0	0	
$[N\frac{3}{2}^-]_1$	N_{1520}	0	0	0	0	
$[N\frac{3}{2}^-]_2$	N_{1700}	0	1	1	1	
$[N\frac{5}{2}^+]_1$	N_{1680}	0	1	2	6	
$[N\frac{5}{2}^+]_2$		1	1	1	3	
$[N\frac{5}{2}^+]_3$		1	0	1	2	
$[N\frac{5}{2}^-]_1$	N_{1675}	2	4	3	5	
$[N\frac{7}{2}^+]_1$		2	2	4	9	
γ		5.929	6.682	6.572	4.937	

contrary to experiment, where the N_{1535} width appears to be smaller or is at most as large as the N_{1650} width (taking into account the experimental uncertainties). Regarding the $L = 1$, $S = \frac{3}{2}$ multiplet $N_{1650} - N_{1675} - N_{1700}$, one notes that the SR parameterizations give approximately the correct ratios of these widths, as it is expected from the corresponding spin-isospin matrix elements, but this effect may be due to a sign change of the transition amplitude, which cannot be seen in the width. These features are not found for the NR parameterizations due to the exceedingly small value of the N_{1650} width.

Concerning the negative-parity N excitations, it is interesting to note that we recover in the $^3P_0$ the properties of structure-dependent and structure-independent resonances. This can be easily understood if one remembers the comparison of the $^3P_0$ with the EEM, see eqs. (3.3-8) and (3.3-9), which shows the similar structure of the decay operators. Specifically, the S-wave resonances N_{1535} and N_{1650} (and likewise also Δ_{1620}) appear to be 'structure-dependent', which results in widths sometimes orders of magnitudes apart for different models. On the other hand, the D-wave resonances N_{1520}, N_{1675}, and N_{1700} (and likewise also Δ_{1700}) are found to be 'structure-independent'. Their decay widths are practically independent of the underlying spectroscopic model.

The decay widths for the Δ resonances are practically all correct for the SR GBE CQM. In case of the other models the one or the other shortcoming appears.

η decays

Table 3.6 gives the results for η decays. Here we use the same spatial part for the meson wave function as for π decays but the constant γ is adjusted so as to reproduce the η decay width of the N_{1535} resonance. Note that this gives values for γ about a factor 3 smaller than for the π decays, in contrast to other

works [80], where the same value was employed to describe both the π and η decays. This has the following reasons:

- The replacement according to eq. (3.3-13).
- We use an unmixed flavor wave function for the η meson, i.e. a pure flavor octet state. For non-strange decays as regarded in this work, a possible mixing would only influence the normalization of this wave function, which can effectively be absorbed into the coupling constant γ.
- Our choice of phase space, as given by eq. (3.1-14). We use a fully relativistic prescription and experimental values for the meson masses, in contrast to ref. [80], where a much higher, "effective" value for the pion mass was employed.

A quick estimate of the magnitudes of these three effects shows indeed that we end up with about a factor of 3 difference in the constant γ between π and η decays.

The η widths of the Roper resonance N_{1440} for the GBE parameterizations (NR as well as SR) are rigorously zero, since in both cases the theoretically predicted masses lie below the η threshold, in accordance with experiment. For the OGE parameterizations, the decay $N_{1440} \to N\eta$ is possible, the corresponding widths remain rather small, however.

In total, there are several resonances predicted with considerable branching ratios in the η decay channel. Only for the N_{1535} and N_{1650} resonances one can compare to experiment, since these are the only ones with an experimental width assigned by the PDG [43]. The relative magnitudes of the experimental decay widths in both of these cases are missed by all theoretical models. This is again reminiscent of the EEM, where a similar effect was found. One may expect that the decays of these resonances are quite sensitive to the tensor forces in the quark-quark interaction, as it was the case in the EEM. The inclusion of these force components will be discussed in the next subsection.

In addition to N_{1535} and N_{1650}, also the widths of the N_{1710} and the N_{1720} resonances come out appreciably large. The PDG does not quote any experimental data for these states. This does not necessarily mean that their widths are vanishing or too small to be measured. It may simply be the case that experimental ambiguities do not (yet) allow for a reliable determination. In fact, there are single partial-wave analyses that assign an appreciable η decay width, for example, also to the N_{1710}, see refs. [52, 187, 188].

Results with tensor force

In table 3.7 we give the results for decay widths for the GBE model including the tensor force. Comparison with the corresponding results from the EEM, table 3.4, shows that there are very few qualitative differences. The most notable being the decays of the radial excitations, in particular the Roper resonance. Evidently, the presence of the meson wave function in the decay operator pushes the zero in the decay amplitude to much larger values of q (compare fig. 3.3), resulting in an appreciable width also for the radial excitations. Also the width of the N_{1710} resonance gets enhanced, which is unfortunate in this case, because it comes out far too large now. For the rest of the resonances, the results are indeed very similar to ones following from the EEM, even though some of the exceedingly large values of table 3.4 seem to get somewhat suppressed now. In particular, in the $N\eta$ channel, where again the right ordering of the decay widths of the N_{1535} and the N_{1650} resonances is predicted, also the width of the third $\frac{1}{2}^-$ width gets strongly reduced.

As compared to experimental data, there persist the typical problems: the $N_{1720} \to N\pi$ and the $N_{1535} \to N\pi$ widths are far too large and also the $N_{1650} \to N\eta$ is still not small enough. This may be traced back, in analogy with the analytical results of the harmonic oscillator model, see table 3.1, to the small extension of the baryon wave function, as it was discussed in the section on the EEM. The fact that we recover such a number of similarities in different decay models using different wave functions, while the simple harmonic oscillator with a larger (unphysical) value of the parameter b does relatively well, seems to be an indication for either the need of more extended wave functions or the need for a mechanism to suppress the ω-dependent terms in the decay operator.

Also the fact that the NR parameterizations apparently perform better than the SR ones (as evidenced

Table 3.7: Decay widths of N^* resonances from the GBE SR potential with tensor component in the M$^3P_0$. A Gaussian-type meson wave function with $r_\pi = r_\eta = 0.565$ fm was employed. Experimental data are from ref. [43].

$[N^{J^\pi}]_n$	N^*	$\Gamma(N^* \to N\pi)$	exp.	$\Gamma(N^* \to N\eta)$	exp.
$[N^{\frac{1}{2}^+}]_2$	N_{1440}	646	$(227 \pm 18)^{+70}_{-59}$		
$[N^{\frac{1}{2}^+}]_3$	N_{1710}	87	$(15 \pm 5)^{+30}_{-5}$	15	
$[N^{\frac{1}{2}^+}]_4$		70		0	
$[N^{\frac{1}{2}^+}]_5$		5		26	
$[N^{\frac{1}{2}^-}]_1$	N_{1535}	294	$(67 \pm 15)^{+55}_{-17}$	64	$(64 \pm 19)^{+76}_{-15}$
$[N^{\frac{1}{2}^-}]_2$	N_{1650}	176	$(109 \pm 26)^{+36}_{-3}$	33	$(10 \pm 5)^{+4}_{-1}$
$[N^{\frac{1}{2}^-}]_3$		116		10	
$[N^{\frac{1}{2}^-}]_4$		2		1	
$[N^{\frac{3}{2}^+}]_1$	N_{1720}	577	$(23 \pm 8)^{+9}_{-5}$	15	
$[N^{\frac{3}{2}^+}]_2$		33		19	
$[N^{\frac{3}{2}^+}]_3$		9		9	
$[N^{\frac{3}{2}^-}]_1$	N_{1520}	146	$(66 \pm 6)^{+9}_{-5}$	0	
$[N^{\frac{3}{2}^-}]_2$	N_{1700}	64	$(10 \pm 5)^{+3}_{-3}$	0	
$[N^{\frac{3}{2}^-}]_3$		86		3	
$[N^{\frac{3}{2}^-}]_4$		43		0	
$[N^{\frac{5}{2}^+}]_1$	N_{1680}	112	$(85 \pm 7)^{+6}_{-6}$	0	
$[N^{\frac{5}{2}^+}]_2$		1		1	
$[N^{\frac{5}{2}^+}]_3$		9		0	
$[N^{\frac{5}{2}^-}]_1$	N_{1675}	61	$(68 \pm 8)^{+14}_{-4}$	2	
$[N^{\frac{7}{2}^+}]_1$		14		2	
$[\Delta^{\frac{1}{2}^+}]_1$	Δ_{1910}	327	$(56 \pm 19)^{+6}_{-9}$		
$[\Delta^{\frac{1}{2}^+}]_2$		360			
$[\Delta^{\frac{1}{2}^-}]_1$	Δ_{1620}	22	$(38 \pm 8)^{+8}_{-6}$		
$[\Delta^{\frac{3}{2}^+}]_1$	Δ_{1232}	120	$(119 \pm 1)^{+5}_{-5}$		
$[\Delta^{\frac{3}{2}^+}]_2$	Δ_{1600}	87	$(61 \pm 26)^{+26}_{-10}$		
$[\Delta^{\frac{3}{2}^+}]_3$	Δ_{1920}	297	$(25 \pm 15)^{+20}_{-3}$		
$[\Delta^{\frac{3}{2}^+}]_4$		56			
$[\Delta^{\frac{3}{2}^-}]_1$	Δ_{1700}	41	$(45 \pm 15)^{+20}_{-10}$		
$[\Delta^{\frac{5}{2}^+}]_1$	Δ_{1905}	15	$(35 \pm 18)^{+13}_{-3}$		
$[\Delta^{\frac{5}{2}^+}]_2$		12			
	γ	16.525		4.80	

by a simple χ^2 error estimate) hints into the same direction, since the NR wave functions are still a bit larger tan the SR ones, see table 2.4.

The two $\Delta^{\frac{1}{2}^-}$ states, which are very close in energy, compare fig. 2.9, will be difficult to distinguish just by their decay properties: their $N\pi$ widths are very similar in the $^3P_0$ and in the EEM, and in any case much larger than the experimental value of the state Δ_{1910}. On the other hand, the results for $N\pi$ widths of the $\Delta^{\frac{1}{2}^+}$ above the Δ_{1600} resonance seem to indicate that the empirical state Δ_{1920} is rather to be identified with the $[\Delta^{\frac{1}{2}^+}]_4$ state.

Table 3.8: Same as table 3.5 but using a Yukawa-type meson wave function with $r_\pi = 0.565$ fm.

$[N^{J^\pi}]_n$	N^*	$\Gamma(N^* \to N\pi)$ [MeV]				
		GBE SR	GBE NR	OGE SR	OGE NR	exp.
$[N\frac{1}{2}^+]_2$	N_{1440}	528	363	1015	204	$(227 \pm 18)^{+70}_{-59}$
$[N\frac{1}{2}^+]_3$	N_{1710}	59	10	179	7	$(15 \pm 5)^{+30}_{-5}$
$[N\frac{1}{2}^+]_4$		29	3	56	12	
$[N\frac{1}{2}^+]_5$		0	0	0	0	
$[N\frac{1}{2}^-]_1$	N_{1535}	251	31	412	61	$(67 \pm 15)^{+55}_{-17}$
$[N\frac{1}{2}^-]_2$	N_{1650}	39	1	78	3	$(109 \pm 26)^{+36}_{-3}$
$[N\frac{3}{2}^+]_1$	N_{1720}	276	58	545	132	$(23 \pm 8)^{+9}_{-5}$
$[N\frac{3}{2}^+]_2$		16	4	33	0	
$[N\frac{3}{2}^+]_3$		6	0	2	0	
$[N\frac{3}{2}^+]_4$		15	1	28	6	
$[N\frac{3}{2}^+]_5$		0	0	0	0	
$[N\frac{3}{2}^-]_1$	N_{1520}	140	225	109	187	$(66 \pm 6)^{+9}_{-5}$
$[N\frac{3}{2}^-]_2$	N_{1700}	6	7	7	9	$(10 \pm 5)^{+3}_{-3}$
$[N\frac{5}{2}^+]_1$	N_{1680}	98	144	158	379	$(85 \pm 7)^{+6}_{-6}$
$[N\frac{5}{2}^+]_2$		2	2	0	4	
$[N\frac{5}{2}^+]_3$		2	1	3	3	
$[N\frac{5}{2}^-]_1$	N_{1675}	35	42	40	55	$(68 \pm 8)^{+14}_{-4}$
$[N\frac{7}{2}^+]_1$		9	5	13	15	
$[\Delta\frac{1}{2}^+]_1$	Δ_{1910}	16	1	32	0	$(56 \pm 19)^{+6}_{-9}$
$[\Delta\frac{1}{2}^+]_2$		158	14	317	40	
$[\Delta\frac{1}{2}^-]_1$	Δ_{1620}	20	1	39	2	$(38 \pm 8)^{+8}_{-6}$
$[\Delta\frac{3}{2}^+]_1$	Δ_{1232}	120	120	120	120	$(119 \pm 1)^{+5}_{-5}$
$[\Delta\frac{3}{2}^+]_2$	Δ_{1600}	41	49	142	11	$(61 \pm 26)^{+26}_{-10}$
$[\Delta\frac{3}{2}^+]_3$	Δ_{1920}	79	7	158	20	$(25 \pm 15)^{+20}_{-3}$
$[\Delta\frac{3}{2}^+]_4$		14	1	26	6	
$[\Delta\frac{3}{2}^-]_1$	Δ_{1700}	28	35	21	40	$(45 \pm 15)^{+20}_{-10}$
$[\Delta\frac{5}{2}^+]_1$	Δ_{1905}	15	13	24	42	$(35 \pm 18)^{+13}_{-3}$
$[\Delta\frac{5}{2}^+]_2$		7	4	8	11	
$[\Delta\frac{7}{2}^+]_1$		67	60	109	188	
	γ	15.931	14.741	18.854	11.961	

3.3.3 Influence of the Meson Wave Function

The $^3P_0$ decay model has two decisive ingredients: the pair-creation strength γ and the parameter determining the extension of the meson wave function. While the former is merely a multiplicative constant, which may be suitably chosen to scale the overall strength of all decays, the latter is a nonlinear parameter, which may also alter the relative magnitudes of various widths. In the following we consider certain different choices of the meson wave functions and examine their influences on the decay widths.

The wave function of Gaussian type (3.3-6) that has been used so far has the advantage of facilitating the calculations, but it certainly cannot be regarded as a realistic representation of a meson wave function. From the Fourier transform of the electromagnetic pion form factor, one can deduce a pion wave function

Table 3.9: Same as table 3.6 but using a Yukawa-type meson wave function with $r_\eta = 0.565$ fm.

$[N^{J^\pi}]_n$	N^*	$\Gamma(N^* \to N\eta)$ [MeV]				
		GBE SR	GBE NR	OGE SR	OGE NR	exp.
$[N\frac{1}{2}^+]_2$	N_{1440}			6	15	
$[N\frac{1}{2}^+]_3$	N_{1710}	32	7	51	14	
$[N\frac{1}{2}^+]_4$		24	6	34	15	
$[N\frac{1}{2}^+]_5$		0	0	0	1	
$[N\frac{1}{2}^-]_1$	N_{1535}	64	64	64	64	$(64 \pm 19)^{+76}_{-15}$
$[N\frac{1}{2}^-]_2$	N_{1650}	110	59	138	86	$(10 \pm 5)^{+4}_{-1}$
$[N\frac{3}{2}^+]_1$	N_{1720}	14	11	25	22	
$[N\frac{3}{2}^+]_2$		25	57	25	0	
$[N\frac{3}{2}^+]_3$		10	1	37	3	
$[N\frac{3}{2}^+]_4$		12	3	17	7	
$[N\frac{3}{2}^+]_5$		0	0	0	0	
$[N\frac{3}{2}^-]_1$	N_{1520}	0	1	0	1	
$[N\frac{3}{2}^-]_2$	N_{1700}	1	1	1	1	
$[N\frac{5}{2}^+]_1$	N_{1680}	1	2	2	10	
$[N\frac{5}{2}^+]_2$		2	1	2	4	
$[N\frac{5}{2}^+]_3$		1	1	1	3	
$[N\frac{5}{2}^-]_1$	N_{1675}	3	6	3	7	
$[N\frac{7}{2}^+]_1$		3	3	5	13	
γ		6.608	7.022	7.056	5.469	

that takes a Yukawa-like form (see ref. [86]):

$$\Psi_Y(\vec{r}) = \frac{1}{\sqrt{4\pi}} \frac{m}{\sqrt{r}} \exp\left(-\frac{mr}{2}\right). \tag{3.3-14}$$

Here the parameter m is related to the relative distance of the constituent quark and anti-quark of the meson by $\langle r^2 \rangle = 6/m^2$. Even if it is not physically meaningful, this expression may serve as a comparison to the Gaussian form.

A graphical representation of the meson wave functions is given in fig. 3.5, where we compare the above forms to the wave function that follows from the original potential of Bhaduri et al. [84,85]. It can be seen that the exact wave function lies just between the extreme choices of a Yukawa and a Gaussian form. The parameters of eqs. (3.3-6) and (3.3-14) have been fitted to give the same root mean square radius for the pion as the wave function from the potential of refs. [84, 85], that is $r_\pi = 0.565$ fm. For simplicity we use the same parameterization for the wave function of the η meson.

In tables 3.8 and 3.9 we show results for decay widths when employing a Yukawa-like meson wave function, as given by eq. (3.3-14), producing the same meson size as the Gaussian parameterization before. We have adjusted the parameter γ again to fit the Δ and N_{1535} widths for $N\pi$ and $N\eta$ decays, respectively. However, as compared to table 3.5, the values change only little in this case.

By comparing the results in tables 3.5, 3.6 and 3.8, 3.9 it is immediately seen that the specific form of the meson wave function has only a minor influence on the predictions of the decay widths for the π as well as η decay modes. The qualitative features remain essentially unchanged. We have also performed calculations with the exact meson wave function produced by the potential of Bhaduri et al. (as shown in fig. 3.5). They confirm the conclusion that the type of meson wave function is not decisive, provided its extension (meson radius) is kept the same.

We now focus the attention on the dependence of the results on the size of the meson. The meson

Table 3.10: Same as table 3.5 but using a Gaussian-type meson wave function with $r_\pi = 0.36$ fm.

$[N^{J^\pi}]_n$	N^*	$\Gamma(N^* \to N\pi)$ [MeV]				
		GBE SR	GBE NR	OGE SR	OGE NR	exp.
$[N^{\frac{1}{2}^+}]_2$	N_{1440}	240	69	546	44	$(227 \pm 18)^{+70}_{-59}$
$[N^{\frac{1}{2}^+}]_3$	N_{1710}	6	13	63	26	$(15 \pm 5)^{+30}_{-5}$
$[N^{\frac{1}{2}^+}]_4$		53	4	113	30	
$[N^{\frac{1}{2}^+}]_5$		0	0	0	0	
$[N^{\frac{1}{2}^-}]_1$	N_{1535}	584	106	953	195	$(67 \pm 15)^{+55}_{-17}$
$[N^{\frac{1}{2}^-}]_2$	N_{1650}	122	14	227	28	$(109 \pm 26)^{+36}_{-3}$
$[N^{\frac{3}{2}^+}]_1$	N_{1720}	489	85	1063	352	$(23 \pm 8)^{+9}_{-5}$
$[N^{\frac{3}{2}^+}]_2$		2	3	9	0	
$[N^{\frac{3}{2}^+}]_3$		7	1	3	0	
$[N^{\frac{3}{2}^+}]_4$		26	2	56	15	
$[N^{\frac{3}{2}^+}]_5$		0	0	0	0	
$[N^{\frac{3}{2}^-}]_1$	N_{1520}	89	88	81	137	$(66 \pm 6)^{+9}_{-5}$
$[N^{\frac{3}{2}^-}]_2$	N_{1700}	4	4	5	8	$(10 \pm 5)^{+3}_{-3}$
$[N^{\frac{5}{2}^+}]_1$	N_{1680}	50	41	93	226	$(85 \pm 7)^{+6}_{-6}$
$[N^{\frac{5}{2}^+}]_2$		1	1	0	3	
$[N^{\frac{5}{2}^+}]_3$		1	0	1	2	
$[N^{\frac{5}{2}^-}]_1$	N_{1675}	26	22	32	46	$(68 \pm 8)^{+14}_{-4}$
$[N^{\frac{7}{2}^+}]_1$		3	1	6	7	
$[\Delta^{\frac{1}{2}^+}]_1$	Δ_{1910}	2	1	9	8	$(56 \pm 19)^{+6}_{-9}$
$[\Delta^{\frac{1}{2}^+}]_2$		318	32	683	158	
$[\Delta^{\frac{1}{2}^-}]_1$	Δ_{1620}	61	8	106	16	$(38 \pm 8)^{+8}_{-6}$
$[\Delta^{\frac{3}{2}^+}]_1$	Δ_{1232}	120	120	120	120	$(119 \pm 1)^{+5}_{-5}$
$[\Delta^{\frac{3}{2}^+}]_2$	Δ_{1600}	0	2	24	63	$(61 \pm 26)^{+26}_{-10}$
$[\Delta^{\frac{3}{2}^+}]_3$	Δ_{1920}	159	16	342	79	$(25 \pm 15)^{+20}_{-3}$
$[\Delta^{\frac{3}{2}^+}]_4$		26	2	53	15	
$[\Delta^{\frac{3}{2}^-}]_1$	Δ_{1700}	21	18	17	34	$(45 \pm 15)^{+20}_{-10}$
$[\Delta^{\frac{5}{2}^+}]_1$	Δ_{1905}	8	4	14	26	$(35 \pm 18)^{+13}_{-3}$
$[\Delta^{\frac{5}{2}^+}]_2$		3	1	4	5	
$[\Delta^{\frac{7}{2}^+}]_1$		36	18	64	115	
γ		20.575	20.695	22.699	17.997	

wave functions employed in tables 3.5 and 3.8 both correspond to a radius of $r_\pi = 0.565$ fm. In the limit $r_\pi \to 0$ one expects to reproduce the results of the EEM. Thus it is interesting to look at an intermediate regime. Tables 3.10 and 3.11 give the decay widths for the same case as in tables 3.5 and 3.6 but for a Gaussian-type wave function leading to a meson radius as small as 0.36 fm.

First we note that the values for the constant γ obtained in this case are considerably larger than before. This is understandable, since in order to recover the results of the point-like meson limit, one has to compensate for the effect of the δ-function, which then replaces the meson wave function. In particular, for the Gaussian form of eq. (3.3-6) one has the relation

$$(2\pi)^{\frac{3}{2}}\delta(\vec{r}) = \lim_{R\to 0}\left(\frac{\pi}{R^2}\right)^{\frac{3}{4}}\Psi_G(\vec{r}). \qquad (3.3\text{-}15)$$

Table 3.11: Same as table 3.6 but using a Gaussian-type meson wave function with $r_\eta = 0.36$ fm.

$[N^{J^\pi}]_n$	N^*	$\Gamma(N^* \to N\eta)$ [MeV]				
		GBE SR	GBE NR	OGE SR	OGE NR	exp.
$[N\frac{1}{2}^+]_2$	N_{1440}			2	4	
$[N\frac{1}{2}^+]_3$	N_{1710}	9	1	18	4	
$[N\frac{1}{2}^+]_4$		24	6	36	22	
$[N\frac{1}{2}^+]_5$		0	0	0	1	
$[N\frac{1}{2}^-]_1$	N_{1535}	64	64	64	64	$(64 \pm 19)^{+76}_{-15}$
$[N\frac{1}{2}^-]_2$	N_{1650}	128	80	156	109	$(10 \pm 5)^{+4}_{-1}$
$[N\frac{3}{2}^+]_1$	N_{1720}	12	8	24	23	
$[N\frac{3}{2}^+]_2$		8	15	14	0	
$[N\frac{3}{2}^+]_3$		9	1	10	5	
$[N\frac{3}{2}^+]_4$		12	3	18	11	
$[N\frac{3}{2}^+]_5$		0	0	0	0	
$[N\frac{3}{2}^-]_1$	N_{1520}	0	0	3	0	
$[N\frac{3}{2}^-]_2$	N_{1700}	0	0	0	1	
$[N\frac{5}{2}^+]_1$	N_{1680}	0	0	1	3	
$[N\frac{5}{2}^+]_2$		1	0	0	1	
$[N\frac{5}{2}^+]_3$		0	0	0	1	
$[N\frac{5}{2}^-]_1$	N_{1675}	1	2	1	3	
$[N\frac{7}{2}^+]_1$		1	1	2	5	
γ		6.844	10.060	6.430	6.619	

Most of the results for decay widths are now rather different. They follow the general trend towards the predictions typical for the EEM, in particular the small decay width of the Roper resonance, as the first radial excitation of the nucleon. The results of table 3.10 show the corresponding trend rather clearly: for all spectroscopic models the N_{1440} widths come out at least a factor of 2 smaller than before, while one is still rather far away from the point-like limit.

Concerning the η decays one observes that the differences in the widths between the N_{1535} and N_{1650} resonances now increase in all cases. Again this follows the (unpleasant) trend towards the predictions typical for the EEM. As a result it appears favorable to use a decay model that permits the use of meson wave functions with finite extensions.

As a general conclusion from this study one can say that the introduction of a finite size meson wave function in the decay operator does not lead to a striking improvement in predictions for decay widths. The qualitative features of the decay predictions remain mostly the same as in the elementary emission model. The only difference concerns the decay of the radial excitation, the Roper resonance, which in the $^3P_0$ naturally obtains a large width, but this seems possible also in the EEM with more extended wave functions (compare the results in the harmonic oscillator case, table 3.1). Taking into account in addition, that the p^2 component in the decay operator of the EEM, see eq. (3.2-10), that was neglected in all the calculations presented in this work, evidently breaks the orthogonality argument, one is left wondering whether the $^3P_0$ really represents an improvement that is worthwhile to maintain. This is in particular the case if one remembers that the way it was presented here, the $^3P_0$ is based on purely intuitive grounds and lacks a firm theoretic foundation. Further modifications of the corresponding operator, including a form factor [80] or factors $1/E$ [166] have been considered with some success but no spectacular improvement.

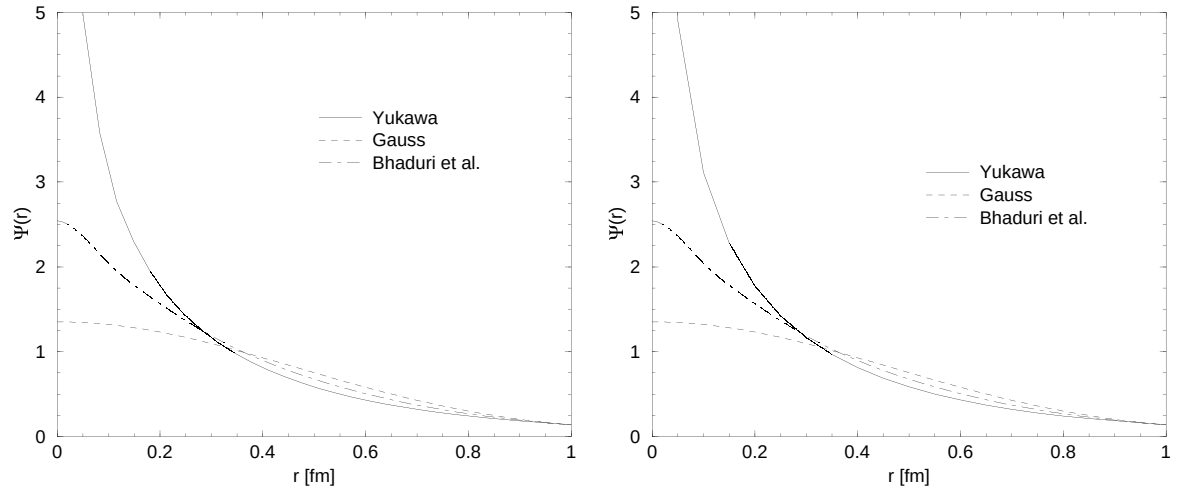

Figure 3.5: Meson wave functions in momentum (left) and configuration space (right). Gaussian and Yukawa forms are compared to the exact wave function following from the original quark-antiquark potential of Bhaduri et al. [84,85].

Numerical accuracy

The question concerning the accuracy of the numerical method employed to solve the three-body Schrödinger equation has been addressed already in the chapter on constituent quark models. While it is often possible to get rather good estimates of resonance masses with relatively simple trial wave functions, the calculation of transition amplitudes is a much more delicate matter. To illustrate this, we compare in table 3.12 results that were obtained employing the hyperspherical harmonics (HH) expansion method for obtaining the baryon wave functions with those resulting from wave functions obtained by the stochastic variational method. The first ones were published in ref. [86], where also a more detailed discussion of the method may be found.

Table 3.12: Comparison of decay widths calculated with wave functions obtained by the stochastic variational (SVM) and the hyperspherical harmonics (HH) method (from ref. [86]) in the OGE NR model. Column A gives the full results of the stochastic variational method, in column B, only the totally symmetric component of the nucleon spatial wave function has been retained.

	Results in the EEM			**Results in the $^3P_0$**			
	SVM		HH	SVM		HH.	exp.
	A	B		A	B		
$N(1440) \to N\pi$	3.02	2.4	3.4	503	525	452	$(227 \pm 18)^{+70}_{-59}$
$N(1520) \to N\pi$	80.5	64.5	64.1	340	295	268	$(66 \pm 6)^{+9}_{-5}$
$N(1535) \to N\pi$	135	208	237	307	402	429	$(67 \pm 15)^{+55}_{-17}$
$N(1650) \to N\pi$	25	46.7	47.9	14.5	44	49.1	$(109 \pm 26)^{+36}_{-3}$
$N(1700) \to N\pi$	5.7	4.08	4.07	23	19	11.5	$(10 \pm 5)^{+3}_{-3}$
$\Delta(1232) \to N\pi$	84	81	79.5	156	157	167	$(119 \pm 1)^{+5}_{-5}$
$\Delta(1600) \to N\pi$	22.2	19.9	20.1	30	19.5	19.8	$(61 \pm 26)^{+26}_{-10}$

It is seen that the results differ quite appreciably between the exact solutions of the SVM (column A) and the HH. In particular for the "structure-dependent" resonances N_{1535} and N_{1650} there appear differences of up to a factor two in the partial widths, which are certainly much larger than the differences

in the predicted masses of the same resonances, which are of the order of some MeV. In order to explain these discrepancies we have calculated the same widths but with a nucleon wave function projected onto its symmetric spin-isospin component. It is seen immediately that the encountered differences are explained by that procedure, indicating that the symmetric part of the nucleon wave function has not been determined precisely enough in ref. [86]. This statement does not concern the principal numerical accuracy of the HH method, but it shows that one has to carefully check the convergence, since obviously, in ref. [86], the expansion in hyperspherical harmonics has been truncated too early. More importantly, this shows that there are certain resonances whose decay widths are especially sensible to a precise numerical solution.

Even though the encountered differences do not change the qualitative conclusions, one should keep in mind that there exist evidently resonances for which it is more important to have a precise solution of the Schrödinger equation than for others. In particular, this concerns once again the structure dependent resonances, whose decay widths are strongly dependent on the form of the nucleon wave function, as evidenced by table 3.12.

The accuracy of the SVM has also been checked by calculations of electromagnetic form factors at high q^2 [189] in constituent quark models, see ref. [190] for an exhaustive discussion.

3.3.4 On the Fourth P_{11} Nucleon Resonance

Generally, constituent quark models predict four P_{11} excited states of the nucleon below or around 2 GeV which are predominantly part of the $N = 2$ band in a harmonic-oscillator basis (see table 2.1). The lightest of these states with a totally symmetric spatial wave function is usually attributed to the Roper resonance, the first radial excitation of the nucleon. Its low mass has presented some problems for conventional CQM's, based on one-gluon exchange (OGE) dynamics, as discussed before, as these models are not able to describe the right level ordering of positive and negative parity states [120]. The second excitation, with a spatial wave function of mixed symmetry, is attributed to the N_{1710} resonance, an identification that is confirmed by studies of decay amplitudes with a specific decay operator [75]. The third state predicted is an orbital momentum $L = 2$ state with quark spin $3/2$ and a mixed symmetric spatial wave function while the fourth is a $L = 1$ state with quark spin $1/2$. The latter one has a totally anti-symmetric spatial wave function and is therefore naturally expected to be the heaviest of these resonances with a weak coupling to the πN decay channel.

The last two states were not found yet by any partial wave analysis, a fact that constitutes part of the problem of "missing states" [175], i.e. the fact that constituent quark models generally predict more states than observed. In ref. [191] it was argued that the lighter of these missing states in the $N = 2$ band can be identified with the fourth P_{11} resonance that was discovered by the Zagreb group in their partial wave analysis based on a multi-channel, multi-resonance, unitary model [52]. It was pointed out that the crucial element for finding this resonance is the fit to the $\pi N \to \eta N$ data, which was carried out with great care in ref. [52]. Results for partial decay widths in the strong decay channels πN, ηN and $\pi\pi N$, as calculated in ref. [80] in a relativized version of a model based on OGE dynamics, were given to confirm the identification. We redisplay these results in table 3.13 together with the experimental results from ref. [52].

It can be seen, that the first OGE state that could correspond to the new solution found by the Zagreb group at $M \simeq 1740$ MeV is the state at $M = 1880$ MeV. A feature that was not discussed in ref. [191] is the fact that the model based on OGE predicts this state to decay more strongly into $N\eta$ than into $N\pi$, a situation that seems to be contradicted by the experimental results (even though one should consider the large error bars in this case).

The fourth state at $M = 1975$ MeV is the totally anti-symmetric and the heaviest one in the $N = 2$ band, as expected. Its weak coupling to the decay channels was used in particular to explain why it has not been seen in any partial wave analysis yet.

The first OGE state in the $N = 4$ band appears at $M = 2065$ MeV and it was assigned to the $P_{11}(N_{2100})$ state of the Particle Data Group [43], which, however, has the status of a 1-star resonance only. Its decay properties are very similar to those of the Roper resonance which indicates the same structure for these two states. However, as for the relative strength of decay amplitudes in the πN and ηN channels, the wrong ordering is again predicted by the OGE as compared to the solution of the

Table 3.13: P_{11}-resonance parameters from different quark models. The first column gives the assignment of the Particle Data Group (PDG, ref. [43]), OGE is from ref. [80], GBE are present results from table 3.7 and the experimental data correspond to the four P_{11}-resonance solution of ref. [52]. For the latter ones we also give the uncertainties in the total width that have to be added to the uncertainty in the partial decay width (the numbers in parentheses). All numbers in MeV.

	OGE			GBE			exp.		
PDG state	Mass	Γ_π	Γ_η	Mass	Γ_π	Γ_η	Mass	Γ_π	Γ_η
$P_{11}(1440)$	1540	412	0	1443	646	0	1439 ± 19	$(271 \pm 18)^{+93}_{-81}$	$(0 \pm 0)^{+0}_{-0}$
$P_{11}(1710)$	1770	18	67	1770	87	15	1729 ± 16	$(40 \pm 40)^{+11}_{-0}$	$(11 \pm 11)^{+6}_{-0}$
P_{11}	1880	8	28	1874	70	0	1740 ± 11	$(39 \pm 39)^{+24}_{-0}$	$(17 \pm 13)^{+5}_{-1}$
P_{11}	1975	4	0	1970	5	26	-	-	-
$P_{11}(2100)$	2065	59	3	2104	4	14	2157 ± 42	$(57 \pm 17)^{+19}_{-11}$	$(295 \pm 18)^{+77}_{-69}$

Zagreb analysis. In fact, just from the decay widths, one would rather guess that this state corresponds to the new solution of the Zagreb group at $M \simeq 1740$ MeV, an identification that is hardly possible in this model because of the large mass of this state in the OGE.

The masses of the lightest resonances in the P_{11} channel predicted by the GBE model with tensor force are redisplayed in table 3.13 and it can be seen that, apart from the Roper resonance, which is better described by the GBE, they correspond almost exactly to the masses of the OGE model. The decay properties are rather different however, as it was first pointed out and discussed in ref. [192].

First we note that for the N_{1710} resonance the GBE model predicts $\Gamma_\eta < \Gamma_\pi$, contrary to the OGE model but in qualitative agreement with the experimental result of the Zagreb analysis. A similar difference appears for the next P_{11} resonance, where again the GBE reproduces roughly the experimental pattern of decay amplitudes, whereas the OGE predicts the opposite ordering.

In order to explain these qualitative differences we have to consider the symmetry structure of the resonances as they are displayed in table 2.7. It is seen immediately, that the GBE state at $M = 1874$ MeV cannot be identified with any of the remaining states in the $N = 2$ band, since it is an almost pure $L = 0$ state. It rather corresponds to the predominantly symmetric solution in the $N = 4$ band, i.e. the second radial excitation of the nucleon after the Roper resonance. The properties of the Goldstone-boson exchange dynamics lead to a strong attraction in symmetric components of the wave function, a property that explained already the low mass of the Roper resonance in this model.

We see also from table 3.13 that the decay properties correspond almost exactly to those of the $N = 4$ state in the OGE model. In particular, we predict the fourth P_{11} resonance to decay more strongly into $N\pi$ than into $N\eta$, as it was found for the new resonance in the Zagreb analysis.

The last two GBE states given in table 3.13 are found to be almost 50% - mixtures of the $L = 2$, $S = 3/2$ and $L = 1$, $S = 1/2$ components. These ones receive a repulsive contribution from the GBE interaction, because they contain quark pairs with anti-symmetric spin-flavor wave functions. This enhances the effect of level inversion with the symmetric state in the $N = 4$ band.

Due to the different symmetry structure it is also expected that they should have smaller branching fractions into the $N\pi$ channel than the lower P_{11} resonances, a feature that is shared with the OGE predictions for the corresponding states. A qualitative difference between the two models again occurs when comparing the $N\eta$ with the $N\pi$ widths: both these resonances give $\Gamma_\eta > \Gamma_\pi$ in the GBE, a relation that is also satisfied by the state at ~ 2157 MeV found in the Zagreb analysis, but contradicted by the predictions of the OGE. This feature is a consequence of the strong mixing of these two states, as evidenced in table 2.7. In fact, the main contribution to the decay widths for both of them comes from the $L = 2$, $S = 3/2$ component which explains their similar decay properties as opposed to the OGE model.

It should be stressed that the inversion of states discussed above is also found in different parameterizations of the GBE interaction. We have checked in particular that in the models of ref. [108,148] as

well as ref. [104, 105], it is always the mainly symmetric state that follows the N_{1710} resonance. A good description of the Roper resonance has also been obtained in a model including a three-body force [89]. Since this one acts mainly on the nucleon and its radial excitations while producing essentially no effect on states with mixed symmetry, one may expect a similar inversion in the upper part of the spectrum as in the GBE model. Unfortunately, calculations of decay widths as presented in ref. [86] do not include the states of interest here.

In addition to πN and ηN widths, also results for the $\pi\pi N$ channel were given in ref. [80] and compared to the results of the Zagreb group. We did not repeat these calculations in the GBE model because of some theoretical ambiguities associated with the determination of a decay operator for quasi-two-body decays [155]. Furthermore the branching fractions extracted from the PWA depend sensitively on the input data of $\pi N \to \pi\pi N$ reactions, but the inelastic data in channels like $\pi\Delta$, ρN, etc., were not explicitly included in the analysis of the Zagreb group [52].

In all the considerations presented above, one has to bear in mind the rather large uncertainties of experimental data which prevents one from drawing definite conclusions about the quality of predictions from any CQM for the moment. However, the inversion of states in the GBE model is a unique and distinguishing feature leading to qualitatively different predictions of decay properties. This would permit a definite discrimination of different models, once the experimental data are determined with sufficient accuracy.

In summary, it was pointed out that the states that are predicted by models based on OGE and GBE dynamics at almost the same mass of $M \simeq 1880$ MeV do not correspond to the same SU(6) $\otimes$ O(3) state in a harmonic oscillator basis. As a consequence they show very different decay properties. In particular, predictions for decay widths using wave functions stemming from GBE dynamics are in qualitative agreement with the recent PWA of ref. [52]. Differences with predictions from the OGE model may allow a discrimination between the two models, which is not possible at the moment due to rather large experimental uncertainties. Clearly, a more precise determination of the resonance parameters discussed in this paper is needed to definitely settle the issue.

3.3.5 The Quest for Foundations of the $^3P_0$

We briefly outline in this section some points that may illuminate the theoretical foundation of the $^3P_0$ model.

In ref. [193] it was noted that if one regards the decay process as due to an interaction Hamiltonian involving Dirac fields

$$H_I = g \int d\vec{x}\, \bar{\Psi}\, \Psi, \tag{3.3-16}$$

then one finds that this gives in the non-relativistic limit identical matrix elements as the $^3P_0$, provided one identifies

$$\gamma = \frac{g}{2m}. \tag{3.3-17}$$

The term of eq. (3.3-16) corresponds just to a mass term in the Hamiltonian (after diagonalization) if $g = m$, so eq. (3.3-17) would imply $\gamma = \frac{1}{2}$. Curiously, this is almost exactly the value that is found from fitting certain decay widths[1] (see eq. (17) in ref. [193], the fit in ref. [153] gave $\gamma \simeq 0.4$).

This suggests that the decay process is mainly due to the pair-creation component of the mass term in the Hamiltonian, and therefore independent of the interaction that is responsible for the binding of the constituents. One would only expect corrections from relativistic effects. It was noted [194] that the Feynman diagram for the decay process depicted in fig. 3.4 gives, in a specific non-relativistic reduction scheme, a transition matrix element between hadron wave functions that resembles the operational structure of the $^3P_0$. This should not be too surprising however, since the $^3P_0$ model was designed by hand to mimic certain of the features following from a field theoretic description.

A phenomenological study of strong decays with a "hybrid" decay operator, that is a linear superposition of the EEM, eq. (3.2-11) and the $^3P_0$, eq. (3.3-1), operators, has not given a significant

[1] This value of γ should not be compared with the numerical values found in this work since they were obtained from meson decays instead of baryon decays and also because of different conventions and definitions.

improvement [195]. The possibility that the $q\bar{q}$–pair is created with different quantum numbers than in the $^3P_0$ (specifically with $^3S_1$ quantum numbers, which is inspired by a flux-tube breaking mechanism) seems to be ruled out by the data [196].

The Flux-Tube Model

In the $^3P_0$ model, the amplitude for creation of a $q\bar{q}$–pair is constant over the whole space. This seems to be an oversimplification, since from intuition one would expect the pair-creation process to take place preferably somewhere between two quarks when they are pulled apart. Furthermore, the probability for pair creation should raise with the inter-quark distance. The flux tube model may be regarded as a generalization of the $^3P_0$ model for the case where the pair-creation constant γ depends on the quark configuration of the decaying resonance.

The flux tube picture has been introduced in ref. [107], see also refs. [152,154], and extensively applied by Stancu and co-workers [159] for the decays of baryon resonances. To gain some qualitative insight into the differences with the $^3P_0$ model, we write the most general form of the pair-creation amplitude in configuration space as

$$\gamma(\vec{x},\vec{y},\vec{z}) = \frac{1}{(2\pi)^{3/2}} \int d\vec{p}_x\, d\vec{p}_y\, d\vec{p}_z\, e^{-i\vec{p}_x\cdot\vec{x} - i\vec{p}_y\cdot\vec{y} - i\vec{p}_z\cdot\vec{z}}\, \gamma(\vec{p}_x,\vec{p}_y,\vec{p}_z), \tag{3.3-18}$$

where the first two arguments denote the internal Jacobi coordinates of the three-quark system and the last one the absolute position of the pair-creation process. The spatial part of the flux tube operator matrix element is then written as

$$\begin{aligned} \mathcal{I}^\mu &= \frac{1}{(2\pi)^{3/2}} \int d\vec{x}\, d\vec{y}\, d\vec{z}\, d\vec{r}\, \gamma(\vec{x},\vec{y},\vec{r})\, \Psi^*_{B'}(\vec{x},\vec{y})\, \Psi^*_M(\vec{y}-\vec{z})\, e^{-i\frac{2}{3}\vec{q}\cdot\vec{y}}\, e^{i\frac{\vec{q}}{2}\cdot(\vec{y}-\vec{z})}\, \mathcal{Y}^\mu_1(-2\vec{q}-2\vec{p}_z)\, \Psi_B(\vec{x},\vec{z}) \\ &= \frac{1}{(2\pi)^{3/2}} \int d\vec{p}_x\, d\vec{p}_y\, d\vec{p}_1\, d\vec{p}_2\, \gamma(\vec{p}_x-\vec{p}_1,\vec{p}_2,0) \\ &\qquad \Psi^*_{B'}(\vec{p}_x,\vec{p}_y+\vec{p}_2+\frac{2}{3}\vec{q})\Psi^*_M(-\vec{p}_y-\frac{\vec{q}}{2})\, \mathcal{Y}^\mu_1(-2\vec{q}-2\vec{p}_y)\, \Psi_B(\vec{p}_1,\vec{p}_y). \end{aligned} \tag{3.3-19}$$

This can be compared to the corresponding quantity of the $^3P_0$ model:

$$\mathcal{I}^\mu = \frac{\gamma}{(2\pi)^{3/2}} \int d\vec{p}_x d\vec{p}_y\, \Psi^*_{B'}(\vec{p}_x,\vec{p}_y+\frac{2}{3}\vec{q})\, \Psi^*_M(-\vec{p}_y-\frac{\vec{q}}{2})\, \mathcal{Y}^\mu_1(-2\vec{q}-2\vec{p}_y)\, \Psi_B(\vec{p}_x,\vec{p}_y). \tag{3.3-20}$$

It is seen that the flux-tube expression reduces to the $^3P_0$ one if we let

$$\gamma(\vec{p}_x-\vec{p}_1,\vec{p}_2,0) = \gamma\, \delta(\vec{p}_x-\vec{p}_1)\, \delta(\vec{p}_2), \tag{3.3-21}$$

with the natural interpretation that the probability of pair creation becomes independent of the quark configuration. The expression of eq. (3.3-19) can also be compared to the form of the transition matrix element that follows from the prescription of Silvestre-Brac and Bonnaz [184], i.e. by letting the pair-creation amplitude γ be a function of the relative momentum of the created $q\bar{q}$–pair. In this case, the amplitude becomes

$$\mathcal{I}^\mu = \frac{1}{(2\pi)^{3/2}} \int d\vec{p}_x\, d\vec{p}_y\, \gamma(-\vec{q}-\vec{p}_y)\, \Psi^*_{B'}(\vec{p}_x,\vec{p}_y+\frac{2}{3}\vec{q})\, \Psi^*_M(-\vec{p}_y-\frac{\vec{q}}{2})\, \mathcal{Y}^\mu_1(-2\vec{q}-2\vec{p}_y)\, \Psi_B(\vec{p}_x,\vec{p}_y). \tag{3.3-22}$$

The pair-creation amplitude γ here depends only on the dynamical variable $\vec{p}_y$, but it is not clear how to obtain this from the more general expression from the flux tube picture, eq. (3.3-19), since there, γ does not depend on this variable. The numerical results for strong decay widths as given by Stancu et al. [159] seem to indicate that an infinite extension for the flux tube (which means $\gamma = const.$) is in fact a good approximation. With this prescription, they recover completely the $^3P_0$.

The Cornell Model

The Cornell group in their study of Charmonium [197–199] has introduced a model where the $q\bar{q}$–pair is created from an exchanged gluon, see fig. (3.6).

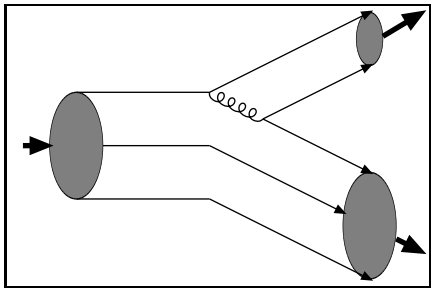

Figure 3.6: Graphical representation of a decay process in the Cornell model.

This has the conceptual advantage that it is the same mechanism that is responsible for the binding and the decays of hadronic states. Consequently, there is no new free parameter in their decay model, all values being in principle determined by the spectroscopy. The operational structure of the decay amplitude that they obtain is very similar to the one of the $^3P_0$, with one important exception: the decay operator contains the derivative of the potential that is responsible for the binding of quarks, and this factor replaces the phenomenological quark-pair creation strength γ of the $^3P_0$. In practice, since they neglect the hyperfine part of the potential and take only a linear confinement (which is evidently the dominant contribution for decay processes), they recover completely the operational structure of the $^3P_0$. One may wonder if residual effects do not play a non-negligible role for decay widths, in particular if one wants to distinguish spectroscopic quark models, like the GBE and the OGE, by their predictions of decay widths.

On the other hand there seem to be indications that the $^3P_0$ already incorporates part of the effects that come from the one-gluon exchange transition potential. We illustrate this in a graphical form. Assume that the emitted meson is described by a Schrödinger-type equation:

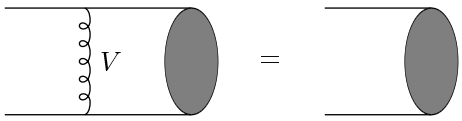

Figure 3.7: Graphical representation of an integral equation with an interaction potential V.

It is not even necessary that the equation be of Schrödinger-type, any sort of equation in the form $P\psi(p) = \int V(p,q)\,dq$ with a two-particle propagator P and an interaction potential V will do, in particular relativistic versions of quasi-potential equations or non-relativistic reductions of the Bethe-Salpeter equation. We see immediately that with this assumption we can absorb the gluon exchange, which is responsible for the quark-pair creation in fig. (3.6), into the meson wave function:

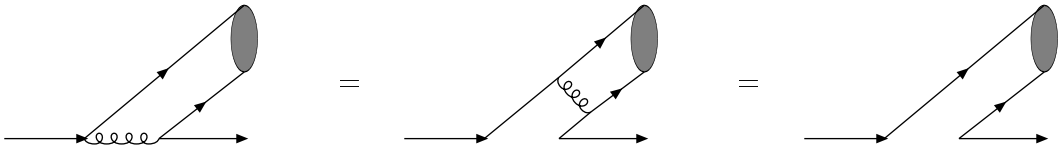

Figure 3.8: Equivalence of the Cornell- and the $^3P_0$-decay model.

What we are left with is a Feynman diagram of the $^3P_0$-type, only the details of the transition operator will depend on the assumptions that go into the description of the emitted meson. This approach, which is in the same spirit as the one underlying the work of ref. [193], is currently investigated [200], in particular with respect to finding a relation between this microscopic formulation and the phenomenological decay models used in practical calculations.

Pair Creation in a Strong Electric Field

It is extremely interesting to mention an analogy with Electrodynamics, where one can obtain an analytic expression for the probability of ee^+-pair creation in a constant, uniform electric field. The exact, non-perturbative result for the probability per unit time and unit volume of ee^+-pair production is given by (see ref. [103, p.193f]):

$$w = \frac{\alpha E^2}{\pi^2} \sum_{n=1}^{\infty} \frac{1}{n^2} \exp\left(-\frac{n\pi m^2}{|eE|}\right), \tag{3.3-23}$$

where α is the fine-structure constant, E the electric field strength and e and m the charge and mass of the electron, respectively. The essential factor here is non-perturbative: $\exp(-\pi m^2/|eE|)$, and it inevitably reminds one of the quantum phenomenon of tunneling through a potential barrier, where a similar factor arises.

Note that the sum on the right hand side of eq. (3.3-23) is bounded from above by $\sum_{n=1}^{\infty} 1/n^2 = \pi^2/6$, but the front factor still suggests a dependence of the probability on the field strength E. This is rather natural and suggests a picture similar to the flux-tube mechanism, where the pair creation depends on the quark configuration, and therefore the field strength at the point, where the pair is created.

In particular, if we assume that the relative momentum of the created $q\bar{q}$–pair is proportional to the color-magnetic field strength, we would expect the pair-creation probability to vary like $w \propto p_{rel}^2$, a trend that seems to be consistent with the phenomenological finding of ref. [184].

In atomic physics, pair creation was never observed directly because of the smallness of typical values of $|eE|$ as compared to m^2. If we take over the analogy to strong interaction physics, where typical field strengths are much larger, it seems rather tempting to describe a strong interaction decay as being due to a tunneling process, in complete analogy to the first explanation of β-decay by Gamow. Unfortunately, it seems rather complicated to obtain an exact formula like eq. (3.3-23) in QCD, because of its nonlinear nature due to gluon self-couplings.

Chapter 4

Summary and Discussion

Die Grenzen meiner Sprache bedeuten die Grenzen meiner Welt.

L. Wittgenstein, Tractatus

Constituent quark models (CQM's) are useful for interpreting the results of partial wave analyses (PWA) that are usually employed to extract the properties of nucleon resonances from the experimental data of pion-nucleon scattering [55]. In the first part of this work we have essentially dealt with theoretical and some experimental issues that are relevant in this area. In this context, we have contributed to the investigation on the proper underlying dynamics between constituent quarks, which is currently a likely subject of polemics [123, 124].

In particular we investigated the theoretical description of π and η decays for N and Δ resonances within different constituent quark models. In the first instance we were interested in the predictions of the specific chiral constituent-quark model whose hyperfine interaction is based on Goldstone-boson exchange (GBE) dynamics [99, 108]. A detailed comparison to the modern experimental data base [43] is provided. We also studied the results relative to the predictions by a traditional constituent quark model [84, 85] based on one-gluon exchange (OGE) but relying on the same type of force components as the GBE CQM. Furthermore we investigated the differences between a semi-relativistic and a non-relativistic description of the baryon states for both types of CQM's. In a second step we investigated the influence of the tensor force component in the GBE interaction on predictions of decay widths.

For the decay mechanism two models were considered separately: the elementary emission model (EEM), which regards the emitted meson as point-like and a modified version of the $^3P_0$ model [86] which allows a more microscopic description of the decay process. We also examined the sensitivity of the results on the ingredients entering the decay operator, notably the analytic form and the extension of the meson wave functions.

From the present results it is still difficult to draw definite conclusions about the relative quality of the wave functions stemming from different CQM's. In fact, the various decay widths seem to be more determined by the choice of the SR or NR parameterizations rather than by the use of either type of dynamics, GBE or OGE. At this stage, we find a number of gross qualitative features that have been observed already before in similar studies along the classical $^3P_0$ decay model. To illustrate this we give in table 4.1 a collection of results from different works that have essentially been compiled from ref. [79].

The values of χ^2 given in table 4.1, as they follow from the definition in eq. (3.2-17), have to be considered as indicative only, since in different approaches, the emphasize has been laid on different aspects and the decay operators are not always the same. It is interesting still to note that the results of the GBE NR parameterization of table 3.5 gives a value of $\chi^2 = 68.0$, which is significantly smaller than the one for the semi-relativistic parameterization. This has to be taken as an indication for the need of a more complete account of relativity. The introduction of semi-relativistic kinematics only is obviously not sufficient to capture the gross features of dynamical observables.

The table also shows that our results are particularly similar to those of Capstick and Roberts, whereas the ones from Stancu and Stassart show some significant differences. However, we remark that the latter ones had to be obtained by calculating a 9-dimensional integral, which was accomplished by

Table 4.1: Comparison of $N^* \to N\pi$ decay widths within constituent quark models calculated with different forms of quark-pair creation models. CR is from ref. [79] (note that these numbers differ from what has been given in the original work, ref. [80]), SST is from ref. [146], the rest are present results from tables 3.5 and 3.7. Experimental data are from ref. [43].

$[N^{J^\pi}]_n$	N^*	$\Gamma(N^* \to N\pi)$ [MeV]					
		CR	SST	OGE SR	GBE SR	GBE+tensor	exp.
$[N\frac{1}{2}^+]_2$	N_{1440}	493	433	1064	517	646	$(227 \pm 18)^{+70}_{-59}$
$[N\frac{1}{2}^+]_3$	N_{1710}	12	3	202	54	87	$(15 \pm 5)^{+30}_{-5}$
$[N\frac{1}{2}^-]_1$	N_{1535}	207	40	462	336	294	$(67 \pm 15)^{+55}_{-17}$
$[N\frac{1}{2}^-]_2$	N_{1650}	115	5	87	53	176	$(109 \pm 26)^{+36}_{-3}$
$[N\frac{3}{2}^+]_1$	N_{1720}	292	50	689	377	577	$(23 \pm 8)^{+9}_{-5}$
$[N\frac{3}{2}^-]_1$	N_{1520}	100	71	108	131	146	$(66 \pm 6)^{+9}_{-5}$
$[N\frac{3}{2}^-]_2$	N_{1700}	36	17	7	6	64	$(10 \pm 5)^{+3}_{-3}$
$[N\frac{5}{2}^+]_1$	N_{1680}	86	94	149	85	112	$(85 \pm 7)^{+6}_{-6}$
$[N\frac{5}{2}^-]_1$	N_{1675}	32	31	40	34	61	$(68 \pm 8)^{+14}_{-4}$
$[\Delta\frac{1}{2}^-]_1$	Δ_{1620}	21	1	41	26	22	$(38 \pm 8)^{+8}_{-6}$
$[\Delta\frac{3}{2}^+]_1$	Δ_{1232}	104	115	120	120	120	$(119 \pm 1)^{+5}_{-5}$
$[\Delta\frac{3}{2}^+]_2$	Δ_{1600}	40	0	174	43	87	$(61 \pm 26)^{+26}_{-10}$
$[\Delta\frac{3}{2}^-]_1$	Δ_{1700}	27	23	20	28	41	$(45 \pm 15)^{+20}_{-10}$
χ^2		125.8	71.6	362.7	108.0	159.7	

a Monte-Carlo routine. Furthermore, variational wave functions were employed that were chosen to give the correct behavior at the origin and at infinity, but we know that it is rather an average, intermediate range in the wave functions which determines the decay amplitudes. In particular, we note that the largest discrepancies occur for just the structure-dependent resonances (the N_{1710}, N_{1535}, N_{1650}, N_{1720} and the Δ_{1620}), which gives rise to some suspicions in view of the discussion of numerical accuracy in the last sections. It just confirms the observation that decay amplitudes of structure-dependent resonances are much more sensitive to a precise determination of the corresponding wave functions than those of structure-independent ones. As a consequence, the resulting low χ^2 in table 4.1 should be considered with some caution.

In any case, our study reveals (and confirms previous such findings) that the description of strong decays of baryon resonances within present CQM's is not yet fully satisfactory. While incorporating the effects of the tensor force helps in a few cases (where configuration mixing effects are important), one may not expect that they will solve the problem caused by the large widths obtained in the SR parameterizations. This problem persists in all cases we considered. Similar findings were made in other works [80, 86, 146]. The reason is probably a large amount of high-momentum components in the wave functions or, equivalently, the smallness of the baryons. In this respect, the better results from the NR CQM also suggest that the weight of the high-momentum components is perhaps too large. The corresponding differences between the NR and SR cases directly originate from the type of kinetic-energy operator employed in the calculation.

On the other hand one must realize that the $^3P_0$ model may also fall short as it is based on intuitive grounds and lacks a firm theoretic foundation. Any attempt to improve upon these semi-phenomenological descriptions has not brought the desired success. A consistent microscopic description of the strong-decay processes within the framework of CQM's thus remains a challenging task, the main difficulty being due to the non-perturbative and relativistic nature of the problem. The ultimate goal would, of course, be a unified description of the resonance spectra and the hadronic, as well as electromagnetic, transitions within the same dynamical scheme.

References for Part I

[1] H. L. Anderson, E. Fermi, E. A. Long, and D. E. Nagle: Phys. Rev. **85**, 936 (1952).

[2] M. Gell-Mann: Phys. Rev. **125**, 1067 (1962).

[3] M. Gell-Mann: Phys. Lett. **8**, 214 (1964).

[4] G. Zweig: CERN-TH-412.

[5] F. Gursey and L. A. Radicati: Phys. Rev. Lett. **13**, 173 (1964).

[6] K. T. Mahanthappa and E.C.G. Sudarshan: Phys. Rev. Lett. **14**, 163 (1965).

[7] V. Halyo *et al.*: Phys. Rev. Lett. **84**, 2576 (2000).

[8] J. D. Bjorken and E. A. Paschos: Phys. Rev. **185**, 1975 (1969).

[9] R. P. Feynman: Phys. Rev. Lett. **23**, 1415 (1969).

[10] O. W. Greenberg: Phys. Rev. Lett. **13**, 598 (1964).

[11] A. J. Bracken and H. S. Green: J. Math. Phys. **14**, 1784 (1973).

[12] S. L. Glashow: Nucl. Phys. **22**, 579 (1961).

[13] S. Weinberg: Phys. Rev. Lett. **19**, 1264 (1967).

[14] A. Salam: In: Elementary Particle Theory, Proceedings of The Nobel Symposium, (1968).

[15] H. Fritzsch, M. Gell-Mann, and H. Leutwyler: Phys. Lett. **B47**, 365 (1973).

[16] A. Chodos, R. L. Jaffe, K. Johnson, C. B. Thorn, and V. F. Weisskopf: Phys. Rev. **D9**, 3471 (1974).

[17] G. E. Brown and M. Rho: Phys. Lett. **B82**, 177 (1979).

[18] A. W. Thomas: J. Phys. **G7**, L283 (1981).

[19] R. H. Dalitz: in *Physique des Hautes Energies. Les Houches Lectures 1965* (C. DeWitt and M. Jacob, eds.), Gordon and Breach, 1965.

[20] D. Faiman and A. W. Hendry: Phys. Rev. **173**, 1720 (1968).

[21] D. Faiman and A. W. Hendry: Phys. Rev. **180**, 1609 (1969).

[22] A. De Rújula, H. Georgi, and S. L. Glashow: Phys. Rev. **D12**, 147 (1975).

[23] N. Isgur and G. Karl: Phys. Rev. **D19**, 2653 (1979).

[24] N. Isgur and G. Karl: Phys. Rev. **D20**, 1191 (1979).

[25] C. Becchi and G. Morpurgo: Phys. Rev. **149**, 1284 (1966).

[26] A. Mitra and M. Ross: Phys. Rev. **158**, 1630 (1967).

[27] L. Micu: Nucl. Phys. **B10**, 521 (1969).

[28] A. Le Yaouanc, L. Oliver, O. Pene, and J.-C. Raynal: Phys. Rev. **D9**, 1415 (1974).

[29] A. Le Yaouanc, L. Oliver, O. Pène, and J.-C. Raynal: Phys. Rev. **D8**, 2223 (1973).

[30] J. J. J. Kokkedee: *The Quark Model* (W.A. Benjamin, 1969).

[31] F. E. Close: *An Introduction to Quarks and Partons* (Academic Press, 1979).

[32] D. Flamm and F. Schöberl: *Introduction to the Quark Model of Elementary Particles: Quantum Numbers, Gauge Theories and Hadron Spectroscopy* (Gordon and Breach, 1986).

[33] A. Le Yaouanc, L. Oliver, O. Pène, and J.-C. Raynal: *Hadron Transitions in the Quark Model* (Gordon and Breach, 1988).

[34] T. Muta: *Foundations of Quantum Chromodynamics* (World Scientific, 1987).

[35] G. Sterman *et al.*: Rev. Mod. Phys. **67**, 157 (1995).

[36] K. G. Wilson: Phys. Rev. **D10**, 2445 (1974).

[37] S. Weinberg: Physica **A96**, 327 (1979).

[38] J. Gasser and H. Leutwyler: Ann. Phys. **158**, 142 (1984).

[39] M. L. Goldberger and S. B. Treiman: Phys. Rev. **110**, 1178 (1958).

[40] M. Gell-Mann, R. J. Oakes, and B. Renner: Phys. Rev. **175**, 2195 (1968).

[41] L. Ya. Glozman: Phys. Lett. **B475**, 329 (2000).

[42] J. R. Taylor: *Scattering Theory* (Wiley & Sons, 1972).

[43] D. E. Groom *et al.*: Eur. Phys. J. **C15**, 1 (2000).

[44] R. E. Cutkosky *et al.*: Phys. Rev. **D20**, 2804 (1979).

[45] G. Höhler: in *Pion Nucleon Scattering. Part 2: Methods and Results of Phenomenological Analyses* (G. Höhler and H. Schopper, eds.), Springer Verlag, 1983.

[46] D. M. Manley and E. M. Saleski: Phys. Rev. **D45**, 4002 (1992).

[47] A. M. Green and S. Wycech: Phys. Rev. **C55**, 2167 (1997).

[48] R. A. Arndt, I. I. Strakovsky, R. L. Workman, and M. M. Pavan: Phys. Rev. **C52**, 2120 (1995).

[49] R. A. Arndt, C. H. Oh, I. I. Strakovsky, R. L. Workman, and F. Dohrmann: Phys. Rev. **C56**, 3005 (1997).

[50] R. A. Arndt, I. I. Strakovsky, and R. L. Workman: Phys. Rev. **C62**, 034005 (2000).

[51] R. A. Arndt, I. I. Strakovsky, and R. L. Workman: Phys. Rev. **C56**, 577 (1997).

[52] M. Batinić, I. Šlaus, A. Švarc, and B. M. K. Nefkens: Phys. Rev. **C51**, 2310 (1995).

[53] R. Workman: Phys. Rev. **C59**, 3441 (1999).

[54] S. Capstick *et al.*: hep-ph/0012238.

[55] S. Simula, B. Saghai, N. C. Mukhopadhyay, and V. D. Burkert, (eds.): Few Body Syst. Suppl. **11** (1999).

[56] K. Hikasa *et al.*: Phys. Rev. **D45**, S1 (1992).

[57] L. Montanet *et al.*: Phys. Rev. **D50**, 1173 (1994).

[58] R. M. Barnett *et al.*: Phys. Rev. **D54**, 1 (1996).

[59] C. Caso *et al.*: Eur. Phys. J. **C3**, 1 (1998).

[60] N. C. Mukhopadhyay, J.-F. Zhang, and M. Benmerrouche: Phys. Lett. **B364**, 1 (1995).

[61] R. A. Arndt, A. M. Green, R. L. Workman, and S. Wycech: Phys. Rev. **C58**, 3636 (1998).

[62] Z. Li and R. Workman: Phys. Rev. **C53**, 549 (1996).

[63] N. Kaiser, P. B. Siegel, and W. Weise: Phys. Lett. **B362**, 23 (1995).

[64] M. Benmerrouche and N. C. Mukhopadhyay: Phys. Rev. Lett. **67**, 1070 (1991).

[65] M. Benmerrouche, N. C. Mukhopadhyay, and J. F. Zhang: Phys. Rev. **D51**, 3237 (1995).

[66] Z. Li: Phys. Rev. **D52**, 4961 (1995).

[67] D. O. Riska: Adv. Nucl. Phys. **22**, 1 (1996).

[68] R. Horgan and R. H. Dalitz: Nucl. Phys. **B66**, 135 (1973).

[69] A. O. Barut and R. Raczka: *Theory of Group Representations and Applications* (World Scientific, 1986).

[70] Fl. Stancu: *Group Theory in Subnuclear Physics* (Clarendon Press, 1996).

[71] I. V. Kurdyumov, Yu. F. Smirnov, K. V. Shitikova, and S. K. E. Samarai: Nucl. Phys. **A145**, 593 (1975).

[72] J. P. Elliott: Proc. Roy. Soc. **A245**, 128 (1958).

[73] J. P. Elliott: Proc. Roy. Soc. **A245**, 562 (1958).

[74] N. Isgur and G. Karl: Phys. Rev. **D18**, 4187 (1978).

[75] R. Koniuk and N. Isgur: Phys. Rev. **D21**, 1868 (1980).

[76] A. J. G. Hey and R. L. Kelly: Phys. Rept. **96**, 71 (1983).

[77] S. Godfrey and N. Isgur: Phys. Rev. **D32**, 189 (1985).

[78] S. Capstick and N. Isgur: Phys. Rev. **D34**, 2809 (1986).

[79] S. Capstick and W. Roberts: nucl-th/0008028.

[80] S. Capstick and W. Roberts: Phys. Rev. **D47**, 1994 (1993).

[81] R. Sartor and Fl. Stancu: Phys. Rev. **D31**, 128 (1985).

[82] Fl. Stancu and P. Stassart: Phys. Lett. **B269**, 243 (1991).

[83] P. Stassart and Fl. Stancu: Z. Phys. **A359**, 321 (1997).

[84] R. K. Bhaduri, L. E. Cohler, and Y. Nogami: Phys. Rev. Lett. **44**, 1369 (1980).

[85] R. K. Bhaduri, L. E. Cohler, and Y. Nogami: Nuovo Cim. **A65**, 376 (1981).

[86] F. Cano, P. Gonzalez, S. Noguera, and B. Desplanques: Nucl. Phys. **A603**, 257 (1996).

[87] S. Capstick, S. Godfrey, N. Isgur, and J. Paton: Phys. Lett. **B175**, 457 (1986).

[88] W. Lucha, F. F. Schöberl, and D. Gromes: Phys. Rept. **200**, 127 (1991).

[89] B. Desplanques *et al.*: Z. Phys. **A343**, 331 (1992).

[90] F. Cano and P. Gonzalez: Phys. Lett. **B431**, 270 (1998).

[91] Fl. Stancu and P. Stassart: Phys. Rev. **D41**, 916 (1990).

[92] R. K. Bhaduri: *Models of the Nucleon* (Addison-Wesley, 1988).

[93] A. Chodos and C. B. Thorn: Phys. Rev. **D12**, 2733 (1975).

[94] A. Manohar and H. Georgi: Nucl. Phys. **B234**, 189 (1984).

[95] D. I. Dyakonov and V. Yu. Petrov: Phys. Lett. **B147**, 351 (1984).

[96] D. I. Dyakonov and V. Yu. Petrov: Nucl. Phys. **B272**, 457 (1986).

[97] Y. Nambu and G. Jona-Lasinio: Phys. Rev. **122**, 345 (1961).

[98] Y. Nambu and G. Jona-Lasinio: Phys. Rev. **124**, 246 (1961).

[99] L. Ya. Glozman and D. O. Riska: Phys. Rept. **268**, 263 (1996).

[100] M. C. Birse and M. K. Banerjee: Phys. Lett. **B136**, 284 (1984).

[101] M. C. Birse and M. K. Banerjee: Phys. Rev. **D31**, 118 (1985).

[102] G. Ripka: *Quarks Bound by Chiral Fields* (Clarendon Press, 1997).

[103] C. Itzykson and J. B. Zuber: *Quantum Field Theory* (McGraw-Hill, 1985).

[104] R. F. Wagenbrunn, L. Ya. Glozman, W. Plessas, and K. Varga: Nucl. Phys. **A663**, 703 (2000).

[105] R. F. Wagenbrunn, L. Ya. Glozman, W. Plessas, and K. Varga: Nucl. Phys. **A666**, 29 (2000).

[106] L. Ya. Glozman, Z. Papp, and W. Plessas: Phys. Lett. **B381**, 311 (1996).

[107] J. Carlson, J. B. Kogut, and V. R. Pandharipande: Phys. Rev. **D28**, 2807 (1983).

[108] L. Ya. Glozman, W. Plessas, K. Varga, and R. F. Wagenbrunn: Phys. Rev. **D58**, 094030 (1998).

[109] L. Ya. Glozman, W. Plessas, K. Varga, and R. F. Wagenbrunn: Nucl. Phys. **A631**, 469c (1998).

[110] J. Carlson, J. Kogut, and V. R. Pandharipande: Phys. Rev. **D27**, 233 (1983).

[111] H. Collins and H. Georgi: Phys. Rev. **D59**, 094010 (1999).

[112] C. E. Carlson, C. D. Carone, J. L. Goity, and R. F. Lebed: Phys. Rev. **D59**, 114008 (1999).

[113] A. Valcarce, A. Faessler, and F. Fernandez: Phys. Lett. **B345**, 367 (1995).

[114] K. Shimizu and M. Koyama: Nucl. Phys. **A646**, 211 (1999).

[115] P. Stassart, Fl. Stancu, J.-M. Richard, and L. Theußl: J. Phys. **G26**, 397 (2000).

[116] R. Machleidt, K. Holinde, and C. Elster: Phys. Rept. **149**, 1 (1987).

[117] D. O. Riska and G. E. Brown: Nucl. Phys. **A653**, 251 (1999).

[118] B. Baumgartner, H. Grosse, and A. Martin: Phys. Lett. **B146**, 363 (1984).

[119] B. Baumgartner, H. Grosse, and A. Martin: Nucl. Phys. **B254**, 528 (1985).

[120] H. Høgaasen and J. M. Richard: Phys. Lett. **B124**, 520 (1983).

[121] D. Gromes and I. O. Stamatescu: Z. Phys. **C3**, 43 (1979).

[122] R. F. Wagenbrunn: Dissertation, Karl-Franzens Universität, Graz, 1998.

[123] N. Isgur: Phys. Rev. **D62**, 054026 (2000).

[124] L. Ya. Glozman: nucl-th/9909021.

[125] R. F. Wagenbrunn, W. Plessas, L. Ya. Glozman, and K. Varga: Few Body Syst. Suppl. **10**, 387 (1999).

[126] L. Ya. Glozman: Phys. Lett. **B494**, 58 (2000).

[127] L. Ya. Glozman: Nucl. Phys. **A663**, 103 (2000).

[128] L. Ya. Glozman: Phys. Lett. **B459**, 589 (1999).

[129] T. Thonhauser: Diplomarbeit, Karl-Franzens Universität, Graz, 1998.

[130] L. A. Blanco, F. Fernández, and A. Valcarce: Phys. Rev. **C59**, 428 (1999).

[131] D. Bartz and Fl. Stancu: Phys. Rev. **C59**, 1756 (1999).

[132] D. Bartz and Fl. Stancu: Phys. Rev. **C60**, 055207 (1999).

[133] Fl. Stancu, S. Pepin, and L. Ya. Glozman: Phys. Rev. **C56**, 2779 (1997).

[134] S. Pepin, Fl. Stancu, M. Genovese, and J.-M. Richard: Phys. Lett. **B393**, 119 (1997).

[135] M. Genovese, J.-M. Richard, Fl. Stancu, and S. Pepin: Phys. Lett. **B425**, 171 (1998).

[136] Fl. Stancu: Phys. Rev. **D58**, 111501 (1998).

[137] S. Pepin and Fl. Stancu: Phys. Rev. **D57**, 4475 (1998).

[138] Fl. Stancu: Few Body Syst. Suppl. **11**, 33 (1999).

[139] Fl. Stancu, S. Pepin, and L. Ya. Glozman: Phys. Rev. **D57**, 4393 (1998).

[140] K. Dannbom, C. Helminen, and D. O. Riska: Nucl. Phys. **A616**, 555 (1997).

[141] R. F. Wagenbrunn, M. Radici, S. Boffi, and P. Demetriou: Eur. Phys. J. **A8**, 385 (2000).

[142] S. Boffi, P. Demetriou, M. Radici, and R. F. Wagenbrunn: Phys. Rev. **C60**, 025206 (1999).

[143] R. F. Wagenbrunn, S. Boffi, W. Klink, W. Plessas, and M. Radici: Phys. Lett. **B511**, 33 (2001).

[144] Z. Papp and W. Plessas: Phys. Rev. **C54**, 50 (1996).

[145] Z. Papp, A. Krassnigg, and W. Plessas: Phys. Rev. **C62**, 044004 (2000).

[146] Fl. Stancu and P. Stassart: Phys. Rev. **D38**, 233 (1988).

[147] S. Moszkowski *et al.*: Phys. Rev. **A62**, 032504 (2000).

[148] L. Ya. Glozman, Z. Papp, W. Plessas, K. Varga, and R. F. Wagenbrunn: Phys. Rev. **C57**, 3406 (1998).

[149] A. Valcarce, P. Gonzalez, F. Fernandez, and V. Vento: Phys. Rev. **C61**, 019803 (2000).

[150] L. Ya. Glozman, Z. Papp, W. Plessas, K. Varga, and R. F. Wagenbrunn: Phys. Rev. **C61**, 019804 (2000).

[151] R. P. Feynman, M. Kislinger, and F. Ravndal: Phys. Rev. **D3**, 2706 (1971).

[152] S. Kumano and V. R. Pandharipande: Phys. Rev. **D38**, 146 (1988).

[153] W. Roberts and B. Silvestre-Brac: Phys. Rev. **D57**, 1694 (1998).

[154] R. Kokoski and N. Isgur: Phys. Rev. **D35**, 907 (1987).

[155] S. Capstick and W. Roberts: Phys. Rev. **D49**, 4570 (1994).

[156] R. E. Cutkosky, C. P. Forsyth, R. E. Hendrick, and R. L. Kelly: Phys. Rev. **D20**, 2839 (1979).

[157] P. Stassart and Fl. Stancu: Phys. Rev. **D42**, 1521 (1990).

[158] Fl. Stancu and P. Stassart: Phys. Rev. **D47**, 2140 (1993).

[159] P. Stassart and Fl. Stancu: Z. Phys. **A351**, 77 (1995).

[160] H. J. Lipkin, H. R. Rubinstein, and H. Stern: Phys. Rev. **161**, 1502 (1967).

[161] D. R. Divgi: Phys. Rev. **175**, 2027 (1968).

[162] R. van Royen and V. F. Weisskopf: Nuovo Cim. **A50**, 617 (1967).

[163] C. P. Forsyth and R. E. Cutkosky: Phys. Rev. Lett. **46**, 576 (1981).

[164] R. Bijker, F. Iachello, and A. Leviatan: Phys. Rev. **D55**, 2862 (1997).

[165] R. Sartor and Fl. Stancu: Phys. Rev. **D34**, 3405 (1986).

[166] F. Cano, P. Gonzalez, B. Desplanques, and S. Noguera: Z. Phys. **A359**, 315 (1997).

[167] J. L. Friar: Phys. Rev. **C10**, 955 (1974).

[168] A. W. Thomas and R. H. Landau: Phys. Rept. **58**, 121 (1980).

[169] M. Bolsterli, W. R. Gibbs, B. F. Gibson, and G. J. Stephenson, Jr.: Phys. Rev. **C10**, 1225 (1974).

[170] M. V. Barnhill: Nucl. Phys. **A131**, 106 (1969).

[171] C. E. Carlson and C. D. Carone: Phys. Lett. **B484**, 260 (2000).

[172] Fl. Stancu and P. Stassart: Phys. Rev. **D39**, 343 (1989).

[173] P. Stassart and Fl. Stancu: in *Quark confinement and the hadron spectrum II* (N. Brambilla and G. M. Prosperi, eds.), World Scientific, 1997.

[174] L. Theußl: Diplomarbeit, Karl-Franzens Universität, Graz, 1997.

[175] S. Capstick: Few Body Syst. Suppl. **11**, 86 (1999).

[176] L. Ya. Glozman and D. O. Riska: Phys. Lett. **B366**, 305 (1996).

[177] L. Ya. Glozman, W. Plessas, L. Theußl, R. F. Wagenbrunn, and K. Varga: πN Newslett. **14**, 99 (1998).

[178] A. Krassnigg: Diplomarbeit, Karl-Franzens Universität, Graz, 1998.

[179] A. Krassnigg, W. Plessas, L. Theußl, R. F. Wagenbrunn, and K. Varga: Few Body Syst. Suppl. **10**, 391 (1999).

[180] J. L. Goity and W. Roberts: Phys. Rev. **D60**, 034001 (1999).

[181] A. Le Yaouanc, L. Oliver, O. Pene, and J.-C. Raynal: Phys. Rev. **D11**, 1272 (1975).

[182] M. B. Gavela, A. Le Yaouanc, L. Oliver, O. Pène, and J. C. Raynal: Phys. Rev. **D25**, 1921 (1982).

[183] M. B. Gavela, A. Le Yaouanc, L. Oliver, O. Pène, and J. C. Raynal: Phys. Rev. **D25**, 1931 (1982).

[184] R. Bonnaz and B. Silvestre-Brac: Few Body Syst. **27**, 163 (1999).

[185] W. Roberts and B. Silvestre-Brac: Few Body Syst. **11**, 171 (1992).

[186] L. Theußl, R. F. Wagenbrunn, B. Desplanques, and W. Plessas: nucl-th/0010099.

[187] M. Batinić, I. Šlaus, and A. Švarc: Phys. Rev. **C52**, 2188 (1995).

[188] T. P. Vrana, S. A. Dytman, and T. S. H. Lee: Phys. Rept. **328**, 181 (2000).

[189] L. Theußl, B. Desplanques, B. Silvestre-Brac, and K. Varga: Few Body Syst. Suppl. **10**, 403 (1999).

[190] B. Desplanques, B. Silvestre-Brac, F. Cano, P. Gonzalez, and S. Noguera: Few Body Syst. **29**, 169 (2000).

[191] S. Capstick, T. S. H. Lee, W. Roberts, and A. Švarc: Phys. Rev. **C59**, 3002 (1999).

[192] L. Theußl and R. F. Wagenbrunn: nucl-th/0104024.

[193] E. S. Ackleh, T. Barnes, and E. S. Swanson: Phys. Rev. **D54**, 6811 (1996).

[194] D. S. Kulshreshtha and A. N. Mitra: Phys. Rev. **D28**, 588 (1983).

[195] A. Nicolet: Stage Maîtrise, Institut des Sciences Nucléaires, Grenoble, 2000.

[196] P. Geiger and E. S. Swanson: Phys. Rev. **D50**, 6855 (1994).

[197] E. Eichten, K. Gottfried, T. Kinoshita, K. D. Lane, and T-M. Yan: Phys. Rev. Lett. **36**, 500 (1976).

[198] E. Eichten, K. Gottfried, T. Kinoshita, K. D. Lane, and T. M. Yan: Phys. Rev. **D17**, 3090 (1978).

[199] E. Eichten, K. Gottfried, T. Kinoshita, K. D. Lane, and T. M. Yan: Phys. Rev. **D21**, 203 (1980).

[200] A. Nicolet: Stage DEA, Institut des Sciences Nucléaires, Grenoble, 2001.

Part II

Relativistic Wave Equations

Chapter 5

Relativistic Bound States

Can such things be,
And overcome us like a summer's cloud,
Without our special wonder?
W. Shakespeare, Macbeth

Like the first part of this work, we shall start the second one with a general theoretical introduction to the problematics of relativistic bound states. We shall discuss the prototype of a relativistic bound-state equation, the Bethe-Salpeter equation, and study some of its simplest cases. The later chapters will then deal with applications and new developments. The most important ones of these include the contribution of non-planar (two-particle irreducible) diagrams to the Bethe-Salpeter interaction kernel, and the derivation of effective, non-relativistic interactions.

5.1 Introduction

The study of bound states presents a principal difficulty when it comes to practical calculations, because of the inadequacy of retaining only a few Feynman diagrams, which is the basis of any perturbative calculation in high-energy physics. The reason is that bound states produce poles in the scattering matrix in the channel in which they appear. However, no such poles exist in any Feynman diagram or any finite sum of them, a pole can only be generated by an infinite sum.

In practice, it is of course impossible to sum an infinity of diagrams, the way one proceeds is usually to find an integral equation, whose solutions may be interpreted as the sum of a certain class of diagrams. But again, no integral equation is able to sum all the diagrams that occur in a certain theory and one has to content oneself with a certain sub-class, which is hoped to be the physically most relevant one.

The prototype of a completely covariant, four-dimensional integral equation is the Bethe-Salpeter equation, and the class of diagrams that are customarily retained in its interaction kernel are those of the ladder type. However, it has to be stressed that this so-called ladder approximation is from the beginning based on computational convenience, rather than physical arguments, and even with this simplification, it is hard enough to draw information from this approach for any realistic system. In particular, the omission of crossed diagrams is believed to be responsible for a certain number of shortcomings of the Bethe-Salpeter equation in ladder approximation. These ones include the wrong one-body limit (the Bethe-Salpeter equation does not reduce to a Dirac- or Klein-Gordon equation in the limit where one of the constituents becomes infinitely massive), the violation of crossing symmetry and the occurrence of abnormal states with all their unusual properties.

Soon after the introduction of the Bethe-Salpeter equation, people therefore started to look for equivalent approaches that take into account all the important features of the fully covariant equation in an effective way.

We shall contribute in the following to the above mentioned developments on two main lines: after a theoretical introduction, we shall first investigate the contribution of non-planar diagrams to the four-dimensional interaction kernel of the Bethe-Salpeter equation. As a second contribution, we investigate

some effective two-body interactions, that are derived from the Bethe-Salpeter equation, emphasizing the important dynamical ingredients required in order to recover results from a covariant approach.

5.2 The Bethe-Salpeter Equation

The Bethe-Salpeter equation was first proposed by Bethe and Salpeter in 1951 [1] and subsequently derived from field-theoretic foundations by Gell-Mann and Low [2] and Schwinger [3–5]. The first explicit solutions of a Bethe-Salpeter equation were given by Wick and Cutkosky [6, 7] in a simple scalar model with a truncated kernel. In spite of its academic character, the Wick-Cutkosky model has given invaluable insight into the general features of the relativistic bound state problem. An early review of the Bethe-Salpeter equation may be found in ref. [8], an extremely useful bibliographic database is provided in ref. [9]. Textbooks that treat the subject on more or less pedagogic levels include the ones by Itzykson and Zuber [10], Gross [11] and Huang [12].

5.2.1 Green's Function and Bethe-Salpeter Amplitude

The Bethe-Salpeter approach to the relativistic two-body bound-state problem assumes that all the needed information about a bound state $|B\rangle$ is contained in the Bethe-Salpeter amplitude (BSA)

$$\Phi(x_1, x_2; P_B) = \left\langle 0 \middle| T\phi_1(x_1)\phi_2(x_2) \middle| B \right\rangle , \tag{5.2-1}$$

and in its conjugate

$$\bar{\Phi}(x_1, x_2; P_B) = \left\langle B \middle| T\phi_1^\dagger(x_1)\phi_2^\dagger(x_2) \middle| 0 \right\rangle . \tag{5.2-2}$$

Here P_B is the bound state four-momentum and field operators are in the Heisenberg representation. Note that

$$\left\langle B \middle| T\phi_1^\dagger(x_1)\phi_2^\dagger(x_2) \middle| 0 \right\rangle = \left\langle 0 \middle| \bar{T}\phi_1(x_1)\phi_2(x_2) \middle| B \right\rangle , \tag{5.2-3}$$

$\bar{T}$ being the anti-chronological time-ordering operator, so we can say that $\bar{\Phi}$ is obtained from Φ through time reversal.

If we introduce the variable $x = x_1 - x_2$ to characterize the two-particle relative-motion, then any linear independent combination $X = \eta_1 x_1 + \eta_2 x_2$ can serve for the description of the system as a whole. Linear independence means $\eta_1 + \eta_2 \neq 0$. In analogy with the non-relativistic center of mass definition, one usually takes

$$\eta_1 = \frac{m_1}{m_1 + m_2} , \qquad \eta_2 = \frac{m_2}{m_1 + m_2} , \tag{5.2-4}$$

where m_1 and m_2 are the masses of the constituents. The equalities $x_1 = X + \eta_2 x$, $x_2 = X - \eta_1 x$ and the fact that the four-momentum operator $\hat{P}$ is the space-time translation operator, enable us to write

$$\phi_1(x_1) = e^{i\hat{P}\cdot X}\phi_1(\eta_2 x)e^{-i\hat{P}\cdot X} , \;\; \phi_2(x_2) = e^{i\hat{P}\cdot X}\phi_2(-\eta_1 x)e^{-i\hat{P}\cdot X} . \tag{5.2-5}$$

Inserting this expression into eq. (5.2-1) we get

$$\langle 0|T\phi_1(x_1)\phi_2(x_2)|B\rangle = e^{-iP_B X}\,\langle 0|T\phi_1(\eta_2 x)\phi_2(-\eta_1 x)|B\rangle . \tag{5.2-6}$$

So, if the reduced Bethe-Salpeter amplitude and its conjugate are introduced

$$\Phi(x; P_B) = (2\pi)^{3/2}\left\langle 0 \middle| T\phi_1(\eta_2 x)\phi_2(-\eta_1 x) \middle| B \right\rangle , \qquad \bar{\Phi}(x; P_B) = (2\pi)^{3/2}\left\langle B \middle| T\phi_1^\dagger(\eta_2 x)\phi_2^\dagger(-\eta_1 x) \middle| 0 \right\rangle , \tag{5.2-7}$$

then

$$\Phi(x_1, x_2; P_B) = (2\pi)^{-3/2}e^{-iP_B X}\Phi(x; P_B), \qquad \bar{\Phi}(x_1, x_2; P_B) = (2\pi)^{-3/2}e^{iP_B X}\bar{\Phi}(x; P_B). \tag{5.2-8}$$

An equation for the Bethe-Salpeter amplitude can be obtained with the help of the four-point Green's function:

$$\mathcal{G}(x_1, x_2; y_1, y_2) = \left\langle 0 \middle| T\phi_1(x_1)\phi_2(x_2)\phi_1^\dagger(y_1)\phi_2^\dagger(y_2) \middle| 0 \right\rangle . \tag{5.2-9}$$

Field operators here are in the Heisenberg representation, so we have the full Green's function, which can be expanded in an infinite perturbation series. Let us rearrange the terms of this series: first of all we sum up self-energy insertions in the propagators of ϕ_1 and ϕ_2, this will give us the full propagators for them, then from the remaining diagrams we separate two-particle irreducible ones, the sum of which will play the role of an interaction operator[1]. This is illustrated graphically in fig. 5.1.

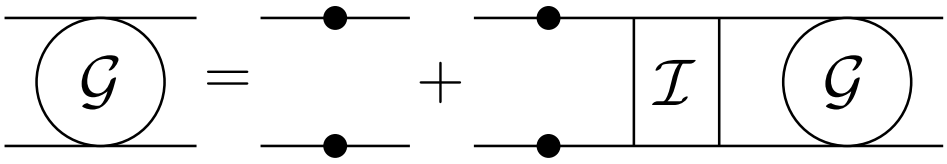

Figure 5.1: Equation for Green's function.

Here the black dots represent the self-energy insertions in the particle propagators and $\mathcal{I}$ is the sum of two-particle irreducible diagrams without external propagators, some of them are shown in fig. 5.2.

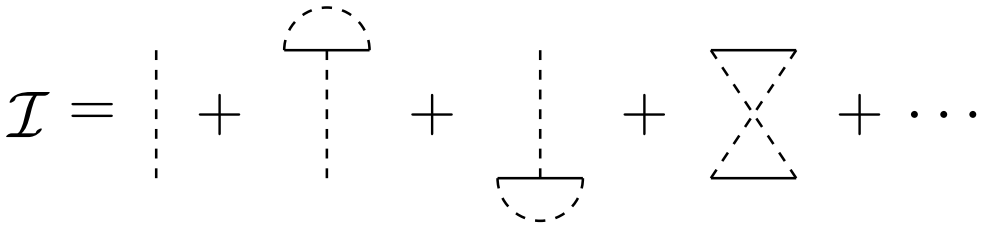

Figure 5.2: Lowest order two-particle irreducible diagrams without external propagators.

The analytic expression of the above integral equation (fig. 5.1) looks like

$$\mathcal{G}(x_1,x_2;y_1,y_2) = \Delta_1(x_1-y_1)\Delta_2(x_2-y_2) + \int dz_1\,dz_2\,dz_1'\,dz_2'\,\Delta_1(x_1-z_1)\,\Delta_2(x_2-z_2)\,\mathcal{I}(z_1,z_2;z_1',z_2')\,\mathcal{G}(z_1',z_2';y_1,y_2), \qquad (5.2\text{-}10)$$

where Δ_i denotes the single-particle propagator for particle i. This one is identical to the two-point vacuum correlation function and is therefore obtained as the solution of a Schwinger-Dyson equation. We get the so called ladder approximation if the full propagator $\Delta(x-y)$ is replaced by the free propagator and in the interaction kernel $\mathcal{I}$ only the first single-particle exchange-term is left, as shown in fig. 5.3.

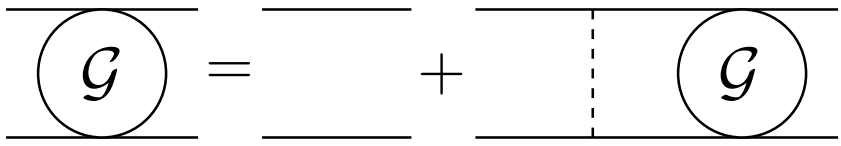

Figure 5.3: Ladder approximation of the equation for Green's functions.

A graphical representation of the iterative solution of this equation (see fig. 5.4) explains the origin of the approximation name.

[1] A diagram is called two-particle reducible, if it can be divided into two disconnected parts by cutting two inner lines.

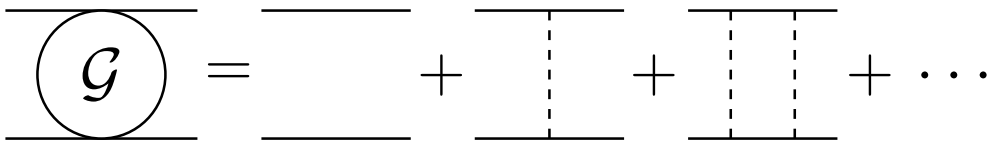

Figure 5.4: Iterative solution of the equation for Green's functions in ladder approximation.

In order to rewrite eq. (5.2-10) in momentum space, let us perform the Fourier transformation

$$\mathcal{G}(x_1,x_2;y_1,y_2) = (2\pi)^{-8}\int dp\,dq\,dP\,e^{-ipx}e^{iqy}e^{-iP(X-Y)}\,\mathcal{G}(p,q;P). \tag{5.2-11}$$

Because of translational invariance, $\mathcal{G}$ depends only on coordinate differences. As an obvious choice of independent differences that can be constructed from the x_1, x_2, y_1, y_2 coordinates, we have taken $x = x_1 - x_2$, $y = y_1 - y_2$ and $X - Y = (\eta_1 x_1 + \eta_2 x_2) - (\eta_1 y_1 + \eta_2 y_2)$.

The propagator in momentum space is defined through the four-dimensional Fourier transformation

$$\Delta(x) = (2\pi)^{-4}\int dp\,e^{-ipx}\Delta(p), \tag{5.2-12}$$

and with the change of variables $p_1 = \eta_1 P + p$, $p_2 = \eta_2 P - p$ we easily find for eq. (5.2-10):

$$\begin{aligned}\mathcal{G}(p,q;P) = {}& \delta(p-q)\Delta_1(\eta_1 P+p)\Delta_2(\eta_2 P-p) + \\ & \Delta_1(\eta_1 P+p)\Delta_2(\eta_2 P-p)\int dq'\,\mathcal{I}(p,q';P)\,\mathcal{G}(q',q;P),\end{aligned} \tag{5.2-13}$$

or

$$[\Delta_1(\eta_1 P+p)\Delta_2(\eta_2 P-p)]^{-1}\mathcal{G}(p,q;P) = \delta(p-q) + \int dq'\,\mathcal{I}(p,q';P)\,\mathcal{G}(q',q;P). \tag{5.2-14}$$

If the following definitions are introduced:

$$(A\cdot B)(p,q;P) = \int dq'\,A(p,q';P)B(q',q;P), \tag{5.2-15}$$

$$\mathcal{K}(p,q;P) = [\Delta_1(\eta_1 P+p)\Delta_2(\eta_2 P-p)]^{-1}\,\delta(p-q), \tag{5.2-16}$$

equation (5.2-14) takes the symbolic form

$$\mathcal{K}\cdot\mathcal{G} = 1 + \mathcal{I}\cdot\mathcal{G}. \tag{5.2-17}$$

Inserting a full set of states $|n\rangle\langle n| = 1$, the Green's function can be rewritten as

$$\begin{aligned}\mathcal{G}(x_1,x_2;y_1,y_2) \equiv {}& \Big\langle 0\Big|T\phi_1(x_1)\phi_2(x_2)\phi_1^\dagger(y_1)\phi_2^\dagger(y_2)\Big|0\Big\rangle = \\ & \Theta\Big(\min[(x_1)_0,(x_2)_0] - \max[(y_1)_0,(y_2)_0]\Big)\times\Big\langle 0\Big|T\phi_1(x_1)\phi_2(x_2)\Big|n\Big\rangle\Big\langle n\Big|T\phi_1^\dagger(y_1)\phi_2^\dagger(y_2)\Big|0\Big\rangle + \\ & \Theta\Big(\min[(x_1)_0,(y_1)_0] - \max[(x_2)_0,(y_2)_0]\Big)\times\Big\langle 0\Big|T\phi_1(x_1)\phi_1^\dagger(y_1)\Big|n\Big\rangle\Big\langle n\Big|T\phi_2(x_2)\phi_2^\dagger(y_2)\Big|0\Big\rangle + \\ & \Theta\Big(\min[(x_1)_0,(y_2)_0] - \max[(x_2)_0,(y_1)_0]\Big)\times\Big\langle 0\Big|T\phi_1(x_1)\phi_2^\dagger(y_2)\Big|n\Big\rangle\Big\langle n\Big|T\phi_2(x_2)\phi_1^\dagger(y_1)\Big|0\Big\rangle + \\ & \Theta\Big(\min[(x_2)_0,(y_1)_0] - \max[(x_1)_0,(y_2)_0]\Big)\times\Big\langle 0\Big|T\phi_2(x_2)\phi_1^\dagger(y_1)\Big|n\Big\rangle\Big\langle n\Big|T\phi_1(x_1)\phi_2^\dagger(y_2)\Big|0\Big\rangle + \\ & \Theta\Big(\min[(x_2)_0,(y_2)_0] - \max[(x_1)_0,(y_1)_0]\Big)\times\Big\langle 0\Big|T\phi_2(x_2)\phi_2^\dagger(y_2)\Big|n\Big\rangle\Big\langle n\Big|T\phi_1(x_1)\phi_1^\dagger(y_1)\Big|0\Big\rangle + \\ & \Theta\Big(\min[(y_1)_0,(y_2)_0] - \max[(x_1)_0,(x_2)_0]\Big)\times\Big\langle 0\Big|T\phi_1^\dagger(y_1)\phi_2^\dagger(y_2)\Big|n\Big\rangle\Big\langle n\Big|T\phi_1(x_1)\phi_2(x_2)\Big|0\Big\rangle,\end{aligned} \tag{5.2-18}$$

where the Θ-functions ensure that physical states can only propagate forward in time. To separate the contribution of a specific two-particle bound state $|B\rangle$, let us substitute

$$|n\rangle\langle n| \longrightarrow \int dP\,\delta(P^2-M^2)\Theta(P_0)\,|B\rangle\langle B|\,, \tag{5.2-19}$$

where we assume a state normalization $\langle\vec{P}\,|\,\vec{Q}\rangle = 2P_0\,\delta(\vec{P}-\vec{Q})$. An action of two annihilation operators over $|B\rangle$ is needed to obtain the vacuum quantum numbers. Only in this case we get a non-zero matrix element in eq. (5.2-18). Therefore the two-particle bound state contribution to the Green's function is

$$B = \int dP\,\Big\langle 0\Big|T\phi_1(x_1)\phi_2(x_2)\Big|B\Big\rangle\Big\langle B\Big|T\phi_1^\dagger(y_1)\phi_2^\dagger(y_2)\Big|0\Big\rangle\times \\ \delta(P^2-M^2)\,\Theta(P_0)\,\Theta\Big(\min\big[(x_1)_0,(x_2)_0\big]-\max\big[(y_1)_0,(y_2)_0\big]\Big). \tag{5.2-20}$$

The integration over dP_0 can be performed by using

$$\delta(P^2-M^2)\,\Theta(P_0) = \frac{\Theta(P_0)}{2P_0}\delta\left(P_0-\sqrt{\vec{P}^2+M^2}\right), \tag{5.2-21}$$

and remembering eqs. (5.2-7) and (5.2-8):

$$B = (2\pi)^{-3}\int\frac{d\vec{P}}{2\omega_B}\Phi(x;P_B)\bar{\Phi}(y,P_B)e^{-i\omega_B(X_0-Y_0)}e^{-i\vec{P}(\vec{X}-\vec{Y})}\,\Theta\left(\min\Big[(x_1)_0,(x_2)_0\Big]-\max\Big[(y_1)_0,(y_2)_0\Big]\right). \tag{5.2-22}$$

Here $P_B=(\omega_B,\vec{P})$ and $\omega_B=\sqrt{\vec{P}^2+M^2}$; M being the bound-state mass. The argument of the Θ function is then expressed as

$$\min\Big[(x_1)_0,(x_2)_0\Big]-\max\Big[(y_1)_0,(y_2)_0\Big] = X_0-Y_0-\frac{1}{2}\,|\,x_0\,|-\frac{1}{2}\,|\,y_0\,|+\frac{1}{2}(\eta_2-\eta_1)(x_0-y_0), \tag{5.2-23}$$

and, using its integral representation

$$\Theta(z) = \frac{i}{2\pi}\int\limits_{-\infty}^{\infty}dk\,\frac{e^{-ikz}}{k+i\epsilon}, \tag{5.2-24}$$

with the variable change $k\to P_0-\omega_B$, we get for eq. (5.2-22):

$$B(x,y;X-Y) = i(2\pi)^{-12}\int dP\,dp\,dq\,e^{-iP(X-Y)}e^{-ipx}e^{iqy}\frac{\Phi(p;P_B)\bar{\Phi}(q;P_B)}{2\omega_B(P_0-\omega_B+i\epsilon)} \\ \times\exp\left\{-i(P_0-\omega_B)[-\frac{1}{2}\,|\,x_0\,|-\frac{1}{2}\,|\,y_0\,|+\frac{1}{2}(\eta_2-\eta_1)(x_0-y_0)]\right\}, \tag{5.2-25}$$

where in the reduced Bethe-Salpeter amplitudes the transition to momentum space was done:

$$\Phi(x,P_B) = (2\pi)^{-4}\int dp\,e^{-ipx}\Phi(p,P_B), \qquad \bar{\Phi}(y,P_B) = (2\pi)^{-4}\int dq\,e^{iqy}\bar{\Phi}(q,P_B). \tag{5.2-26}$$

If we designate for brevity

$$A(p,q;P) = \frac{\Phi(p;P_B)\bar{\Phi}(q;P_B)}{2\omega_B(P_0-\omega_B+i\epsilon)}, \tag{5.2-27}$$

and

$$f(x_0,y_0) = \frac{1}{2}(\eta_2-\eta_1)(x_0-y_0)-\frac{1}{2}\,|\,x_0\,|-\frac{1}{2}\,|\,y_0\,|\,, \tag{5.2-28}$$

then the momentum-space image of B will be

$$B(p,q,P) = (2\pi)^{-4}\int e^{ipx}e^{-iqy}e^{iPX}B(x,y;X)dx\,dy\,dX = \\ i(2\pi)^{-12}\int dx\,dy\,dp'\,dq'e^{i(p-p')x}e^{-i(q-q')y}A(p',q';P')\times\exp\{-i(P_0-\omega_B)f(x_0,y_0)\} \\ \simeq i(2\pi)^{-4}A(p,q;P) \qquad \text{when } P_0\to\omega_B. \tag{5.2-29}$$

Therefore, near the point $P_0=\omega_B$, we have:

$$B(p,q;P) = \frac{i}{(2\pi)^4}\frac{\Phi(p;P_B)\bar{\Phi}(q;P_B)}{2\omega_B(P_0-\omega_B+i\epsilon)}, \tag{5.2-30}$$

that is, the two-particle bound state contribution to $\mathcal{G}(p,q;P)$ has a pole at $P_0=\omega_B$. Other intermediate states $|n\rangle$ will give a regular contribution at this point, if their masses differ from M (and we assume that this is the case). Therefore,

$$\mathcal{G}(p,q;P) \longrightarrow \frac{i}{(2\pi)^4}\frac{\Phi(p;P_B)\bar{\Phi}(q;P_B)}{2\omega_B(P_0-\omega_B+i\epsilon)}\,, \qquad \text{when } P_0\to\omega_B. \tag{5.2-31}$$

5.2.2 Bethe-Salpeter Equation

Let us take $p\neq q$ and $P\to P_B$ in equation (5.2-14) for the Green's function. Taking into account eq. (5.2-31), we get

$$[\Delta_1(\eta_1 P+p)\,\Delta_2(\eta_2 P-p)]^{-1}\,\frac{i}{(2\pi)^4}\frac{\Phi(p;P_B)\bar{\Phi}(q;P_B)}{2\omega_B(P_0-\omega_B+i\epsilon)} = \int dq'\,\mathcal{I}(p,q';P_B)\frac{i}{(2\pi)^4}\frac{\Phi(q';P_B)\bar{\Phi}(q;P_B)}{2\omega_B(P_0-\omega_B+i\epsilon)}. \tag{5.2-32}$$

This implies the Bethe-Salpeter equation (BSE) for the Bethe-Salpeter amplitude:

$$[\Delta_1(\eta_1 P_B+p)\,\Delta_2(\eta_2 P_B-p)]^{-1}\,\Phi(p;P_B) = \int dq'\,\mathcal{I}(p,q';P_B)\,\Phi(q';P_B). \tag{5.2-33}$$

5.2.3 Bethe-Salpeter Equation in Ladder Approximation

Let us consider the Bethe-Salpeter equation in ladder approximation for two scalar particles interacting via scalar quantum exchange. The interaction kernel in this case can be calculated according to standard Feynman rules: every vertex contributes a factor ig and every scalar propagator is given by

$$\Delta(x) = (2\pi)^{-4}\int \frac{e^{-ipx}\,dp}{i[\mu^2-p^2-i\epsilon]}. \tag{5.2-34}$$

Thus,

$$\mathcal{I}(x,y;X-Y) = -g_1g_2\;\Delta(x)\;\delta(x_1-y_1)\;\delta(x_2-y_2) = -g_1g_2\,\Delta(x)\;\delta(x-y)\;\delta(X-Y), \tag{5.2-35}$$

its momentum-space image being

$$\mathcal{I}(p,q;P) = (2\pi)^{-4}\int e^{ipx}e^{-iqy}e^{-iPX}\mathcal{I}(x,y;X)\;dx\;dy\;dX = \frac{ig_1g_2}{(2\pi)^4}\frac{1}{\mu^2-(p-q)^2-i\epsilon}. \tag{5.2-36}$$

Let us substitute this into eq. (5.2-33) and let us take $\vec{P}_B=0$. As a result, we get the rest-frame Bethe-Salpeter equation in ladder approximation:

$$\left[m_1^2+\vec{p}^{\,2}-(\eta_1P_0+p_0)^2\right]\left[m_2^2+\vec{p}^{\,2}-(\eta_2P_0-p_0)^2\right]\Phi(p;P_0) = \frac{\lambda}{i\pi^2}\int d^4q\frac{\Phi(q;P_0)}{\mu^2-(p-q)^2-i\epsilon}, \tag{5.2-37}$$

where we have introduced a coupling constant $\lambda=g_1g_2/(16\pi^2)$ which has the dimension of a mass squared.

This integral equation has a singular kernel, so standard mathematical tools are inapplicable to it. But the singularity in

$$\frac{1}{\mu^2-(p_0-q_0)^2+(\vec{p}-\vec{q})^2-i\epsilon} \tag{5.2-38}$$

disappears if we suppose that p_0 and q_0 are purely imaginary. The procedure of such a transition to imaginary time (energy-) variables is called a "Wick rotation" and it assumes two things: the analytic continuation of $\Phi(p;P_B)$ in the complex p_0-plane and a rotation of the dq_0 integration contour from the real to the imaginary axis. During this rotation, the integration contour must not cross any singularities of the integrand. So it is necessary to study the analytic properties of the amplitude $\Phi(p;P_B)$.

5.2.4 Analytic Properties of the Bethe-Salpeter Amplitude

Let us consider the reduced Bethe-Salpeter amplitude

$$(2\pi)^{-3/2}\Phi(x;P) = \langle 0|T\phi_1(\eta_2 x)\phi_2(-\eta_1 x)|B\rangle = \Theta(x_0)f(x;P) + \Theta(-x_0)g(x;P), \tag{5.2-39}$$

where

$$f(x;P) = \langle 0|T\phi_1(\eta_2 x)\phi_2(-\eta_1 x)|B\rangle \qquad \text{and} \qquad g(x;P) = \langle 0|T\phi_2(-\eta_1 x)\phi_1(\eta_2 x)|B\rangle\,. \tag{5.2-40}$$

Each of these functions can be transformed by using a complete set of states:

$$1 = |n\rangle\langle n| \equiv \sum_\alpha \int dp\,|p,\alpha\rangle\langle p,\alpha|\,, \tag{5.2-41}$$

where α represents discrete quantum numbers of the state $|n\rangle$ and p its four-momentum. We shall consider in the following $f(x;P)$ only, the arguments for $g(x;P)$ being completely analogous. Taking into account the identities

$$\phi_1(\eta_2 x) = e^{i\eta_2 x\cdot\hat{P}}\phi_1(0)e^{-i\eta_2 x\cdot\hat{P}} \qquad \text{and} \qquad \phi_2(-\eta_1 x) = e^{-i\eta_1 x\cdot\hat{P}}\phi_2(0)e^{i\eta_1 x\cdot\hat{P}}, \tag{5.2-42}$$

we calculate easily

$$f(x;P) = \int dp\, e^{-i(p-\eta_1 P)x} f(p;P), \tag{5.2-43}$$

where we have designated

$$f(p;P) = \sum_\alpha \langle 0|\phi_1(0)|p,\alpha\rangle\langle p,\alpha|\phi_2(0)|B\rangle\,. \tag{5.2-44}$$

The matrix element $\langle 0|\phi_1(0)|p,\alpha\rangle$ is different from zero only if $|p,\alpha\rangle$ has the same quantum numbers as the ϕ_1 field quantum. But among all the states with quantum numbers of the first particle, it is just this particle which has the smallest invariant mass, otherwise it would not be stable [6]. Therefore $f(p;P) \neq 0$ only if $p_0 \geq \sqrt{m_1^2 + \vec{p}^{\,2}}$, and we can write

$$\begin{aligned} f(x;P) = \int dp\, e^{-i(p-\eta_1 P)\cdot x} f(p;P)\,\Theta(p_0 - \sqrt{m_1^2 + \vec{p}^{\,2}}) = \\ \int dq\, e^{-iq\cdot x} f(\eta_1 P + q;P)\,\Theta\left(q_0 + \eta_1 P_0 - \sqrt{m_1^2 + (\vec{q} + \eta_1\vec{P})^2}\right). \end{aligned} \tag{5.2-45}$$

This last equation, if we designate

$$\tilde{f}(q;P) = f(\eta_1 P + q;P)\,, \qquad \omega_+ = \sqrt{m_1^2 + (\vec{q} + \eta_1\vec{P})^2} - \eta_1 P_0, \tag{5.2-46}$$

can be rewritten as

$$f(x;P) = \int d\vec{q} \int_{\omega_+}^{\infty} dq_0\, e^{-iqx}\tilde{f}(q;P). \tag{5.2-47}$$

The crucial point is now the observation that

$$\omega_+ \geq m_1 - \eta_1 P_0 = \frac{m_1}{m_1 + m_2}(m_1 + m_2 - P_0). \tag{5.2-48}$$

In the rest frame, P_0 is equal to the bound state mass, therefore $m_1 + m_2 > P_0$. This implies that $\omega_+ > 0$, and only positive frequencies contribute to $f(x;P)$. Analogously, only negative frequencies contribute to $g(x;P)$ (in the rest frame of the bound system). As a result we get for the reduced Bethe-Salpeter amplitude of eq. (5.2-39):

$$\begin{aligned} (2\pi)^{-3/2}\Phi(x;P) \quad = \quad \Theta(x_0)\int d\vec{q}\int_{\omega_+(\vec{q};P)}^{\infty} dq_0\, e^{-iq\cdot x}\tilde{f}(q;P) \;+ \\ \Theta(-x_0)\int d\vec{q}\int_{-\infty}^{\omega_-(\vec{q};P)} dq_0\, e^{-iq\cdot x}\tilde{g}(q;P). \end{aligned} \tag{5.2-49}$$

In the rest frame we always have $\omega_+ > 0$, and $\omega_- < 0$. If we consider x_0 as a complex variable, then eq. (5.2-49) shows that $\Phi(x;P)$ can be analytically continued to the lower half-plane in the region $-\pi < \arg x_0 \leq 0$. Similarly, it can be analytically continued to the upper half-plane in the region $0 < \arg x_0 \leq \pi$.

To deal with eq. (5.2-37), we need the analytic properties of the amplitude in momentum space. Let us consider therefore the Fourier transformation of eq. (5.2-49). Performing the integrals over $d\vec{x}$, $d\vec{q}$ and dx_0, we obtain

$$(2\pi)^{-9/2}\Phi(p;P) = i\int_{\omega_+(\vec{p})}^{\infty} dq_0 \frac{\tilde{f}(q_0,\vec{p};P)}{p_0 - q_0 + i\epsilon} - i\int_{-\infty}^{\omega_-(\vec{p})} dq_0 \frac{\tilde{g}(q_0,\vec{p};P)}{p_0 - q_0 - i\epsilon}. \tag{5.2-50}$$

While integrating over dx_0, we had to assume that the amplitude exists for real values of p_0, i.e., that the integral converges. This necessitates the introduction if the infinitesimal parameter ϵ.

We see that $\Phi(p;P)$ is an analytic function in the complex p_0-plane, with two cuts from ω_+ to $+\infty$ and from $-\infty$ to ω_- (see fig. 5.5). The analytic continuation from the lower to the upper half plane is ensured by the existence of a gap between these two cuts, which in turn is guaranteed by the strict inequalities $\omega_+ > 0$, and $\omega_- < 0$ in the rest frame of the bound system.

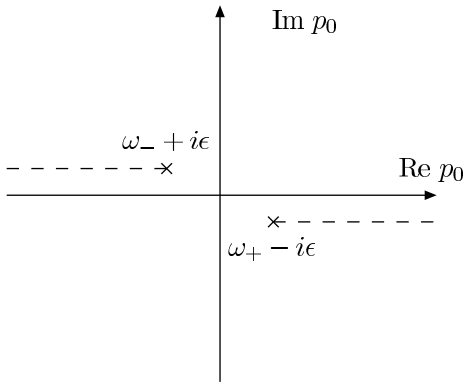

Figure 5.5: Analytic properties of the Bethe-Salpeter amplitude.

Note that the sense of rotation implied by eq. (5.2-50) is opposite to the one in the x_0 plane: from the real p_0 axis one goes continuously into the upper half-plane if $p_0 > \omega_+ > 0$ and into the lower half plane if $p_0 < \omega_- < 0$.

5.2.5 Wick Rotation

We shall now use the analytic properties of the Bethe-Salpeter amplitude to transform the Bethe-Salpeter equation by a rotation of the integration axis in the complex p_0 plane. On the right hand side of eq. (5.2-37) we have the following integral over dq_0:

$$\int_{-\infty}^{\infty} dq_0 \frac{\Phi(q;P_0)}{\mu^2 - (p_0 - q_0)^2 + (\vec{p} - \vec{q})^2 - i\epsilon}. \tag{5.2-51}$$

Its integrand has singularities at $q_0 = p_0 \pm \sqrt{\mu^2 + (\vec{p}^2 - \vec{q}^2) - i\epsilon}$. We shall assume in the following that $p_0 > 0$, (the reasoning for the case $p_0 < 0$ being completely analogous), so that depending on the magnitude of the two terms, the singularities will lie as shown in fig. 5.6. Therefore,

$$\oint_C dq_0 \frac{\Phi(q;P_0)}{\mu^2 - (p_0 - q_0)^2 + (\vec{p} - \vec{q})^2 - i\epsilon} = 0, \tag{5.2-52}$$

where the integration contour C is also shown in fig. 5.6.

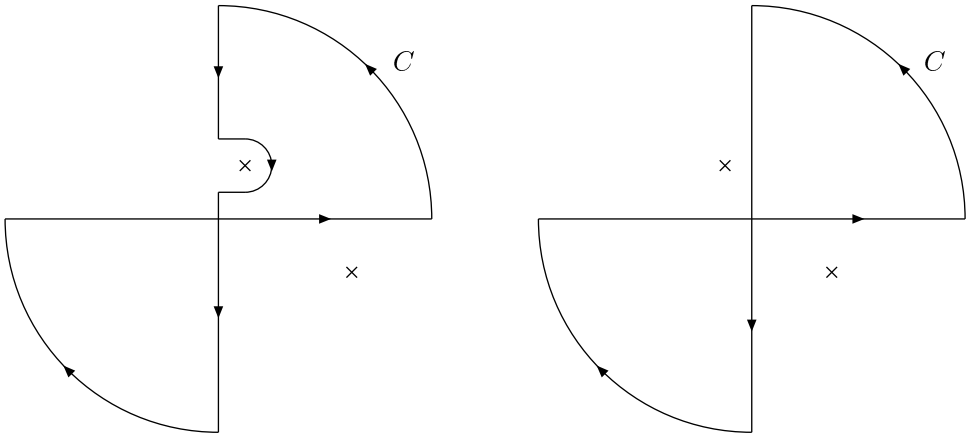

Figure 5.6: Integration contour and singularities before the Wick rotation.

Eq. (5.2-52) is of course guaranteed by the preceding discussion of analytic properties of the Bethe-Salpeter amplitude, which showed that the amplitude $\Phi(q;P_0)$ is an analytic function everywhere in the area covered by C.

The contributions from the two infinite quarter circles of C tends to zero, provided the Bethe-Salpeter amplitude vanishes sufficiently rapidly. Eq. (5.2-52) then implies that the dq_0-integral over the real axis can be replaced by that over the C_i contour, which follows the imaginary axis but goes around the $p_0 - \sqrt{\mu^2 + (\vec{p}-\vec{q})^2 - i\epsilon}$ pole in the case of the left hand side of fig. 5.6. Therefore,

$$[m_1^2 + \vec{p}^2 - (\eta_1 P_0 + p_0)^2][m_2^2 + \vec{p}^2 - (\eta_2 P_0 - p_0)^2]\Phi(p;P_0) = \frac{\lambda}{i\pi^2}\int d\vec{q}\int\limits_{C_i} dq_0 \frac{\Phi(q;P_0)}{\mu^2 - (p_0-q_0)^2 + (\vec{p}-\vec{q})^2 - i\epsilon}. \qquad (5.2\text{-}53)$$

If now we begin to rotate p_0 counterclockwise, both sides of eq. (5.2-53) remain well defined. When we reach the imaginary axis $p_0 = ip_4$, the disposition of the singularities of the integrand will be as in fig. 5.6 but with the poles rotated by $-90°$. This means that the dangerous pole on the left hand side of fig. 5.6 has crossed the imaginary axis, so the C_i contour can be straightened and it will coincide with the imaginary axis. On the right hand side of fig. 5.6, none of the poles crosses the imaginary axis, so the contour can be left invariant. Therefore eq. (5.2-53) becomes:

$$[m_1^2 + \vec{p}^2 - (\eta_1 P_0 + ip_4)^2][m_2^2 + \vec{p}^2 - (\eta_2 P_0 - ip_4)^2]\Phi(ip_4,\vec{p};P_0) = \frac{\lambda}{i\pi^2}\int d\vec{q}\int\limits_{-i\infty}^{i\infty} dq_0 \frac{\Phi(q;P_0)}{\mu^2 - (ip_4-q_0)^2 + (\vec{p}-\vec{q})^2 - i\epsilon}. \qquad (5.2\text{-}54)$$

Let us make the variable change $q_0 \to iq_4$ in the integral over dq_0:

$$[m_1^2 + \vec{p}^2 + (p_4 - i\eta_1 P_0)^2][m_2^2 + \vec{p}^2 + (p_4 + i\eta_2 P_0)^2]\Phi(ip_4,\vec{p};P_0) = \frac{\lambda}{\pi^2}\int d\vec{q}\int\limits_{-\infty}^{\infty} dq_4 \frac{\Phi(iq_4,\vec{q};P_0)}{\mu^2 + (p_4-q_4)^2 + (\vec{p}-\vec{q})^2}. \qquad (5.2\text{-}55)$$

If we now introduce Euclidean four-vectors $\tilde{p} = (\vec{p},p_4)$, $\tilde{q} = (\vec{q},q_4)$ and an amplitude $\tilde{\Phi}(\tilde{p};P_0) = \Phi(ip_4,\vec{p};P_0)$ (which is defined by the analytic continuation of the Bethe-Salpeter amplitude), then the above equation can be rewritten as

$$\left[m_1^2 + \vec{p}^2 + (p_4 - i\eta_1 P_0)^2\right]\left[[m_2^2 + \vec{p}^2 + (p_4 + i\eta_2 P_0)^2]\right]\tilde{\Phi}(\tilde{p};P_0) = \frac{\lambda}{\pi^2}\int d^4\tilde{q}\,\frac{\tilde{\Phi}(\tilde{q};P_0)}{\mu^2 + (\tilde{p}-\tilde{q})^2}. \qquad (5.2\text{-}56)$$

This is the Wick rotated, rest frame, Bethe-Salpeter equation in ladder approximation.

We remark that eq. (5.2-56) has the structure of an eigen-value equation, but contrary to the non-relativistic Schrödinger case, the eigen-value λ is associated with the coupling constant of the potential and not with the energy of the system. Technically, there is of course no problem, once we have determined λ as a function of energy E, we can invert the relation without loss of numerical accuracy. There is however a change in language, in particular, if we will talk about the "ground state" of the theory in the following, we will often mean the state with the lowest coupling constant for a given energy. We also note that the eigen-value structure of the Bethe-Salpeter equation is only recovered in ladder approximation, where the interaction is just given by the lowest order term in the coupling constant.

We note that for the equal-mass case, $m_1 = m_2 = m$, we have from eq. (5.2-4) $\eta_1 = \eta_2 = \frac{1}{2}$, and the left hand side of eq. (5.2-56) becomes real:

$$\left[\left(m^2 + \tilde{p}^2 - \frac{P_0^2}{4}\right)^2 + p_4^2 P_0^2\right] \tilde{\Phi}(\tilde{p}; P_0) = \frac{\lambda}{\pi^2} \int d^4\tilde{q}\, \frac{\tilde{\Phi}(\tilde{q}; P_0)}{\mu^2 + (\tilde{p} - \tilde{q})^2}, \tag{5.2-57}$$

where $\tilde{p}^2 = \vec{p}^{\,2} + p_4^2$. For the general case of unequal masses, eq. (5.2-56) will give complex solutions, a complication that we shall avoid in the rest of this work by sticking to the equal-mass case. Note also that eq. (5.2-57) is an O(4)-invariant equation in the limit where $P_0^2 = 0$. This symmetry will be exploited in the following for finding solutions of the Bethe-Salpeter equation.

5.2.6 Normalization Condition

The homogeneous Bethe-Salpeter equation leaves the normalization of the Bethe-Salpeter amplitude undetermined, but we can use eq. (5.2-17), $\mathcal{G} \cdot (\mathcal{K} - \mathcal{I}) = 1$, which, differentiated with respect to P_0, gives

$$\frac{\partial \mathcal{G}}{\partial P_0}(\mathcal{K} - \mathcal{I}) + \mathcal{G}\left(\frac{\partial \mathcal{K}}{\partial P_0} - \frac{\partial \mathcal{I}}{\partial P_0}\right) = 0, \tag{5.2-58}$$

that is

$$\frac{\partial \mathcal{G}}{\partial P_0} = -\mathcal{G}\,\left(\frac{\partial \mathcal{K}}{\partial P_0} - \frac{\partial \mathcal{I}}{\partial P_0}\right)\,\mathcal{G}. \tag{5.2-59}$$

Let us consider this equation near the point $P_0 = \omega_B$, where eq. (5.2-31) for the Green's function is valid:

$$-\frac{i}{(2\pi)^4}\frac{\Phi(p; P_B)\bar{\Phi}(q; P_B)}{2\omega_B(P_0 - \omega_B + i\epsilon)^2} = -\int dq'\, dq''\, \frac{i}{(2\pi)^4}\frac{\Phi(p; P_B)\bar{\Phi}(q'; P_B)}{2\omega_B(P_0 - \omega_B + i\epsilon)} \left[\frac{\partial}{\partial P_0}(\mathcal{K} - \mathcal{I})\right](q', q'') \quad \frac{i}{(2\pi)^4}\frac{\Phi(q''; P_B)\bar{\Phi}(q; P_B)}{2\omega_B(P_0 - \omega_B + i\epsilon)}. \tag{5.2-60}$$

This gives the following normalization condition:

$$\frac{i}{(2\pi)^4}\int dp\, dq\, \bar{\Phi}(p; P_B)\left[\frac{\partial}{\partial P_0}(\mathcal{K} - \mathcal{I})\right]_{P_0 = \omega_B}(p, q)\,\Phi(q; P_B) = 2\omega_B. \tag{5.2-61}$$

Orthonormality relations in ladder approximation

From eq. (5.2-61), using the fact that in ladder approximation, the interaction kernel $\mathcal{I}$ does not depend on the total energy of the system, we obtain the following normalization condition for the Bethe-Salpeter amplitude:

$$\int \frac{d^4p}{(2\pi)^4}\,\bar{\Phi}_P(p)\,\frac{\partial}{\partial P_0}\,\left\{\left[\left(\frac{P}{2} + p\right)^2 - m^2\right]\left[\left(\frac{P}{2} - p\right)^2 - m^2\right]\right\}\,\Phi_P(p) = 2iP_0, \tag{5.2-62}$$

or, after a Wick rotation in Euclidean space[1],

$$\int \frac{d^4p}{(2\pi)^4}\,\bar{\Phi}_P(p)\,\left[\frac{1}{2}\Big(\frac{P^2}{4}-p^2-m^2\Big)+p_0^2\right]\,\Phi_P(p)=1. \tag{5.2-63}$$

For the sake of discussion, we shall write the Bethe-Salpeter equation as an eigen-value equation for the coupling constant λ in the form $L\Phi=\lambda V\Phi$, with operators L and V in momentum space:

$$\underbrace{\left[\left(p^2+m^2-\epsilon^2\right)^2+4\epsilon^2\,p_0^2\right]}_{\mathrm{L}}\;\;\Phi(p)\;\;=\;\;\lambda\;\;\underbrace{\frac{1}{\pi^2}\int\frac{d^4q}{(p-q)^2+\mu^2}}_{\mathrm{V}}\;\;\Phi(q). \tag{5.2-64}$$

Here we introduced the parameter $\epsilon=P_0/2$, which will play the role of the total energy of the system. With this form it is easy to verify that two solutions that give different energies ϵ_i and ϵ_j for the same coupling constant λ satisfy an orthogonality relation of a form that resembles eq. (5.2-63), so that we can write the following orthonormality condition:

$$\int \frac{d^4p}{(2\pi)^4}\,\bar{\Phi}_i(p)\,\left[\frac{1}{2}\Big(\frac{\epsilon_i^2+\epsilon_j^2}{2}-p^2-m^2\Big)+p_0^2\right]\,\Phi_j(p)=\delta_{ij}. \tag{5.2-65}$$

Alternatively, one can show an orthogonality relation for two solutions that give the same energy for different coupling constants λ_i and λ_j :

$$\int \frac{d^4p}{(2\pi)^4}\,\bar{\Phi}_i(p)\,L\,\Phi_j(p)=0,\qquad i\neq j. \tag{5.2-66}$$

A normalization condition in the form of eq. (5.2-66) may be obtained by differentiating eq. (5.2-64) with respect to ϵ^2, multiplying from the left with $\bar{\Phi}_i$ and integrating over d^4p. Together with the normalization of eq. (5.2-65), we end up with the following orthonormality relations for solutions of the scalar Bethe-Salpeter equation in ladder approximation:

$$\epsilon_i=\epsilon_j:\qquad \int \frac{d^4p}{(2\pi)^4}\,\bar{\Phi}_i(p)\,L\,\Phi_j(p)=\frac{\lambda}{\lambda'}\,\delta_{ij}, \tag{5.2-67}$$

$$\lambda_i=\lambda_j:\qquad \int \frac{d^4p}{(2\pi)^4}\,\bar{\Phi}_i(p)\,L'\,\Phi_j(p)=\delta_{ij}. \tag{5.2-68}$$

where the prime designates differentiation with respect to $s=4\epsilon^2$ and in the last relation we have to replace ϵ^2 by $\frac{1}{2}(\epsilon_i^2+\epsilon_j^2)$ after taking the derivative of L.

5.3 The Wick-Cutkosky Model

The Wick-Cutkosky model (WCM) corresponds to the Bethe-Salpeter equation in ladder approximation for two scalar particles interacting via massless quanta exchange. It has been introduced and thoroughly investigated by Wick [6] and Cutkosky [7]. In their pioneering work, due to the special symmetry of the problem, they have found an explicit expression for the Bethe-Salpeter amplitude in this model. The reason why the WCM has been investigated so extensively in the past, in spite of its "toy-model" character, is not exclusively a consequence of its illustrative value. Even though it is quite the simplest case of a relativistic bound-state problem that one can think of, the WCM already provides the main features, advantages and problems, of more realistic treatments. Quite the most prominent one is the occurrence of abnormal states, that are excitations in the relative-time (or energy-) variable. In the WCM, these states are easily classified (and distinguished numerically) according to the symmetry of the amplitudes under time reversal. The physical relevance of these states is not clarified yet, since the original conjecture by Wick, it is generally believed that they represent artifacts of the ladder approximation.

We shall use this model in the following to illustrate general properties of the relativistic bound-state problem, discuss numerical techniques to solve the equation and calculate form factors in this approach. An extensive overview of the Wick-Cutkosky model may be found in ref. [13], a more pedagogic introduction is given in ref. [14].

[1]For simplicity, we denote vectors in Euclidean and in Minkowski space by the same symbols from now on.

5.3.1 Introduction

After the Wick rotation, the rest frame Bethe-Salpeter equation corresponding to the equal-mass Wick-Cutkosky model (that is eq. (5.2-57) for $\mu = 0$) takes the form

$$\left[\left(m^2 + p^2 - E^2\right)^2 + 4\,p_4^2\,E^2\right]\Phi(p) = \frac{\lambda}{\pi^2}\int d^4q\,\frac{\Phi(q)}{(p-q)^2}, \tag{5.3-1}$$

where $E = P_0/2$ (also denote ϵ in other parts of this work) is the total mass of the system and p, q are Euclidean four-vectors.

To investigate the mathematical structure of eq. (5.3-1), let us consider first the simplest case that was already mentioned above, where the total energy of the system is equal to zero[1]: $E = 0$. Setting also $m = 1$, eq. (5.3-1) becomes

$$(p^2+1)^2\Phi(p) = \frac{\lambda}{\pi^2}\int d^4q\,\frac{\Phi(q)}{(p-q)^2}. \tag{5.3-2}$$

Let us show, that one of its solutions is $\Phi(p) = (p^2+1)^{-3}$. To this end we expand the denominator of the integrand on the right hand side of eq. (5.3-2) into four-dimensional spherical harmonic functions (see App. D):

$$\frac{1}{(p-q)^2} = 2\pi^2\sum_{nlm}\left[\frac{\Theta(p-q)}{p^2}\frac{1}{n+1}\left(\frac{q}{p}\right)^n + \frac{\Theta(q-p)}{q^2}\frac{1}{n+1}\left(\frac{p}{q}\right)^n\right]|nlm\rangle^*\,(\hat{p})\,|nlm\rangle\,(\hat{q}). \tag{5.3-3}$$

Then we can calculate the integral

$$\int\frac{d^4q}{(p-q)^2(q^2+1)^3} = 2\sqrt{2}\pi^3\left\{\frac{1}{p^2}\int_0^p\frac{q^3dq}{(q^2+1)^3} + \int_p^\infty\frac{qdq}{(q^2+1)^3}\right\}|000\rangle = \frac{\sqrt{2}}{2}\pi^3\frac{|000\rangle}{p^2+1}. \tag{5.3-4}$$

Now, since $|000\rangle = \frac{1}{\sqrt{2}\pi}$, we see that $\phi(p) = (p^2+1)^{-3}$ is indeed a solution of eq. (5.3-2) with an eigenvalue $\lambda = 2$.

The most interesting thing about this solution is that we can indicate its analogue in the non-relativistic problem of the hydrogen atom. The Schrödinger equation

$$\left[-\frac{\Delta}{2m} + V(\vec{r})\right]\Psi(\vec{r}) = E\Psi(\vec{r}) \tag{5.3-5}$$

in momentum space becomes an integral equation

$$(\vec{p}^{\,2} + p_0^2)\Psi(\vec{p}) = \frac{me^2}{\pi^2}\int\frac{\Psi(\vec{q})}{(\vec{p}-\vec{q})^2}\,d\vec{q}, \tag{5.3-6}$$

where $p_0^2 = -2mE$ (we consider a discrete spectrum and therefore $E < 0$). One of the solutions of this equation is $\Psi(\vec{p}) = (\vec{p}^{\,2} + p_0^2)^{-2}$, which corresponds to the $E = -(me^4)/2$ ground state of the hydrogen atom. This analogy is only valid on a mathematical level, since the solution in the Wick-Cutkosky model corresponds to the zero-mass case only. However, if the analogy between the solutions of eq. (5.3-2) and eq. (5.3-6) is not accidental, one can expect that the same methods, which are used in dealing with the hydrogen atom [15], will be useful also for eq. (5.3-2) and maybe even for eq. (5.3-1).

Let us proceed by showing, that we can in fact find a complete set of analytic solutions for eq. (5.3-2). Using the identity

$$\Box\frac{1}{(p-q)^2} = -4\pi^2\,\delta^4(p-q), \tag{5.3-7}$$

where $\Box$ is the (Euclidean) d'Alembert operator, see eq. (D.1-5), and p, q are Euclidean four-vectors, we can transform the integral equation into a differential equation:

$$\Box\Psi(p) = -4\lambda\frac{\Psi(p)}{(1+p^2)^2}, \tag{5.3-8}$$

[1] We remark that in the rest frame, $E = 0$ is, of course, unphysical: a massless bound state has no rest frame.

where we have introduced a new function $\Psi(p) = (p^2+1)^2\Phi(p)$. This is an O(4)-invariant equation, so the solutions can be factorized into orbital and radial parts: $\Psi(p) = \psi(p^2)|\kappa lm\rangle$. If we make the variable change $p^2 = \frac{1+z}{1-z}$, equation (5.3-8) is reduced to the one-dimensional differential equation

$$(1-z^2)\psi'' + 2(1-z)\psi' - \frac{\kappa(\kappa+2)}{1-z^2}\psi = -\lambda\psi. \tag{5.3-9}$$

This equation admits solutions in terms of Gegenbauer polynomials $C_n^\kappa(z)$ in the form

$$\psi(z) = (1-z)(1-z^2)^{\kappa/2}\, C_n^{\kappa+3/2}(z), \tag{5.3-10}$$

with eigenvalues $\lambda = (n+\kappa+1)(n+\kappa+2)$. So a complete set of solutions of eq. (5.3-2) is given by:

$$\Phi_{n\kappa lm}(p) = \frac{|p|^\kappa}{(1+p^2)^{\kappa+3}}\, C_n^{\kappa+3/2}\left(\frac{p^2-1}{p^2+1}\right)|\kappa lm\rangle\,. \tag{5.3-11}$$

These solutions have a definite parity with respect to time inversion because of the symmetry property of the O(4) spherical harmonics: $|\kappa lm\rangle \to (-1)^{\kappa-l}|\kappa lm\rangle$. Let us display explicitly the lowest solutions with angular momentum $l=0$: after the ground state $\Phi_{0000}(p) = (p^2+1)^{-3}$ with $\lambda = 2$ we have two states with $\lambda = 6$ (not normalized):

$$\Phi_{1000}(p) = \frac{1-p^2}{(1+p^2)^4}, \qquad \Phi_{0100}(p) = \frac{p_0}{(1+p^2)^4}. \tag{5.3-12}$$

This illustrates explicitly that the states with odd quantum numbers κ are odd functions of the relative-time (here: energy-) variable p_0. In general, whenever the Bethe-Salpeter amplitude has a zero as a function of the relative-time variable, one speaks of an abnormal solution of the Bethe-Salpeter equation. We note that apart from the odd-parity functions mentioned above, we also have even abnormal solutions, the ones with an even $\kappa \neq 0$. An interesting discussion of these abnormal states together with a compilation of their surprising properties, may be found in ref. [16].

Before we discuss the general properties of the solutions (5.3-11), let us first find the complete spectrum of eq. (5.3-1) for arbitrary energies E.

5.3.2 Different Methods of Solution

There exist several methods to solve a Bethe-Salpeter equation, some more fit for a numerical treatment [17,18], some that make certain analytic properties more explicit [19,20]. We shall briefly discuss the most important of these approaches.

Numerical integration

For a finite energy E the Bethe-Salpeter equation of the Wick-Cutkosky model, eq. (5.3-1), can still be converted into a partial differential equation [21] as before by applying the d'Alembert operator $\Box$. The generalization of eq. (5.3-8) is:

$$\Box\Psi(p) = -4\lambda\frac{\Psi(p)}{(p^2+1-E^2)^2 + 4E^2p_0^2}, \tag{5.3-13}$$

where the function $\Psi(p)$ is now written as $\Psi(p) = \left[(p^2+m^2-E^2)^2 + 4E^2p_0^2\right]\Phi(p)$. This equation is no longer O(4)-invariant for $E \neq 0$, but it is still invariant under rotations in three-dimensional space. We can therefore separate the angular variables. Defining the spatial variable $p_s = \sqrt{p_x^2+p_y^2+p_z^2}$, we express $\Psi(p)$ in the form

$$\Psi(p) = \Psi(p_0, p_s)Y_l^m(\theta,\phi). \tag{5.3-14}$$

Introducing the dimensionless variables $\epsilon = E/m$, $\rho_0 = p_0/m$ and $\rho_s = p_s/m$, eq. (5.3-13) takes the form (see ref. [21]):

$$\left(\frac{\partial^2}{\partial\rho_0^2} + \frac{1}{\rho_s}\frac{\partial^2}{\partial\rho_s^2}\rho_s - \frac{l(l+1)}{\rho_s^2}\right)\Psi(\rho_0,\rho_s) = -\frac{4\lambda}{m^2}\frac{\Psi(\rho_0,\rho_s)}{[(\rho_0^2+\rho_s^2+1-\epsilon^2)^2 + 4\rho_0^2\epsilon^2]}. \tag{5.3-15}$$

From this equation it follows that the form of the solution near the singularity at $\rho_s = 0$ is

$$\lim_{\rho_s \to 0} \Psi(\rho_0, \rho_s) \sim \rho_s^l. \tag{5.3-16}$$

We write $\Psi(\rho_0, \rho_s)$ in a form that incorporates this behaviour:

$$\Psi(\rho_0, \rho_s) = \rho_0^{l'} \rho_s^l \xi(\rho_0, \rho_s), \tag{5.3-17}$$

where the function $\xi(\rho_0, \rho_s)$ has to be finite at $\rho_s = 0$ and has to satisfy the boundary conditions

$$\lim_{\rho_0 \to \pm\infty} \xi(\rho_0, \rho_s) = \lim_{\rho_s \to \infty} \xi(\rho_0, \rho_s) = 0. \tag{5.3-18}$$

We shall therefore expand it in terms of some basis functions:

$$\xi(\rho_0, \rho_s) = \sum_{i=1}^{I_{max}} C_i G_i(\rho_0, \rho_s), \tag{5.3-19}$$

that are chosen to be of Gaussian type:

$$G_i(\rho_0, \rho_s) = e^{-\alpha_i \rho_0^2 - \beta_i \rho_s^2}. \tag{5.3-20}$$

These basis functions are even functions of the "time variable" ρ_0, this is the reason why we wrote an explicit factor $\rho_0^{l'}$ in eq. (5.3-17), in order to allow for odd solutions, too. (Since eq. (5.3-15) is invariant with respect to the time reversal transformation $\rho_0 \to -\rho_0$, all the solutions have to be either even or odd functions of ρ_0.) In practice, we always have $l' = 0$ or 1. Now we rewrite eq. (5.3-15) as an equation for $\xi(\rho_0, \rho_s)$:

$$\begin{aligned} \Big\{ l'(l'-1)\rho_0^{l'-2}\rho_s^{l+1} + 2l'\rho_0^{l'-1}\rho_s^{l+1}\frac{\partial}{\partial\rho_0} + \rho_s^{l+1}\rho_0^{l'}\frac{\partial^2}{\partial\rho_0^2} + \\ 2(l+1)\rho_0^{l'}\rho_s^{l}\frac{\partial}{\partial\rho_s} + \rho_0^{l'}\rho_s^{l+1}\frac{\partial^2}{\partial\rho_s^2} \Big\} \xi(\rho_0, \rho_s) = \\ -\frac{4\lambda}{m^2} \frac{\rho_0^{l'}\rho_s^{l+1}\xi(\rho_0, \rho_s)}{[(\rho_0^2 + \rho_s^2 + 1 - \epsilon^2)^2 + 4\rho_0^2\epsilon^2]}. \end{aligned} \tag{5.3-21}$$

If we now insert eq. (5.3-19), multiply both sides with $\rho_0^{l'}\rho_s^{l+1}G_j$ and integrate over ρ_s and ρ_0, we see, that we obtain a generalized eigen-value equation of the form

$$AC = \frac{\lambda}{m^2} BC, \tag{5.3-22}$$

where the matrices A and B are both positive-definite and symmetric. The elements of the column matrix C are the expansion coefficients of eq. (5.3-19) and the elements of the matrices A and B are given by

$$\begin{aligned} A_{ij} &= -\int_{-\infty}^{\infty} d\rho_0 \int_0^{\infty} d\rho_s \, G_j \, \rho_0^{2l'} \rho_s^{2l+1} \\ &\quad \Big\{ l'(l'-1)\rho_0^{-2}\rho_s + 2l'\rho_0^{-1}\rho_s\frac{\partial}{\partial\rho_0} + \rho_s\frac{\partial^2}{\partial\rho_0^2} + 2(l+1)\frac{\partial}{\partial\rho_s} + \rho_s\frac{\partial^2}{\partial\rho_s^2} \Big\} G_i. \end{aligned} \tag{5.3-23}$$

$$B_{ij} = 4\int_{-\infty}^{\infty} d\rho_0 \int_0^{\infty} d\rho_s \frac{G_j \, \rho_0^{2l'} \rho_s^{2(l+1)} \, G_i}{[(\rho_0^2 + \rho_s^2 + 1 - \epsilon^2)^2 + 4\rho_0^2\epsilon^2]}. \tag{5.3-24}$$

The necessary integrals to calculate these matrix elements are given in App. C.

The result for the spectrum of the Wick-Cutkosky model is shown in fig. 5.7. One immediately recovers the additional O(4) symmetry for the case $\epsilon^2 = 0$ due to the degeneracy of the eigen-values for $n+\kappa = const.$, as discussed after eq. (5.3-8). For finite values of ϵ^2 this degeneracy is broken such that the normal states ($\kappa = 0$) are always the lowest ones. For a given $n+\kappa = N$, one has the following ordering of energies $\epsilon_{n,\kappa}$ at a fixed coupling constant λ: $\epsilon_{n,\kappa} > \epsilon_{n+1,\kappa-1}$. Miscellaneous properties of the eigen-values of the Bethe-Salpeter equation in the Wick-Cutkosky model have been studied in refs. [22, 23]. We note

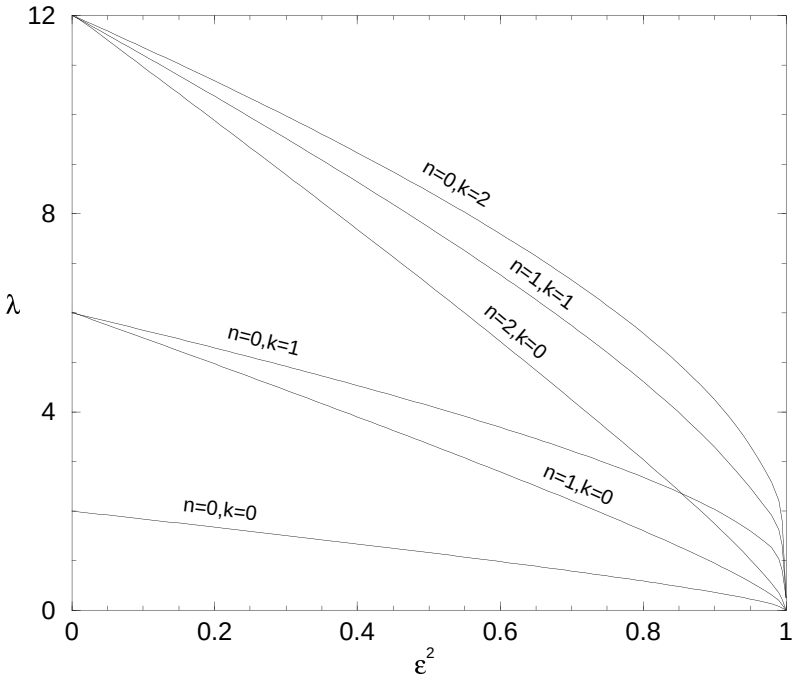

Figure 5.7: Spectrum of the Wick-Cutkosky model.

furthermore that the normal solutions tend to a zero binding energy ($\epsilon^2 \to 1$) for a vanishing coupling constant $\lambda \to 0$, as expected from the non-relativistic (weak-binding) limit. The corresponding limit for the abnormal solutions ($\kappa \neq 0$) is hard to guess from fig. 5.7, in fact there are some numerical problems in this limit due to the slow convergence of the integrals in eq. (C.3-7). The determination of the exact behaviour of these solutions in the limit $\epsilon^2 \to 1$ demands a much more subtle analysis, as demonstrated in the next subsection.

The integral representation method

Because of the zero mass of the exchanged boson, the Wick-Cutkosky model has an extra symmetry just like the non-relativistic Schrödinger equation for the hydrogen atom, as demonstrated above. Due to this property, Wick was able to show that the four-dimensional integral equation (5.3-1) can be reduced to a one-dimensional differential equation. There are several ways of doing this, the most prominent one being the integral representation method worked out by Wick and Cutkosky. For the simple case $n = l + 1$, it is possible to show that

$$\Phi_{nlm}(p) = \int_{-1}^{1} \frac{g(z)\,dz}{[p^2 + 2izp\cdot\eta + 1 - \eta^2]^{n+2}}\,\mathcal{Y}_l^m(\vec{p}) \tag{5.3-25}$$

is a solution of the Bethe-Salpeter equation (5.3-1), provided the function $g(z)$ satisfies the differential equation

$$(1-z^2)\,g_n''(z) + 2(n-1)\,z\,g_n'(z) - n(n-1)\,g_n(z) + \lambda\frac{g_n(z)}{1-\eta^2+\eta^2\,z^2} = 0, \tag{5.3-26}$$

with the boundary conditions $g_n(\pm 1) = 0$. In these formulas, η is an arbitrary four-vector with $\eta^2 = \epsilon^2$, so conveniently it is chosen to be the total four-momentum of the system. The functions $g(z)$ are commonly called Cutkosky functions.

Equation (5.3-26) can be solved with high numerical accuracy, for instance by employing the Numerov-algorithm [24]. We show some examples of solutions in figs. 5.8 and 5.9. The first case corresponds to solutions for a strong coupling case, $\alpha = 3$, the second one to a moderate coupling of $\alpha = 1$. The coupling constant α here is related to the eigen-value λ of eq. (5.3-26) by $\lambda = \pi\alpha$, and it has the advantage of being

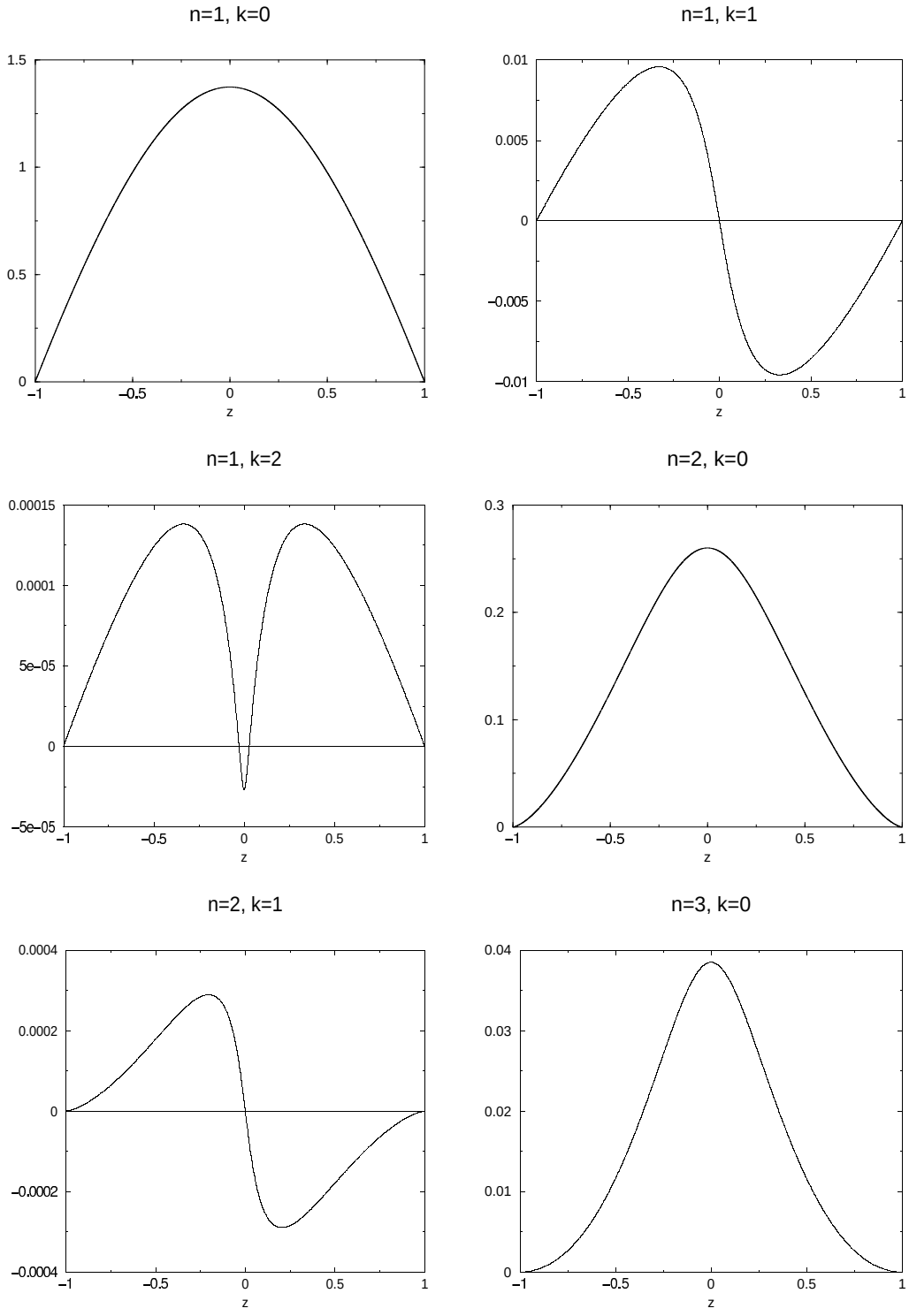

Figure 5.8: Examples of Cutkosky functions for $\alpha = 3$.

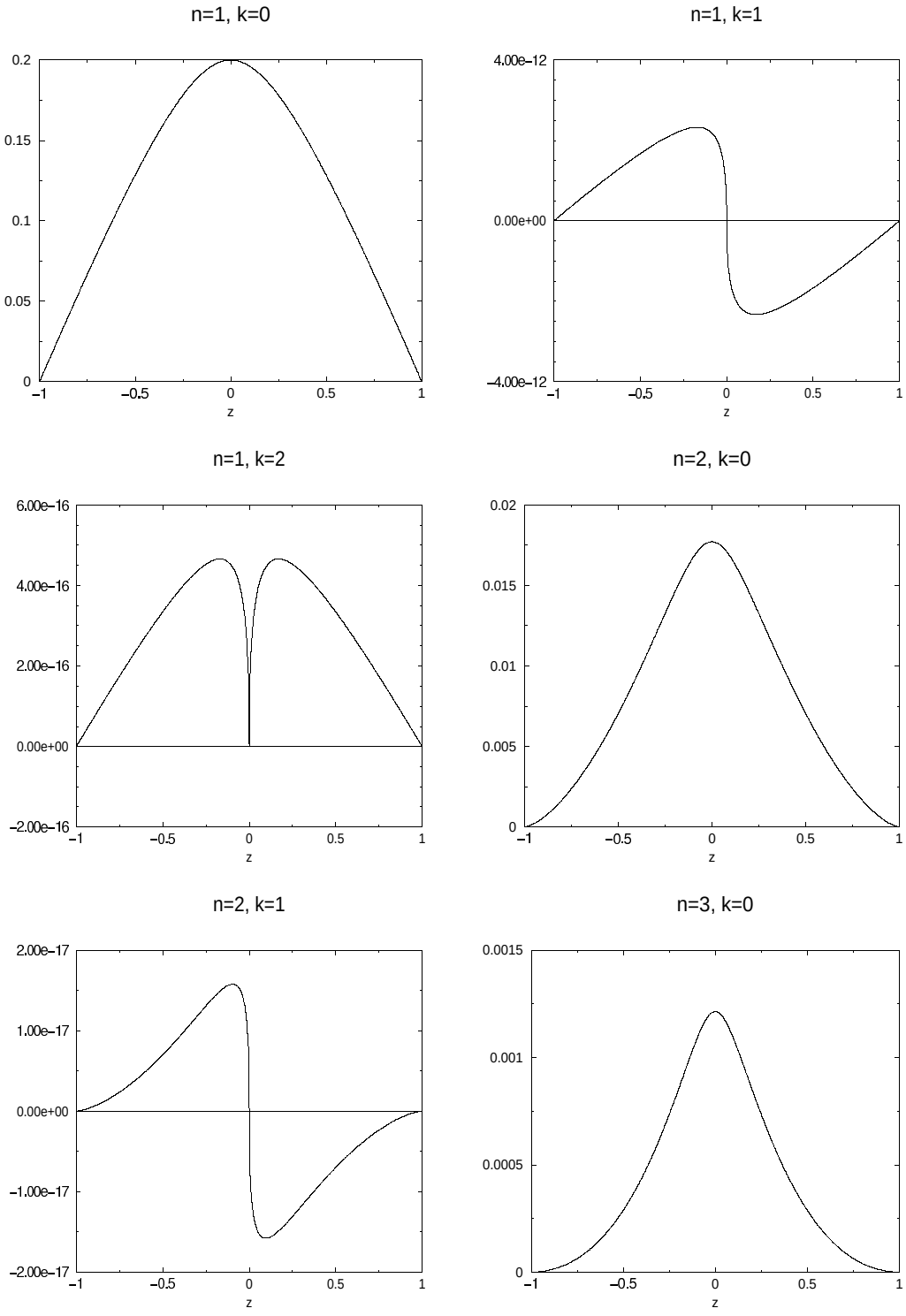

Figure 5.9: Examples of Cutkosky functions for $\alpha = 1$.

directly comparable to the fine structure constant of QED. We see from the figures that the abnormal solutions ($\kappa \neq 0$) are easily identified in this approach by the number of zeros of their Cutkosky function in the interval $-1 < z < 1$.

Two special cases are particularly interesting when solving eq. (5.3-26), one that corresponds to the deep-binding (or ultra-relativistic) limit, $\eta^2 \to 0$, the other one to the weak-binding (or non-relativistic) limit with $\eta^2 \to 1$.

- $\eta^2 = 0$:

  In this case it is easily seen, that a general solution of eq. (5.3-26) is given by

  $$g_n(z) = \left(1 - z^2\right)^n \, C_\kappa^{n+\frac{1}{2}}(z), \tag{5.3-27}$$

  involving the Gegenbauer polynomials $C_\kappa^n(z)$. The eigen-values in this case are given by $\lambda = (n+\kappa)(n+\kappa+1)$. This is of course just a special case of the general solution found before, see eq. (5.3-11).

- $\eta^2 = 1$:

  This case is much more delicate and one has to consider very carefully the limit $\eta^2 \to 1$. For the normal states ($\kappa = 0$), Wick noted that the factor $1/(1-\eta^2+\eta^2 z^2)$ tends to $\delta(z)/\sqrt{1-\eta^2}$, which gives solutions in the form

  $$g_n(z) = (1 - |\, z \,|)^n \,. \tag{5.3-28}$$

  In particular, these solutions reproduce the spectrum of the non-relativistic hydrogen atom in the weak-binding limit: $B \sim \frac{\alpha^2}{4n^2}$, where B is the binding energy. Even more impressive, also the non-relativistic wave functions of the hydrogen atom are recovered [7], so we can say that the Wick-Cutkosky model, applied to normal states, reduces exactly to the non-relativistic Schrödinger equation with a Coulomb potential in the weak-binding limit.

  The second case corresponds to the abnormal solutions in this limit ($\kappa \neq 0$). Eq. (5.3-26) then takes the form

  $$(1-z^2)\, g_n''(z) + 2(n-1)\, g_n'(z) - n(n-1)\, g_n(z) + \frac{\lambda}{z^2}\, g_n(z) = 0, \tag{5.3-29}$$

  which gives solutions

  $$g_n(z) = \left(1 - z^2\right)^n \, z^{\rho+\frac{1}{2}} \, F\left[\frac{2n+2\rho+3}{4}, \frac{2n+2\rho+1}{4}; n+1; 1-z^2\right]. \tag{5.3-30}$$

  Here F is a hypergeometric function and $\rho = \sqrt{1/4 - \lambda}$. It was then shown that the eigen-values λ tend to the value $\lambda \to 1/4$ for vanishing binding energy and that the abnormal solutions therefore do not exist below this critical value of the coupling constant. This has led to the notion that abnormal solutions do not have a non-relativistic limit, which is very often repeated in the literature. This is not exactly true however, since there is a well-defined limit when the binding energy goes to zero (and the constituents therefore become non-relativistic). What does not exist is the weak-coupling limit, since the coupling constant is always greater than zero. A very elegant proof of this particularity may be found in ref. [25].

Expansion in spherical harmonics

We shall finally outline two methods that are also applicable to the more general case when the exchanged meson has a finite mass μ[1]. The first one is inspired by the observation that the Bethe-Salpeter equation has an exact O(4) symmetry for $E = 0$, so that the solution is proportional to a four-dimensional spherical harmonic function (see App. D). When this symmetry gets broken, we can write the general

[1]Some authors refer to this model as the 'massive Wick-Cutkosky model'. We do not follow this terminology, because the finite mass of the exchanged boson destroys the almost defining property of the Wick-Cutkosky model: the additional O(4) symmetry. We prefer to use the terms 'scalar model' or '$\varphi^2\chi$ theory'.

solution of the Bethe-Salpeter equation as an expansion into these spherical harmonics, which form a complete set on the four-dimensional sphere. This method is known since a very long time [17,26] and it is still used in many numerical calculations today. In particular, the convergence of the eigen-values in this expansion scheme has been studied in ref. [27].

As an illustration, we note the expansion of the kernel function on the right hand side of eq. (5.2-56):

$$\frac{1}{(p-q)^2+\mu^2} = \sum_{klm} V_k(p,q) \frac{2\pi^2}{k+1} \, |klm\rangle^*_{(\hat{p})} \, |klm\rangle_{(\hat{q})} \,, \tag{5.3-31}$$

with

$$V_k(p,q) = \frac{1}{pq\left[z+\sqrt{z^2-1}\right]^{k+1}}, \qquad z = \frac{p^2+q^2+\mu^2}{2pq}. \tag{5.3-32}$$

Note that in the special case $\mu = 0$, eq. (5.3-31) reduces to the expression (5.3-3) given earlier. After some straightforward algebra, the Bethe-Salpeter equation can then be converted into an infinite set of coupled one-dimensional integral equations, which can be treated by standard numerical means.

Solution in configuration space

Let us write the Bethe-Salpeter equation in the same form as in eq. (5.2-64). Performing a Fourier transformation in four-dimensional Euclidean space, and denoting the operators in configuration space again by L and V, we get [17]:

$$L\Psi = \lambda V \Psi, \tag{5.3-33}$$

with

$$L = \left(-\Box + 1 - \epsilon^2\right)^2 - 4\epsilon^2 \frac{\partial^2}{\partial x_0^2}, \qquad \Box = \sum_{i=1}^{4} \frac{\partial^2}{\partial x_i^2}, \tag{5.3-34}$$

and

$$V(R) = \frac{1}{\pi^2} \int d^4q \frac{e^{-iq\cdot x}}{q^2+\mu^2} = \frac{4\mu}{R} K_1(\mu R), \qquad R = \left(\sum_{i=1}^{4} x_i^2\right)^{1/2}. \tag{5.3-35}$$

In the last equation, $K_1(x)$ is a modified Bessel function. Note that for $\mu = 0$ the potential becomes $V(R) = 4/R^2$, which is just the Coulomb potential in four dimensions.

Again, we expand the solutions Ψ of eq. (5.3-33) in four-dimensional spherical harmonics, which implies that we have to determine a set of functions of one variable R only. We then arrive at the structure of our trial function

$$\Psi = \sum_n R^n \, f_{nl}(R) \;\; |nlm\rangle \,, \tag{5.3-36}$$

where the factor R^n follows from the asymptotic behaviour of the wave function at the origin. For $R \to \infty$, the Bethe-Salpeter amplitude is known to decay exponentially [6,7], so that a natural choice for a variational basis function would be a simple exponential [17]. For calculational convenience, we chose a Gaussian basis:

$$f_{nl}(R) = \sum_i c_i \; e^{-\alpha_i R^2}, \tag{5.3-37}$$

the slight loss in accuracy being more than compensated by the possibility of easily increasing the number of terms in the expansion. The nonlinear parameters α_i in eq. (5.3-37) are chosen stochastically, a method that was already successfully applied in other domains of physics [28] and in the first part of this work (see App. B).

Note that due to the transformation properties of the spherical harmonic functions, the sum in eq. (5.3-36) always runs over either even or odd values of n, according to the quantum numbers of the state. In particular this allows us to calculate states of different relative time-parity separately.

The numerical performance of the method is very satisfactory as regarding precision and computing time. As in ref. [27], we found the convergence in terms of hyper-spherical harmonics slowest in case of a small mass of the exchanged meson and small binding energies. In this case, the expansion in eq. (5.3-36) was pushed up to $n_{max} = 30$. In eq. (5.3-37), we extended the sum up to $i_{max} = 25$, the results being practically unchanged by the addition of the last few terms.

5.3.3 Normalization

We shall briefly discuss the application of the normalization condition eq. (5.2-63) to the case of the Wick-Cutcosky model [29]. With the general representation for the Bethe-Salpeter amplitude of eq. (5.3-25), and with the help of a Feynman transformation, see eq. (C.3-5), one easily obtains:

$$I_1 = -\frac{\pi}{2}\frac{(2n-1)!!}{(2n)!!}\int_0^1 x^{n+1}(1-x)^{n+1}dx\int_{-1}^1 dz\int_{-1}^1 dz'\frac{g_n(z)\,g_n(z')}{\left\{1+\epsilon^2\left[zx+z'(1-x)\right]^2-\epsilon^2\right\}^{n+2}}. \quad (5.3\text{-}38)$$

For a properly normalized solution according to eq. (5.2-68), we require $I_1 = 1$. For the case of eq. (5.2-67) we introduce an analogous factor that we call I_3:

$$I_3 = \frac{\pi}{2^{2n+1}}\frac{(2n)!}{[(n+1)!]^2}\,J, \quad (5.3\text{-}39)$$

with [30, 31]

$$J = \int_0^1 x^{n+1}(1-x)^{n+1}dx\int_{-1}^1 dz\int_{-1}^1 dz' g_n(z)\,g_n(z')\left(\frac{\partial^2}{\partial\alpha\,\partial\beta}\left[(\alpha+\beta)^2-4\alpha\beta\epsilon^2\right]^{-n-1}\right)\Bigg|_{\beta=1-\alpha}, \quad (5.3\text{-}40)$$

and $\alpha = \frac{1}{2}[(1+z)x+(1+z')(1-x)]$. The equivalence of the two normalization factors I_1 and I_3 is of course guaranteed by the corresponding relations of eqs (5.2-68) and (5.2-67):

$$\frac{I_1}{I_3} = \frac{\lambda'}{\lambda}. \quad (5.3\text{-}41)$$

There exists a third possibility of normalizing the Cutkosky functions $g(z)$, which is much simpler and more elegant than the ones discussed above. It is based on the observation, that the differential equation for $g(z)$, eq. (5.3-26) can be brought into a Schrödinger-like form $y''(z) = A(z)\,y(z)$ with the change of variables $g(z) = (1-z^2)^{(n-1)/2}\,y(z)$. One can then deduce an orthonormality relation in the form

$$\int_{-1}^1 \frac{y_i(z)\,y_j(z)}{\left(z^2+\frac{1}{\epsilon_i^2}-1\right)\left(z^2+\frac{1}{\epsilon_j^2}-1\right)} = 0, \qquad i\neq j, \quad (5.3\text{-}42)$$

which suggests a normalization factor

$$I_2 = \int_{-1}^1 \frac{y_i^2(z)}{\left(z^2+\frac{1}{\epsilon^2}-1\right)^2}. \quad (5.3\text{-}43)$$

This normalization has a priori no relation with the normalization of the four-point Green's function for a bound state and therefore has no physical meaning by itself. It is however technically much easier to calculate the factor I_2 (one has to evaluate a one-dimensional integral only instead of a three-dimensional one). It is therefore interesting to note that for the ground state solution of eq. (5.3-26) with $n = 1$, there exists a very simple relation between the two normalizations:

$$\frac{I_1}{I_2} = -\frac{\pi}{128(\epsilon^4-\epsilon^6)}\left(\frac{\int_{-1}^1 g_1(z)\,dz}{g_1(0)}\right)^2. \quad (5.3\text{-}44)$$

The different possibilities of normalization and their inter-relations have been studied in ref. [32]. It seems to be possible to generalize the relation (5.3-44) to the case of excited states, but no general solution has been found yet.

5.3.4 Form Factors in the Wick-Cutkosky Model

Calculations of form factors [33–35] often retain in a first approximation the single-particle current (impulse approximation). In most approaches, this contribution has to be completed by at least two-body currents, especially to fulfil current conservation. This also holds for relativistic approaches where a covariant calculation of the single-particle current does not necessarily imply a complete account of the physical process. For each relativistic approach, it is therefore important to test the degree of validity by comparing its predictions to a case where an exact calculation can be performed. Neglecting vertex and

mass corrections, as usually done on the basis that they are partly incorporated in the physical inputs, such an exact calculation is generally believed to be provided by the Bethe-Salpeter equation with an appropriate interaction kernel.

A particular case of interest is the Wick-Cutkosky model, where calculations of form factors can be performed rather easily. Contrary to other approaches, there is no need to add two-body currents. The contribution of the single-particle current is sufficient in the Bethe-Salpeter equation in ladder approximation to ensure current conservation [36]. This can be checked explicitly with the expressions of the matrix elements of the current.

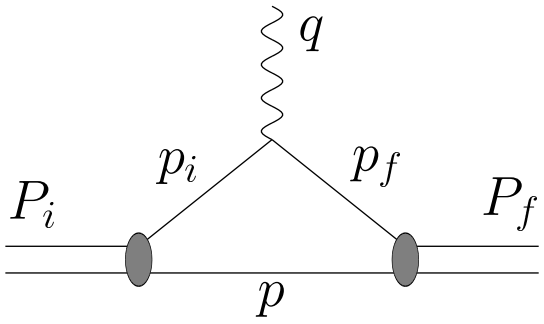

Figure 5.10: Representation of a virtual photon absorption on a two-body system with the kinematical definitions.

The contribution which we are interested in is shown in fig. 5.10. The general expression of the corresponding matrix element between two states with $l = 0$, possibly different, is given by

$$\langle f|j^\mu|i\rangle = F_1(q^2)\,(P_f^\mu + P_i^\mu) + F_2(q^2)\,q^\mu, \tag{5.3-45}$$

$$\langle f|s|i\rangle = F_0(q^2), \tag{5.3-46}$$

where $q^\mu = P_f^\mu - P_i^\mu$, and j^μ is related to a vector probe (electromagnetic case) while s gives the current of a scalar probe. Current conservation imposes constraints on the form factors $F_1(q^2)$ and $F_2(q^2)$. For an elastic process, $F_2(q^2)$ has to vanish but this result automatically stems from symmetry arguments alone. It does not imply that current conservation holds at the operator level, as it should. For an inelastic process, the following relationship has to be fulfilled:

$$F_1(q^2)\,(M_f^2 - M_i^2) + F_2(q^2)\,q^2 = 0. \tag{5.3-47}$$

For the Wick-Cutkosky model, the general expression of the matrix element of the currents, that reduce to single-particle ones in this case, can be written in terms of the Bethe-Salpeter amplitudes $\chi_P(p)$:

$$\langle f|j^\mu|i\rangle = i\int \frac{d^4p}{(2\pi)^4}\,\chi_{P_f}\Big(\frac{1}{2}P_f - p\Big)\,\Big(P_f^\mu + P_i^\mu - 2p^\mu\Big)\,(p^2 - m^2)\,\chi_{P_i}\Big(\frac{1}{2}P_i - p\Big), \tag{5.3-48}$$

$$\langle f|s|i\rangle = i\int \frac{d^4p}{(2\pi)^4}\,\chi_{P_f}\Big(\frac{1}{2}P_f - p\Big)\,(p^2 - m^2)\,\chi_{P_i}\Big(\frac{1}{2}P_i - p\Big). \tag{5.3-49}$$

With the general representation in terms of Cutkosky functions, eq. (5.3-25), one gets the following expressions for the form factors F_0, F_1 and F_2:

$$F_0(q^2) = -\frac{3\pi}{8}\int_{-1}^{1} dz\,g(z)\int_{-1}^{1} dz'\,g(z')\int_0^1 x^2(1-x)^2\frac{dx}{(2\pi)^4}\frac{m^2 + A + \frac{1}{3}a}{a^4}, \tag{5.3-50}$$

$$F_1(q^2) = -\frac{3\pi}{16}\int_{-1}^{1} dz\,g(z)\int_{-1}^{1} dz'\,g(z')\int_0^1 x^2(1-x)^2\frac{dx}{(2\pi)^4} \times\frac{(m^2 + A)\,\{2 - x(1+z) - (1-x)(1+z)\} + \frac{2}{3}a}{a^4}, \tag{5.3-51}$$

Table 5.1: Scalar and electromagnetic form factors in the Wick-Cutkosky model. $F_i(n\kappa \to n'\kappa')$ denotes the form factors of eq. (5.3-50)-(5.3-52) for a transition of a state with $n\kappa$ to $n'\kappa'$ quantum numbers. Wave functions employed are those that give solutions for $\alpha = \pi\lambda = 3$.

	Q^2/m^2				
	0	0.01	0.1	1.0	10.0
$F_0(10 \to 10)$	2.255	2.246	2.161	1.535	0.264
$F_0(11 \to 10)$	2.05	1.70	4.96-1	8.55-3	-3.28-5
$F_0(12 \to 10)$	2.00	0.11	7.70-4	1.70-6	-2.6-8?
$F_1(10 \to 10)$	1.0	0.996	0.962	0.705	0.139
$F_1(11 \to 11)$	1.0	0.828	0.238	3.57-3	-3.57-3
$F_1(12 \to 12)$	1.0	5.50-2	3.83-4	8.68-7	-1.53-8?
$F_1(11 \to 10)$	8.0-8?	2.63-4	2.35-3	9.37-3	2.50-3
$F_1(12 \to 10)$	2.0-4?	2.0-4?	2.6-4?	5.7-4	-2.1-4?
$F_2(11 \to 10)$	-4.03-2	-3.98-2	-3.56-2	-1.42-2	-3.78-4
$F_2(12 \to 10)$	-3.94-2	-3.89-2	-3.47-2	-1.38-2	-3.69-4

$$F_2(q^2) = \frac{3\pi}{16}\int_{-1}^{1} dz\, g(z) \int_{-1}^{1} dz'\, g(z') \int_0^1 x^2(1-x)^2 \frac{dx}{(2\pi)^4} \times \frac{(1-x)(1+z') - x(1+z)}{a^4}(m^2 + A), \tag{5.3-52}$$

with the following factors

$$A = m^2 - \frac{x}{2}(1+z)P^2 - \frac{1-x}{2}(1+z')P'^2, \qquad a = -Q^2 - A, \tag{5.3-53}$$

and the kinematical quantities

$$P' = P + q, \qquad Q^2 = -q^2, \qquad P^2 = M^2, \qquad P'^2 = M'^2, \qquad 2P\cdot P' = M^2 + M'^2 + Q^2,$$
$$4Q^2 = x^2(1+z)^2M^2 + (1-x)^2(1+z')^2M'^2 + 2x(1-x)(1+z)(1+z')P\cdot P'. \tag{5.3-54}$$

In table 5.1 we present results for various form factors in the Wick-Cutkosky model for solutions of the Bethe-Salpeter equation with $\alpha = \pi\lambda = 3$. They were obtained by evaluating numerically the three-dimensional integrals in eqs. (5.3-50) - (5.3-52). We note that we encountered certain numerical difficulties, where the integrals did not converge in terms of the integration step. This was in particular the case for large momentum transfers and for certain excited states with small binding energy. Numerical results that were not completely converged are marked by a question mark[1] in table 5.1. Integrating analytically over the variable x in eqs. (5.3-50) - (5.3-52) improved evidently the computation time, but not the numerical accuracy. The problem seems therefore related to the properties of the Cutkosky functions in a specific domain of z-values. The situation gets worse for smaller coupling constants, for the case $\alpha = 1$ for instance, we were able to find stable solutions for the ground state only.

As for a physical interpretation, we note that the form factors of abnormal states do not show any particular difference as compared to those of normal ones, the drop-off at large Q^2 being determined by the binding energy of the excited state.

[1]Note that the inelastic transition form factors $F_1(11 \to 10)$ and $F_1(12 \to 10)$ are rigorously zero at zero momentum transfer. The observed deviation in table 5.1 gives therefore an estimate of the numerical accuracy in this case.

Table 5.2: Comparison of electromagnetic form factors $F_1(Q^2)$ for different prescriptions with the non-relativistic results. The coupling constant employed is $\alpha = \pi\lambda = 0.08$, which gives an exact binding energy of $BE = 1.233 - 3$ in the Wick-Cutkosky model. The binding energy that corresponds to the non-relativistic expression is $BE = \alpha^2/4 = 1.6 - 3$. The results with the non-relativistic expression of the binding energy in the Wick-Cutkosky model were divided by a factor 0.5213 in order to have the same normalization as in the exact case.

Q^2/m^2	exact $g(z)$ exact BE	exact $g(z)$ $BE = \alpha^2/4$	$g(z) = \wedge$ exact BE	$g(z) = \wedge$ $BE = \alpha^2/4$	non-rel. exact BE	non-rel. $BE = \alpha^2/4$
0	1.0	1.0	1.0002	1.0	1.0	1.0
0.01	4.39-1	5.16-1	4.39-1	5.16-1	4.40-1	5.17-1
1	3.62-4	6.03-4	3.63-4	6.03-4	3.743-4	6.231-4
25	5.13-7	7.84-7	5.14-7	9.30-7	6.217-7	1.046-6

The Wick-Cutkosky model model was used by Karmanov and Smirnov as a test of the description of form factors in the light-front approach for systems composed of scalar particles with small binding energy [37]. They used the non-relativistic expression, $-\alpha^2/(4n^2)$, for the binding energy, which differs from the exact one, but this does not seem to affect their conclusion. Interestingly enough, the comparison of the exact calculation with the non-relativistic one does not show much difference up to $Q^2 \simeq 100\, m^2$, where m is the constituent mass. It is only beyond that value, that relativistic corrections with a log character slowly begin to show up.

In table 5.2 we compare the effects of the different approximations employed by Karmanov and Smirnov, i.e., the use of a non-relativistic expression for the binding energy, and the replacement of the exact Cutkosky function $g(z)$ by its non-relativistic limit $g(z) = 1 - |\, z\, |$. We also give the non-relativistic result in the same table which is determined from

$$F_1(q^2)_{nonrel} = \frac{1}{\left(1 + \frac{Q^2}{16 m\, BE}\right)^2}, \tag{5.3-55}$$

where BE is the binding energy. It is seen immediately, that the exact form of the Cutkosky function $g(z)$ is not important for the numerical values of the form factors, small differences occurring only at large momentum transfers. The results do depend however on the value of the binding energy. Taking the non-relativistic expression, as done by Karmanov and Smirnov, the form factors differ by about 50%, even after a renormalization in order to get the same form factor at the origin. It is surprising however, that the non-relativistic calculation gives very close results in all cases, provided the same binding energy is used in eq. (5.3-55).

While there are several works that report results of form factors in the light-front approach [38,39], the so-called point-form approach has been much less exploited. In ref. [40] it was proposed to make a similar test as the one of Karmanov and Smirnov for the point form of relativistic quantum mechanics, which is another one of the forms proposed by Dirac, beside the instant and the light-front forms [41]. This form, which is much less known than the other two, has been developed in [42] and recently used for a calculation of form factors of the deuteron [43] and the nucleon [44]. In both cases, the form factors decrease faster with Q^2 than the non-relativistic ones. In the first case, the discrepancy with experiment tends to increase while, in the other one, it almost vanishes. In ref. [40], a sample of results like the one presented above was used to test the validity of the single-current approximation in the point-form approach and gave insight into the results presented in refs. [43,44].

Again, it was found that the non-relativistic approach does particularly well up to momentum transfers of 3-4 times the constituent mass, including the case of a strong binding. While the point-form approach does correctly for small bindings and small couplings, large discrepancies with the exact results appear as soon as the momentum transfer or the coupling increases. A major lesson of these results is that relativistic effects are not necessarily important and that most probably, for any non-relativistic calculation of form factors, there exists a covariant calculation (the exact one in the present case) which gives very close results

over a large range of momentum transfers. However, this does not mean that such a calculation contains all relativistic effects and is physically relevant, especially with respect to current conservation. An example is provided by the deuteron electro-disintegration near threshold in the light-front approach [45]. Two covariant calculations of the transition form factors have been shown to be very close to the non-relativistic ones up to $Q^2 = 10$ (GeV/c)^2 [46], completely missing the contribution due to the pair term, whose relativistic character is well known.

Although it is not quite certain, there is good reason to believe that the non-relativistic calculation does relatively well because it fulfils current conservation. With this respect, the failure of the point-form approach is likely to reside in the incomplete character of the current operator [47]. Whether a minimal set of two-body currents will be sufficient to provide results in better agreement with the exact ones is not clear however.

The results presented in ref. [40] cannot be applied directly to the calculation of the deuteron or nucleon form factors [43,44]. However, the qualitative similarity in the results strongly suggests that the kinematical boost, which provided a nice description of the nucleon form factors, represents an incomplete account of relativistic effects. More likely, the agreement is the consequence of neglecting significant contributions to the current. This conclusion is to be preferred with two respects:

- It leaves some room for the well known contribution of the coupling of the nucleon to the photon through vector-meson exchange (vector-meson dominance mechanism), which roughly provides half of the proton's squared charge radius.
- On the other hand, it leaves room for another relativistic effect related to the nature of the coupling of the constituents to the exchanged boson. This effect increases the form factor at high Q^2 rather than the opposite as in ref. [44]. It is known to explain the different asymptotic form factors in a non-relativistic and a relativistic calculation in QCD, which scale like $1/Q^8$ and $1/Q^4$, respectively (see for instance refs. [33,48]).

Altogether, two-body currents should produce quite sizeable contributions. Their role seems to be more essential in the point form than in other approaches.

5.4 Crossed-Boson Exchange Contribution to the Interaction Kernel

The necessity of introducing a contribution due to the crossed-boson exchange in the interaction kernel entering the Bethe-Salpeter equation [1] has been referred to many times in the literature [49–53]. This component of the interaction is indeed required if one wants the Bethe-Salpeter equation to reproduce results obtained with the Dirac or Klein-Gordon equations, which are known to provide a good account of the energy spectrum of charged particles in the field of a heavy system (one-body limit). At the same time it removes an undesirable contribution of the order $\alpha^3 \log\alpha$ (or α^3) expected from the simplest ladder approximation [54], indirectly supporting the validity of the instantaneous approximation in describing the one-boson exchange contribution to the two-body interaction. Transparent details about the derivation of the above result are scarcely found however and, thus, it may be thought that it is pertinent to QED or to the one-body limit. The role of the spin and charge of the exchanged boson, as well as its mass, is hardly mentioned.

Recently, Nieuwenhuis and Tjon [55], employing the Feynman-Schwinger representation (FSR), performed a calculation of the energy for a system of two equal-mass constituents with zero spin exchanging a zero spin massive boson. They found large differences with the ladder Bethe-Salpeter approximation, pointing to the contribution of crossed-boson exchanges. Their binding energies are also larger than those obtained from various equations inspired by the instantaneous (equal time) approximation.

The contribution of the crossed two-boson exchange was recently considered for a scattering process [56]. We shall concentrate in the following on the energy of bound states in the framework of the Bethe-Salpeter equation. Some results in this case were reported in ref. [57], but only for the ground state and for equal masses of the constituents and the exchanged particle. This study, which was presented in ref. [58], is obviously motivated by the works mentioned above, which provide separate benchmarks. In

the first case, it may allow one to determine which part of the disagreement between the FSR results and those obtained from the Bethe-Salpeter equation is due to the crossed two-boson exchange. In the second case, it is interesting to see whether results of a relativistic framework confirm the qualitative features evidenced by a non-relativistic approach.

5.4.1 Dispersion Relations for Feynman Diagrams

We shall briefly outline the procedure of putting Feynman diagrams into the form of dispersion relations. This is done for the simple case where all the particles are scalar and have the same mass. We follow here the presentation of Mandelstam [59], who first demonstrated the possibility of the procedure, the generalization to the unequal-mass case may be found in ref. [10, p. 312].

We start by specifying the kinematics of the box diagram in fig. 5.11, which is a planar, fourth-order perturbation graph for the reaction $A + B \to C + D$.

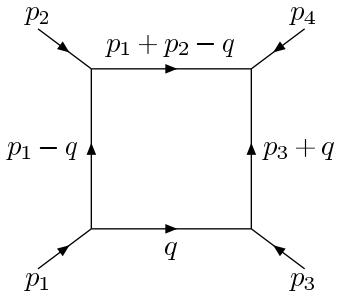

Figure 5.11: Kinematics for the box diagram.

Its analytic expression is given by

$$T = \frac{ig^4}{(2\pi)^4} \int \frac{d^4 q}{[(p_1 - q)^2 - m^2]\,[(p_1 + p_2 - q)^2 - m^2]\,[(p_3 + q)^2 - m^2]\,(q^2 - m^2)}, \tag{5.4-1}$$

where all masses are assumed to be equal and the external lines are taken on-mass shell: $p_i^2 = m^2$. Therefore, the amplitude of eq. (5.4-1) is a function of two invariants, the Mandelstam variables s and t [60]. In order to establish a dispersion relation for this quantity, it will be demonstrated that if t is fixed, real and negative, T is an analytic function of s with no singularities in the complex plane. It is indeed easy to verify, by using the usual Feynman-parameterization, eq. (C.3-5), that the denominator under the integral never vanishes for s real and under the expected threshold[1]. It follows that T can be written in the form

$$T(s,t) = \frac{1}{\pi} \int_{4m^2}^{\infty} d\,s' \frac{\mathrm{Im}\,T(s',t)}{s' - s}. \tag{5.4-2}$$

We will now explicitly calculate the imaginary part of T from eq. (5.4-1). To this end, remembering that the masses in the denominator of the integral carry an infinitesimal imaginary part, we rewrite each factor in eq. (5.4-1) in the form

$$\begin{aligned} \frac{1}{(q_0 - p_0)^2 - (\vec{q} - \vec{p})^2 - m^2 + i\epsilon} \;=\; & \frac{\mathcal{P}}{(q_0 - p_0)^2 - (\vec{q} - \vec{p})^2 - m^2} \\ & - \frac{i\pi}{2q_0} \delta\left\{q_0 - p_0 + \sqrt{(\vec{q} - \vec{p})^2 - m^2 - i\epsilon}\right\} \\ & - \frac{i\pi}{2q_0} \delta\left\{q_0 - p_0 - \sqrt{(\vec{q} - \vec{p})^2 - m^2 - i\epsilon}\right\}, \end{aligned} \tag{5.4-3}$$

[1] This is true if there do not occur any anomalous thresholds, i.e. the mass of any particle must not be greater than the sum of the masses of the two particles meeting it at one vertex. Since we take here the external particles on-mass shell, this condition is always satisfied.

where $\mathcal{P}$ means principal part. Expanding out the product one finds that only terms with two principal parts and two δ functions contribute to the imaginary part of T:

$$\left(\frac{i\pi}{2q_0}\right)^2 \left[\delta\left\{q_0 - p_{12_0} + \sqrt{\vec{q}^2+m^2-i\epsilon}\right\} + \delta\left\{q_0 - p_{12_0} - \sqrt{\vec{q}^2+m^2-i\epsilon}\right\}\right] \times\left[\delta\left\{q_0 + \sqrt{\vec{q}^2+m^2-i\epsilon}\right\} + \delta\left\{q_0 - \sqrt{\vec{q}^2+m^2-i\epsilon}\right\}\right] =$$
$$2\left(\frac{i\pi}{2q_0}\right)^2 \left[\delta\left\{q_0 - p_{12_0} + \sqrt{\vec{q}^2+m^2-i\epsilon}\right\}\,\delta\left\{q_0 - \sqrt{\vec{q}^2+m^2-i\epsilon}\right\} + \delta\left\{q_0 - p_{12_0} - \sqrt{\vec{q}^2+m^2-i\epsilon}\right\}\,\delta\left\{q_0 + \sqrt{\vec{q}^2+m^2-i\epsilon}\right\}\right]. \tag{5.4-4}$$

Here we have made use of the fact that we work in the center of momentum frame, so that $\vec{p}_1 + \vec{p}_2 = 0$, and we write short p_{12_0} for $(p_1+p_2)_0$. The second term in the square bracket of eq. (5.4-4) is always zero, because $p_{12} > 0$, so with the general relation

$$\frac{1}{2q_0}\delta\left\{q_0 - \sqrt{\vec{q}^2-m^2}\right\} = \delta\left(q^2-m^2\right)\Theta(q_0), \tag{5.4-5}$$

we obtain for the imaginary part of T:

$$\mathrm{Im}\,T = \frac{g^4}{8\pi^2}\int d^4q \frac{\delta\left(q^2-m^2\right)\,\delta\left\{(p_1+p_2-q)^2-m^2\right\}\,\Theta(q_0)\,\Theta(p_{12_0}-q_0)}{[(p_1-q)^2-m^2]\,[(p_3+q)^2-m^2]}\,; \qquad s > 4m^2. \tag{5.4-6}$$

We note in passing that this expression is identical to the one that is obtained by the application of the Cutkosky cutting rules [61].

Writing for the integration element in eq. (5.4-6) $d^4q = dq_0\, q^2 dq\, d\Omega$ and making use of the δ functions, one easily carries out the integrations over q_0 and q:

$$\mathrm{Im}\,T = \frac{g^4}{32\pi^2}\frac{q}{\sqrt{s}}\int \frac{d\Omega}{[m^2-2p_1\cdot q]\,[m^2+2p_3\cdot q]}, \tag{5.4-7}$$

where $q_0 = \sqrt{s}/2$ and q is the center-of-mass momentum. The integral over the angles is a bit more tedious. Introducing the variable $z = 1 + \frac{t}{2q^2}$, it may be expressed as

$$\begin{aligned}\mathrm{Im}\,T &= \frac{g^4}{32\pi^2}\frac{q}{\sqrt{s}}\int_{-1}^{1}dx\int_0^{2\pi}\frac{d\phi}{[2q^2(x-1)-m^2]\left\{2q^2[zx+\sqrt{1-z^2}\sqrt{1-x^2}\cos\phi-1]-m^2\right\}} \\ &= \frac{g^4}{8\pi\sqrt{\kappa}}\log\frac{\alpha+\frac{q}{\sqrt{s}}\sqrt{\kappa}}{\alpha-\frac{q}{\sqrt{s}}\sqrt{\kappa}}\,\Theta(s-4m^2),\end{aligned} \tag{5.4-8}$$

with

$$\alpha(s,t) = t(s-4m^2) + 2m^2(3m^2-s), \tag{5.4-9}$$
$$\kappa(s,t) = 4st\left[t(s-4m^2) + 4m^2(3m^2-s)\right]. \tag{5.4-10}$$

In order to examine the analytic properties of $\mathrm{Im}\,T$ we note that we can rewrite eq. (5.4-8) in the form

$$\mathrm{Im}\,T = \frac{g^4}{4\pi\sqrt{\kappa}}\log\frac{\frac{\kappa}{4st}+\frac{q}{\sqrt{s}}\sqrt{\kappa}}{\frac{\kappa}{4st}-\frac{q}{\sqrt{s}}\sqrt{\kappa}}\,\Theta(s-4m^2) = \frac{g^4}{2\pi\sqrt{\kappa}}\,\Theta(s-4m^2)\int_0^z\frac{du}{1-u^2}, \tag{5.4-11}$$

where the parameter z is now given by

$$z = \sqrt{\frac{t}{t-4m^2\frac{s-3m^2}{s-4m^2}}}. \tag{5.4-12}$$

The right hand side of eq. (5.4-11) is an analytic function of z as long as κ is positive and $|\,z\,| < 1$, i.e. $t < 4m^2$. Otherwise, there is a cut along the real axis where both κ and t are positive. The discontinuity across the cut is given by

$$\mathrm{Im}\,T(z\,|_{t+i\epsilon}) - \mathrm{Im}\,T(z\,|_{t-i\epsilon}) = -\frac{g^4}{2\pi\sqrt{\kappa}}(i\pi), \tag{5.4-13}$$

from which it follows at once that the expression for the box diagram, eq. (5.4-1) satisfies a double dispersion relation of the form

$$T(s,t) = \frac{g^4}{\pi^2} \int ds'dt' \frac{\rho(s',t')}{(s'-s)(t'-t)}, \tag{5.4-14}$$

where the double spectral function ρ is given by

$$\rho(s,t) = -\frac{\Theta(s-4m^2)\,\Theta(t-4m^2)\,\Theta(\kappa)}{4\sqrt{\kappa}}. \tag{5.4-15}$$

What we are interested in is not the box diagram, which in a four-dimensional integral equation gets generated by the iteration of the one-particle exchange term, but rather the crossed-box diagram. This is obtained from fig. 5.11 by the interchange $p_1 \leftrightarrow p_3$, or in other words by the crossing operation $s \leftrightarrow u$. It can be shown that the same reasoning as discussed above is applicable in this case, so we can expect to use the expression of the crossed-box diagram in the form of a dispersion relation in a Bethe-Salpeter equation.

5.4.2 The Crossed Box

For definiteness, we first recall the expression of the Bethe-Salpeter equation for two scalar particles of equal mass, interacting via the exchange of another scalar particle. It is given in momentum space by:

$$\left(m^2 - (\frac{P}{2}+p)^2\right)\left(m^2 - (\frac{P}{2}-p)^2\right)\Phi(p,P) = i\int \frac{d^4p'}{(2\pi)^4}\,K(p,p',P)\,\Phi(p',P), \tag{5.4-16}$$

where the quantities m, P and p represent the mass of the constituents, their total and their relative momenta, respectively. $K(p,p',P)$ represents the interaction kernel which contains a well determined contribution due to a single-boson exchange:

$$K^{(1)} = -\frac{g^2}{\mu^2 - t} = -\frac{g^2}{\mu^2 - (p-p')^2 - i\epsilon}, \tag{5.4-17}$$

which has been extensively used in the literature. In this equation, the coupling g^2 has the dimension of a mass squared. The quantity $g^2/4m^2$ is directly comparable to the coupling g^2_{MNN}, frequently used in hadronic physics or to $4\pi\,\alpha$, where α is the usual QED coupling. In terms of the coupling constant λ that was used so far, we have the relation $g^2/4m^2 = 4\pi^2\lambda$. The full kernel K also contains multi-boson exchange contributions that eq. (5.4-17) cannot account for, namely of the non-ladder type. Examples of such contributions are shown in fig. 5.12 involving crossed two- and three-boson exchanges.

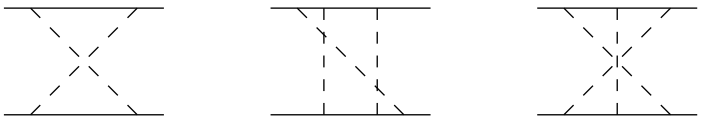

Figure 5.12: Two- and three crossed-boson exchanges.

Dealing with the crossed two-boson exchange should not raise difficulties if the expression of its contribution was tractable [62]. This one, as derived from the Feynman diagram of fig. 5.12a, is quite complicated and, moreover, not amenable to the mathematical methods generally employed in solving eq. (5.4-16). Expressions for scalar one-loop integrals have been given in ref. [63], where it was shown that the scalar box-diagram of fig. 5.11 for instance, can be expressed as a combination of Spence functions. However, from the results of the last section, we know that there exists an expression for the on-shell amplitude that has a structure similar to eq. (5.4-17). It consists in writing a double dispersion relation with respect to the t and u variables [59]:

$$K^{(2)}(s,t,u) = -\frac{g^4}{8\pi^2}\int_{4\mu^2}^{\infty}\int_{4m^2}^{\infty}\frac{dt'}{t'-t-i\epsilon}\,\frac{du'}{u'-u-i\epsilon}\,\frac{1}{\sqrt{\kappa(u',t')}}\,\Theta\left(\kappa(u',t')\right), \tag{5.4-18}$$

with (compare eq. (5.4-10))

$$\kappa(u',t') = u'\,t'\,[(t'-4\mu^2)(u'-4m^2)-4\mu^4]. \tag{5.4-19}$$

The quantities s, t and u represent the standard Mandelstam variables. For a physical process, they verify the equality $s+t+u=4m^2$. The integration in eq. (5.4-18) runs over the domain $t'>4\mu^2$, $u'>4m^2$ where the quantity $\kappa(u',t')$ entering the square root function is positive. One of the integrations in eq. (5.4-18) can be performed analytically, allowing one to write:

$$K^{(2)} = -\frac{g^4}{8\pi^2}\int_{4\mu^2}^{\infty}\frac{dt'}{t'-t-i\epsilon}\,\frac{1}{2\sqrt{\kappa(u,t')}}\,\log\left(\frac{\alpha(u,t')+\frac{1}{2}\sqrt{\frac{t'-4\mu^2}{t'}}\sqrt{\kappa(u,t')}}{\alpha(u,t')-\frac{1}{2}\sqrt{\frac{t'-4\mu^2}{t'}}\sqrt{\kappa(u,t')}}\right), \tag{5.4-20}$$

with (compare eq. (5.4-9))

$$\alpha(u,t') = \frac{1}{4}\,[(4m^2-u)(t'-4\mu^2)+4\mu^4-u(t'-4\mu^2)]. \tag{5.4-21}$$

The expression for $\alpha(u,t')$ has been written as the sum of two terms appearing in a product form in the second term of the numerator and denominator of the log function in eq. (5.4-20). This suggests an alternative expression for the last factor in eq. (5.4-20) (to be used with care)[1]:

$$\frac{1}{2}\log\left(\frac{\alpha(u,t')+\frac{1}{2}\sqrt{\frac{t'-4\mu^2}{t'}}\sqrt{\kappa(u,t')}}{\alpha(u,t')-\frac{1}{2}\sqrt{\frac{t'-4\mu^2}{t'}}\sqrt{\kappa(u,t')}}\right) = \log\left(\frac{\sqrt{(4m^2-u)(t'-4\mu^2)+4\mu^4}+\sqrt{-u\,(t'-4\mu^2)}}{\sqrt{(4m^2-u)(t'-4\mu^2)+4\mu^4}-\sqrt{-u\,(t'-4\mu^2)}}\right). \tag{5.4-22}$$

Methods based on dispersion relations are powerful ones, allowing one to make off-shell extrapolations of on-energy shell amplitudes, sometimes far from the physical domain. This extrapolation is not unique however (it is not clear a priori how to extrapolate an amplitude which is equal to zero on-energy shell), and it may thus result some uncertainty in a calculation involving a limited number of exchanged bosons.

Without considering all possibilities, the dependence on the variable u of the crossed two-boson exchange contribution given by eq. (5.4-20) can provide some insight on the above uncertainties. Indeed, the variable u, which is an independent one in eq. (5.4-20), can be replaced by $4m^2-s-t$ on-energy shell, thus introducing a possible dependence on the variables s and t. The dependence on s makes the interaction energy dependent. There is nothing wrong with this feature but it is not certain that it is physically relevant. It may well be an economical way to account for higher order processes. On the other hand, its arbitrary character should be removed by considering explicitly the contribution of these higher processes. In any case, the effect of the dependence on s gives some order of magnitude for contributions not included in the present work. The dependence on t through the dependence on u raises another type of problem. It is illustrated by rewriting the factor appearing in eq. (5.4-18):

$$\frac{1}{(t'-t)(u'-u)} = \frac{1}{(t'-t)(u'+s-4m^2+t)} = \left(\frac{1}{t'-t}+\frac{1}{u'+s-4m^2+t}\right)\,\frac{1}{u'+s-4m^2+t'}. \tag{5.4-23}$$

While the first term in the bracket has mathematical properties similar to eq. (5.4-17), the second term evidences different properties, poles appearing for negative values of t. This prevents us from applying the Wick rotation and, with it, the numerical methods employed to solve eq. (5.4-16).

In the following, we will consider various choices about the off-shell extrapolation of eq. (5.4-20). For non-relativistic systems, we expect the uncertainties to be small, in relation with the fact that the quantity u appearing in the factor $(u'-u)$ in the denominator of eq. (5.4-18) is small in comparison with u' ($>4m^2$).

[1] Expressions for $K^{(2)}$ differing from eq. (5.4-22) by the front factor may be found in the literature (two times smaller in ref. [59] and two times too large in ref. [10], which is perhaps due to the consideration of identical particles).

Our first choice assumes that $u = 0$, as it was done in studies relative to the contribution of two-pion exchange to the nucleon-nucleon force [64]. It is quite conservative and possibly appropriate for a non-relativistic approach, which assumes that the potential is energy independent. The expression of $K^{(2)}$ is then given by:

$$K^{(2)} = -\frac{g^4}{8\pi^2}\int_{4\mu^2}^{\infty}\frac{dt'}{t'-t}\sqrt{\frac{t'-4\mu^2}{t'}}\;\frac{1}{2(\mu^4+m^2(t'-4\mu^2))}. \tag{5.4-24}$$

A second choice consists in replacing the variable u in eq. (5.4-20) by the factor $4m^2 - s - t'$. Upon inspection, one finds that this is equivalent to neglecting the second term in the bracket of eq. (5.4-23). The corresponding interaction kernel is given by:

$$K^{(2)} = -\frac{g^4}{8\pi^2}\int_{4\mu^2}^{\infty}\frac{dt'}{t'-t}\sqrt{\frac{t'-4\mu^2}{t'}}\;\frac{1}{AB}\;\log\frac{A+B}{A-B}, \tag{5.4-25}$$

with

$$A = \sqrt{(t'-2\mu^2)^2 + s\,(t'-4\mu^2)}, \quad B = \sqrt{(t'+s-4m^2)(t'-4\mu^2)}. \tag{5.4-26}$$

This expression depends on the variable s and, thus, can provide some order of magnitude for the effect due to higher order processes. Its effect can be directly compared to that in the non-relativistic limit corresponding to $s = 4m^2$, whose expression, also conservative, is given by:

$$K^{(2)} = -\frac{g^4}{8\pi^2}\int_{4\mu^2}^{\infty}\frac{dt'}{t'-t}\sqrt{\frac{t'-4\mu^2}{t'}}\;\frac{1}{AB}\;\log\frac{A+B}{A-B}, \tag{5.4-27}$$

with

$$A = \sqrt{(t'-2\mu^2)^2 + 4m^2\,(t'-4\mu^2)}, \quad B = \sqrt{t'\,(t'-4\mu^2)}. \tag{5.4-28}$$

A last expression of interest corresponds to the non-relativistic limit where $m \to \infty$. Not surprisingly, it is identical to that obtained by considering time ordered diagrams in the same limit and may be written as:

$$K^{(2)} = -\frac{g^4}{8\pi^2}\int_{4\mu^2}^{\infty}\frac{dt'}{t'-t}\sqrt{\frac{t'-4\mu^2}{t'}}\;\frac{1}{2m^2(t'-4\mu^2)}. \tag{5.4-29}$$

In this last expression, the possible effect of off-shell extrapolations might be studied by replacing the factor m^2 by $s/4$.

As a theoretical model, the Bethe-Salpeter equation is most often used with an interaction kernel derived from the exchange of a scalar neutral particle. Anticipating on the conclusion that the contribution of the crossed two-boson exchange in this case could be strongly misleading, we also considered the case of the exchange of bosons that would carry some "isospin" [65]. In particular, for the case of two isospin 1/2 constituents and an isospin 1 exchange particle, a factor $\vec{\tau}_1.\vec{\tau}_2$ would appear in the single boson exchange contribution, eq. (5.4-17), while a factor $(3 + 2\vec{\tau}_1.\vec{\tau}_2)$ should be inserted in the expressions involving the crossed two-boson exchange, eqs. (5.4-24) - (5.4-29). The factor relative to the iterated one-boson exchange would be $(3 - 2\vec{\tau}_1.\vec{\tau}_2)$. For a state with an "isospin" equal to 1, the factor $\vec{\tau}_1.\vec{\tau}_2$ is equal to 1 and thus the single boson exchange, eq. (5.4-17), remains unchanged. It is easily checked that the factor relative to the iterated single boson exchange, $(3 - 2\vec{\tau}_1.\vec{\tau}_2)$, is also equal to 1 (as well as for the multi-iterated exchanges). On the contrary, for the crossed two-boson exchange, the factor $(3 + 2\vec{\tau}_1.\vec{\tau}_2)$ makes a strong difference. It is equal to 5 instead of 1. Its consequences and the possible role of crossed-boson exchange in restoring the validity of the instantaneous approximation lost in the ladder Bethe-Salpeter equation will be examined in in the following.

Numerical method

In order to solve eq. (5.4-16) we transform the Bethe-Salpeter equation into configuration space and expand the Bethe-Salpeter amplitude in a series of O(4) harmonics. This method was discussed earlier, see eq. (5.3-33), and it may be generalized in a straightforward manner to the case of higher order diagrams.

The potential function of eq. (5.3-35) was obtained from the one-meson exchange Feynman diagram, which gave a contribution (in Minkowski space and momentum representation)

$$K^{(1)} = (4\pi)^2 m^2 \frac{\lambda}{t-\mu^2}. \tag{5.4-30}$$

With the results of the last sections, the contribution of the crossed diagram can be expressed with the help of a dispersion relation in the form

$$K^{(2)} = (4\pi)^2\, 2m^4 \int_{4\mu^2}^{\infty} \frac{\lambda^2}{t-t'}\; F(t')\; dt', \tag{5.4-31}$$

where the spectral function $F(t')$ is given by one of the t-independent forms under the integrals of eqs. (5.4-24) - (5.4-29).

Now, since for all the cases considered here, $F(t')$ is an analytic function everywhere in the integration domain, we are allowed to carry out the Wick rotation, and by making the transition to configuration space we obtain the generalization of eq. (5.3-33),

$$L\Psi = \lambda V\Psi + \lambda^2 W\Psi, \tag{5.4-32}$$

where the potential function associated with the crossed-boson exchange is given by

$$W(s,R) = \frac{8}{R}\int_{4\mu^2}^{\infty} \sqrt{t'}\; K_1(R\sqrt{t'})\; F(t')\; dt'. \tag{5.4-33}$$

We have indicated in eq. (5.4-33) by the functional argument that contrary to V, the new function W may also depend on the total energy of the system, i.e. the Mandelstam variable s. For the choices of $F(t')$ that we consider here, this is only the case for eq. (5.4-25). As we see, eq. (5.4-32) is no longer a simple eigen-value problem, but it has to be solved by searching the zeros of the determinant

$$\mathrm{Det}\left[\langle L - \lambda V - \lambda^2 W\rangle\right] \tag{5.4-34}$$

as a function of λ.

Results and comparison with other approaches

We first present results for the ground state mass as a function of the dimensionless coupling constant $g^2/4\pi m^2 = 4\pi\lambda$ for the case $\mu/m = 0.15$. The reason for this choice is that we can directly compare our results to those of Nieuwenhuis and Tjon [55], who reported the first calculation of bound state properties beyond the ladder approximation using the Feynman- Schwinger representation [66,67]. Since this formulation takes into account all ladder and crossed-ladder diagrams, we may expect the results of the present approach to lie somewhere between those of the ladder and the Feynman-Schwinger calculations. If the perturbative series expansion of the Bethe-Salpeter kernel turns out to converge reasonably fast, which we would like to be the case, our results should actually be closer to those of the Feynman-Schwinger approach. This would imply that even higher order terms of the kernel could safely be neglected in perturbative calculations.

In fig. 5.13 we show the ladder results and the Feynman-Schwinger results (taken from ref. [55]) together with the various off-shell extrapolations given by eqs. (5.4-24) - (5.4-29). For small couplings, the differences between these various choices are small compared to the difference between the ladder and the Feynman-Schwinger results, allowing one to make safe statements about the contribution of the crossed two-boson exchange diagram. The binding energies so obtained are found just about halfway between the FSR- and the ladder results. The remaining, still considerable, disagreement with the exact binding energies of the non-perturbative approach makes us believe, that even higher order terms than the crossed two-boson exchange term in the kernel are essential for doing reliable calculations within the Bethe-Salpeter framework at large coupling.

The inset of fig. 5.13 shows the evolution of our solutions over the whole range of binding energies. It can be seen that the solution corresponding to the parameterization of eq. (5.4-25) shows a double-valued structure with a lower branch where the binding energy decreases with increasing coupling. This is a

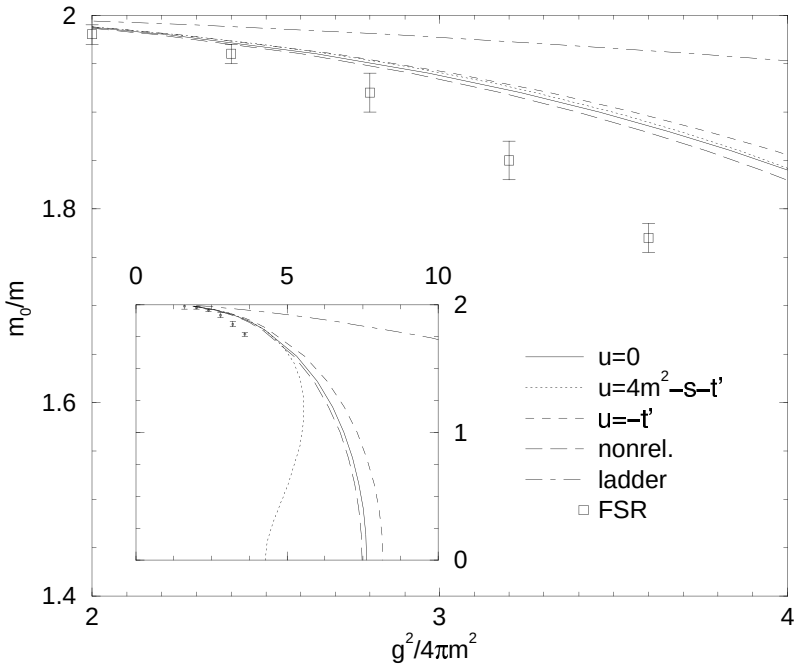

Figure 5.13: Ground state mass m_0 of the scalar theory as a function of the dimensionless coupling constant $g^2/4\pi m^2$ for $\mu/m = 0.15$. The solid, dotted, dashed and long dashed lines correspond to the solutions with the spectral functions of eqs. (5.4-24) to (5.4-29), respectively. The dashed-dotted line gives the ladder result, the boxes represent the non-perturbative results of Nieuwenhuis and Tjon [55]. The inset shows the evolution of the various solutions over the whole range of bound state energy values.

consequence of the energy dependence of this choice, since replacing s by $4m^2$, which corresponds to eq. (5.4-27), renders the curve monotonically decreasing. It is however interesting to note that the lower branch does not start off at a coupling constant equal to 0 for $s = 0$, as it is the case, for instance, for the Gross equation, (see below). Also the lower branch solution of the equal mass Klein-Gordon equation goes through 0 for $s = 0$.

This qualitative difference to well known facts led us to investigate the μ dependence of our results. It was found that, from a value of the exchanged particles mass of about $\mu \sim 0.5$ on, the curves become monotonically decreasing even for the choice of eq. (5.4-25). On the other hand, for $\mu \to 0$, the lower branch tends to $s = 0$ for vanishing coupling. This is no surprise however, since for $\mu = 0$ the integral of eq. (5.4-25) diverges, a reminiscent of the original infrared divergence of the box diagram. This is somehow a pity, since the case $\mu = 0$, in the ladder approximation, corresponds to the Wick-Cutkosky model, which for $s = 0$ admits analytic solutions in the form $\lambda = N(N+1)$, see eq. (5.3-11). With the crossed box diagram included, all these solutions become degenerate at $\lambda = 0$. We shall not comment any more on this subject, as we believe that further theoretical work is required in order to correctly account for the contribution of the crossed box diagram in the case $\mu = 0$. Note however that it is not possible from the present results to estimate the influence of the infra-red divergence of the crossed-box diagram even for $\mu = 0.15$. If this one would not be negligible in the present case, we should expect the results of fig. 5.13 to be even further away from the complete non-perturbative ones.

Nieuwenhuis and Tjon also give a detailed comparison of their results with those of various quasi-potential equations. They considered the Blankenbecler-Sugar, Logunov-Tavkhelidze (BSLT) equation [68, 69], the equal-time (ET) equation [70, 71] and the Gross equation [72, 73]. Generally, these equations reduce the description from a four-dimensional to a three-dimensional one by making an ansatz for the propagators and the potentials involved. Specifically, the propagator factor of the Bethe-Salpeter equation in ladder approximation

$$S^{-1}(p)\Phi(p) = \frac{1}{(2\pi)^4} \int d^4p'\, V(p-p')\, \Phi(p'), \tag{5.4-35}$$

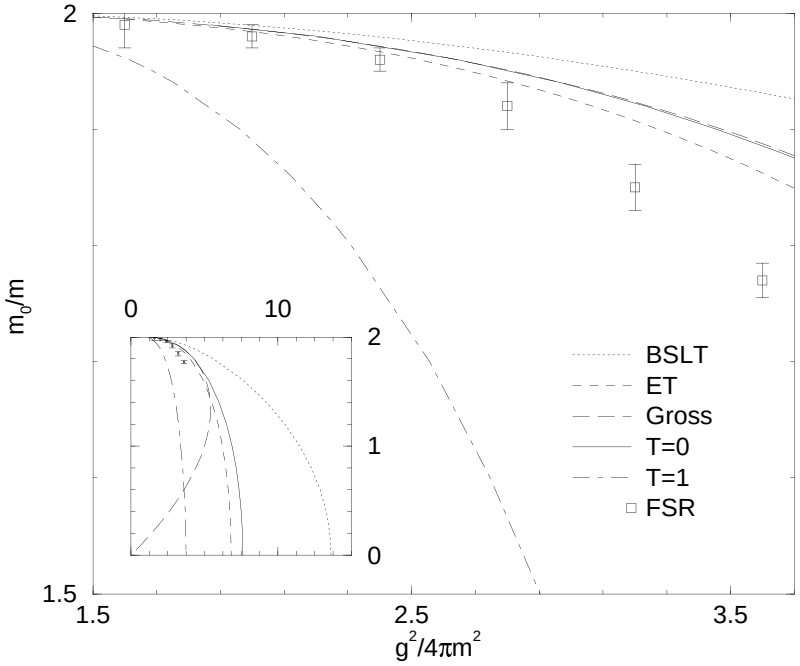

Figure 5.14: Comparison of ground state masses obtained in various quasi-potential equations with the results of the scalar theory in case of charge-less (solid line) and charged (dash-dotted line) particles. The latter one applies for a state of total isospin 1. Both curves correspond to the choice $u = 0$ of eq. (5.4-24). The boxes represent the non-perturbative Feynman-Schwinger results of ref. [55].

(that is eq. (5.4-16) after the Wick rotation) is replaced by the following forms in the various approaches (compare ref. [55]):

$$S_{\rm QPE}(p) \overset{\rm BSLT}{=} \frac{1}{4\sqrt{\vec{p}^2+m^2}} \frac{2\pi\,\delta(p_0)}{\vec{p}^2+m^2-\frac{1}{4}s}, \tag{5.4-36}$$

$$\overset{\rm ET}{=} \frac{1}{4\sqrt{\vec{p}^2+m^2}} \frac{2\pi\,\delta(p_0)}{\vec{p}^2+m^2-\frac{1}{4}s} \left(2-\frac{s}{4(\vec{p}^2+m^2)}\right), \tag{5.4-37}$$

$$\overset{\rm Gross}{=} \frac{1}{4\sqrt{s}\sqrt{\vec{p}^2+m^2}} \frac{2\pi\,\delta\left(p_0+\frac{1}{2}\sqrt{s}-\sqrt{\vec{p}^2+m^2}\right)}{\sqrt{\vec{p}^2+m^2}-\frac{1}{2}\sqrt{s}}. \tag{5.4-38}$$

In the potential function $V(p-p') = K^{(1)}(p,p',P)$ for the BSLT and ET equations, the time component is simply neglected:

$$V(p-p') = g^2 \frac{1}{(\vec{p}-\vec{p}\,')^2+\mu^2}, \tag{5.4-39}$$

whereas for the Gross equation, V takes the form

$$V(p-p') = g^2 \frac{1}{(\vec{p}-\vec{p}\,')^2-(\omega-\omega')^2+\mu^2}, \tag{5.4-40}$$

with $\omega = \sqrt{\vec{p}^2+m^2}-\frac{1}{2}\sqrt{s}$ and $\omega' = \sqrt{\vec{p}\,'^2+m^2}-\frac{1}{2}\sqrt{s}$.

In ref. [55] it was found that all the binding energies obtained in these quasi-potential models are distributed between the energies of the FSR- and the ladder calculations. In fig. 5.14 we compare our results with those of the equations specified above. For small coupling constants, we find that our binding energies, represented by the choice $u = 0$ indicated in fig. 5.14, are remarkably close to those of the ET and Gross equation.

Since it is often conjectured that results like these may tend to support the validity of the instantaneous approximation, it was pointed out in ref. [58], that this is true only for the specific model considered here. In fact, one can quickly convince oneself of the special nature of this approximate agreement by considering

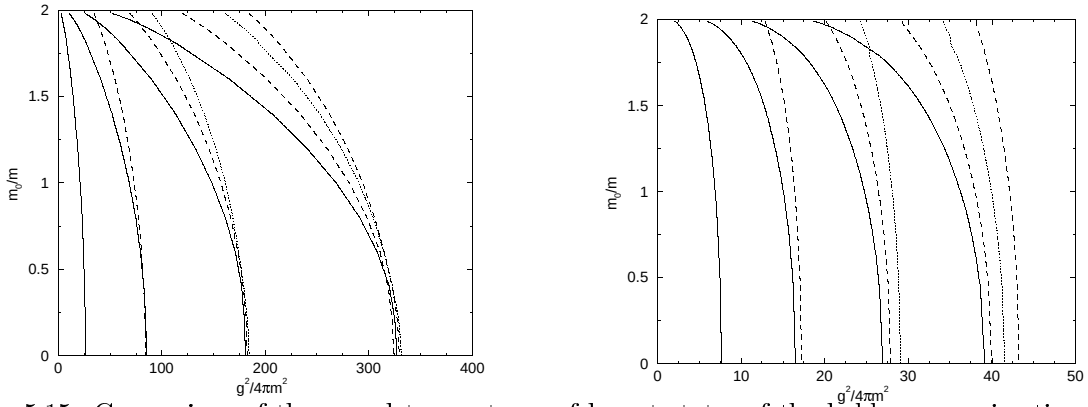

Figure 5.15: Comparison of the complete spectrum of lowest states of the ladder approximation (left) and the one obtained by the inclusion of the crossed box diagram (right) for a spatial orbital angular momentum $l = 0$. The solid lines give the normal solutions, dotted and dashed lines give abnormal solutions with even and odd time-parity, respectively.

another specific case, where the involved particles would carry some sort of isospin. For the case already mentioned earlier, the contribution of the crossed box for a state of isospin 1 gets multiplied by a factor five, whereas the ladder terms remain unchanged. It can be seen in fig. 5.14, that the corresponding curve even largely overshoots the Feynman-Schwinger points. The inset of fig. 5.14 shows again the evolution of the curves over the whole range of binding energies where one can see the unphysical lower branch of the Gross equation already mentioned above and discussed in ref. [55].

Let us finally note that results quite similar to the ones presented here can also be obtained in a non-relativistic scheme. Details about this approach, as presented in ref. [74], will be discussed in the next chapter.

Excited states

In fig. 5.15 we show the complete spectrum of lowest states for a spatial orbital angular momentum $l = 0$ and an exchanged particle of mass $\mu = 0.15$. The spectrum of the ladder approximation, on the left hand side, is very similar to the one of the Wick-Cutkosky model. There are normal and abnormal solutions, the latter ones corresponding to excitations in the relative time variable. For $s = 0$ an approximate degeneracy appears. This can be traced back to the extra symmetry that occurs in the Wick-Cutkosky model, i.e. for $\mu = 0$, when $s \to 0$. Like in this model, the normal states tend to the correct non-relativistic limit when the coupling gets small, whereas the abnormal states exist only for larger values of the coupling constant. The only qualitative difference to the Wick-Cutkosky model is the fact that the different abnormal solutions do not tend to a common value of the coupling constant when the binding energy becomes small.

The spectrum gets considerably changed quantitatively by the inclusion of the crossed box diagram. On the right hand side of fig. 5.15 we show the results for the energy independent choice $u = 0$ of eq. (5.4-24). First note the different scale in the coupling constant. Generally, the crossed box increases the binding energies for all states as compared with the ladder results.

Second, it has to be stated that we still find abnormal solutions with in fact similar properties as in the ladder approximation. Ever since the initial conjecture of Wick, it has been repeatedly claimed in the literature, that these abnormal states should be spurious consequences of the ladder approximation. The mere existence of these states beyond the ladder approximation is therefore already an interesting result by itself.

As for the qualitative properties of the solutions, we see that the normal ones still behave normally, that is, they seem to have the correct weak binding limit. Also the abnormal solutions behave like in the ladder approximation in this limit, since they tend to different but larger values of the coupling constant. In the strong-binding limit however, the approximate degeneracy of states is severely lifted. This could have been expected, since the effect of the term on the right hand side of eq. (5.4-24) is similar to the

ladder term, eq. (5.4-17), with a much higher effective mass μ.

The crossing of states that is observed in fig. 5.15 does not cause any numerical problems if it occurs between solutions of opposite time-parity, since as outlined before, we calculate even- and odd time-parity solutions separately. There occurs however a problem for the even time-parity case. Since the normal solutions all tend to a value that is closer to zero than the limit of the abnormal solutions, the former ones necessarily cross some of the latter ones, if they initially belonged to a higher O(4) multiplet. This leads to a perturbation of the eigenvalues near the crossing region, which can be clearly seen from fig. 5.15 in the case of the two positive time-parity abnormal solutions. The effect is in principle also present in the ladder approximation, but it seems somehow less pronounced there. In fact, taking a closer look at the crossing region, one finds rather a repulsion of the two solutions, with no real crossing taking place. In this region, it is obviously not possible to identify the two solutions due to configuration mixing. It is only by the smooth continuation of the curves after the crossing, that the solutions were identified in order to draw the graph of fig. 5.15. The curve for the abnormal solution after the crossing is however not expected to be meaningful anymore, since it gets repeatedly perturbed by all the normal states crossing it.

5.4.3 The Crossed Double-Box

Given the results of fig. 5.13, it is obvious that the simple crossed box does not explain the difference in binding energy between the ladder results and the completely non-perturbative ones. Assuming that the FSR-results of ref. [55] give the correct final answer for the sum of all two-particle irreducible diagrams in the interaction kernel, we see that the crossed-box graph brings us only about half the way to the exact solution. This is not a very satisfactory result for a perturbative approach, where we would like even higher-order terms to be negligible. We are therefore led to investigate the contribution of the crossed double-box, which is the contribution to the interaction kernel at order g^6. At this order, we have the two topologically different diagrams that are shown in fig. 5.12b,c (page 117).

Denoting by T^{3X} the sum of the two diagrams of figs. 5.12b and 5.12c, we write again a dispersion relation in the form

$$T^{3X}(s,t) = \iint ds'dt' \frac{\rho^{3X}(s',t')}{(s'-s)(t'-t)}, \tag{5.4-41}$$

which results in a contribution to the interaction kernel at the order λ^6

$$K^{(3)} = -\frac{g^6}{128\pi^5} \int_{9\mu^2}^{\infty} \frac{dt'}{t'-t}\, G(t'). \tag{5.4-42}$$

We thus end up with the generalization of eq. (5.4-32):

$$L\Psi = \lambda V\Psi + \lambda^2 W\Psi + \lambda^3 U\Psi, \tag{5.4-43}$$

where the function $U(R)$ is related to the spectral function $G(t')$ of eq. (5.4-42) by

$$U(R) = \frac{1}{2\pi R} \int_{9\mu^2}^{\infty} \sqrt{t'} K_1(R\sqrt{t'}) G(t') dt'. \tag{5.4-44}$$

The only difference with the case of the crossed-box diagram is, that we do not have an analytic representation of the spectral function $G(t')$, but it has to be determined numerically. This is most easily done for the choice $u = 0$, compare eq. (5.4-24), in time ordered perturbation theory, where summing the energy denominators of all possible time-orderings of the graphs b and c of fig. 5.12 leads to a surprisingly simple result. This was noted already by Kaiser [75,76] in his calculation of the NN potential to two-loop order in the framework of chiral perturbation theory. The remarkable fact is, that it is only the sum of diagrams that simplifies in that way, each term in the sum remains a complicated multi-dimensional integral.

With the spectral function $G(t')$ determined numerically, we can solve eq. (5.4-43) in the same way as we solved eq. (5.4-32), i.e. by searching the zeros of the determinant occurring in eq. (5.4-43). The result for the ground state solution is shown on the left-hand side of fig 5.16 where we immediately note the unpleasant feature that the ground state energy drops below the results of the FSR solution.

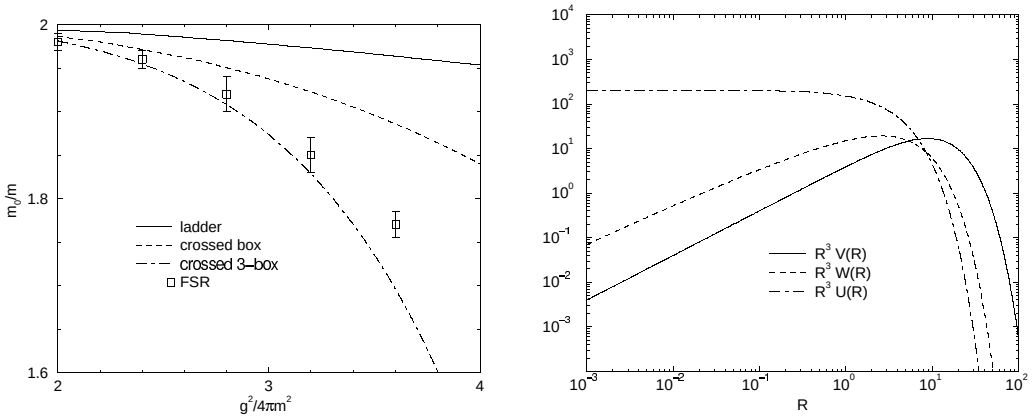

Figure 5.16: Comparison of the ground states of the Bethe-Salpeter equation in ladder approximation with the crossed box and the crossed double-box diagram included with the non-perturbative results of ref. [55] (left-hand side). On the right, the different potential functions of eq. (5.4-43) are displayed.

We know from the analytic properties of the interaction kernel in the scalar theory, that each term in the perturbative expansion is explicitly positive, so if there exists a definite numerical limit, we have to approach it from one side only. In other words, every diagram that we add to our eq. (5.4-43) will move the corresponding results further away from the FSR-curve. The strong effect of the crossed double-box may be illustrated by a graphical representation of the potential functions that appear in eq. (5.4-43), which is given on the right-hand side of fig. 5.16. We see in particular that the function U associated with the crossed double-box has a $1/R^3$ singularity at the origin which gives a notable contribution to the matrix elements (since the volume element in four-dimensional Euclidean space is proportional to R^3).

Assuming the FSR results to be correct, we have to conclude that there is something wrong with our prescription of calculating the contribution to the Bethe-Salpeter interaction kernel in perturbation theory via dispersion relations. We recall in particular, that the result by Mandelstam, discussed in section 5.4.1, is strictly valid only for the case where the external particles are on-shell. We know that this is an approximation, since in a Bethe-Salpeter equation we need the full off-shell amplitude. Even though the dispersion relations may be generalized to the arbitrary-mass case [10], there would arise complications due to anomalous thresholds, that would spoil the mathematical similarity of the different terms in the expansion. Furthermore, by regarding the different off-shell extrapolations of the spectral function $F(t')$ in eqs. (5.4-24) - (5.4-29), we thought to obtain an estimate of the uncertainty due to these off-shell effects, which were found to be small from the results in fig. 5.13. The present results now indicate definitely that the use of dispersion relations in the Bethe-Salpeter interaction kernel overestimate the binding energy of the system.

Another effect of importance here is the infra-red divergence of any loop diagram in the scalar theory. Approaching the limit $\mu \to 0$, this divergence should be felt in a certain way, and it might well be that the dispersion relations are especially sensitive to this limit. This effect is present already in the crossed-box diagram, for the crossed double-box, it gets of course even further enhanced.

Looking back to the case of the crossed-box only, this means that already this contribution should be even smaller than what we got from our calculations. This conclusion is confirmed by independent calculations[1], which shows that the convergence of the Bethe-Salpeter interaction kernel in powers of the coupling constant is indeed very slow. This casts serious doubts on the relevance of any perturbative calculations in such a scheme. A possible way of including effectively an infinity of two-particle irreducible diagrams in the Bethe-Salpeter interaction kernel has been sketched in ref. [77], but the method has never been applied in numerical investigations[2].

In fig. 5.17 finally, we compare the complete spectra of the Bethe-Salpeter equation in ladder approximation, with the crossed box and with the crossed double-box included. We do not need to comment

[1] J.A. Tjon, I.A. Afnan, D. Phillips: private communication
[2] C. Schwartz: private communication.

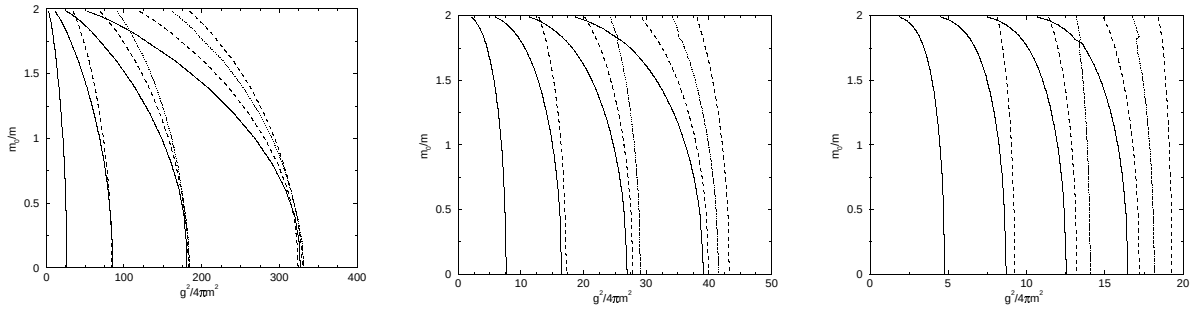

Figure 5.17: Comparison of the complete spectrum of $l = 0$ states in ladder approximation (left), with the inclusion of the crossed-box diagram (center), and with the crossed double-box diagram included (right). The solid lines give the normal solutions, dotted and dashed lines give abnormal solutions with even and odd time-parity, respectively.

this graph any further, since the qualitative features are completely the same as in the case of the crossed box only. The basic net effect is an attraction of all the states, in such a way that the normal ones are effected the strongest. Again, we cannot conclude that the abnormal states are artifacts of the ladder approximation, as conjectured by Wick [6], even though they only appear at coupling constants where the single-particle exchange approximation is certainly not valid anymore.

5.5 More Complicated Systems

So far we have only dealt with the simplest system that one can imagine: a bound state of two scalar particles that interact via the exchange of a third scalar particle of different mass μ. This model is certainly not a realistic one and it is often referred to as a "toy-model", implying in a certain under-tone that it is good fun to deal with it, without gaining any insight into a realistic physical situation. We shall indicate in this section very briefly that to deal with such simple models may still be useful and deliver important informations for the approach of more complete situations.

5.5.1 The Spinor Equation

As a first step in the direction of a more realistic model, let us consider the case where the two constituents are fermions and therefore carry a spin, while the exchanged particle stays scalar. The consideration of such a system was mainly motivated by the study of the fine structure of the hydrogen atom [78]. A complete review of the spinor Bethe-Salpeter equation may be found in ref. [79], numerical solutions have been given by Suttorp [80, 81], see also ref. [82], while the notorious question about abnormal states has been raised in ref. [83].

The general spinor Bethe-Salpeter equation may be written as

$$\left[\gamma\cdot p+\frac{M}{2}\gamma_0-m\right]\chi(p)\left[\gamma\cdot p-\frac{M}{2}\gamma_0-m\right]=-i\frac{\lambda}{\pi^2}\int d^4q\,\frac{\Gamma_\mu\,\chi(q)\,\Gamma^\mu}{(p-q)^2-\mu^2}. \tag{5.5-1}$$

Note that now the Bethe-Salpeter amplitude is no longer a scalar function but a spinor in Dirac space, and all the operators are corresponding matrices. Like in the scalar case we are allowed to carry out the Wick rotation:

$$\left[(ip_0+\frac{M}{2})\gamma_0-\vec{\gamma}\cdot\vec{p}-m\right]\chi(p)\left[(ip_0-\frac{M}{2})\gamma_0-\vec{\gamma}\cdot\vec{p}-m\right]=-\frac{\lambda}{\pi^2}\int d^4q\,\frac{\Gamma_\mu\,\chi(q)\,\Gamma^\mu}{(p-q)^2+\mu^2}. \tag{5.5-2}$$

We shall stick to the idea that we want to model a bound state of nucleons that interact by the exchange of a pion, so we adopt a pseudo-scalar coupling, in which case we have $\Gamma_\mu = (\gamma_5, 0, 0, 0)$. We then introduce

the following basis in Dirac space:

$$\begin{aligned} \Phi_1 &= \tfrac{1}{2}\gamma_5 \\ \Phi_2 &= \tfrac{1}{2}\gamma_5\gamma_0 \\ \Phi_3 &= \tfrac{1}{2|\vec{p}|}\gamma_5\vec{\gamma}\cdot\vec{p} \\ \Phi_4 &= \tfrac{1}{2|\vec{p}|}\gamma_5\gamma_0\vec{\gamma}\cdot\vec{p}. \end{aligned} \tag{5.5-3}$$

With the following definition of a scalar product, this basis is orthogonal:

$$\langle\Phi_i,\Phi_j\rangle := \mathrm{Tr}\left\{\Phi_i^\dagger\Phi_j\right\} = \mathrm{diag}\,(1,1,-1,-1). \tag{5.5-4}$$

We now expand the Bethe-Salpeter amplitude, which is a 4×4 matrix in Dirac space, in this basis:

$$\chi(p) = \sum_{i=1}^{4}\chi_i(p)\,\Phi_i, \tag{5.5-5}$$

where the coefficient functions $\chi_i(p)$ are scalar functions of p. We make the same expansion of the whole left- and right-hand sides of the Bethe-Salpeter equation (5.5-2), for instance:

$$\left[(ip_0+\frac{M}{2})\gamma_0-\vec{\gamma}\cdot\vec{p}-m\right]\chi(p)\left[(ip_0-\frac{M}{2})\gamma_0-\vec{\gamma}\cdot\vec{p}-m\right] = \sum_{i=1}^{4} f_i(p)\,\Phi_i, \tag{5.5-6}$$

so that

$$f_i(p) = \pm\sum_{j=1}^{4}\chi_j(p)\,Tr\left\{\Phi_i^\dagger\left[(ip_0+\frac{M}{2})\gamma_0-\vec{\gamma}\cdot\vec{p}-m\right]\Phi_j\left[(ip_0-\frac{M}{2})\gamma_0-\vec{\gamma}\cdot\vec{p}-m\right]\right\}, \tag{5.5-7}$$

where the sign in front corresponds to the one of eq. (5.5-4). After a similar expansion of the right-hand side we finally arrive at

$$B_{ij}\,\chi_j(p)\,\Phi_i = -\frac{\lambda}{\pi^2}\int d^4q\,\frac{A_{ij}\,\chi_j(q)}{(p-q)^2+\mu^2}\,\Phi_i, \tag{5.5-8}$$

with the matrices $A_{ij} = \mathrm{diag}\,(1,-1,1,-1)$ and

$$B_{ij} = \begin{pmatrix} p^2+m^2+\frac{M^2}{4} & mM & 0 & -M|\vec{p}| \\ mM & p_0^2-|\vec{p}|^2+m^2+\frac{M^2}{4} & -2ip_0|\vec{p}| & -2m|\vec{p}| \\ 0 & 2ip_0|\vec{p}| & -p_0^2+|\vec{p}|^2+m^2-\frac{M^2}{4} & 2imp_0 \\ M|\vec{p}| & 2m|\vec{p}| & 2imp_0 & -p^2-\frac{M^2}{4}+m^2 \end{pmatrix}. \tag{5.5-9}$$

In particular, for a massless bound state, $M=0$, we see that the equation for the amplitude χ_1 decouples from the rest and satisfies an equation of the same kind as in the scalar problem. This indicates, that the time that we spent on the "toy-models" of the last sections may not have been completely useless, since the same methods that were developed there are applicable to the more realistic system of the spinor problem.

5.5.2 The Three-Body Problem

The relativistic three-body problem is not only interesting from a theoretical point of view. Realistic calculations of the triton binding energy with modern nucleon-nucleon potentials (excluding three-body forces) result in a discrepancy of ~ 1 MeV as compared to the experimentally observed value of -8.48 MeV. There are several works that attempt a relativistic calculation of this quantity in different approaches [84–87]. All of these include contributions coming from relativistic kinematics, but none treats the full Dirac-structure of the nucleon, or investigates effects from a relativistic treatment of the NN dynamics. Also the investigation of baryons as bound states of three quarks in a relativistic, four-dimensional framework would be of highest current interest. Such systems are usually treated either in a quark-diquark approach [88], where the number of effective degrees of freedom is reduced, or in one of

numerous reduction formalisms of the Bethe-Salpeter equation, where the dimensionality of the problem is reduced [89–92].

The Bethe-Salpeter equation for a three-body bound state amplitude has been written down a long time ago [93], and it appears that with the numerical techniques developed for the two-body problem, it is today amenable to numerical solutions. This would allow a consistent comparison with results that have already been obtained in different quasi-potential formalisms. The corresponding calculations in the light-front approach [94] are currently under way [95]. An interesting topic in this context would be the investigation of relativistic effects in relation with three-body forces.

So far, three-body calculations have only been carried out in three-dimensional, or quasi-potential reductions of the Bethe-Salpeter equation [96–98], the full four-dimensional problem remains unadressed. The ϕ^3 model, i.e. the scalar "toy-model" discussed so far, applied to the three-body case, has been especially treated in ref. [99].

We shall only sketch very superficially the problematics for the scalar theory. Let us write down the general form of a three-body Bethe-Salpeter equation:

$$S^{-1}(p_1)\,S^{-1}(p_2)\,S^{-1}(p_3)\,\chi(p_1,p_2,p_3) = \int dp_1' dp_2' dp_3'\,V(p_i,p_i')\,\chi(p_1',p_2',p_3'), \tag{5.5-10}$$

where the $S(p_i)$ are the single-particle propagators, V is the potential (the sum of all three-particle irreducible Feynman diagrams), and $p_i = \{p_1,p_2,p_3\}, p_i' = \{p_1',p_2',p_3'\}$.

In the following we shall consider the equal mass case only and work in the center of mass system. For the potential, we shall immediately restrict ourselves to the ladder approximation, that is, only one-particle exchange terms are kept, as shown in fig. 5.18.

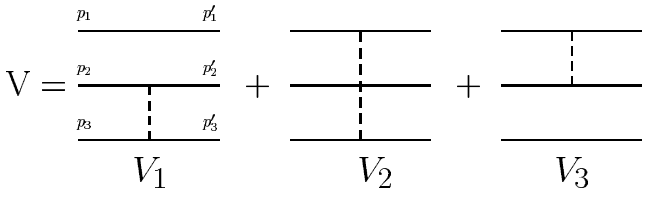

Figure 5.18: Three-body potential in ladder approximation

We denote by V_i the term where particles j and k interact, where $\{ijk\}$ are cyclic permutations of $\{123\}$, so that (omitting a δ function for overall momentum conservation)

$$V_i = \frac{g^2\delta(p_i - p_i')}{(p_j - p_j')^2 - \mu^2}\,S^{-1}(p_i). \tag{5.5-11}$$

Now we introduce Jacobi coordinates analogously to the three-dimensional case:

$$\begin{array}{l|l|l} p_x = \frac{1}{2}(p_1 - p_2) & p_1 = p_x + \frac{1}{2}p_y + \frac{1}{3}P & \\ p_y = \frac{1}{3}(p_1 + p_2 - 2p_3) & p_2 = -p_x + \frac{1}{2}p_y + \frac{1}{3}P & dp_1dp_2dp_3 = dp_x dp_y dP. \\ P = p_1 + p_2 + p_3 & p_3 = \; -p_y + \frac{1}{3}P & \end{array} \tag{5.5-12}$$

With this change of variables we can write $\chi(p_1,p_2,p_3) = \delta(P - p_1 - p_2 - p_3)\chi(p_x,p_y)$ and $V(p_i,p_i') = \delta(\sum p_i - \sum p_i')\sum V_i(p_x,p_y,p_x',p_y')$, where the terms of the potential become:

$$\begin{aligned} V_1 &= g^2\,\frac{\delta\left[p_x - p_x' + \frac{1}{2}(p_y - p_y')\right]}{4(p_x - p_x')^2 - \mu^2}\,S^{-1}(p_1), \\ V_2 &= g^2\,\frac{\delta\left[-(p_x - p_x') + \frac{1}{2}(p_y - p_y')\right]}{4(p_x - p_x')^2 - \mu^2}\,S^{-1}(p_2), \\ V_3 &= g^2\,\frac{\delta\left[p_y - p_y'\right]}{(p_x - p_x')^2 - \mu^2}\,S^{-1}(p_3). \end{aligned} \tag{5.5-13}$$

So we arrive at our final equation

$$S^{-1}(p_1)S^{-1}(p_2)S^{-1}(p_3)\chi(p_x,p_y) = g^2\, S^{-1}(p_1)\int dp'_x \frac{\chi\,(p'_x, p_y + 2(p_x - p'_x))}{4(p_x - p'_x)^2 - \mu^2} + g^2\, S^{-1}(p_2)\int dp'_x \frac{\chi\,(p'_x, p_y - 2(p_x - p'_x))}{4(p_x - p'_x)^2 - \mu^2} + g^2\, S^{-1}(p_3)\int dp'_x \frac{\chi\,(p'_x, p_y)}{(p_x - p'_x)^2 - \mu^2}. \qquad (5.5\text{-}14)$$

From the structure of this equation some general properties can be deduced immediately. First it can be checked that

$$\chi(-p_x, p_y) = \pm\chi(p_x, p_y). \qquad (5.5\text{-}15)$$

This means in particular, that the Bethe-Salpeter amplitude is either an even or odd function of the relative time variable[1] of particles 1 and 2, and by permutation symmetry, this has to be true for the other particle pairs, too. Furthermore, since the second Jacobi coordinate p_y can be expressed as a combination of relative particle momenta only, we conclude

$$\chi(p_x, -p_y) = \pm\chi(p_x, p_y), \qquad (5.5\text{-}16)$$

where the sign corresponds to the one of eq. (5.5-15), such that $\chi(-p_x, -p_y) = +\chi(p_x, p_y)$. This symmetry in the relative time components is an obvious analogue to the two-body case, and it will simplify the search for solutions of eq. (5.5-14). Finally, from eq. (5.5-14) it follows that

$$\chi(p_x, -p_y, -P) = \pm\chi(p_x, p_y, P), \qquad (5.5\text{-}17)$$

so that by inverting the time component of the second Jacobi coordinate, we get a negative energy solution for the same coupling constant. This, too, is a complete analogue to the two-body problem, where the spectrum is symmetric with respect to energy inversion.

We also note, that the Wick rotation is only necessary with respect to the first Jacobi coordinate p_x and it will be allowed under the same circumstances as in the two-body case. For computational convenience, it will of course be advisable, to pass to a Euclidean metric also for the second Jacobi coordinate p_y.

Using the Gaussian expansion method, the solution of eq. (5.5-14) will have the form

$$\chi(p_x, p_y) = \sum c_i e^{-\alpha_i p_x^2 - \beta_i p_y^2} p_x^{n_x} \left|n_x l_x m_x\right\rangle_{(\hat{p}_x)} p_y^{n_y} \left|n_y l_y m_y\right\rangle_{(\hat{p}_y)}. \qquad (5.5\text{-}18)$$

To solve eq. (5.5-14) one can again make use of the techniques that were developed in the two-body problem, especially concerning the algebra with four-dimensional spherical harmonics. In particular, if we exploit the symmetry of the Bethe-Salpeter amplitude as discussed above, we can write in complete analogy to the non-relativistic case

$$\langle\chi|V|\chi\rangle = \sum_{i=1}^{3} \langle\chi|V_i|\chi\rangle = 3\,\langle\chi|V_3|\chi\rangle\,. \qquad (5.5\text{-}19)$$

Therefore, the three-body Bethe-Salpeter equation (5.5-14) becomes again a very simple eigen-value equation that may be solved by the usual diagonalization procedure.

[1] The same is true of course for the spatial variables also, it is just interesting to note the analogy with the two-body case here.

Chapter 6

Three-Dimensional Approaches

Lorsqu'on a compris qu'il y a quelque chose que l'on ne comprend pas,
on est en bonne voie pour comprendre au fond pas mal de choses.

J. Gaardener, Le Mystère de la Patience

It should have become clear by now, that the description of relativistic bound states in the Bethe-Salpeter formalism, in spite of its theoretic foundations, presents difficulties not only on a practical (computational) level, but also on a fundamental level. In particular, the absence of a quantum-mechanical probability interpretation due to the presence of a relative-time variable, has historically led to the introduction of a multitude of different reduction formalisms. In general, these ones tempt to eliminate the relative-time degree of freedom by making some assumptions on the propagators and the interaction potential of the theory [100, 101]. We shall contribute in this chapter to the study of such three-dimensional approaches to the relativistic bound-state problem, with a strong emphasis on the question of what ingredients in the dynamics are necessary in order to account for results stemming from a covariant calculation.

6.1 Introduction

Understanding the discrepancies for binding energies obtained from different approaches, ranging from the ladder Bethe-Salpeter equation at one extreme [1] to a non-relativistic equation with a so-called instantaneous one-boson exchange interaction at the other extreme, has been and is still a subject which raises considerable interest and curiosity [74]. Although it is more founded theoretically, the Bethe-Salpeter equation in ladder approximation (along with other approaches) does not reproduce the spectrum of atomic systems, like the Dirac or Klein-Gordon equations. These last equations assume a potential which is apparently consistent with an instantaneous propagation of the exchanged boson, and their success has certainly contributed substantially in founding this approximation as a model for non-relativistic interactions.

It has been suggested that the problem was specific to QED together with the one-body limit [54] and irrelevant outside this case, when bosons are massive or the one-body limit does not apply. Although proofs are not transparent and rely on some approximations, allowing authors to have doubt [102, 103], it is generally conjectured that including the contribution of crossed-boson exchange terms would resolve the problem, see ref. [58] and the discussion in the last chapter. It was clearly stated that the Bethe-Salpeter equation applied to the Wick-Cutkosky model does not support the validity of the instantaneous approximation [24]. Instead, there is agreement with results from an energy-dependent interaction [56, 104]. One might suspect therefore that the instantaneous approximation in fact provides an incomplete account of the essential dynamics in a non-relativistic scheme.

In ref. [65], Amghar and Desplanques, starting from a field-theory based approach, derived an effective interaction to be used in a non-relativistic framework. The resulting interaction, which was also obtained on a different basis in earlier works [105–107], was found to involve, as the most important effect, a renormalization of the so-called instantaneous approximation. For small couplings, the renormalization factor is given by the probability of the system being in a two-body component, without accompanying

bosons in flight. A close relation between wave functions issued from the field-theory (energy-dependent) scheme and the non-relativistic scheme (using an effective interaction) was found. It was suggested that the spectra obtained from the Bethe-Salpeter or other field-theory based approaches and the one resulting from the effective interaction could be quite similar for the lowest states.

This was confirmed in ref. [74], which completed the work performed in ref. [65] for wave functions, and extended it to the Bethe-Salpeter equation [58]. The important conclusion of these investigations is the statement that reproducing results from the Bethe-Salpeter equation in a non-relativistic scheme demands a proper account of the many-body character of the interaction, rather than the relativistic covariance of the equation.

The main idea of these works was that information obtained from the Bethe-Salpeter equation and a non-relativistic approach, the one more founded theoretically, the other closer to a physical interpretation, can complement each other. Quite generally, the aim was to derive effective interactions in a given scheme, which demands a proper 'feeling' of which physics is behind a given equation. This motivation has some similarity with the one underlying the work of Bhaduri and Brack who tried to reproduce the spectrum of the Dirac equation with an effective interaction in a non-relativistic approach [108]. The difference between this work and the one discussed here is in the dynamics: coupling of large and small components in one case, coupling of two-body components with components involving mesons in flight in the other. A renormalization of the instantaneous one-boson exchange interaction has been considered in refs. [109–111] and [112]. These works have in common with the one that will be presented in the following that they take into account effects beyond some perturbative scale, but they differ in the way how this physics is incorporated, parameterized in one case, theoretically motivated in the other.

6.2 Effective Interactions

In this section, we present the various approaches that will be used in the following to calculate binding energies of two-body systems. These ones will be compared to the results of the Bethe-Salpeter equation, that will serve as a benchmark set since they are obtained in a manifestly relativistic-covariant way.

6.2.1 Description of Two-Body Systems: Different Approaches

The first approach is of course the one based on the Bethe-Salpeter equation, where we shall at first restrict ourselves to the ladder approximation. This has been extensively discussed in the last chapter, we shall in particular retain the form of eq. (5.4-16) with the interaction kernel of eq. (5.4-17).

The field-theory foundation is more transparent in an approach which is based on time-ordered diagrams and, therefore, gives an interaction that depends on the total energy of the system, E. This energy dependence is a reminiscent of the fact that the two-body system under consideration is coupled to components with bosons in flight.

We shall then derive an approach with an effective interaction where the energy dependence has been eliminated. This interaction differs in particular from the instantaneous one-boson exchange approximation, which is frequently employed in non-relativistic descriptions of two-body systems.

Energy-dependent interaction from time-ordered perturbation theory

Little is known about the Schrödinger equation with an energy-dependent potential, like for instance the fact that Levinson's theorem still keeps its validity [113]. The complications encountered have generally led physicists to conclude that it is probably preferable not to touch this subject [114–116]. We know, however, that a proper development of Feynman-diagrams in time-ordered perturbation theory (TOPT) necessarily leads to energy-dependent interaction potentials [117]. In such a case one no longer deals with a Schrödinger equation in its proper sense, since the energy does not play the role of a simple eigen-value anymore. It has become customary however, still to refer to such equations as Schrödinger equations with an energy-dependent potential.

The single-boson exchange contribution that we want to consider first is represented by the time-ordered diagrams of fig. 6.1.

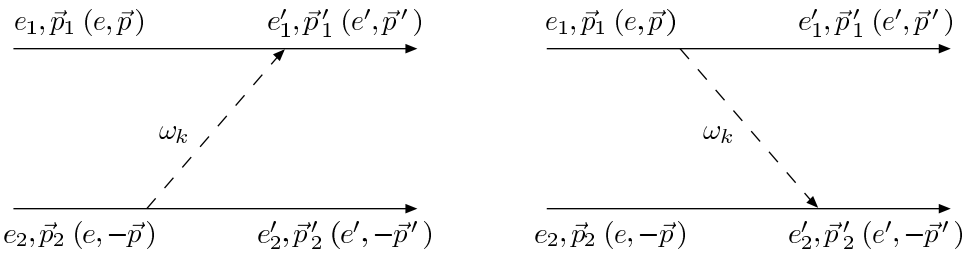

Figure 6.1: Time-ordered single-boson exchange contributions to the two-body interaction with indication of the kinematics in an arbitrary frame and in the center of mass (in parentheses).

The corresponding interaction is easily obtained from second-order perturbation theory:

$$V_E^{(1)}(,\vec{p}_2,\vec{p}'_1,\vec{p}'_2) = \frac{g^2\, O_1\, O_2}{2\,\omega_k}\,\sqrt{\frac{m^2}{e_1 e_2}}\,\left(\frac{1}{E-\omega_k-e_1-e'_2}+\frac{1}{E-\omega_k-e_2-e'_1}\right)\sqrt{\frac{m^2}{e'_1 e'_2}}, \tag{6.2-1}$$

with $\omega_k = \sqrt{\mu^2+(\vec{p}_1-\vec{p}_1\,')^2}$, $e_i = \sqrt{m^2+\vec{p}_i^{\,2}}$ and $e'_i = \sqrt{m^2+\vec{p}_i^{\,\prime 2}}$. If energy is conserved, this equation allows one to recover the standard Feynman propagator. In the center of mass, the two terms representing the contributions of the diagrams displayed in fig. 6.1 are equal. Equation (6.2-1) then simplifies and reads:

$$V_E^{(1)}(\vec{p},\vec{p}\,') = \frac{g^2\, O_1\, O_2}{\omega_k}\,\frac{m}{e}\,\left(\frac{1}{E-\omega_k-e-e'}\right)\,\frac{m}{e'}, \tag{6.2-2}$$

with $\omega_k = \sqrt{\mu^2+\vec{k}^{\,2}}$, $\vec{k}=\vec{p}-\vec{p}\,'$, $e=\sqrt{m^2+\vec{p}^{\,2}}$ and $e'=\sqrt{m^2+\vec{p}\,'^2}$, where $\vec{p}$ and $\vec{p}\,'$ represent the relative three-momenta of the constituent particles. The two normalization factors, m/e and m/e' in eq. (6.2-2), are appropriate for the case where the total free energy of the constituent particles has the semi-relativistic expression, $e=\sqrt{m^2+\vec{p}^{\,2}}$, the corresponding equation to be fulfilled being of the Klein type [118]:

$$(2\,e-E)\,\psi(\vec{p}) = -\int\frac{d\vec{p}\,'}{(2\pi)^3}\,\left(V_E^{(1)}(\vec{p},\vec{p}\,')+\cdots\right)\,\psi(\vec{p}\,'). \tag{6.2-3}$$

The dots represent multi-boson exchange terms, some of which will be explicitly considered in the following. The important feature of the interaction (6.2-2) is its dependence on the total energy of the system, E, which prevents one from using it in a Schrödinger equation without some caution[1].

We remark that the above equation may be obtained from the Bethe-Salpeter equation, eq. (5.4-16), by putting:

$$\left(m^2-(\frac{P}{2}+p)^2\right)\,\left(m^2-(\frac{P}{2}-p)^2\right)\,\Phi(p,P)\simeq$$
$$(2\,e)^2\,\left(e-\frac{E}{2}-p_0\right)\,\left(e-\frac{E}{2}+p_0\right)\,\Phi(p,P)\equiv\frac{2\,e}{E}\,(2e-E)\,\psi(\vec{p}), \tag{6.2-4}$$

consistently neglecting the dependence on p_0 (but not p'_0!) in the kernel as well as corrections of order $(E-2e)/2E$ (we assume that the mass of the exchanged boson, μ, is smaller than the constituent mass, m). In accordance with the center of mass validity of eq. (6.2-2), P_0 has been replaced by E. It should be emphasized that an equation like eq. (6.2-3) (or similar ones used below) can always be put into the form of a 4-dimensional, but non-covariant equation, as exemplified by:

$$(2e-E)\,\psi(\vec{p}) = i\int\frac{d^4p'}{(2\pi)^4}\,\frac{\left(V_E^{(1)}(\vec{p},\vec{p}\,')+\cdots\right)\,\,(2e'-E)\,\psi(\vec{p}\,')}{\left(e'-\frac{E}{2}-p'_0+i\epsilon\right)\,\left(e'-\frac{E}{2}+p'_0+i\epsilon\right)}. \tag{6.2-5}$$

A non-relativistic, but still energy-dependent form of eq. (6.2-3) may be used:

$$\left(\frac{p^2}{m}-(E-2m)\right)\,\psi(\vec{p}) = -\int\frac{d\vec{p}\,'}{(2\pi)^3}\,\left(V_E^{(1)}(\vec{p},\vec{p}\,')+\cdots\right)\,\psi(\vec{p}\,'), \tag{6.2-6}$$

[1]Note that this energy dependence has the same origin as the one in the full Bonn model of the NN interaction [119].

where the normalization factors m/e appearing in $V_E^{(1)}$ should be consistently neglected. This last equation represents an intermediate step in our effort to derive an effective non-relativistic interaction in the next subsection.

In order to make a meaningful comparison with the ladder Bethe-Salpeter approach, box-type multi-boson exchange contributions to the interaction V_E should be considered[1]. Some of them are shown in fig. 6.2.

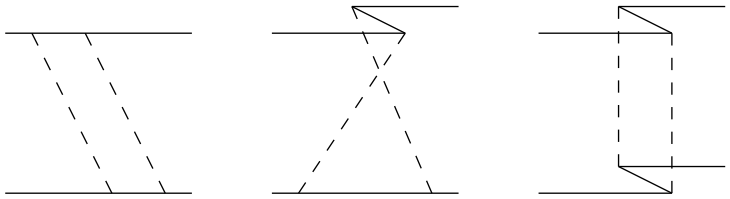

Figure 6.2: Box-type two-boson exchange contributions to the two-body interaction in time-ordered perturbation theory.

The most important one corresponds to diagram a) in this figure. Its contribution is of order $(1/m)^0$ and has the same magnitude as the off-shell effects due to the presence of the term $E - e - e'$ in the denominator of eq. (6.2-2) (see also ref. [65]). Its expression is given by:

$$V^{(2a)}(\vec{p},\vec{p}\,') = -\frac{g^4}{2}\int \frac{d\vec{q}}{(2\pi)^3}\,\frac{m}{e}\frac{(O_1\,O_2)\,(O_1\,O_2)}{\omega\,\omega'}\frac{m}{e'}\left(\frac{m}{e_q}\right)^2 \times\frac{1}{(\omega+e+e_q-E)}\,\frac{1}{(\omega'+e'+e_q-E)}\,\frac{1}{(\omega+\omega'+e+e'-E)}, \qquad (6.2\text{-}7)$$

with $\omega = \sqrt{\mu^2+(\vec{p}-\vec{q}\,)^2}$, $\omega' = \sqrt{\mu^2+(\vec{p}\,'-\vec{q}\,)^2}$ and $e_q = \sqrt{m^2+\vec{q}^{\,2}}$. The quantity $\vec{q}$ represents the momentum of the constituent particle in the intermediate state and the operators O_i are put between parentheses to emphasize that they do not necessarily commute.

As we do not pay much attention to contributions of order g^6, one could be tempted to drop terms like $E - e - e'$ in the denominator of eq. (6.2-7), which are of the same order. Doing this also has the advantage that the integral of eq. (6.2-7) can be worked out analytically (see Appendix C.3). We shall nevertheless retain the full expression of eq. (6.2-7) in our calculations, in order to deal consistently with the energy dependence of the box diagram. Numerically, the effect of the latter one turned out to be substantial. On the other hand, contributions of Z-diagrams like fig. 6.2b,c have a typical relativistic character and are of order $(1/m)^1$ and $(1/m)^3$, respectively.

Energy-independent approach and effective interaction

In order to get an energy-independent interaction from the general interaction kernel given by eq. (6.2-2), the energy dependence of the latter one was approximated in ref. [65] by a linear term (see also refs. [117, 120] for examples in relation with this approach):

$$\frac{1}{E-2m-\omega_k-\frac{\vec{p}^{\,2}}{2m}-\frac{\vec{p}\,'^{\,2}}{2m}} = -\frac{1}{\omega_k} - \frac{E-2m-\frac{\vec{p}^{\,2}}{2m}-\frac{\vec{p}\,'^{\,2}}{2m}}{\omega_k^2}+\cdots, \qquad (6.2\text{-}8)$$

[1] In the Bethe-Salpeter equation, since there is no time ordering in the four-dimensional approach, these ones are automatically generated by the ladder term.

where we replaced, as we shall do from now on, the relativistic expressions for the kinetic energies by their non-relativistic counterparts.

The second term on the right hand side of eq. (6.2-8), after insertion in eqs. (6.2-3) or (6.2-6), was then removed by a transformation which is formally similar to the one introduced by Perey and Saxon [121] in order to change a linear energy-dependent term of an optical potential into a dependence on the squared momentum and vice versa. The inverse transformation is used for solving an equation with a squared momentum-dependent term when employing the Numerov algorithm. In both cases, it has no definite physical ground beyond its mathematical character. The transformation which was performed here is more in the spirit of the Foldy-Wouthuysen one [122], see ref. [65] for details. It implicitly corresponds to introducing effective degrees of freedom with the drawback that the interaction generally acquires a non-local character. An expansion similar to that given in eq. (6.2-8) was used by Lahiff and Afnan [123, 124], so that some of our results obtained with the full energy dependence of the interaction kernel have a relationship to theirs. However, these authors have not considered the possibility of removing the energy dependence by the transformation mentioned above. The resulting energy-independent interaction was the main object of studies in the work presented in ref. [74].

Since the expansion parameter in eq. (6.2-8) is roughly equivalent to the interaction strength, this equation makes sense only as long as the coupling is not too large. In ref. [74], an essential improvement upon the approximation of eq. (6.2-8) was introduced, extending to massive bosons what was done in ref. [65] for the zero-mass case.

Starting from the formal expression of the interaction in configuration space:

$$V_E(r) = g^2\, O_1\, O_2\, \frac{1}{2\pi^2} \int \frac{dk k^2 j_0(kr)}{\omega_k \left(E - 2m - \omega_k - \frac{\vec{p}^{\,2}}{2m} - \frac{\vec{p}^{\,\prime\,2}}{2m} \right)}, \tag{6.2-9}$$

it was assumed that the quantity $E - 2m - \vec{p}^{\,2}/2m - \vec{p}^{\,\prime\,2}/2m$ in the denominator under the integral can be approximated by the effective potential we want to determine. This procedure is often used in other domains of physics where it underlies for instance the Thomas-Fermi-, WKB-, or eikonal approximations [125, 126], and it immediately provides a self-consistency equation:

$$V^{nr}_{eff,sc}(r) = -g^2\, O_1\, O_2\, \frac{1}{2\pi^2} \int \frac{dk k^2 j_0(kr)}{\omega_k \left(\omega_k - V^{nr}_{eff,sc}(r) \right)}. \tag{6.2-10}$$

By neglecting the effective interaction under the integral, one recovers the standard expression of the instantaneous one-boson exchange potential:

$$V_0(r) = -g^2\, O_1\, O_2\, \frac{e^{-\mu r}}{4\pi r}. \tag{6.2-11}$$

One can go a step further and make an expansion of the right-hand side of eq. (6.2-10) up to first order in the effective potential:

$$V^{nr}_{eff}(r) = V_0(r) - V^{nr}_{eff}(r)\, V_1(r), \tag{6.2-12}$$

where

$$V_1(r) = g^2\, O_1\, O_2\, \frac{1}{2\pi^2} \int \frac{dk k^2 j_0(kr)}{(\omega_k)^3} = \frac{g^2\, O_1\, O_2}{2\pi^2}\, K_0(\mu r). \tag{6.2-13}$$

By rearranging terms in eq. (6.2-12), one recovers the expression of the effective interaction given in ref. [65]:

$$V^{nr}_{eff}(r) = \frac{V_0(r) + \cdots}{(1 + V_1(r) + \cdots)}, \tag{6.2-14}$$

where the dots may account for two, three, ... boson exchanges. This expression has a simple interpretation in the limit of small couplings. It corresponds to the instantaneous approximation potential renormalized by the probability that the system is in a two-body component. Note that the self-consistent potential of eq. (6.2-10) can be put in a form analogous to eq. (6.2-14), with a generalized renormalization factor:

$$V^{nr}_{eff,sc}(r) = \frac{V_0(r) + \cdots}{1 + \frac{g^2\, O_1\, O_2}{2\pi^2} \int \frac{dk k^2 j_0(kr)}{\omega_k^2 \left(\omega_k - V^{nr}_{eff,sc}(r) \right)} + \cdots}. \tag{6.2-15}$$

While making the above developments, we assumed that the operator p^2 could be treated as a number. To go beyond this approximation, an expansion of the denominator in eq. (6.2-9) should be performed in the vicinity of

$$E - 2m - \frac{\vec{p}^{\,2}}{2m} - \frac{\vec{p}^{\,\prime 2}}{2m} \simeq V^{nr}_{eff,sc}(r). \tag{6.2-16}$$

This approximate equality is valid provided it is applied to a solution of a Schrödinger equation. One thus gets up to first order in the expansion:

$$V_E(r) = V^{nr}_{eff,sc}(r) + \frac{1}{2}\left\{\left(\frac{\vec{p}^{\,2}}{m} + V^{nr}_{eff,sc}(r) + 2m - E\right), V_{1,sc}(r)\right\}, \tag{6.2-17}$$

where

$$V_{1,sc}(r) = g^2\, O_1\, O_2\, \frac{1}{2\pi^2} \int \frac{dk k^2 j_0(kr)}{\omega_k \left(\omega_k - V^{nr}_{eff,sc}(r)\right)^2} \tag{6.2-18}$$

generalizes the result given by eq. (6.2-13). The expression of eq. (6.2-17) can now be inserted in the equation that corresponds to eq. (6.2-6) in configuration space. One thus gets the following equation with an energy-dependent interaction:

$$\left(V^{nr}_{eff,sc}(r)(1 + V_{1,sc}(r)) + \frac{1}{2}\left\{\frac{\vec{p}^{\,2}}{m}, \left(1 + V_{1,sc}(r)\right)\right\} - (E - 2m)\left(1 + V_{1,sc}(r)\right)\right)\psi(r) = 0. \tag{6.2-19}$$

The equation relative to the energy-independent scheme is obtained by multiplying eq. (6.2-19) from the left by $\left(1 + V_{1,sc}(r)\right)^{-1/2}$ and making the substitution:

$$\psi(r) = \left(1 + V_{1,sc}(r)\right)^{-1/2} \phi(r). \tag{6.2-20}$$

One thus gets a usual non-relativistic Schrödinger equation:

$$\left(V_{eff}(r) + \frac{\vec{p}^{\,2}}{m} - (E - 2m)\right)\phi(r) = 0, \tag{6.2-21}$$

with an effective potential

$$V_{eff}(r) = V^{nr}_{eff,sc}(r) - \frac{1}{4m} \frac{\left(\vec{\nabla} V_{1,sc}(r)\right)^2}{\left(1 + V_{1,sc}(r)\right)^2}. \tag{6.2-22}$$

The (presumably) dominant first term, of order $(1/m)^0$ in eq. (6.2-22), has a typical non-relativistic character. It can be checked that its contribution to order g^4 (i.e. including the box diagram, fig. 6.2a) is identical to the one obtained by subtracting from the Feynman two-boson exchange diagram that part resulting from iterating the one-boson exchange. This represents another way of calculating the contributions to energy-independent potentials with the range of two-boson exchange [64,127]. However, the present approach allows one to take into account higher order corrections that are relevant when $V_{1,sc}(r)$ becomes large. The second term in eq. (6.2-22) is required for consistency with eq. (6.2-19) and, most importantly, it represents the first correction to the approximation given by eq. (6.2-16) at the denominator of eq. (6.2-9). Being of a higher order in $1/m$, it was neglected in the calculations presented in ref. [74]. This is consistent with neglecting other relativistic corrections of the same order, especially the normalization factors m/e present in eq. (6.2-2). These ones provide some non-locality that, most probably, could be accounted for in the above developments [128], but at the price of a tremendous numerical work [129]. For the same reason, we will retain, for the numerical calculations presented below, the expression of the self-consistent, effective potential given by the solution of eq. (6.2-10).

The dressed (effective) character of the object described by $\phi(r)$, eq. (6.2-21), is better seen by looking at the expression of the norm in the local approximation:

$$N = \int d\vec{r}\, \left(\frac{\phi^2(r)}{\left(1 + V_{1,sc}(r)\right)} + \frac{\phi^2(r)\, V_{1,sc}(r)}{\left(1 + V_{1,sc}(r)\right)}\right) = \int d\vec{r}\, \left(\psi^2(r) + \psi(r)\, V_{1,sc}(r)\, \psi(r)\right). \tag{6.2-23}$$

The quantity $\phi^2(r)$ describes a hybrid state that is a coherent superposition of two components, with weights respectively given by $1/(1+V_{1,sc}(r))$ and $V_{1,sc}(r)/(1+V_{1,sc}(r))$. The first one, which from eq. (6.2-20) is seen to be described by $\psi(r)$, corresponds to the bare two-body component. The second one, which corresponds to a three-body component, has a more complicated structure. The relation in this case can be obtained from the expression of the component with one boson in flight:

$$|\text{boson} + 2\,\text{constituents}\rangle = \frac{1}{E-\omega_k-e_1-e_2}\,H_I\,|2\,\text{constituents}\rangle, \tag{6.2-24}$$

where H_I is the boson-constituent interaction. Using this expression, it can be checked that the part corresponding to extra bosons in flight (discarding the boson cloud of the constituents) provides a contribution to the normalization given by $\int d\vec{r}\,\psi^2(r)(-\partial V_E(r)/\partial E)$. The identification with the last term in eq. (6.2-23) is achieved via the expression given by eq. (6.2-17), or equivalently from an explicit calculation starting with eq. (6.2-9), allowing one to directly obtain eq. (6.2-18). This illustrates vividly that working with the effective degrees of freedom ϕ, we implicitly include many-body effects in our calculations. How important they are will be discussed when we present our results.

Instantaneous one-boson exchange approximation

It is clearly noted that the potential of eq. (6.2-22) does not correspond to the so-called instantaneous approximation given by $V_0(r)$ in eq. (6.2-11). This one, which is often used as a reference, underlies many models dealing with hadronic systems and, at first sight, the well known Coulomb potential. It is usually justified as follows. Starting from the covariant expression for a boson propagator in configuration space,

$$i\Delta(x_1-x_2) = \int \frac{d^4q}{(2\pi)^4}\,\frac{e^{iq\cdot(x_1-x_2)}}{\mu^2+\vec{q}^{\,2}-q_0^2-i\epsilon}, \tag{6.2-25}$$

and assuming that the energy transfer q_0 is small, one gets

$$i\Delta(x_1-x_2) \simeq \delta(t_1-t_2)\,\frac{e^{-\mu\,r}}{4\pi r}, \quad (\text{with } r=|\vec{r}_1-\vec{r}_2|). \tag{6.2-26}$$

The assumption of q_0 being small is valid for a Born amplitude in the non-relativistic domain. Beyond this approximation, q_0, which is an integration variable at the r.h.s. of eq. (6.2-25), is not limited to small values. It may be large and, in particular, can give rise to singularities when $q_0=\pm\sqrt{\mu^2+\vec{q}^{\,2}}$. These poles are responsible for the renormalization of the so-called instantaneous potential, eq. (6.2-11), leading to the effective potential of eq. (6.2-22). Their contributions are omitted in the spectator approach [72] where they could allow one to symmetrize the role of the two constituent particles. This omission is generally justified by the fact that these extra contributions are cancelled by crossed-boson exchange diagrams, thus recovering an instantaneous-like single-boson exchange interaction. However, this only works for neutral, spin-less bosons, which discards two important cases in hadronic physics: pions and gluons.

While the potentials of eqs. (6.2-11) and (6.2-22) both have an instantaneous character, there is not necessarily a contradiction as they do not correspond to the same mathematical description. In the first case, one works with asymptotic, bare particles that exchange bosons. In the second, one has dressed particles that are eigenstates of the Hamiltonian, incorporating components with bosons in flight. It will become clear from our results that the effects implicitly incorporated in the effective interaction account at least partially for the dynamics of the original relative time (or energy) variable, which has been integrated out, as for instance in eq. (6.2-3). The effects under discussion may therefore not be relativistic ones as sometimes advocated in the literature. Instead, they are quite similar to those appearing in the many-body problem. In the case of the nucleon-nucleus interaction for instance, they originate from the energy dependence of the optical potential due to the coupling to other channels, whose effects can be partly incorporated in mean-field approximations through a contribution to the effective mass. The close relationship between the quasi-particle strength introduced in ref. [126], $Z=(1-d(\Delta V(E))/dE)^{-1}$, and the quantity $(1+V_1)^{-1}$ appearing in many equations of the present section, is evident.

Being justified in Born approximation, the one-boson exchange instantaneous approximation cannot correctly account for higher order (off-shell) effects. How large these ones are will be discussed in the

next sections where binding energies are compared with corresponding ones of more complete approaches. The above statement also applies to the many quasi-potential approaches that have been considered in the literature [68–72, 130], often with the idea to provide some link to the Bethe-Salpeter equation. Frequently, they differ by the two-particle propagator while using an interaction similar to the so-called instantaneous approximation [131–133]. Little attention has been given to a significant modification of the interaction, like the one provided by a renormalization as given by eq. (6.2-22). This one, as will be seen below, is essential to reveal the close relationship with the Bethe-Salpeter equation. Note that, in the domain of hadronic physics, this renormalization is accounted for correctly in different ways at the two-pion level in the Paris [127] and full Bonn [119] models of the NN interaction, but treated phenomenologically in most other ones.

Energy-dependent corrections beyond the instantaneous approximation, which we are interested in here, have different names, depending on the domain where they are employed: norm corrections in the case of mesonic exchange currents [134], dispersive effects in scattering processes involving composite systems [126] or retardation effects in two-body scattering [119]. It is remarked that retardation effects sometimes represent different kind of corrections, involving terms of the order $(\Delta E/\omega)^2$ [51], rather than the ones retained here, that involve terms of the order $\Delta E/\omega$. As already mentioned, the former ones are of the order $(1/m)^2$, and have a typical relativistic character.

6.2.2 Results in Ladder Approximation

In ref. [74] binding energies were calculated in ladder approximation using the different approaches described in the last section. Explicitly, these ones include:

- the Bethe-Salpeter (B.S.) equation, eq. (5.4-16), together with an interaction kernel given by eq. (5.4-17) (ladder approximation),
- a semi-relativistic equation, eq. (6.2-3), with an energy-dependent potential V_E given by eq. (6.2-2),
- the standard non-relativistic Schrödinger equation, eq. (6.2-21), together with an effective interaction ($V_{eff,sc}$) given by eq. (6.2-10), which accounts for energy-dependent effects in a self-consistent calculation,
- the same equation, but with an effective interaction (V_{eff}) as given by eq. (6.2-14), accounting for energy-dependent effects only at the lowest order,
- the same equation in the so-called instantaneous approximation (IA) with an interaction given by eq. (6.2-11).

In fig. 6.3, we plot the potential functions of the last three of these approaches in configuration space with the box contribution included for two values of the coupling constant and two values of the boson mass. It can be seen that the effective potentials are significantly smaller in magnitude than the one from the instantaneous approximation, especially at small distances, the effect being larger for V_{eff} than for its self-consistent version, $V_{eff,sc}$.

In the following, we give results for two different boson masses as well as different angular momenta. In the second, third and fourth approaches, the results with and without the contribution of the box diagram (fig. 6.2a) are considered, so that a comparison with the Bethe-Salpeter approach is fully relevant at order $(1/m)^0$.

Finite-mass boson case

Calculations have been performed with boson masses $\mu = 0.15\,m$ and $\mu = 0.5\,m$, a choice that was made in earlier works [55, 135]. In the instantaneous approximation, these results are not independent. The ratio of the binding energy and the squared boson mass is a unique function of the ratio of the coupling constant and the boson mass:

$$\frac{m\,E_{be}}{\mu^2} = f\left(\frac{\alpha m}{\mu}\right). \tag{6.2-27}$$

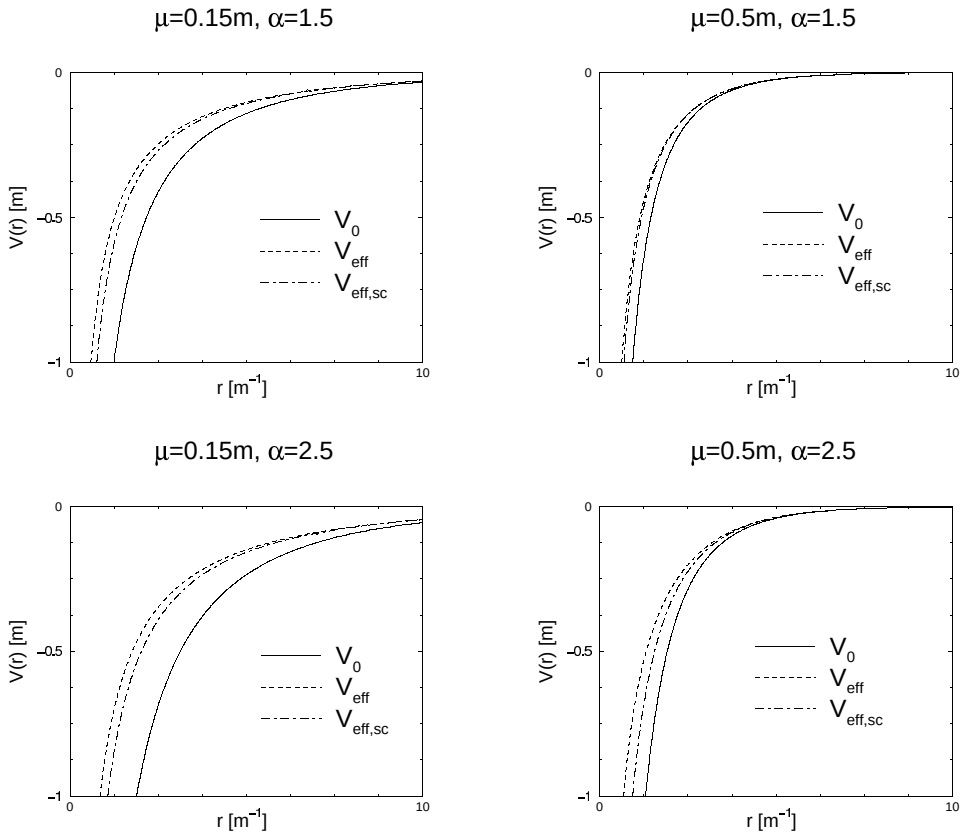

Figure 6.3: Representation of non-relativistic potentials for two values of α and two values of μ. V_0 is the instantaneous potential of eq. (6.2-11), V_{eff} is the effective potential of eq. (6.2-14) and $V_{eff,sc}$ gives the self-consistent, effective potential of eq. (6.2-10).

For the coupling constant, $\alpha = g^2/4\pi$, we considered ranges appropriate for the states under consideration, in order to provide a significant insight on the variation of the binding energy with the strength of the interaction. Some of the binding energies may be quite large, questioning their physical relevance. However, this should not spoil the comparison of the different approaches we are considering, which is our main intent. For the angular momentum, we obviously considered the ground state with $l = 0$ (table 6.1), but also the first excited states with $l = 0$ (denoted 0*) and $l = 1$. The energies for the latter ones, which are degenerate in the case of zero-mass boson exchange, are presented in table 6.2. Their examination may provide useful information on the role of the combined effect of the coupling strength and the boson mass.

Concerning the binding energies of the lowest $l = 1$ state and the first excited state with $l = 0$, some track of the degeneracy expected for a Coulomb potential can be seen in table 6.2 (for states that are not too weakly bound). It is interesting however to observe the relative order of these states in the various approaches. In the instantaneous approximation the total energy of the first excited state with $l = 0$ is always smaller than the one of the $l = 1$ state for all values of the coupling constant, as expected from a theorem involving the concavity of the potential [136, 137]. The situation is however different in the energy-dependent model, and in the Bethe-Salpeter case, where a crossing of the 2s and 1p states occurs. This peculiarity is illustrated in fig. 6.4, where we plot the ratio of binding energies of the two states for the various approaches. This feature, together with the principal possibility of the description of abnormal states, as discussed earlier, shows the dynamical importance of the energy dependence of the interaction for describing also excited states.

Table 6.1: Binding energies calculated in ladder approximation for massive scalar bosons (in units of the constituent mass m). Results are presented here as a function of the coupling constant α for the ground state ($l = 0$) and two boson masses ($\mu = 0.15\,m$ and $\mu = 0.5\,m$). Five cases have been considered: the Bethe-Salpeter equation (B.S., eqs. (5.4-16, 5.4-17)), an energy-dependent model (V_E, eqs. (6.2-2, 6.2-3)), an effective non-relativistic interaction ($V^{nr}_{eff,sc}$, eqs. (6.2-21, 6.2-10)), a simplified version of this effective interaction (V^{nr}_{eff}, eqs. (6.2-21, 6.2-14)) and, slightly apart, the so-called instantaneous approximation (IA^{nr}, eqs. (6.2-21, 6.2-11)). In the second, third and fourth cases, the binding energies calculated without the contribution of the box diagram are given in parentheses. The superscript nr signifies that the calculations are performed with an interaction derived at the lowest order, $(1/m)^0$.

μ/m	α	B.S.	V_E ($-$box)	$V^{nr}_{eff,sc}$ ($-$box)	V^{nr}_{eff} ($-$box)	IA^{nr}
	0.50	0.0059	0.0052 (0.0045)	0.0062 (0.0051)	0.0055 (0.0040)	0.013
	0.75	0.023	0.020 (0.017)	0.023 (0.020)	0.020 (0.014)	0.056
.15	1.00	0.047	0.039 (0.034)	0.048 (0.039)	0.038 (0.026)	0.129
	1.25	0.076	0.061 (0.052)	0.076 (0.063)	0.059 (0.037)	0.233
	1.50	0.109	0.084 (0.073)	0.108 (0.088)	0.081 (0.047)	0.367
	1.50	0.0125	0.0071 (0.0051)	0.0144 (0.0090)	0.0098 (0.0028)	0.093
	1.75	0.028	0.017 (0.013)	0.031 (0.021)	0.023 (0.008)	0.180
.50	2.00	0.049	0.030 (0.024)	0.053 (0.037)	0.038 (0.014)	0.296
	2.25	0.073	0.045 (0.036)	0.078 (0.056)	0.056 (0.022)	0.442
	2.50	0.100	0.061 (0.050)	0.106 (0.077)	0.077 (0.030)	0.619

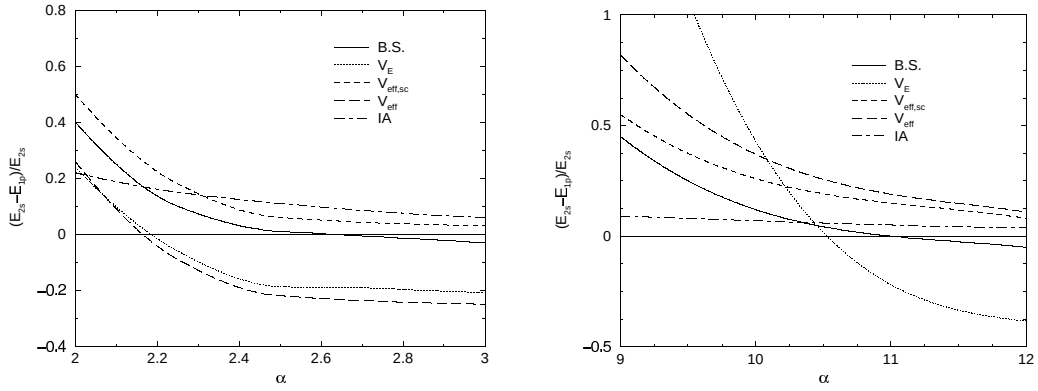

Figure 6.4: Relative ordering of binding energies of the first radial (2s) and orbital (1p) excited states for different approaches. The figure on the left corresponds to the case $\mu = 0.15\,m$, the one on the right to $\mu = 0.5\,m$.

Zero-mass boson case

Binding energies for the zero-mass boson case have been considered in various works from different viewpoints (see for instance refs. [24, 104, 138, 139]). Those for the Wick-Cutkosky model obtained with the Bethe-Salpeter equation in ref. [24] are complemented here by a few more values for different coupling constants, α. Binding energies calculated with the energy-dependent interaction, V_E, may be compared to those obtained using the memory-function approach in ref. [104]. The latter one includes higher order corrections in $1/m$, but neglects the contribution of the box diagram (fig. 6.2a). The two last sets of numbers considered here correspond to binding energies calculated in a non-relativistic approach with an effective Coulomb interaction accounting for energy-dependent effects, and the bare Coulomb interaction

Table 6.2: Same as table 6.1 for excited states with $l = 0^*$ and $l = 1$. Bars indicate that there is either no bound state or that its binding energy, being too small, cannot be determined reliably.

μ/m	l	α	B.S.	V_E (−box)	$V^{nr}_{eff,sc}$ (−box)	V^{nr}_{eff} (−box)	IA^{nr}
		2.00	0.005	0.003 (0.002)	0.006 (0.004)	0.003 (—)	0.054
		2.25	0.010	0.006 (0.004)	0.011 (0.007)	0.005 (—)	0.086
	0^*	2.50	0.015	0.009 (0.007)	0.016 (0.011)	0.009 (0.001)	0.124
		2.75	0.022	0.013 (0.010)	0.023 (0.015)	0.013 (0.002)	0.170
		3.00	0.029	0.018 (0.014)	0.030 (0.021)	0.018 (0.003)	0.223
0.15							
		2.00	0.003	0.002 (0.001)	0.003 (0.001)	0.002 (—)	0.042
		2.25	0.009	0.006 (0.003)	0.009 (0.005)	0.006 (0.001)	0.073
	1	2.50	0.015	0.011 (0.007)	0.015 (0.009)	0.011 (0.003)	0.111
		2.75	0.022	0.016 (0.011)	0.022 (0.014)	0.016 (0.005)	0.156
		3.00	0.030	0.022 (0.016)	0.029 (0.020)	0.022 (0.007)	0.209
		9	0.022	(—) (—)	0.031 (0.012)	0.017 (—)	1.787
		10	0.042	0.004 (0.001)	0.053 (0.024)	0.035 (—)	2.494
	0^*	11	0.067	0.012 (0.005)	0.079 (0.040)	0.057 (—)	3.324
		12	0.096	0.022 (0.011)	0.108 (0.058)	0.084 (—)	4.279
0.5							
		9	0.012	(—) (—)	0.014 (—)	(—) (—)	1.627
		10	0.037	0.003 (—)	0.039 (0.008)	0.022 (—)	2.327
	1	11	0.067	0.015 (0.002)	0.067 (0.026)	0.046 (—)	3.150
		12	0.101	0.031 (0.012)	0.099 (0.046)	0.075 (—)	4.099

as a reference. The binding energy for these cases is then given by the standard analytic expression:

$$|E_{be}| = \frac{\alpha^2}{4n^2} \quad \left(\text{or } \frac{\alpha^2_{eff,sc}}{4n^2}\right), \tag{6.2-28}$$

where the relation between $\alpha_{eff,sc}$ and α, first studied in ref. [65], is given in the simplest case by:

$$\alpha_{eff,sc} = \frac{\alpha}{1+\alpha\, J} = \alpha(1-\alpha_{eff,sc}\, J), \;\; \text{with } J = \frac{2}{\pi}\int_0^\infty \frac{dy\, j_0(y)}{\alpha_{eff,sc}+y}. \tag{6.2-29}$$

This equation can also be obtained from eq. (6.2-10) for the zero-mass boson case. It can be improved by incorporating the contribution of the box diagram, in which case it gets modified as follows:

$$\alpha_{eff,sc} = \frac{\alpha(1+\alpha J^b)}{1+\alpha\, J} = \alpha(1+\alpha J^b - \alpha_{eff,sc}\, J), \tag{6.2-30}$$

where J is still given by the integral in eq. (6.2-29). The quantity J^b, which involves the contribution of the box diagram (fig. 6.2a), is given by:

$$J^b = \frac{1}{\pi^2}\int_0^\infty dx\, j_0(x) \int_0^\infty \frac{x\, dy}{y(\alpha_{eff,sc}+y)} \log\left(\frac{(\alpha_{eff,sc}+|x+y|)(\alpha_{eff,sc}+y+|x-y|)}{(\alpha_{eff,sc}+|x-y|)(\alpha_{eff,sc}+y+|x+y|)}\right), \tag{6.2-31}$$

where the second integral becomes equal to $4\log 2$ in the limit of small $\alpha_{eff,sc}$. It is calculated from an expression similar to eq. (6.2-7) where the terms $E - p^2/m$ appearing in the full expression have been kept and approximated by $-\alpha_{eff,sc}/r$. This is consistent with the calculation of J, allowing one to factorize

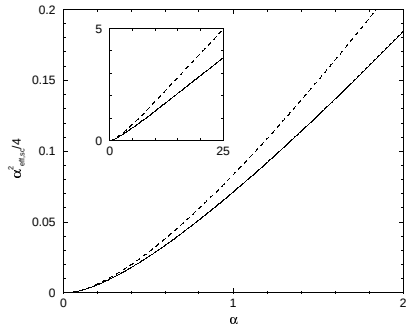

Figure 6.5: Representation of $\alpha^2_{eff,sc}/4$ as a function of the bare coupling α. The solid line corresponds to the solution of eq. (6.2-29), the dashed line to the one of eq. (6.2-30). The inset shows the linear asymptotic behaviour for large α.

a local Coulomb-type contribution.

While the relation of J^b to the two-boson exchange can be traced back without too much difficulty, this is not so obvious for the quantity J which was obtained by accounting for off-shell effects arising from one-boson exchange. However, it is possible to rewrite J in a form that is formally similar to eq. (6.2-31) by using the identity:

$$\sin(y) = \frac{1}{\pi}\int_0^\infty dx\, \sin(x)\, \log\left(\frac{|x+y|}{|x-y|}\right),$$

from which one gets:

$$J = \frac{2}{\pi^2}\int_0^\infty dx\, j_0(x) \int_0^\infty \frac{dy\quad x}{y(\alpha_{eff,sc}+y)}\, \log\left(\frac{|x+y|}{|x-y|}\right). \tag{6.2-32}$$

Curves showing $\alpha_{eff,sc}$ as a function of the coupling α are given in fig. 6.5 for the different cases corresponding to eqs. (6.2-29) and (6.2-30). More precisely, we represent the quantity $\alpha^2_{eff,sc}/4$ as a function of α. This one offers the advantage of being directly comparable to the binding energy obtained for the lowest $l = 0$ state in a non-relativistic Coulomb-like potential, $-\alpha_{eff,sc}/r$ (we set $m = 1$ here). For large couplings, $\alpha_{eff,sc}$ varies like $\sqrt{\alpha}$, which can be checked from eq. (6.2-29) or equivalently from eq. (6.2-10) in the limit of a large effective potential. One gets the asymptotic relation $\alpha^2_{eff,sc} \to (2/\pi)\,\alpha$ for one-boson exchange, eq. (6.2-29) and $\alpha^2_{eff,sc} \to 2/[\pi(\sqrt{3}-1)]\,\alpha$ when also including two-boson exchange, eq. (6.2-30). The corresponding result for the Wick-Cutkosky model would be $\alpha^2_{eff,sc} \to (4/\pi)\,\alpha$.

The different results for the binding energies are given in table 6.3. The results of V^{nr}_{eff} relative to those of $V^{nr}_{eff,sc}$ are very similar to the corresponding ones of table 6.1, so we do not give the numbers here. In the case of V_E, the small binding energies obtained here for small couplings cannot be reliably determined by the variational procedure that we employ. Only values for relatively large couplings are given here, in order to allow for a comparison of different approaches. Note also, that for the energy-dependent interaction, V_E, binding energies for excited states are not degenerate, as it is the case for all the other models considered here, even though the splitting is expected to be small. The numbers that we present in table 6.3 for this case correspond to the state with the highest value of angular momentum, l, in that row.

Discussion of results in ladder approximation

The tables presented above clearly show that results from the B.S., V_E and $V_{eff,sc}$ approaches are very close to each other but definitely depart from the ones of the instantaneous approximation. This is true for the massive- as well as the zero-mass boson case. The contribution of the box diagram, without affecting the above conclusion, significantly helps in narrowing the gap between the Bethe-Salpeter approach and those accounting for energy-dependent effects, V_E and $V_{eff,sc}$.

Table 6.3: Binding energies calculated in ladder approximation for zero-mass scalar bosons (Wick-Cutkosky model). Results (in units of the constituent mass m) are presented here as a function of the coupling constant α for the ground state ($l = 0$) as well as excited states ($l = 0^*, 1, 0^{**}, 1^*, 2$). Four cases from the previous tables have been considered here: the Bethe-Salpeter equation (B.S.), an energy-dependent model (V_E), an effective interaction $V^{nr}_{eff,sc}$ and, slightly apart, the so-called instantaneous approximation(IA^{nr}). For V_E the binding energies for excited states, which are not degenerate in this case, given in the table correspond to the highest orbital momentum l only. Bars indicate that the corresponding binding energy is too small to be determined reliably using the same numerical method as for the other numbers in the same column.

α	l	B.S.	V_E ($-$box)	$V^{nr}_{eff,sc}$ ($-$box)	IA^{nr}
	0,	1.274-5	(—)	1.274-5 (1.266-5)	1.331-5
1/137.036	$0^*, 1$,	0.318-5	(—)	0.318-5 (0.316-5)	0.333-5
	$0^{**}, 1^*, 2$,	0.141-5	(—)	0.141-5 (0.140-5)	0.148-5
	0,	1.849-3	(—)	1.859-3 (1.770-3)	2.500-3
0.10	$0^*, 1$,	0.465-3	(—)	0.465-3 (0.442-3)	0.625-3
	$0^{**}, 1^*, 2$,	0.207-3	(—)	0.207-3 (0.197-3)	0.278-3
	0,	2.867-2	(—)	2.883-2 (2.547-2)	6.250-2
0.50	$0^*, 1$,	0.727-2	(—)	0.721-2 (0.637-2)	1.562-2
	$0^{**}, 1^*, 2$,	0.324-2	(—)	0.320-2 (0.283-2)	0.694-2
	0,	0.842-1	0.725-1 (0.637-1)	0.832-1 (0.711-1)	2.50-1
1.00	$0^*, 1$,	0.213-1	0.202-1 (0.174-1)	0.208-1 (0.178-1)	0.62-1
	$0^{**}, 1^*, 2$,	0.095-1	0.093-1 (0.081-1)	0.092-1 (0.079-1)	0.28-1
	0,	1.545-1	1.239-1 (1.071-1)	1.494-1 (1.247-1)	5.62-1
1.50	$0^*, 1$,	0.388-1	0.353-1 (0.300-1)	0.373-1 (0.312-1)	1.41-1
	$0^{**}, 1^*, 2$,	0.173-1	0.164-1 (0.138-1)	0.166-1 (0.139-1)	0.62-1

For the case $\mu = 0$, due to the way the effective potential is derived, the binding energies obtained in this approach evidence the degeneracy pattern of the Wick-Cutkosky model in ladder approximation, as do the IA results (which is just the degeneracy of the well-known Coulomb problem in this case). Less trivial is the fact that the same effective potential does equally well for the ground- and excited states, indicating that the important dynamics has been properly captured by this approach.

The calculations with effective interactions ($V^{nr}_{eff,sc}$ and V^{nr}_{eff}) have neglected various corrections of relativistic order. The binding energies obtained in these approaches are likely to be overestimated because the largest corrections are expected from the normalization factors m/e, that have a repulsive character. These corrections would get partly cancelled however by the attractive second term in eq. (6.2-22), which has been neglected in the calculations. Even though they are probably not small on the scale of the total energy of the system, one should compare them to the differences between results obtained with $V^{nr}_{eff,sc}$ and IA^{nr}, which roughly amount to factors 2-3 ($\mu = 0.15\,m$) and 6 ($\mu = 0.50\,m$).

In view of these corrections due to factors m/e, it is remarkable still, that differences with the Bethe-Salpeter results are rather small in many cases, in particular as compared to the results of the energy-dependent approach, V_E. Taking into account the normalization factors m/e would have the welcome effect of bringing values obtained with $V^{nr}_{eff,sc}$ ($-$box) closer to those obtained with V_E ($-$box). This would leave some room for the contribution of Z-type diagrams as well as diagrams with higher-order boson exchanges. These ones give an attractive contribution in the present model and become more important when the coupling gets stronger.

It is also noted that the differences between the B.S. and V_E results decrease with l. As these differences mainly originate from Z-type diagrams, which produce a $1/r^2$ contribution to the interaction

in the non-relativistic limit, it is expected that their effect will be reduced by the centrifugal barrier, providing an explanation for the above observation.

The results presented in tables 6.1 - 6.3 indicate that the range of validity of a non-relativistic approach should be larger than what is often inferred from the results of the instantaneous approximation. In particular, contrary to the statement made in ref. [140], it seems to be possible in a non-relativistic approach to account for binding energies obtained in relativistic calculations even for large couplings, provided one includes in the interaction corrections that account for the many-body character of the problem. In other words, the differences between results obtained from the Bethe-Salpeter equation with those stemming from its (various) instantaneous approximations, are only minorily due to the relativistic covariance of the former approach, but largely a consequence of many-body effects, that the Bethe-Salpeter equation implicitly includes.

6.2.3 Results with Crossed-Boson Exchange

We shall now consider the role of genuine crossed two-boson exchanges in the different approaches discussed before. We shall consider in particular those diagrams that are of the same order as the correction brought about by the renormalization factor $(1+V_1(r))^{-1}$ in eq. (6.2-14), or what generalizes this quantity in eq. (6.2-15). We first recall the general expression for these contributions and subsequently look at particular cases for both neutral and charged bosons. Contrary to the ladder case, we shall only consider the case of massive boson exchange here. The reason is of course the infra-red divergence of the Feynman diagram for the crossed box, which makes it impossible to use in a perturbative calculation of the Bethe-Salpeter kernel.

General considerations

The full expression of the crossed two-boson exchange contribution to the Bethe-Salpeter equation, as discussed in chapter 5.4, is taken from ref. [58], where it was put into the form of a dispersion relation. Among the different expressions given in this work, we retain here the choice of eq. (5.4-24) with $u=0$, which gives an energy-independent interaction kernel. The other expressions give close results, provided the binding energy is not too large, compare fig. 5.13.

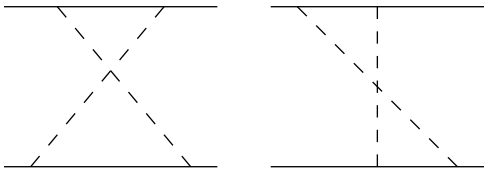

Figure 6.6: Crossed two-boson exchange contributions to the two-body interaction in time-ordered perturbation theory.

The expressions appropriate for the energy-dependent picture are obtained from the time-ordered diagrams shown in fig. 6.6 that have to be added to the box diagram of fig. 6.2a. They are given by:

$$V^{(2b)}(\vec{p},\vec{p}\,') = -\frac{g^4}{2}\int\frac{d\vec{q}}{(2\pi)^3}\,\frac{m}{e_q}\frac{m}{e}\,\frac{O_1\,(O_1\cdot O_2)\,O_2}{\omega\,\omega'}\,\frac{m}{e'}\frac{m}{e_{q'}} \times\frac{1}{(\omega+e+e_q-E)}\frac{1}{(\omega'+e'+e_q-E)}\frac{1}{(\omega+\omega'+e_q+e_{q'}-E)}, \qquad (6.2\text{-}33)$$

$$V^{(2c)}(\vec{p},\vec{p}\,') = -\frac{g^4}{2}\int\frac{d\vec{q}}{(2\pi)^3}\,\frac{m}{e_q}\frac{m}{e}\,\frac{O_1\,(O_1\cdot O_2)\,O_2}{\omega\,\omega'}\,\frac{m}{e'}\frac{m}{e_{q'}} \times\frac{1}{(\omega+e+e_q-E)}\frac{1}{(\omega+e'+e_{q'}-E)}$$

$$\times \left\{ \frac{1}{(\omega+\omega'+e+e'-E)} + \frac{1}{(\omega+\omega'+e_q+e_{q'}-E)} \right\}. \qquad (6.2\text{-}34)$$

In addition to the factors defined after eq. (6.2-7), we have used here $e_{q'} = \sqrt{m^2+\vec{q}'^{\,2}}$ with $\vec{q}' = \vec{q}-(\vec{p}+\vec{p}')$. Z-type diagrams have a higher order in $1/m$ and are expected to be smaller. They are not incorporated in eqs. (6.2-33) and (6.2-34). By retaining terms of the lowest order, $(1/m)^0$, one gets the expression of the crossed two-boson exchange that we will include in $V^{nr}_{eff,sc}$ and V^{nr}_{eff}. It can be checked that it is equal to the contribution obtained with the dispersion relation, eq. (5.4-24), in the same limit.

For a charged boson, the crossed-box contribution depends on the isospin of the state under consideration. We will consider the case of a state with $T=1$, where it provides further attraction. The effective interaction then reads:

$$V^{nr}_{eff} = V_0 \, \frac{1+\bar{V}^{(2a)}+\kappa\,(\bar{V}^{(2b)}+\bar{V}^{(2c)})}{1+\bar{V}^{(2a)}+\bar{V}^{(2b)}+\bar{V}^{(2c)}}, \qquad (6.2\text{-}35)$$

where the barred potentials are the same as the ones defined in eqs. (6.2-7), (6.2-33) and (6.2-34), but without the isospin operators O_i. The factor κ is the result of the isospin algebra. For a charged boson, $\kappa=5$, whereas for a neutral boson, $\kappa=1$, in which case the expression greatly simplifies, leaving V_0 as an effective interaction. Note that, up to order $(1/m)^0$, this cancellation is expected to hold at all orders in the coupling g^2, i.e. even including multi-boson exchange diagrams [65]. The effective interaction is thus also given by V_0 in this case.

Results

The results for the massive boson case are displayed in table 6.4. Comparing with the ladder case (table 6.1), we see that the crossed box for the neutral boson exchange multiplies the binding energies by factors $\sim$1.5 – 2 in all models except the instantaneous approximation, which is unaffected. As in the ladder approximation, binding energies for the energy-dependent and the non-relativistic self-consistent effective-interaction approaches are relatively close to each other in the neutral-boson model. The differences, that tend to increase with the coupling and the boson mass, can be understood as being primarily due to the omission of factors $\sqrt{m/e}$ in the non-relativistic calculation. Taking this into account, it can be considered that the effective self-consistent interaction, $V^{nr}_{eff,sc}$, incorporates the relevant physics underlying the energy-dependent interaction, V_E, which it was derived from. However, contrary to the ladder approximation (table 6.1), the corresponding results significantly depart from those obtained with the Bethe-Salpeter equation or the (non self-consistent) effective interaction, V^{nr}_{eff}, which both are close (or identical) to the results obtained in the instantaneous approximation. We emphasize again that the exact equality of the two last columns simply results from the identity, $V^{nr}_{eff}=V_0$, which holds for this particular case, see eq. (6.2-35) for $\kappa=1$.

Apart from results in the instantaneous approximation, those for charged boson exchange show a quite similar pattern as in the neutral boson case. The exact degeneracy between results of the instantaneous approximation and V^{nr}_{eff} is lifted now, see eq. (6.2-35) for $\kappa=5$. To estimate the relative importance of the boson charge one can compare binding energies for the same coupling constant $\alpha=0.5$ and the same boson mass $\mu=0.15$. We see that results from the B.S. and V^{nr}_{eff} approaches get multiplied by a factor $\sim$10, those from V_E and $V^{nr}_{eff,sc}$ by a factor $\sim$3, while the instantaneous approximation result stays the same when going from neutral to charged boson exchange. This illustrates the very limited range of applicability of the instantaneous approximation, which by definition cannot account for any structure different from a scalar, neutral exchange in the interaction.

We note finally that in the charged boson case, the boson mass μ plays a non-negligible role. Binding energies from the V_E model for instance are larger than those in the instantaneous approximation for the case $\mu=0.15$ while they are smaller for $\mu=0.5$. This is possibly an effect of the infra-red divergence of the crossed-box diagram, which may be more important for charged-boson exchange, where the interaction is much more attractive than in the neutral boson case.

Discussion of results with crossed-boson exchange

By incorporating the contribution of crossed diagrams, we expected the different approaches, B.S., V_E, $V^{nr}_{eff,sc}$ and V^{nr}_{eff}, to produce a pattern similar to the one evidenced by these models in ladder approxima-

Table 6.4: Ground-state binding energies calculated for massive, scalar bosons without and with charge (in units of the constituent mass m), including the box- and the crossed-box contribution. Results for the charged-boson case correspond to a state with total isospin equal to 1. As in the previous section, five cases have been considered: the Bethe-Salpeter equation (B.S.), an energy-dependent model (V_E), an effective interaction ($V^{nr}_{eff,sc}$), an approximate version of the latter one (V^{nr}_{eff}) and, slightly apart, the so-called instantaneous approximation(IA^{nr}).

μ/m	α	B.S.	V_E	$V^{nr}_{eff,sc}$	V^{nr}_{eff}	IA^{nr}
neutral case						
	0.50	0.013	0.0076	0.0096	0.013	0.013
	0.75	0.062	0.027	0.035	0.056	0.056
.15	1.00	0.158	0.054	0.071	0.129	0.129
	1.25	0.324	0.083	0.114	0.233	0.233
	1.50	0.593	0.115	0.161	0.367	0.367
	1.50	0.077	0.014	0.034	0.093	0.093
	1.75	0.162	0.029	0.064	0.180	0.180
.50	2.00	0.290	0.047	0.101	0.296	0.296
	2.25	0.479	0.068	0.143	0.442	0.442
	2.50	0.761	0.092	0.189	0.619	0.619
charged case						
	0.30	0.0062	0.0015	0.0024	0.0095	0.00046
	0.40	0.037	0.0083	0.012	0.053	0.0046
.15	0.50	0.107	0.020	0.028	0.152	0.013
	0.60	0.229	0.034	0.049	0.322	0.027
	0.70	0.425	0.050	0.073	0.573	0.045
	0.90	0.092	0.0007	0.011	0.336	0.0007
.50	1.00	0.183	0.0041	0.023	0.59	0.0052
	1.10	0.319	0.0098	0.040	0.93	0.0138
	1.20	0.517	0.0170	0.061	1.36	0.0267

tion. As shown in table 6.4, this is not the case. It is important to note that the B.S. results are not as reliable here than in the ladder approximation case. The results for the B.S. approach given in table 6.4 rely on dispersion relations for calculating the crossed-boson exchange contribution [58]. As argued at the end of section 5.4, we suspect the dispersion relation approach to the Bethe-Salpeter equation to overestimate the binding energy of a two-body system. This means that binding energies reported in table 6.4 for the Bethe-Salpeter equation have to be considered upper limits of the exact results, which is consistent with the fact that the energy-dependent potential gives smaller values in all cases.

This conclusion is supported by independent calculations of the crossed-box diagram[1]. Exact results for the Bethe-Salpeter equation with the crossed box included as communicated by Daniel Phillips give for instance a value of 0.08 for the binding energy in the case $\mu = 0.15$, $\alpha = 1$ in the neutral boson model. This is very close to the corresponding result of $V^{nr}_{eff,sc}$ and slightly larger than the one from V_E. Extrapolating the remaining results of our dispersion relation approach in this way, we indeed end up with a picture very similar to the ladder approximation. All the arguments as discussed in the last section equally apply in the present case, in particular as regarding the contribution of Z-type and higher-order

[1] J.A. Tjon, I.A. Afnan, D. Phillips: private communication

diagrams in establishing the equivalence of the V_E and $V^{nr}_{eff,sc}$ approaches.

The reason for the failure of the dispersion relation approach may be partly due to the possible proximity of a situation where the binding energy would rapidly increase while the coupling approaches a critical value. More probably, it seems that the dispersion-relation approach does not take fully into account the renormalization effects that V_E and $V^{nr}_{eff,sc}$ implicitly incorporate.

Furthermore, we recall the effect of the infra-red divergence of the crossed-box diagram. This was discussed in the last chapter, the present results allow for a somewhat more quantitative estimate of the effect. Comparing the B.S. and V_E results in the neutral boson case for the same coupling constant $\alpha = 1$ but different boson masses, we find that they both differ by about the same factor of 5. For the charged boson case we do not have results at the same coupling constant, however, corresponding numbers for $\alpha = 0.7$, $\mu = 0.15$ and $\alpha = 0.9$, $\mu = 0.5$ give rather similar ratios of 9 and 13, respectively. This indicates that the influence of the infra-red divergence is probably not the reason of the over-binding in the dispersion relation approach.

What remains as a possible explanation are the the off-mass shell effects that were neglected in the determination of the spectral function in the dispersion relation for the box diagram. Taking $p_i^2 \neq m_i^2$ in eq. (5.4-1) would require a much more complicated analysis, with a careful discussion of anomalous thresholds, whose outcome, in particular with respect to the applicability of the resulting expressions, is not clear.

In summary we can say that the consideration of crossed-boson exchange does not modify the general conclusions drawn from the ladder results. A careful discussion of results however demands a much more detailed analysis and special attention as for the source of certain properties. What one can learn in any case is the very restricted validity range of the instantaneous approximation, which becomes strikingly clear by the consideration of charged-boson exchange.

From our results it must be concluded that the apparent success of the instantaneous approximation in the neutral boson case is largely misleading. The reason is that retardation corrections to the propagators cancel exactly the contribution of crossed diagrams in this particular case, but this is not generally true [111]. This property is hardly mentioned in the literature especially in the field of hadronic physics, where the instantaneous approximation is often justified by its success in QED. As we have shown, this success is misleading as it supposes that the retardation effect and the crossed-boson exchange contribution largely cancel each other. Employing the instantaneous approximation in hadronic physics without any regard to the charge or spin of the exchanged boson, is therefore inappropriate. This has to be kept in mind if one intends to apply this approximation to more realistic models, in particular involving pion or gluon exchange, even if in practice, one may hope to remedy this shortcoming by the fitting of certain model parameters, as done in any realistic potential model.

6.3 Abnormal Solutions

We have discussed at some length already that the covariant Bethe-Salpeter equation admits not only ordinary (so called normal), but also abnormal solutions that have no non-relativistic analogue[1]. Such solutions were first discovered and discussed in the framework of the Wick-Cutkosky model where it became clear that they are related to excitations of the relative-time (or, in momentum space, relative-energy) degree of freedom. It also turned out that the norm of these solutions is proportional to the relative-time parity of the Bethe-Salpeter amplitude, which can be both positive or negative [30,31]. This makes a quantum-mechanical (probabilistic) interpretation of the Bethe-Salpeter amplitude problematic.

These difficulties usually provide sufficient motivation (apart from technical simplicity) to consider a three-dimensional reduction of the Bethe-Salpeter equation. In these so-called quasi-potential approaches, the wave functions do not present the negative-norm problem as they are defined as the equal-time Bethe-Salpeter amplitude. Amplitudes which are odd with respect to the relative time can not survive in the equal-time limit. However, there are also abnormal solutions which are even functions of relative time, so one might expect them to show up in the quasi-potential approach as well.

[1] To be exact: They have no weak-coupling limit, see discussion on page 108.

Furthermore, eliminating the original relative-time degree of freedom immediately raises the question whether an essential dynamical ingredient is lost in this step and if yes, how to recover it. The main motivation of the work presented in the last section and in ref. [74] came from the conviction that the dynamics involving the relative time can indeed be accounted for in a non-relativistic scheme. If this is the case, also excited states should be well described in an effective approach. This is why we put some emphasis on the simultaneous description of ground and excited states when we presented results in the last section. Being excitations in the fourth dimension, it is difficult to imagine describing abnormal states in a three-dimensional formalism. It was noted however [141, 142] that just this may be achieved by an energy-dependent potential.

The essential feature in this context is the dependence of the quasi-potential on the total energy of the system, even if the kernel of the original Bethe-Salpeter equation did not depend on it, like in ladder approximation. Excitations of the relative-time degree of freedom are thereby transformed into the energy dependence of the quasi-potential, so one again may expect some "extra" solutions to show up even in a three-dimensional formalism.

The existence of such "extra" solutions (i.e. solutions that do not have an analogue when the energy dependence in the potential is neglected) of the Schrödinger equation was analytically demonstrated in ref. [143]. The authors considered the equivalent of eq. (6.2-6) for the zero-mass boson case ($\mu = 0$):

$$\left(\frac{\vec{p}^{\,2}}{m} + E\right)\Psi(\vec{p}) = \frac{\alpha}{2\pi^2}\int d\vec{q}\,\frac{\Psi(\vec{q})}{|\vec{p}-\vec{q}|(E+|\vec{p}-\vec{q}\,|)}, \tag{6.3-1}$$

where $\alpha = e^2/4\pi$ is the fine structure constant and $E > 0$ is the binding energy. Neglecting the energy dependence in the denominator under the integral, as usually done, we recover the familiar non-relativistic Coulomb problem. Keeping the energy dependence, this equation was then analyzed in coordinate space:

$$\left(\frac{\Delta}{m} - E\right)\Psi(\vec{r}) = V_E(r)\Psi(\vec{r}), \tag{6.3-2}$$

where

$$V_E(r) = -\frac{2\alpha}{\pi}\frac{f(Er)}{r}, \tag{6.3-3}$$

and

$$f(x) = \mathrm{Ci}(x)\sin(x) - \mathrm{si}(x)\cos(x). \tag{6.3-4}$$

Here $\mathrm{si}(x) = \mathrm{Si}(x) - \pi/2$, and $\mathrm{Si}(x)$ and $\mathrm{Ci}(x)$ are the integral sine and cosine functions, respectively [144]. In spite of the occurrence of trigonometric functions, $f(x)$ is monotonically decreasing and non-negative. From its known asymptotics, it was found that for $E > 0$, the potential (6.3-3) behaves like:

$$V_E(r)\big|_{Er\ll 1} \sim -\frac{\alpha}{r}\left[1 + \frac{2}{\pi}Er\log(Er) + \frac{2}{\pi}(\gamma - 1)Er\right], \tag{6.3-5}$$

$$V_E(r)\big|_{Er\gg 1} \sim -\frac{2\alpha}{\pi E}\frac{1}{r^2}, \tag{6.3-6}$$

where $\gamma = 0.5772\ldots$ is the Euler constant. When $E = 0$ we have a pure Coulomb potential:

$$V_{E=0}(r) = -\frac{\alpha}{r}. \tag{6.3-7}$$

We see that the asymptotic behaviour of the potential at infinity differs from the Coulomb one if we preserve the energy dependence in the potential. The question now arises whether there appear "extra" solutions of the Schrödinger equation because of this difference. Let us therefore study the asymptotic solution of the radial Schrödinger equation for the case where only the term of eq. (6.3-6) is kept in the potential [145]. With the Ansatz $\Psi(\vec{r}) = (\chi(r)/r)\,Y_l^m(\hat{r})$ we get for $Er \gg 1$:

$$\chi''(r) - \left[\kappa^2 - \frac{\gamma(E)}{r^2}\right]\chi(r) = 0, \qquad Er \gg 1, \tag{6.3-8}$$

where

$$\kappa^2 = mE, \qquad \gamma(E) = 2\alpha m/\pi E - l(l+1). \tag{6.3-9}$$

The general solution of this equation with the appropriate behaviour at infinity involves a modified Bessel function:

$$\chi(r) = \sqrt{r}\, K_{\sqrt{\frac{1}{4}-\gamma(E)}}(\kappa r), \qquad Er \gg 1. \tag{6.3-10}$$

The function $K_\nu(z)$ has zeros on the real axis only for imaginary indices ν. So there are the following possibilities:

- $\gamma(E) < 1/4$: The function $\chi(r)$ has no zeros, so the Schrödinger equation with the potential (6.3-3) has no additional solutions apart from the ones implied by the short-range part of the potential.
- $\gamma(E) > 1/4$: The index of the Bessel function in eq. (6.3-10) is imaginary and the solution $\chi(r)$ has an infinite number of zeros, i.e. there may occur an infinite number of additional discrete levels.

According to the second case, the additional discrete levels may arise only for

$$\frac{2\alpha m}{\pi E} > \frac{1}{4} + l(l+1) \qquad \text{or} \qquad \alpha > \frac{\pi E}{8m} + l(l+1)\frac{\pi E}{2m}. \tag{6.3-11}$$

At first sight it seems that this condition can be satisfied for usual values of $\alpha \approx 1/137$. However, a careful examination of the zeros of the function $K_\nu(z)$ reveals the opposite situation.

Here our reasoning will differ from the one presented in ref. [143], where it was argued that the function $K_\nu(z)$ for imaginary ν has an infinite number of zeros for $z \to \infty$. In fig. 6.7 we give an example of such a function for the case $\nu = i$ which was calculated numerically using the relation [144]

$$K_{i\nu}(z) = \int_0^\infty e^{-z\,\cosh t} \cos(\nu t)\, dt, \quad \mathrm{Re}\, z > 0. \tag{6.3-12}$$

We see that contrary to the claim in ref. [143], the function $K_i(z)$ has its infinity of zeros around the origin and falls exponentially for large z. This may be seen more clearly from the asymptotic solution of eq. (6.3-8) for the case $r \ll 1$, where we get $\chi \sim \sqrt{r}\cos\left(\sqrt{\gamma(E) - 1/4}\log(r/r_0) + const.\right)$ as a solution, while for $r \gg 1$ we have of course $\chi \sim \exp(-\kappa r)$. Obviously there is one largest zero of the function $K_{i\nu}(z)$ and it can be shown [146] that it lies in the region $z < \nu$.

For real ν and z, let us write for brevity $w = K_{i\nu}(z)$ and denote the largest zeros of w, w' and w'' by z_0, z_0' and z_0'', respectively. From the asymptotic form of w (see fig. 6.7) it is clear that $z_0 < z_0' < z_0''$. If we now take $z = z_0''$ in the differential equation satisfied by w,

$$z\frac{\partial}{\partial z}\left(z\, w'\right) = \left(z^2 - \nu^2\right) w, \tag{6.3-13}$$

we obtain $z_0''\, w'(z_0'') = \left(z_0''^2 - \nu^2\right)\, w(z_0'')$. Thus, from the fact that $w'(z_0'')$ is negative while $w(z_0'')$ is positive, we deduce that $z_0'' < \nu$ and hence from the above relation $z_0 < \nu$.

If the asymptotic solution of eq. (6.3-10) is to lead to an additional eigenstate of the Schrödinger equation, we must demand at least one of the zeros to lie in the asymptotic region $Er \gg 1$. Together with the above relation we then have the following conditions for the occurrence of "extra" solutions of the Schrödinger equation with an energy-dependent potential:

$$\kappa r = \sqrt{mE}\, r = \sqrt{\frac{m}{E}}\, Er \gg \sqrt{\frac{m}{E}} \qquad \text{and} \qquad \kappa r < \sqrt{\gamma(E) - \frac{1}{4}}, \tag{6.3-14}$$

or equivalently

$$\alpha \gg \frac{\pi}{2} + \frac{\pi E}{2m}\left[\frac{1}{4} + l(l+1)\right]. \tag{6.3-15}$$

We note in particular, that for vanishing binding energy, $E \to 0$, the coupling constant is bounded from below by a finite, non-zero value. Therefore, the additional solutions, if they exist, do not have a weak-coupling limit, since the coupling constant does not vanish when the binding energy goes to zero.

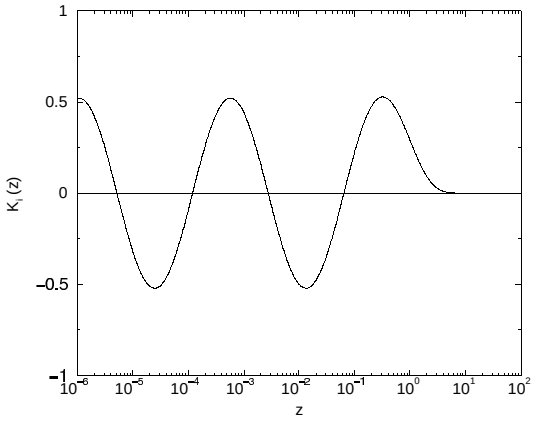

Figure 6.7: Modified Bessel function $K_\nu(z)$ with imaginary index $\nu = i$.

This is a complete analogy to the Wick-Cutkosky model, where the corresponding relation was given by $\alpha = \pi\lambda \to \pi/4$ for vanishing binding energy[1].

Thus, the asymptotic behaviour of the Schrödinger equation with an energy-dependent potential indicates the existence of additional, discrete levels apart from the Coulombic ones. They occur however only at large values of the coupling constant α, i.e. in a region where the single-photon (ladder) approximation is certainly not justified anymore.

The formal similarity of these extra solutions to the abnormal solutions of the Bethe-Salpeter equation is obvious. The essential observation is that when we neglect the energy-dependence in a quasi-potential, the asymptotic behaviour of the potential changes discontinuously and the abnormal solutions disappear. Their existence is therefore a consequence of off-energy-shell effects.

Summing up, we can say that it seems possible to account for abnormal states even in a three-dimensional formalism. Unfortunately, neither of the effective interaction potentials that were used earlier, eq. (6.2-10) and eq. (6.2-14), even though they are supposed to account for a part of the energy dependence of the original potential that they were derived from, will be able to produce these supplementary states. The reason is, that they both have the same asymptotic behaviour for large distances in configuration space as the original Coulomb potential, so the argument of ref. [143] does not apply. This shows the non-perturbative nature of these states and the necessity of keeping track of the full energy dependence of the original potential if one wants to account for them. However, from a calculational point of view, it seems to be difficult to identify these solutions numerically, since there is no obvious criterion to distinguish them from normal ones. For that reason and in order to render a comparison meaningful for all approaches considered, we only investigated normal states in this work.

[1] Establishing a definite limit for abnormal solutions for $E \to 0$, in particular regarding the difference with the value $\pi/2$ in eq. (6.3-15), demands certainly a more careful analyses of the original equation (6.3-1). It would be very nice to recover the same result as in the relativistic case, this would imply that the Wick-Cutkosky model reduces exactly to the non-relativistic Schrödinger problem, including abnormal solutions (see the discussion on page 108). If there remains a difference, however, we do not expect it to be due to relativistic effects, like the omission of factors m/e in eq. (6.3-15), because, remember, we are looking here at the non-relativistic limit, even if we are in the strong-coupling regime.

Chapter 7

Summary and Discussion

Nun lehrt mich die Erfahrung zwar, was dasei, und wie es sei,
niemals aber daß es notwendiger Weise so und nicht anders sein müsse.

I. Kant, Prolegomena

In the second part of this work, we have contributed to the study of crossed two-boson exchange to the binding energy of a system made of two distinguishable particles in the Bethe-Salpeter equation. For the range of coupling constants where a comparison is possible, the crossed-box contribution accounts for roughly half of the total effect, as compared to the complete non-perturbative results of the FSR approach, the disagreement tending to increase with the coupling. This is consistent with the expectation that the role of multi-boson exchanges not included here should increase similarly. The result is however somewhat disturbing. It implies that the convergence of the Bethe-Salpeter approach in terms of an expansion of the interaction kernel in the coupling constant is likely to be slow. This conclusion was confirmed by estimating the contribution of crossed three-boson exchange diagrams to the interaction kernel. This study also led to the definite conclusion that the dispersion relation approach to calculate Feynman diagrams actually overestimates the binding energy due to off-mass shell effects.

Amazingly, our results, which include crossed two-boson exchange contributions, are close to those obtained with the instantaneous approximation, where these contributions are absent. The specific character of this coincidence was demonstrated by the consideration of a model with "charged" bosons, which leads to a different conclusion, showing that the validity of the instantaneous approximation is limited to the Born approximation.

In the course of our study of abnormal states we were led to investigate form factors (electromagnetic and scalar ones) in the Wick-Cutkosky model. While the results of this investigation did not provide a clear interpretation of these states, it was amazing to note that again, the non-relativistic approach does particularly well even for large momentum transfers and for large couplings. This seems to indicate that the effects under consideration are not necessarily relativistic ones, but a clear interpretation demands a more detailed analysis, which is currently under way.

In a second line of attack we investigated different three-dimensional approaches based on, and derived from the Bethe-Salpeter equation, in particular an equation with an energy-dependent interaction and a non-relativistic equation with an energy-independent, effective interaction. This has been done for the ladder approximation as well as the more complete approach involving crossed-boson exchanges with the idea that approximation schemes should not be limited to one of these cases. Up to departures of relativistic order, we found a strong continuity between the results from different approaches in ladder approximation. The inclusion of crossed-diagram contributions confirmed the earlier conclusion that the way of accounting for higher order diagrams in the Bethe-Salpeter equation via dispersion relations leads to an overestimation of the binding energy in this approach.

The reasons why we are able to account in a non-relativistic approach for results of the Bethe-Salpeter equation in ladder approximation deserve some explanation. The difference between results obtained with the Bethe-Salpeter equation and those using the instantaneous single-boson exchange approximation in a non-relativistic approach is not due to relativity, as sometimes advocated, but to the fact that the

latter misses the field-theory character underlying the former. Since a field-theory can be dealt with in a non-relativistic scheme, it should be no surprise that one is able to get rid of the above difference even in a non-relativistic approach. The so-called instantaneous approximation, often employed to provide some non-relativistic interaction, simply represents a too naïve view of what the interaction in a non-relativistic picture should be, missing many-body effects in its determination.

The main effect of the effective interactions in the small coupling limit is a renormalization of the so-called instantaneous interaction by the probability of having two constituents only without bosons in flight. The improvement we introduced in calculating the effective interaction is quite significant. While we do not attain the same level of agreement as more elaborate calculations in some cases, we believe that the effect is fully relevant. It allows in particular to identify ingredients missing in the effective interaction, especially those in relation with non-locality effects, which are obviously more difficult to incorporate. In any case, our results cast serious doubts on the possibility of reliably describing physical systems in the strong-interaction regime by only retaining one-boson exchange contributions. This could be however partly remedied by fitting parameters of a certain model, as it is done for the NN interaction models.

Results for zero-mass bosons were presented only in ladder approximation due to calculational difficulties in relation with the infra-red divergence of the crossed-box diagram. It is clear that the zero-mass boson case needs to be more elaborated, especially in view of possible applications in QED or QCD. The cancellation between the renormalization of the instantaneous approximation interaction and the effect of the crossed-boson exchange, which is expected in the massive neutral-boson case at order $(1/m)^0$, and has been partly obtained in our calculations, is more difficult to be achieved in the zero-mass case. The reason is that solving a certain integral equation allows one to sum up an infinite set of contributions with increasing order, but also an increasingly divergent character in the infra-red limit. This prevents one from reproducing numerically the above expected cancellation without considering an infinite set of selected crossed-boson exchange terms with similar properties. From present results and further studies performed separately, it is clear that the convergence of the Bethe-Salpeter kernel to the full result is likely to be slow for couplings of the order $\alpha \simeq 1$.

Contrary to a common belief, the dynamics involving the relative time variable can be accounted for partly, if not totally, in a three-dimensional approach, in a way which is not Lorentz-covariant however. We have illustrated in particular, that there do arise also "abnormal" solutions in a three-dimensional approach, if the energy dependence of the potential is taken into account.

All studies presented here have been performed in a model involving scalar particles only. This greatly simplifies the discussion by providing a better insight on the origin of various corrections (renormalization of the instantaneous approximation interaction, relativistic corrections, etc.). In spite of the fact that this system is not an especially realistic one, we nevertheless believe that our conclusions have some general character. The most important one is probably the very limited validity range of the instantaneous one-boson exchange approximation which, strictly speaking, is valid only for small energy transfers and therefore only makes sense for the Born amplitude in the non-relativistic regime. Its apparent success in QED or in hadronic physics is largely misleading. It rather points to large contributions from multi-boson exchanges. In the case of QED, they are required to recover the Coulomb potential, whereas in hadronic physics, they provide a more microscopic description of the forces, most often simulated by instantaneous exchanges of single bosons with fitted parameters.

References for Part II

[1] E. E. Salpeter and H. A. Bethe: Phys. Rev. **84**, 1232 (1951).

[2] M. Gell-Mann and F. Low: Phys. Rev. **84**, 350 (1951).

[3] J. Schwinger: Proc. Nat. Acad. Sci. **37**, 452 (1951).

[4] J. Schwinger: Proc. Nat. Acad. Sci. **37**, 455 (1951).

[5] J. Schwinger: Phys. Rev. **91**, 713 (1953).

[6] G. C. Wick: Phys. Rev. **96**, 1124 (1954).

[7] R. E. Cutkosky: Phys. Rev. **96**, 1135 (1954).

[8] N. Nakanishi: Prog. Theor. Phys. Suppl. **43**, 1 (1969).

[9] M.-T. Noda: Prog. Theor. Phys. Suppl. **95**, 78 (1988).

[10] C. Itzykson and J. B. Zuber: *Quantum Field Theory* (McGraw-Hill, 1985).

[11] F. Gross: *Relativistic Quantum Mechanics and Field Theory* (Wiley Interscience, 1993).

[12] K. Huang: *Quantum Field Theory* (Wiley Interscience, 1998).

[13] N. Nakanishi: Prog. Theor. Phys. Suppl. **95**, 1 (1988).

[14] Z. K. Silagadze: hep-ph/9803307.

[15] V. A. Fock: Z. Phys. **98**, 145 (1935).

[16] S. Ahlig and R. Alkofer: Ann. Phys. **275**, 113 (1999).

[17] C. Schwartz: Phys. Rev. **137**, 717 (1965).

[18] E. zur Linden and H. Mitter: Nuovo Cim. **61B**, 389 (1969).

[19] H. S. Green: Nuovo Cim. **5**, 866 (1957).

[20] G. B. Mainland and L. A. Parson: J. Math. Phys. **32**, 1072 (1991).

[21] G. B. Mainland and J. R. Spence: Few Body Syst. **19**, 109 (1995).

[22] N. Setô: Prog. Theor. Phys. **56**, 919 (1976).

[23] N. Setô: Prog. Theor. Phys. **57**, 1403 (1977).

[24] B. Silvestre-Brac, A. Bilal, C. Gignoux, and P. Schuck: Phys. Rev. **D29**, 2275 (1984).

[25] R. E. Cutkosky and G. C. Wick: Phys. Rev. **101**, 1830 (1956).

[26] D. Kershaw, H. Snodgrass, and C. Zemach: Phys. Rev. **D2**, 2806 (1970).

[27] T. Nieuwenhuis and J. A. Tjon: Few Body Syst. **21**, 167 (1996).

[28] Y. Suzuki and K. Varga: *Stochastic Variational Approach to Quantum-Mechanical Few-Body Problems* (Springer Verlag, 1998).

[29] D. Lurié, A. J. MacFarlane, and Y. Takahashi: Phys. Rev. **140B**, 1091 (1965).

[30] N. Nakanishi: Phys. Rev. **138**, B1182 (1965), [Erratum: Phys. Rev. **139** (1965) B1].

[31] N. Nakanishi: Phys. Rev. **139**, B1401 (1965).

[32] F. Rahoui: Stage Maîtrise, Institut des Sciences Nucléaires, Grenoble, 1999.

[33] C. Alabiso and G. Schierholz: Phys. Rev. **D10**, 960 (1974).

[34] C. Alabiso and G. Schierholz: Phys. Rev. **D11**, 1905 (1975).

[35] S. Singh: Phys. Rev. **D6**, 1648 (1972).

[36] G. Rupp and J. A. Tjon: Phys. Rev. **C41**, 472 (1990).

[37] V. A. Karmanov and A. V. Smirnov: Nucl. Phys. **A546**, 691 (1992).

[38] V. A. Karmanov and A. V. Smirnov: Nucl. Phys. **A575**, 520 (1994).

[39] V. A. Karmanov and J. F. Mathiot: Nucl. Phys. **A602**, 388 (1996).

[40] B. Desplanques and L. Theußl: nucl-th/0102060.

[41] P. A. M. Dirac: Rev. Mod. Phys. **21**, 392 (1949).

[42] W. H. Klink: Phys. Rev. **C58**, 3587 (1998).

[43] T. W. Allen, W. H. Klink, and W. N. Polyzou: Phys. Rev. **C63**, 034002 (2001).

[44] R. F. Wagenbrunn, S. Boffi, W. Klink, W. Plessas, and M. Radici: Phys. Lett. **B511**, 33 (2001).

[45] A. Amghar, B. Desplanques, and V. A. Karmanov: Nucl. Phys. **A567**, 919 (1994).

[46] B. D. Keister: Phys. Rev. **C37**, 1765 (1988).

[47] W. H. Klink: nucl-th/0012033.

[48] B. Desplanques, B. Silvestre-Brac, F. Cano, P. Gonzalez, and S. Noguera: Few Body Syst. **29**, 169 (2000).

[49] I. T. Todorov: Phys. Rev. **D3**, 2351 (1971).

[50] E. Brezin, C. Itzykson, and J. Zinn-Justin: Phys. Rev. **D1**, 2349 (1970).

[51] J. L. Friar: Phys. Rev. **C22**, 796 (1980).

[52] F. Gross: Phys. Rev. **C26**, 2203 (1982).

[53] A. R. Neghabian and W. Glöckle: Can. J. Phys. **61**, 85 (1983).

[54] G. Feldman, T. Fulton, and J. Townsend: Phys. Rev. **D7**, 1814 (1973).

[55] T. Nieuwenhuis and J. A. Tjon: Phys. Rev. Lett. **77**, 814 (1996).

[56] D. R. Phillips and I. R. Afnan: Phys. Rev. **C54**, 1542 (1996).

[57] M. J. Levine and J. Wright: Phys. Rev. **D2**, 2509 (1970).

[58] L. Theußl and B. Desplanques: Few Body Syst. **30**, 5 (2001).

[59] S. Mandelstam: Phys. Rev. **115**, 1741 (1959).

[60] S. Mandelstam: Proc. Roy. Soc. Lond. **A233**, 248 (1955).

[61] R. E. Cutkosky: J. Math. Phys. **1**, 429 (1960).

[62] M. J. Zuilhof and J. A. Tjon: Phys. Rev. **C26**, 1277 (1982).

[63] G. 't Hooft and M. Veltman: Nucl. Phys. **B153**, 365 (1979).

[64] M. Chemtob, J. W. Durso, and D. O. Riska: Nucl. Phys. **B38**, 141 (1972).

[65] A. Amghar and B. Desplanques: Few Body Syst. **28**, 65 (2000).

[66] Yu. A. Simonov and J. A. Tjon: Ann. Phys. **228**, 1 (1993).

[67] Ç. Şavklı, J. A. Tjon, and F. Gross: Phys. Rev. **C60**, 055210 (1999).

[68] R. Blankenbecler and R. Sugar: Phys. Rev. **142**, 1051 (1966).

[69] A. A. Logunov and A. N. Tavkhelidze: Nuovo Cim. **29**, 380 (1963).

[70] E. Hummel and J. A. Tjon: Phys. Rev. **C49**, 21 (1994).

[71] N. K. Devine and S. J. Wallace: Phys. Rev. **C51**, 3222 (1995).

[72] F. Gross: Phys. Rev. **186**, 1448 (1969).

[73] F. Gross: Phys. Rev. **D10**, 223 (1974).

[74] A. Amghar, B. Desplanques, and L. Theußl: nucl-th/0012051, to be published in Nucl. Phys. A.

[75] N. Kaiser: Phys. Rev. **C61**, 014003 (2000).

[76] N. Kaiser: Phys. Rev. **C62**, 024001 (2000).

[77] C. Schwartz: in *Three-Particle Scattering in Quantum Mechanics* (J. Gillespie and J. Nuttal, eds.), W.A. Benjamin, 1968.

[78] E. E. Salpeter: Phys. Rev. **87**, 328 (1952).

[79] N. Setô: Prog. Theor. Phys. Suppl. **95**, 25 (1988).

[80] L. G. Suttorp: Nuovo Cim. **A29**, 225 (1975).

[81] L. G. Suttorp: Ann. Phys. **113**, 257 (1978).

[82] I. Fukui and N. Setô: Prog. Theor. Phys. **65**, 1026 (1981).

[83] N. Setô: Prog. Theor. Phys. **64**, 1026 (1980).

[84] G. Rupp and J. A. Tjon: Phys. Rev. **C45**, 2133 (1992).

[85] G. Rupp and J. A. Tjon: Phys. Rev. **C37**, 1729 (1988).

[86] F. Sammarruca, D. P. Xu, and R. Machleidt: Phys. Rev. **C46**, 1636 (1992).

[87] J. L. Forest, V. R. Pandharipande, and J. L. Friar: Phys. Rev. **C52**, 568 (1995).

[88] M. Oettel: Dissertation, Eberhard-Karls-Universität, Tübingen, 2000, nucl-th/0012067.

[89] J. Bijtebier: J. Phys. **G26**, 871 (2000).

[90] A. N. Mitra: Int. J. Mod. Phys. **A14**, 4781 (1999).

[91] A. N. Mitra and A. Mittal: Phys. Rev. **D29**, 1399 (1984).

[92] D. S. Kulshreshtha and A. N. Mitra: Phys. Rev. **D37**, 1268 (1988).

[93] J.G. Taylor: Phys. Rev. **150**, 1321 (1966).

[94] J. Carbonell, B. Desplanques, V. A. Karmanov, and J. F. Mathiot: Phys. Rept. **300**, 215 (1998).

[95] J. P. B. C. de Melo, A. E. A. Amorim, L. Tomio, and T. Frederico: J. Phys. **G27**, 1031 (2001).

[96] P. Dulany and S. J. Wallace: Phys. Rev. **C56**, 2992 (1997).

[97] F. Gross: Phys. Rev. **C26**, 2226 (1982).

[98] E. van Faassen and J. A. Tjon: Phys. Rev. **C33**, 2105 (1986).

[99] A. N. Kvinikhidze and B. Blankleider: Nucl. Phys. **A574**, 788 (1994).

[100] J. Bijtebier and J. Broekaert: J. Phys. **G22**, 559 (1996).

[101] J. Bijtebier and J. Broekaert: J. Phys. **G22**, 1727 (1996).

[102] J. W. Darewych: Can. J. Phys. **76**, 523 (1998).

[103] B. Ding and J. Darewych: J. Phys. **G26**, 907 (2000).

[104] A. Bilal and P. Schuck: Phys. Rev. **D31**, 2045 (1985).

[105] N. Fukuda, K. Sawada, and M. Taketani: Prog. Theor. Phys. **12**, 156 (1954).

[106] S. Ôkubo: Prog. Theor. Phys. **12**, 603 (1954).

[107] M. Sugawara and S. Ôkubo: Phys. Rev. **117**, 605 (1960).

[108] R. K. Bhaduri and M. Brack: Phys. Rev. **D25**, 1443 (1982).

[109] G. P. Lepage: nucl-th/9706029.

[110] W. E. Caswell and G. P. Lepage: Phys. Rev. **A18**, 810 (1978).

[111] W. E. Caswell and G. P. Lepage: Phys. Lett. **B167**, 437 (1986).

[112] S. S. Schweber: Ann. Phys. **20**, 61 (1962).

[113] F. Calogero and G. Jagannathan: Nuovo Cim. **47**, 178 (1967).

[114] J. L. Friar: Ann. Phys. **81**, 332 (1973).

[115] J. L. Friar: Phys. Rev. **C10**, 955 (1974).

[116] J. L. Friar: Nucl. Phys. **A264**, 455 (1976).

[117] B. Desplanques: Phys. Lett. **B203**, 200 (1988).

[118] A. Klein: Phys. Rev. **90**, 1101 (1953).

[119] R. Machleidt, K. Holinde, and C. Elster: Phys. Rept. **149**, 1 (1987).

[120] B. Desplanques: in *Trends in Nuclear Physics, 100 Years Later. Les Houches Lectures 1996* (H. Nifenecker, J.-P. Blaizot, G. F. Bertsch, W. Weise, and F. David, eds.), North Holland, 1998.

[121] F. G. Perey and D. S. Saxon: Phys. Lett. **10**, 107 (1964).

[122] L. L. Foldy and S. A. Wouthuysen: Phys. Rev. **78**, 29 (1950).

[123] A. D. Lahiff and I. R. Afnan: Phys. Rev. **C56**, 2387 (1997).

[124] A. D. Lahiff and I. R. Afnan: Phys. Rev. **C60**, 024608 (1999).

[125] P. Ring and P. Schuck: *The Nuclear Many-Body Problem* (Springer Verlag, 1980).

[126] C. Mahaux, P. F. Bortignon, R. A. Broglia, and C. H. Dasso: Phys. Rept. **120**, 1 (1985).

[127] M. Lacombe *et al.*: Phys. Rev. **C21**, 861 (1980).

[128] E. Moulin and N. Ploquin: Stage Maîtrise, Institut des Sciences Nucléaires, Grenoble, 2000.

[129] Ch. Elster, E. E. Evans, H. Kamada, and W. Glöckle: Few-Body Syst. **21**, 25 (1996).

[130] V. G. Kadyshevsky: Nucl. Phys. **B6**, 125 (1968).

[131] V. Pascalutsa and J. A. Tjon: Phys. Lett. **B435**, 245 (1998).

[132] D. R. Phillips and S. J. Wallace: Phys. Rev. **C54**, 507 (1996).

[133] D. R. Phillips and S. J. Wallace: Few Body Syst. **24**, 175 (1998).

[134] M. Chemtob: in *Mesons in Nuclei* (M. Rho and D. Wilkinson, eds.), North-Holland, 1979.

[135] J. H. O. Sales, T. Frederico, B. V. Carlson, and P. U. Sauer: Phys. Rev. **C61**, 044003 (2000).

[136] B. Baumgartner, H. Grosse, and A. Martin: Phys. Lett. **B146**, 363 (1984).

[137] B. Baumgartner, H. Grosse, and A. Martin: Nucl. Phys. **B254**, 528 (1985).

[138] C.-R. Ji and R. J. Furnstahl: Phys. Lett. **B167**, 11 (1986).

[139] C.-R. Ji: Phys. Lett. **B167**, 16 (1986).

[140] M. Mangin-Brinet and J. Carbonell: Phys. Lett. **B474**, 237 (2000).

[141] J. Bijtebier and J. Broekaert: Nuovo Cim. **107A**, 1275 (1994).

[142] J. Bijtebier: Nucl. Phys. **A623**, 498 (1997).

[143] A. A. Khelashvili, G. A. Khelashvili, N. Kiknadze, and T. P. Nadareishvili: quant-ph/9907078.

[144] M. Abramowitz and I. A. Stegun, (eds.): *Handbook of Mathematical Functions* (Dover, 1965).

[145] L. D. Landau and E. M. Lifshitz: *Quantum Mechanics* (Pergamon Press, 1958).

[146] G. N. Watson: *A Treatise on the Theory of Bessel Functions* (Cambridge University Press, 1966).

Chapter 8

Conclusion

Regardez le ciel. Demandez-vous : Le mouton oui ou non a-t-il mangé la fleur ?
Et vous verrez comme tout change ...
Et aucune grande personne ne comprendra jamais que ça a tellement d'importance !
A. de Saint-Exupéry, Le Petit Prince

Dans ce travail nous avons étudié quelques sujets spécifiques qui sont en relation avec la description des systèmes en interaction forte. Plus particulièrement, nous avons tenté d'illustrer le long chemin qui sépare l'approche aux états liés basée sur la théorie des champs de la description des hadrons physiques, tels que les résonances baryoniques. Les difficultés conceptuelles et techniques que l'on rencontre généralement dans les approches "fondamentales" sont souvent des raisons suffisantes pour se contenter des modèles phénoménologiques de la structure hadronique, le plus populaire étant le modèle des quarks constituants. De tels modèles sont utiles pour l'interprétation des résultats des analyses en ondes partielles, qui sont habituellement employées pour extraire les propriétés des résonances nucléoniques à partir des données expérimentales de la diffusion pion-nucléon.

Dans la première partie de cette thèse, nous avons traité essentiellement de quelques sujets théoriques et expérimentaux qui sont pertinents dans ce domaine. En particulier, nous avons contribué à la recherche actuelle sur l'interaction entre quarks constituants, ce qui est un sujet de discussion très à la mode. Nous avons concentré nos recherches sur la description théorique des désintégrations π et η des résonances N et Δ dans le contexte des différents modèles des quarks constituants.

En premier lieu, nous nous sommes intéressés aux prédictions du modèle spécifique des quarks constituants dont l'interaction hyperfine est basée sur la dynamique de l'échange des bosons de Goldstone. Nous avons également étudié les résultats relatifs aux prédictions d'un modèle plus traditionel basé sur l'échange d'un gluon et nous avons établi une comparaison détaillée avec la base de données expérimentales.

De plus, nous avons étudié les différences qui existent entre des descriptions semi-relativistes et non-relativistes des états des baryons pour les deux types de modèles, où 'semi-relativiste' signifie que seulement la forme relativiste de l'opérateur d'énergie cinétique a été utilisée, mais que les corrections relativistes dans la dynamique ont été négligées. Dans une seconde étape, nous avons étudié l'influence de la force tenseur dans l'interaction GBE sur la prédiction des largeurs de désintégration.

En ce qui concerne le mécanisme de désintégration, nous avons utilisé deux modèles différents: le modèle d'émission élémentaire, où le méson émis est considéré comme n'ayant aucune structure interne; et une version modifiée du modèle populaire $^3P_0$, où la désintégration a lieu au travers de la création d'une paire $q\bar{q}$ à partir du vide.

Au vu des résultats obtenus dans notre étude, il est difficile de tirer des conclusions définitives sur la qualité relative des fonctions d'ondes provenant des différents modèles de quarks constituants.

A ce stade de la recherche, nous retrouvons un certain nombre de propriétés qualitatives qui ont déjà été observées dans d'autres recherches. L'introduction seule d'une cinématique semi-relativiste n'est pas à l'évidence suffisante pour reproduire les propriétés globales des observables dynamiques et ne représente même pas une amélioration par rapport au traitement non-relativiste. Dans tous les cas, notre étude

révèle que la description des désintégrations fortes des résonances baryoniques dans le cadre de modèles de quarks constituants n'est pas encore complètement satisfaisante. Les effets de la force tenseur sont importants seulement dans quelques cas où le mélange des configurations n'est pas négligeable. La raison de la mauvaise description des désintégrations hadroniques est probablement due au poids des composants à hautes impulsions dans la fonction d'onde, ou, de la même manière, à la petite taille des baryons. Cela est également suggéré par les résultats quelque peu meilleurs obtenus par les paramétrisations non relativistes, qui donnent des fonctions d'ondes baryoniques légèrement plus étendues. D'autre part, il est évident que les modèles de désintégrations fortes ne sont pas sans défaut puisqu'ils sont principalement déduits d'une façon intuitive. Aucune tentative d'amélioration de ces approches semi-phénoménologiques n'a apporté jusqu'à présent le succès escompté. Une description microscopique cohérente des processus de désintégrations fortes dans le cadre des modèles de quarks constituants reste ainsi une tâche considérable, dont la difficulté principale est due à la nature non-perturbative et relativiste du problème. Bien évidemment, le but ultime serait d'arriver à une description unifiée des spectres des résonances et des transitions hadroniques, ainsi que des transitions électromagnétiques, dans le cadre du même schéma dynamique.

Dans la seconde partie de notre étude nous avons contribué à la recherche sur le rôle de l'échange de deux bosons croisés pour l'énergie de liaison d'un système composé de deux particules discernables dans l'équation de Bethe-Salpeter. Pour des valeurs de la constante de couplage permettant une comparaison, la contribution de la boîte croisée contribue à peu près pour la moitié de l'effet total, par rapport aux résultats de l'approche Feynman-Schwinger. Les désaccords augmentent avec le couplage, ce qui nous conforte dans l'idée que le rôle des échanges multi-bosons non inclus ici devrait augmenter de façon similaire. L'estimation de la contribution des diagrammes d'échange de trois bosons croisés au noyau d'interaction nous a amené à la conclusion, que l'approche avec relations de dispersion pour calculer des diagrammes de Feynman surestime effectivement l'énergie de liaison à cause des effets hors couches. Ce résultat est cependant quelque peu inquiètant en ce qui concerne des applications possibles, car il implique que la convergence du noyau d'interaction de Bethe-Salpeter en terme d'un développement dans la constante de couplage sera probablement très lent. Il est surprenant de constater que nos résultats qui incluent des contributions de l'échange de deux bosons croisés sont proches de ceux obtenus avec l'approximation instantanée, où ces contributions sont absentes.

Le caractère spécial de cette coïncidence a été démontré en étudiant un modèle avec des bosons chargés, ce qui a amené à des conclusions différentes, qui démontre que la validité de l'approximation instantanée est limitée à l'approximation de Born.

Au cours de notre étude des états anormaux nous avons été amené à évaluer les facteurs de forme (électromagnétiques ainsi que scalaires) dans le modèle de Wick-Cutkosky. Bien que les résultats de cette recherche n'aient pas pu fournir une interprétation précise de ces états, il était surprenant de constater que une fois encore, l'approche non relativiste fonctionne particulièrement bien, même pour des transferts d'impulsion assez élevés et pour des couplages assez forts. Cela semble indiquer que les effets considérés ne sont pas nécessairement des effets relativistes, mais une interprétation plus précise éxigerait une analyse plus détaillée, étude qui est actuellement en cours.

Dans une seconde étape, nous avons étudié différentes approches tri-dimensionelles, qui proviennent de l'équation de Bethe-Salpeter dans une réduction non relativiste, en particulier une équation avec une interaction dépendant de l'énergie et une équation non relativiste avec une interaction effective qui n'en dépend pas.

Cela a été accompli dans l'approximation en échelle, mais aussi pour le cas plus complet qui inclut des échanges de bosons croisés, avec l'idée qu'un certain schéma d'approximation ne doit pas être limité à un seul cas. A l'exception des effets d'ordre relativiste nous avons trouvé une forte continuité entre les résultats des différentes approches dans l'approximation en échelle. L'inclusion des diagrammes croisés a comfirmé la conclusion précédente que l'estimation des diagrammes d'ordre plus élevé dans l'équation de Bethe-Salpeter en utilisant des relations de dispersion conduit à une surestimation de l'énergie de liaison dans cette approche.

Les raisons pour lesquelles nous pouvons reproduire des résultats de l'équation de Bethe-Salpeter dans une approche non-relativiste méritent une explication. Les différences entre les résultats obtenus avec l'équation de Bethe-Salpeter et ceux utilisants l'approximation instantanée dans une approche non relativiste ne sont pas dues à la relativité, comme il est parfois affirmé, mais au fait que cette dernière n'inclut

pas le caractère "théorie des champs" qui est à la base de l'approche de Bethe-Salpeter. Puisqu'il est possible de traiter une théorie des champs dans un schéma non relativiste cela n'est pas une surprise que l'on puisse éliminer les différences ci-dessus mentionnées même dans le cadre d'une approche non relativiste. L'approximation instantanée, souvent employée pour fournir une interaction non relativiste représente simplement une vue trop naïve de ce que l'interaction devrait être dans un schéma non relativiste, en particulier en ce qui concerne les "effets à plusieurs corps" dans sa détermination.

Des résultats pour le cas d'un boson avec masse nulle ont été présentés seulement dans l'approximation en échelle à cause de difficultés de calcul en relation avec la divergence infra-rouge du diagramme croisé. Il est évident que le cas d'un boson de masse zéro a besoin d'être plus élaboré, spécialement en vue des applications possibles dans la QED ou QCD.

Contrairement à l'opinion générale, la dynamique de la variable du temps relatif peut être pris en compte partiellement, si ce n'est totalement, dans une approche tri-dimensionelle, qui n'est pas, cependant, invariante de Lorentz. En particulier, nous avons illustré par un exemple spécifique, qu'il émerge aussi des solutions anormales dans une approche tri-dimensionelle si la dépendance en énergie du potentiel est proprement prise en compte.

Toutes les recherches, dont les résultats sont présentés dans la seconde partie de ce travail, ont été réalisées dans le cadre d'un modèle qui ne contient que des particules scalaires. Cela simplifie la discussion en permettant une meilleure vue sur l'origine des diverses corrections (renormalisation de l'interaction instantanée, corrections relativistes, etc.). Bien que ce système ne soit pas particulièrement réaliste, nous pensons néanmoins que nos conclusions possèdent un caractère général. Le plus important est probablement le domaine de validité très limité de l'approximation instantanée qui est au sens strict valide uniquement pour des faibles transferts d'énergie et qui n'a de sens que pour l'amplitude de Born dans un régime non relativiste. Son succès apparent en QED ou en physique hadronique est en grande partie trompeur et indique plutôt des contributions importantes des diagrammes croisés. Dans le cadre de la QED ces échanges croisés sont nécessaires pour retrouver le potentiel de Coulomb, tandis qu'en physique hadronique ils fournissent une description plus microscopique des forces qui sont le plus souvent simulées par l'échange instantané d'un seul boson avec des paramètres ajustés.

En conclusion, nous constatons que le travail présenté ici reste largement à faire dans le régime à couplages forts, particulièrement en ce qui concerne les difficultés rencontrées dans la première partie, où les interactions effectives ont été obtenues à partir de l'échange instantané des gluons ou des bosons de Goldstone. Bien qu'il semble difficile de généraliser au problème à trois corps les méthodes d'obtention des interactions effectives qui ne dependent pas d'énergie, il est évident qu'on a besoin d'un traitement plus microscopique de la dynamique pour décrire la physique des baryons et des mésons d'une façon satisfaisante.

Bibliography

This is a collection of all the references cited in this work, including titles and eventual e-print numbers. The items are ordered alphabetically by the author's name(s).

[AA99] S. Ahlig and R. Alkofer: *(In-)consistencies in the relativistic description of excited states in the Bethe-Salpeter equation*, Ann. Phys. **275** (1999), 113–147, (hep-th/9810241).

[ABS96] E. S. Ackleh, T. Barnes, and E. S. Swanson: *On the mechanism of open-flavor strong decays*, Phys. Rev. **D54** (1996), 6811–6829, (hep-ph/9604355).

[AD00] A. Amghar and B. Desplanques: *Relationship of field-theory based single-boson-exchange potentials to static ones*, Few Body Syst. **28** (2000), 65–101, (nucl-th/9910001).

[ADK94] A. Amghar, B. Desplanques, and V. A. Karmanov: *The deuteron electrodisintegration near threshold in the light front dynamics*, Nucl. Phys. **A567** (1994), 919–936.

[ADT00] A. Amghar, B. Desplanques, and L. Theußl: *From the Bethe-Salpeter equation to non-relativistic approaches with effective two-body interactions*, nucl-th/0012051, to be published in Nucl. Phys. A.

[AF+52] H. L. Anderson, E. Fermi, E. A. Long, and D. E. Nagle: *Total cross sections of positive pions in hydrogen*, Phys. Rev. **85** (1952), 936.

[AG+98] R. A. Arndt, A. M. Green, R. L. Workman, and S. Wycech: *The energies and residues of the nucleon resonances N(1535) and N(1650)*, Phys. Rev. **C58** (1998), 3636–3640, (nucl-th/9807009).

[AKP01] T. W. Allen, W. H. Klink, and W. N. Polyzou: *Point-form analysis of elastic deuteron form factors*, Phys. Rev. **C63** (2001), 034002, (nucl-th/0005050).

[AO+97] R. A. Arndt, C. H. Oh, I. I. Strakovsky, R. L. Workman, and F. Dohrmann: *Nucleon-nucleon elastic scattering analysis to 2.5 GeV*, Phys. Rev. **C56** (1997), 3005–3013, (nucl-th/9706003).

[AS65] M. Abramowitz and I. A. Stegun (eds.): *Handbook of Mathematical Functions*, Dover, 1965.

[AS74] C. Alabiso and G. Schierholz: *Asymptotic behavior of form factors for two- and three-body bound states*, Phys. Rev. **D10** (1974), 960–967.

[AS75] C. Alabiso and G. Schierholz: *Asymptotic behavior of form factors for two- and three-body bound states. II. Spin-$\frac{1}{2}$ constituents*, Phys. Rev. **D11** (1975), 1905–1914.

[AS+95] R. A. Arndt, I. I. Strakovsky, R. L. Workman, and M. M. Pavan: *Updated analysis of πN elastic scattering data to 2.1 GeV: The baryon spectrum*, Phys. Rev. **C52** (1995), 2120–2130, (nucl-th/9505040).

[ASW97] R. A. Arndt, I. I. Strakovsky, and R. L. Workman: *Pion photoproduction in the Δ resonance region*, Phys. Rev. **C56** (1997), 577–578, (nucl-th/9702039).

[ASW00] R. A. Arndt, I. I. Strakovsky, and R. L. Workman: *Nucleon-nucleon elastic scattering to 3 GeV*, Phys. Rev. **C62** (2000), 034005, (nucl-th/0004039).

[B+96] R. M. Barnett et al.: *Review of particle physics. Particle Data Group*, Phys. Rev. **D54** (1996), 1–720.

[Bar69] M. V. Barnhill: *Ambiguity of the "Galilean-invariant" operator for pion absorption by nuclei*, Nucl. Phys. **A131** (1969), 106–112.

[BB70] D. Basu and S. N. Biswas: *O(5) harmonics and abnormal solutions in the Bethe-Salpeter equation*, J. Math. Phys. **11** (1970), 1204–1209.

[BB82] R. K. Bhaduri and M. Brack: *Schrödinger versus Dirac equation for a massless quark*, Phys. Rev. **D25** (1982), 1443–1446.

[BB84] M. C. Birse and M. K. Banerjee: *A chiral soliton model of nucleon and delta*, Phys. Lett. **B136** (1984), 284–288.

[BB85] M. C. Birse and M. K. Banerjee: *Chiral model for nucleon and delta*, Phys. Rev. **D31** (1985), 118–127.

[BB94] J. Bijtebier and J. Broekaert: *What happens with the relative time excitations after a three-dimensional reduction of the Bethe-Salpeter equation?*, Nuovo Cim. **107A** (1994), 1275–1292.

[BB96a] J. Bijtebier and J. Broekaert: *On the three-dimensional reductions of the Bethe-Salpeter equation and their one-body limits (two-fermion case)*, J. Phys. **G22** (1996), 559–578.

[BB96b] J. Bijtebier and J. Broekaert: *On the three-dimensional reductions of the Bethe-Salpeter equation and their one-body limits (two-boson and boson - fermion cases)*, J. Phys. **G22** (1996), 1727–1740.

[BCN80] R. K. Bhaduri, L. E. Cohler, and Y. Nogami: *Quark-quark interaction and the nonrelativistic quark model*, Phys. Rev. Lett. **44** (1980), 1369–1372.

[BCN81] R. K. Bhaduri, L. E. Cohler, and Y. Nogami: *A unified potential for mesons and baryons*, Nuovo Cim. **A65** (1981), 376–390.

[BD+99] S. Boffi, P. Demetriou, M. Radici, and R. F. Wagenbrunn: *Nucleon form factors in a chiral constituent-quark model*, Phys. Rev. **C60** (1999), 025206, (hep-ph/9811483).

[BFV99] L. A. Blanco, F. Fernández, and A. Valcarce: *Light meson spectra and chiral quark cluster models*, Phys. Rev. **C59** (1999), 428–434.

[BG73] A. J. Bracken and H. S. Green: *Parastatistics and quark model*, J. Math. Phys. **14** (1973), 1784–1793.

[BG+74] M. Bolsterli, W. R. Gibbs, B. F. Gibson, and G. J. Stephenson, Jr.: *Galilean-invariance ambiguity in the nonrelativistic pion-nucleon absorption operator*, Phys. Rev. **C10** (1974), 1225–1226.

[BGM84] B. Baumgartner, H. Grosse, and A. Martin: *The Laplacian of the potential and the order of energy levels*, Phys. Lett. **B146** (1984), 363–366.

[BGM85] B. Baumgartner, H. Grosse, and A. Martin: *Order of levels in potential models*, Nucl. Phys. **B254** (1985), 528–542.

[Bha88] R. K. Bhaduri: *Models of the Nucleon*, Addison-Wesley, 1988.

[BI66a] M. Bander and C. Itzykson: *Group theory and the hydrogen atom (I)*, Rev. Mod. Phys. **38** (1966), 330–345.

[BI66b] M. Bander and C. Itzykson: *Group theory and the hydrogen atom (II)*, Rev. Mod. Phys. **38** (1966), 346–358.

[Bie61] L. C. Biedenharn: *Wigner coefficients for the R_4 group and some applications*, J. Math. Phys. **2** (1961), 433–441.

[Bij97] J. Bijtebier: *Bethe-Salpeter equation: 3D reductions, heavy mass limits and abnormal solutions*, Nucl. Phys. **A623** (1997), 498–518, (nucl-th/9703028).

[Bij00] J. Bijtebier: *A cluster-separable Born approximation for the three-dimensional reduction of the three-fermion Bethe-Salpeter equation*, J. Phys. **G26** (2000), 871–886, (hep-th/9907122).

[BIL97] R. Bijker, F. Iachello, and A. Leviatan: *Strong decays of nonstrange q^3 baryons*, Phys. Rev. **D55** (1997), 2862–2873, (nucl-th/9608057).

[BIZJ70] E. Brezin, C. Itzykson, and J. Zinn-Justin: *Relativistic Balmer formula including recoil effects*, Phys. Rev. **D1** (1970), 2349–2355.

[BM66] C. Becchi and G. Morpurgo: *Connection between BBP and VPP vertices in the quark model*, Phys. Rev. **149** (1966), 1284–1287.

[BM91] M. Benmerrouche and N. C. Mukhopadhyay: *η Photoproduction from threshold through the $S_{11}(1535)$ resonance*, Phys. Rev. Lett. **67** (1991), 1070–1073.

[BMZ95] M. Benmerrouche, N. C. Mukhopadhyay, and J. F. Zhang: *Effective Lagrangian approach to the theory of η photoproduction in the N*(1535) region*, Phys. Rev. **D51** (1995), 3237–3266, (hep-ph/9412248).

[BP69] J. D. Bjorken and E. A. Paschos: *Inelastic electron-proton and γ-proton scattering, and the structure of the nucleon*, Phys. Rev. **185** (1969), 1975–1982.

[BR79] G. E. Brown and M. Rho: *The little bag*, Phys. Lett. **B82** (1979), 177–180.

[BR86] A. O. Barut and R. Raczka: *Theory of Group Representations and Applications*, World Scientific, 1986.

[BS66] R. Blankenbecler and R. Sugar: *Linear integral equations for relativistic multichannel scattering*, Phys. Rev. **142** (1966), 1051–1059.

[BS85] A. Bilal and P. Schuck: *Memory-function approach to retardation effects in the relativistic two-body problem*, Phys. Rev. **D31** (1985), 2045–2075.

[BŠ+95] M. Batinić, I. Šlaus, A. Švarc, and B. M. K. Nefkens: *$\pi N \to \eta\ N$ and $\eta\ N \to \eta\ N$ partial-wave T matrices in a coupled, three-channel model*, Phys. Rev. **C51** (1995), 2310–2325, (nucl-th/9501011).

[BS99a] D. Bartz and Fl. Stancu: *Important configurations for NN processes in a Goldstone boson exchange model*, Phys. Rev. **C59** (1999), 1756–1761, (hep-ph/9810385).

[BS99b] D. Bartz and Fl. Stancu: *NN interaction in a Goldstone boson exchange model*, Phys. Rev. **C60** (1999), 055207, (hep-ph/9903533).

[BSB99] R. Bonnaz and B. Silvestre-Brac: *Discussion of the $^3P_0$ model applied to the decay of mesons into two mesons*, Few Body Syst. **27** (1999), 163–187.

[BŠŠ95] M. Batinić, I. Šlaus, and A. Švarc: *ηN S-wave scattering length in a three-coupled-channel, multiresonance, unitary model*, Phys. Rev. **C52** (1995), 2188–2194, (nucl-th/9502017).

[C+79] R. E. Cutkosky et al.: *Pion - nucleon partial wave analysis*, Phys. Rev. **D20** (1979), 2804–2838.

[C+98] C. Caso et al.: *Review of particle physics. Particle Data Group*, Eur. Phys. J. **C3** (1998), 1–794.

[C+00] S. Capstick et al.: *Key issues in hadronic physics*, hep-ph/0012238.

[Cap99] S. Capstick: *Missing baryons*, Few Body Syst. Suppl. **11** (1999), 86–93.

[CC+99] C. E. Carlson, C. D. Carone, J. L. Goity, and R. F. Lebed: *Operator analysis of $l = 1$ baryon masses in large N_c QCD*, Phys. Rev. **D59** (1999), 114008, (hep-ph/9812440).

[CC00] C. E. Carlson and C. D. Carone: *Predictions for decays of radially excited baryons*, Phys. Lett. **B484** (2000), 260–266, (hep-ph/0005144).

[CD+98] J. Carbonell, B. Desplanques, V. A. Karmanov, and J. F. Mathiot: *Explicitly covariant light-front dynamics and relativistic few-body systems*, Phys. Rept. **300** (1998), 215–347, (nucl-th/9804029).

[CDR72] M. Chemtob, J. W. Durso, and D. O. Riska: *Two-pion-exchange nucleon-nucleon potential*, Nucl. Phys. **B38** (1972), 141–206.

[CF+79] R. E. Cutkosky, C. P. Forsyth, R. E. Hendrick, and R. L. Kelly: *Pion - nucleon partial wave amplitudes*, Phys. Rev. **D20** (1979), 2839–2853.

[CG+86] S. Capstick, S. Godfrey, N. Isgur, and J. Paton: *Taking the 'naïve' and 'non-relativistic' out of the quark potential model*, Phys. Lett. **B175** (1986), 457–461.

[CG+96] F. Cano, P. Gonzalez, S. Noguera, and B. Desplanques: *Strong pionic decays of baryons from a spectroscopic quark model*, Nucl. Phys. **A603** (1996), 257–280, (nucl-th/9606038).

[CG+97] F. Cano, P. Gonzalez, B. Desplanques, and S. Noguera: *A (p/E) calculation of strong pionic decays of baryons*, Z. Phys. **A359** (1997), 315–319, (nucl-th/9706027).

[CG98] F. Cano and P. Gonzalez: *A consistent explanation of the Roper phenomenology*, Phys. Lett. **B431** (1998), 270–276, (nucl-th/9804071).

[CG99] H. Collins and H. Georgi: *S(3) and the $l = 1$ baryons in the quark model and the chiral quark model*, Phys. Rev. **D59** (1999), 094010, (hep-ph/9810392).

[Che79] M. Chemtob: *Meson theory of nuclear vector and axial vector exchange currents*, in: Mesons in Nuclei (M. Rho and D. Wilkinson, eds.), North-Holland, 1979, pp. 495–593.

[CI86] S. Capstick and N. Isgur: *Baryons in a relativized quark model with chromodynamics*, Phys. Rev. **D34** (1986), 2809–2835.

[CJ67] F. Calogero and G. Jagannathan: *Levinson's theorem for energy-dependend potentials*, Nuovo Cim. **47** (1967), 178–188.

[CJ+74] A. Chodos, R. L. Jaffe, K. Johnson, C. B. Thorn, and V. F. Weisskopf: *A new extended model of hadrons*, Phys. Rev. **D9** (1974), 3471–3495.

[CKP83a] J. Carlson, J. Kogut, and V. R. Pandharipande: *Quark model for baryons based on quantum chromodynamics*, Phys. Rev. **D27** (1983), 233–243.

[CKP83b] J. Carlson, J. B. Kogut, and V. R. Pandharipande: *Hadron spectroscopy in a flux-tube quark model*, Phys. Rev. **D28** (1983), 2807–2817.

[CL78] W. E. Caswell and G. P. Lepage: *Reduction of the Bethe-Salpeter equation to an equivalent Schrödinger equation, with applications*, Phys. Rev. **A18** (1978), 810–819.

[CL86] W. E. Caswell and G. P. Lepage: *Effective lagrangians for bound state problems in QED, QCD, and other field theories*, Phys. Lett. **B167** (1986), 437–442.

[CL+99] S. Capstick, T. S. H. Lee, W. Roberts, and A. Švarc: *Evidence for the fourth P_{11} resonance predicted by the constituent quark model*, Phys. Rev. **C59** (1999), 3002–3004, (nucl-th/9904005).

[Clo79] F. E. Close: *An Introduction to Quarks and Partons*, Academic Press, 1979.

[CR93] S. Capstick and W. Roberts: *$N\pi$ decays of baryons in a relativized model*, Phys. Rev. **D47** (1993), 1994–2010.

[CR94] S. Capstick and W. Roberts: *Quasi-two-body decays of nonstrange baryons*, Phys. Rev. **D49** (1994), 4570–4586, (nucl-th/9310030).

[CR00] S. Capstick and W. Roberts: *Quark models of baryon masses and decays*, nucl-th/0008028.

[CT75] A. Chodos and C. B. Thorn: *Chiral invariance in a bag theory*, Phys. Rev. **D12** (1975), 2733–2743.

[Cut54] R. E. Cutkosky: *Solutions of a Bethe-Salpeter equation*, Phys. Rev. **96** (1954), 1135–1141.

[Cut60] R. E. Cutkosky: *Singularities and discontinuities of Feynman amplitudes*, J. Math. Phys. **1** (1960), 429–433.

[CW56] R. E. Cutkosky and G. C. Wick: *Spectrum of a Bethe-Salpeter equation*, Phys. Rev. **101** (1956), 1830–1831.

[Dal65] R. H. Dalitz: *Quark models for the "elementary particles"*, in: Physique des Hautes Energies. Les Houches Lectures 1965 (C. DeWitt and M. Jacob, eds.), Gordon and Breach, 1965.

[Dar98] J. W. Darewych: *Some exact solutions of reduced scalar Yukawa theory*, Can. J. Phys. **76** (1998), 523–537, (nucl-th/9807006).

[DD00] B. Ding and J. Darewych: *A variational calculation of particle antiparticle bound states in the scalar Yukawa model*, J. Phys. **G26** (2000), 907–925, (nucl-th/9908022).

[Des88] B. Desplanques: *Deuteron D-state probability and energy-dependent NN interactions*, Phys. Lett. **B203** (1988), 200–204.

[Des98] B. Desplanques: *Electromagnetic and weak interactions in nuclei*, in: Trends in Nuclear Physics, 100 Years Later. Les Houches Lectures 1996 (H. Nifenecker, J.-P. Blaizot, G. F. Bertsch, W. Weise, and F. David, eds.), North Holland, 1998.

[DG+92] B. Desplanques, C. Gignoux, B. Silvestre-Brac, P. Gonzáles, J. Navarro, and S. Noguera: *The baryonic spectrum in a constituent quark model including a three-body force*, Z. Phys. **A343** (1992), 331–336.

[DHR97] K. Dannbom, C. Helminen, and D. O. Riska: *Baryon magnetic moments and axial coupling constants with relativistic and exchange current effects*, Nucl. Phys. **A616** (1997), 555–574, (hep-ph/9610384).

[Dir49] P. A. M. Dirac: *Forms of relativistic dynamics*, Rev. Mod. Phys. **21** (1949), 392–399.

[Div68] D. R. Divgi: *Decays of negative-parity baryons in a quark model*, Phys. Rev. **175** (1968), 2027–2029.

[dMA+01] J. P. B. C. de Melo, A. E. A. Amorim, L. Tomio, and T. Frederico: *Lower bound to the mass of a relativistic three-boson system in the light-cone*, J. Phys. **G27** (2001), 1031–1042, (hep-ph/0102129).

[Dom67] G. Domokos: *Four-dimensional symmetry*, Phys. Rev. **159** (1967), 1387–1403.

[DP84] D. I. Dyakonov and V. Yu. Petrov: *Chiral condensate in the instanton vacuum*, Phys. Lett. **B147** (1984), 351–356.

[DP86] D. I. Dyakonov and V. Yu. Petrov: *A theory of light quarks in the instanton vacuum*, Nucl. Phys. **B272** (1986), 457–489.

[DS64] G. Domokos and P. Suranyi: *Bound states and analytic properties in angular momentum*, Nucl. Phys. **54** (1964), 529–548.

[DSB+00] B. Desplanques, B. Silvestre-Brac, F. Cano, P. Gonzalez, and S. Noguera: *Nucleon form factors at high q^2 within constituent quark models*, Few Body Syst. **29** (2000), 169–222, (nucl-th/9910006).

[DT01] B. Desplanques and L. Theußl: *Validity of the one-body current for the calculation of form factors in the point form of relativistic quantum mechanics*, nucl-th/0102060.

[DW95] N. K. Devine and S. J. Wallace: *Instant two-body equation in Breit frame*, Phys. Rev. **C51** (1995), 3222–3231.

[DW97] P. Dulany and S. J. Wallace: *Relativistic three-body bound states and the reduction from four to three dimensions*, Phys. Rev. **C56** (1997), 2992–3004, (nucl-th/9712022).

[EE+96] Ch. Elster, E. E. Evans, H. Kamada, and W. Glöckle: *Nonlocality in the nucleon-nucleon interaction due to minimal relativity factors: Effects on two-nucleon observables and the three-nucleon binding energy*, Few-Body Syst. **21** (1996), 25–45.

[EG+76] E. Eichten, K. Gottfried, T. Kinoshita, K. D. Lane, and T-M. Yan: *The interplay of confinement and decay in the spectrum of charmonium*, Phys. Rev. Lett. **36** (1976), 500–504.

[EG+78] E. Eichten, K. Gottfried, T. Kinoshita, K. D. Lane, and T. M. Yan: *Charmonium: The model*, Phys. Rev. **D17** (1978), 3090–3117.

[EG+80] E. Eichten, K. Gottfried, T. Kinoshita, K. D. Lane, and T. M. Yan: *Charmonium: Comparison with experiment*, Phys. Rev. **D21** (1980), 203–233.

[Ell58a] J. P. Elliott: *Collective motion in the nuclear shell model I. Classification schemes for states of mixed configurations*, Proc. Roy. Soc. **A245** (1958), 128–145.

[Ell58b] J. P. Elliott: *Collective motion in the nuclear shell model II. The introduction of intrinsic wave-functions*, Proc. Roy. Soc. **A245** (1958), 562–581.

[FC81] C. P. Forsyth and R. E. Cutkosky: *Masses and widths of odd-parity N and Δ resonances*, Phys. Rev. Lett. **46** (1981), 576–579.

[Fey69] R. P. Feynman: *Very high-energy collisions of hadrons*, Phys. Rev. Lett. **23** (1969), 1415–1417.

[FFT73] G. Feldman, T. Fulton, and J. Townsend: *Wick equation, the infinite - momentum frame, and perturbation theory*, Phys. Rev. **D7** (1973), 1814–1824.

[FGML73] H. Fritzsch, M. Gell-Mann, and H. Leutwyler: *Advantages of the color octet gluon picture*, Phys. Lett. **B47** (1973), 365–368.

[FH68] D. Faiman and A. W. Hendry: *Harmonic-oscillator model for baryons*, Phys. Rev. **173** (1968), 1720–1729.

[FH69] D. Faiman and A. W. Hendry: *Harmonic-oscillator model for baryons*, Phys. Rev. **180** (1969), 1609–1610.

[FKR71] R. P. Feynman, M. Kislinger, and F. Ravndal: *Current matrix elements from a relativistic quark model*, Phys. Rev. **D3** (1971), 2706–2732.

[Foc35] V. A. Fock: *Zur Theorie des Wasserstoffatoms*, Z. Phys. **98** (1935), 145–154.

[FPF95] J. L. Forest, V. R. Pandharipande, and J. L. Friar: *Relativistic nuclear hamiltonians*, Phys. Rev. **C52** (1995), 568–575.

[Fri73] J. L. Friar: *Relativistic corrections to electron scattering by ^2H, ^3He, and $^4He^*$*, Ann. Phys. **81** (1973), 332–363.

[Fri74] J. L. Friar: *Pion-nucleon absorbtion operator ambiguity*, Phys. Rev. **C10** (1974), 955–957.

[Fri76] J. L. Friar: *Relativistic corrections to electron scattering. II. Inelastic scattering*, Nucl. Phys. **A264** (1976), 455–483.

[Fri80] J. L. Friar: *Retardation, quasipotential equations, and relativistic corrections to the deuteron charge operator*, Phys. Rev. **C22** (1980), 796–812.

[FS81] I. Fukui and N. Setô: *On the structure of the continuous spectra in the spinor- spinor Bethe-Salpeter equation*, Prog. Theor. Phys. **65** (1981), 1026–1040.

[FS86] D. Flamm and F. Schöberl: *Introduction to the Quark Model of Elementary Particles: Quantum Numbers, Gauge Theories and Hadron Spectroscopy*, Gordon and Breach, 1986.

[FST54] N. Fukuda, K. Sawada, and M. Taketani: *On the construction of potential in field theory*, Prog. Theor. Phys. **12** (1954), 156–166.

[FW50] L. L. Foldy and S. A. Wouthuysen: *On the Dirac theory of spin 1/2 particle and its nonrelativistic limit*, Phys. Rev. **78** (1950), 29–36.

[G+00] D. E. Groom et al.: *Review of particle physics. Particle Data Group*, Eur. Phys. J. **C15** (2000), 1.

[GI85] S. Godfrey and N. Isgur: *Mesons in a relativized quark model with chromodynamics*, Phys. Rev. **D32** (1985), 189–231.

[GK94] L. Ya. Glozman and E. I. Kuchina: *Baryon-baryon components in the deuteron as quark-exchange currents*, Phys. Rev. **C49** (1994), 1149–1165.

[GL84] J. Gasser and H. Leutwyler: *Chiral perturbation theory to one loop*, Ann. Phys. **158** (1984), 142–210.

[Gla61] S. L. Glashow: *Partial symmetries of weak interactions*, Nucl. Phys. **22** (1961), 579–588.

[Glö83] W. Glöckle: *The Quantum Mechanical Few-Body Problem*, Springer Verlag, 1983.

[Glo99a] L. Ya. Glozman: *Chiral quarks, chiral limit, nonanalytic terms and baryon spectroscopy*, Phys. Lett. **B459** (1999), 589–593, (hep-ph/9904459).

[Glo99b] L. Ya. Glozman: *Reply to Isgur's 'Critique of a pion exchange model for interquark forces'*, nucl-th/9909021.

[Glo00a] L. Ya. Glozman: *Chiral aspects of baryon structure in the quark model*, Phys. Lett. **B494** (2000), 58–62, (hep-ph/0004229).

[Glo00b] L. Ya. Glozman: *Origins of the baryon spectrum*, Nucl. Phys. **A663** (2000), 103–112, (hep-ph/9908423).

[Glo00c] L. Ya. Glozman: *Parity doublets and chiral symmetry restoration in baryon spectrum*, Phys. Lett. **B475** (2000), 329–334, (hep-ph/9908207).

[GM62] M. Gell-Mann: *Symmetries of baryons and mesons*, Phys. Rev. **125** (1962), 1067–1084.

[GM64] M. Gell-Mann: *A schematic model of baryons and mesons*, Phys. Lett. **8** (1964), 214–215.

[GML51] M. Gell-Mann and F. Low: *Bound states in quantum field theory*, Phys. Rev. **84** (1951), 350–354.

[GMOR68] M. Gell-Mann, R. J. Oakes, and B. Renner: *Behavior of current divergences under SU(3)×SU(3)*, Phys. Rev. **175** (1968), 2195–2199.

[GP+98a] L. Ya. Glozman, Z. Papp, W. Plessas, K. Varga, and R. F. Wagenbrunn: *Effective Q-Q interactions in constituent quark models*, Phys. Rev. **C57** (1998), 3406–3413, (nucl-th/9705011).

[GP+98b] L. Ya. Glozman, W. Plessas, L. Theußl, R. F. Wagenbrunn, and K. Varga: *Baryon excitation spectra and hadronic decays of resonances in a semirelativistic chiral quark model*, πN Newslett. **14** (1998), 99–108.

[GP+98c] L. Ya. Glozman, W. Plessas, K. Varga, and R. F. Wagenbrunn: *Light and strange baryons in a chiral quark model with Goldstone-boson-exchange interactions*, Nucl. Phys. **A631** (1998), 469c–472c.

[GP+98d] L. Ya. Glozman, W. Plessas, K. Varga, and R. F. Wagenbrunn: *Unified description of light- and strange-baryon spectra*, Phys. Rev. **D58** (1998), 094030, (hep-ph/9706507).

[GP+00] L. Ya. Glozman, Z. Papp, W. Plessas, K. Varga, and R. F. Wagenbrunn: *Reply to 'Comment on "Effective Q-Q interactions in constituent quark models" '*, Phys. Rev. **C61** (2000), 019804.

[GPP96] L. Ya. Glozman, Z. Papp, and W. Plessas: *Light baryons in a constituent quark model with chiral dynamics*, Phys. Lett. **B381** (1996), 311–316, (hep-ph/9601353).

[GR64] F. Gursey and L. A. Radicati: *Spin and unitary spin independence of strong interactions*, Phys. Rev. Lett. **13** (1964), 173–175.

[GR80] I. S. Gradshteyn and I. M. Ryzhik: *Table of Integrals, Series and Products*, Academic Press, 1980.

[GR96a] L. Ya. Glozman and D. O. Riska: *Quark model explanation of the $N^* \to N\eta$ branching ratios*, Phys. Lett. **B366** (1996), 305–310, (hep-ph/9508327).

[GR96b] L. Ya. Glozman and D. O. Riska: *The spectrum of the nucleons and the strange hyperons and chiral dynamics*, Phys. Rept. **268** (1996), 263–303, (hep-ph/9505422).

[GR+98] M. Genovese, J.-M. Richard, Fl. Stancu, and S. Pepin: *Heavy-flavour pentaquarks in a chiral constituent quark model*, Phys. Lett. **B425** (1998), 171–176, (hep-ph/9712452).

[GR99] J. L. Goity and W. Roberts: *A relativistic chiral quark model for pseudoscalar emission from heavy mesons*, Phys. Rev. **D60** (1999), 034001, (hep-ph/9809312).

[Gre57] H. S. Green: *Separability of a covariant wave equation*, Nuovo Cim. **5** (1957), 866–871.

[Gre64] O. W. Greenberg: *Spin and unitary-spin independence in a paraquark model of baryons and mesons*, Phys. Rev. Lett. **13** (1964), 598–602.

[Gro69] F. Gross: *Three-dimensional covariant integral equations for low- energy systems*, Phys. Rev. **186** (1969), 1448–1462.

[Gro74] F. Gross: *A new theory of nuclear forces. Relativistic origin of the repulsive core*, Phys. Rev. **D10** (1974), 223–242.

[Gro82a] F. Gross: *Relativistic few-body problem. I. Two-body equations*, Phys. Rev. **C26** (1982), 2203–2225.

[Gro82b] F. Gross: *Relativistic few-body problem. II. Three-body equations and three-body forces*, Phys. Rev. **C26** (1982), 2226–2241.

[Gro93] F. Gross: *Relativistic Quantum Mechanics and Field Theory*, Wiley Interscience, 1993.

[GS79] D. Gromes and I. O. Stamatescu: *Baryon spectrum and the forces between quarks*, Z. Phys. **C3** (1979), 43–50.

[GS94] P. Geiger and E. S. Swanson: *Distinguishing among strong decay models*, Phys. Rev. **D50** (1994), 6855–6862, (hep-ph/9405238).

[GT58] M. L. Goldberger and S. B. Treiman: *Decay of the pi meson*, Phys. Rev. **110** (1958), 1178–1184.

[GW97] A. M. Green and S. Wycech: *η-nucleon scattering length and effective range*, Phys. Rev. **C55** (1997), 2167–2170, (nucl-th/9703009).

[GY+82a] M. B. Gavela, A. Le Yaouanc, L. Oliver, O. Pène, and J. C. Raynal: *Pionic decays and saturation of current algebra sum rules in a nonrelativistic expansion of the quark shell model*, Phys. Rev. **D25** (1982), 1921–1930.

[GY+82b] M. B. Gavela, A. Le Yaouanc, L. Oliver, O. Pène, and J. C. Raynal: *General proof of the saturation of the Adler-Weisberger sum rule in a quark shell model*, Phys. Rev. **D25** (1982), 1931–1936.

[H+92] K. Hikasa et al.: *Review of particle properties. Particle Data Group*, Phys. Rev. **D45** (1992), S1.

[H+00] V. Halyo et al.: *Search for free fractional electric charge elementary particles*, Phys. Rev. Lett. **84** (2000), 2576–2579, (hep-ex/9910064).

[HD73] R. Horgan and R. H. Dalitz: *Baryon spectroscopy and the quark shell model. 1. The framework, basic formulae, and matrix elements*, Nucl. Phys. **B66** (1973), 135–172.

[HK83] A. J. G. Hey and R. L. Kelly: *Baryon spectroscopy*, Phys. Rept. **96** (1983), 71–204.

[Höh83] G. Höhler: *Elastic and charge exchange scattering of elementary particles*, in: Pion Nucleon Scattering. Part 2: Methods and Results of Phenomenological Analyses (G. Höhler and H. Schopper, eds.), Springer Verlag, 1983.

[HR83] H. Høgaasen and J. M. Richard: *Nucleon resonances and the quark model*, Phys. Lett. **B124** (1983), 520–522.

[HT94] E. Hummel and J. A. Tjon: *Relativistic description of electron scattering on the deuteron*, Phys. Rev. **C49** (1994), 21–39, (nucl-th/9309004).

[Hua98] K. Huang: *Quantum Field Theory*, Wiley Interscience, 1998.

[IK78] N. Isgur and G. Karl: *P-wave baryons in the quark model*, Phys. Rev. **D18** (1978), 4187–4205.

[IK79a] N. Isgur and G. Karl: *Positive-parity excited baryons in a quark model with hyperfine interactions*, Phys. Rev. **D19** (1979), 2653–2677.

[IK79b] N. Isgur and G. Karl: *Ground-state baryons in a quark model with hyperfine interactions*, Phys. Rev. **D20** (1979), 1191–1194.

[Isg00] N. Isgur: *Critique of a pion exchange model for interquark forces*, Phys. Rev. **D62** (2000), 054026, (nucl-th/9908028).

[IZ85] C. Itzykson and J. B. Zuber: *Quantum Field Theory*, McGraw-Hill, 1985.

[JF86] C.-R. Ji and R. J. Furnstahl: *Bound state spectrum from the light-cone two-body equation in ϕ^3-theories*, Phys. Lett. **B167** (1986), 11–15.

[JF+01] O. Juillet, S. Fleck, L. Theußl, J.-M. Richard, and K. Varga: *Lower bound on fermion binding energies*, Phys. Rev. **B63** (2001), 037102, (quant-ph/0008048).

[Ji86] C.-R. Ji: *Analytic calculation of the bound state spectrum in the light-cone two-body equation*, Phys. Lett. **B167** (1986), 16–20.

[Kad68] V. G. Kadyshevsky: *Quasipotential type equation for the relativistic scattering amplitude*, Nucl. Phys. **B6** (1968), 125–148.

[Kai00a] N. Kaiser: *Chiral 3π exchange NN potentials: Results for representation-invariant classes of diagrams*, Phys. Rev. **C61** (2000), 014003, (nucl-th/9910044).

[Kai00b] N. Kaiser: *Chiral 3π exchange NN potentials: Results for diagrams proportional to g_A^4 and g_A^6*, Phys. Rev. **C62** (2000), 024001, (nucl-th/9912054).

[KB94] A. N. Kvinikhidze and B. Blankleider: *Covariant three body equations in ϕ^3 field theory*, Nucl. Phys. **A574** (1994), 788–818, (nucl-th/9402010).

[Kei88] B. D. Keister: *Front-form hamiltonian dynamics of deuteron electrodisintegration*, Phys. Rev. **C37** (1988), 1765–1767.

[KI80] R. Koniuk and N. Isgur: *Baryon decays in a quark model with chromodynamics*, Phys. Rev. **D21** (1980), 1868–1886.

[KI87] R. Kokoski and N. Isgur: *Meson decays by flux tube breaking*, Phys. Rev. **D35** (1987), 907–933.

[KK+99] A. A. Khelashvili, G. A. Khelashvili, N. Kiknadze, and T. P. Nadareishvili: *On the abnormal type anomalous solutions of quasipotential equations*, quant-ph/9907078.

[Kle53] A. Klein: *The Damm-Dancoff formalism and the symmetric pseudoscalar theory of nuclear forces*, Phys. Rev. **90** (1953), 1101–1115.

[Kli98] W. H. Klink: *Point form relativistic quantum mechanics and electromagnetic form factors*, Phys. Rev. **C58** (1998), 3587–3604.

[Kli00] W. H. Klink: *Point form electrodynamics and the construction of conserved current operators*, nucl-th/0012033.

[KM83] D. S. Kulshreshtha and A. N. Mitra: *Bethe-Salpeter basis for quark-pair-creation model: Understanding of VPP, VPγ and P$\gamma\gamma$ couplings*, Phys. Rev. **D28** (1983), 588–596.

[KM88] D. S. Kulshreshtha and A. N. Mitra: *Null-plane formulation of Bethe-Salpeter qqq dynamics: Baryon mass spectra*, Phys. Rev. **D37** (1988), 1268–1278.

[KM96] V. A. Karmanov and J. F. Mathiot: *On the calculation of the nucleon electromagnetic form-factors in light front dynamics*, Nucl. Phys. **A602** (1996), 388–404.

[KMW76] E. G. Kalnins, W. Miller, Jr., and P. Winternitz: *The group O(4), separation of variables and the hydrogen atom*, SIAM J. Appl. Math. **30** (1976), 630–664.

[Kok69] J. J. J. Kokkedee: *The Quark Model*, W.A. Benjamin, 1969.

[KP88] S. Kumano and V. R. Pandharipande: *Decay of mesons in flux-tube quark model*, Phys. Rev. **D38** (1988), 146–151.

[KP+99] A. Krassnigg, W. Plessas, L. Theußl, R. F. Wagenbrunn, and K. Varga: *Hadronic decays of light and strange baryon resonances in the GBE constituent quark model*, Few Body Syst. Suppl. **10** (1999), 391–394.

[Kra98] A. Krassnigg: *Hadronic decays in a semirelativistic constituent quark model*, Diplomarbeit, Karl-Franzens Universität, Graz, 1998.

[KS+75] I. V. Kurdyumov, Yu. F. Smirnov, K. V. Shitikova, and S. K. E. Samarai: *Translationally invariant shell model*, Nucl. Phys. **A145** (1975), 593–612.

[KS92] V. A. Karmanov and A. V. Smirnov: *Electromagnetic form-factors in the light front dynamics*, Nucl. Phys. **A546** (1992), 691–717.

[KS94] V. A. Karmanov and A. V. Smirnov: *Deuteron electromagnetic form-factors in the light front dynamics*, Nucl. Phys. **A575** (1994), 520–548.

[KSW95] N. Kaiser, P. B. Siegel, and W. Weise: *Chiral dynamics and the $S_{11}(1535)$ nucleon resonance*, Phys. Lett. **B362** (1995), 23–28, (nucl-th/9507036).

[KSZ70] D. Kershaw, H. Snodgrass, and C. Zemach: *Methods for the Bethe-Salpeter equation. I. Special functions and expansions in spherical harmonics*, Phys. Rev. **D2** (1970), 2806–2819.

[LA97] A. D. Lahiff and I. R. Afnan: *Role of retardation in three-dimensional relativistic equations*, Phys. Rev. **C56** (1997), 2387–2395, (nucl-th/9708037).

[LA99] A. D. Lahiff and I. R. Afnan: *Solution of the Bethe-Salpeter equation for pion-nucleon scattering*, Phys. Rev. **C60** (1999), 024608, (nucl-th/9903058).

[Lep97] G. P. Lepage: *How to renormalize the Schrödinger equation*, nucl-th/9706029.

[Li95] Z. Li: *The η photoproduction of nucleons and the structure of the resonance $S_{11}(1535)$ in the quark model*, Phys. Rev. **D52** (1995), 4961–4970, (nucl-th/9506033).

[LL58] L. D. Landau and E. M. Lifshitz: *Quantum Mechanics*, Pergamon Press, 1958.

[LL+80] M. Lacombe, B. Loiseau, J.-M. Richard, R. Vinh Mau, J. Côté, P. Pirès, and R. de Tourreil: *Parametrization of the Paris N-N potential*, Phys. Rev. **C21** (1980), 861–873.

[LMT65] D. Lurié, A. J. MacFarlane, and Y. Takahashi: *Normalization of Bethe-Salpeter wave functions*, Phys. Rev. **140B** (1965), 1091–1099.

[LRS67] H. J. Lipkin, H. R. Rubinstein, and H. Stern: *Strong and weak decays with meson emission*, Phys. Rev. **161** (1967), 1502–1504.

[LSG91] W. Lucha, F. F. Schöberl, and D. Gromes: *Bound states of quarks*, Phys. Rept. **200** (1991), 127–240.

[LT63] A. A. Logunov and A. N. Tavkhelidze: *Quasioptical approach in quantum field theory*, Nuovo Cim. **29** (1963), 380–399.

[LW70] M. J. Levine and J. Wright: *Comment on nonplanar graphs and the Bethe-Salpeter equation*, Phys. Rev. **D2** (1970), 2509–2510.

[LW96] Z. Li and R. Workman: *Do we have three S_{11} resonances in the second resonance region?*, Phys. Rev. **C53** (1996), 549–552, (nucl-th/9511041).

[M+94] L. Montanet et al.: *Review of particle properties. Particle Data Group*, Phys. Rev. **D50** (1994), 1173–1823.

[Mai86] G. B. Mainland: *Electromagnetic binding of a minimally interacting, relativistic spin 0 and spin 1/2 constituent: Zero four-momentum solutions*, J. Math. Phys. **27** (1986), 1344–1350.

[Man55] S. Mandelstam: *Dynamical variables in the Bethe-Salpeter formalism*, Proc. Roy. Soc. Lond. **A233** (1955), 248–266.

[Man59] S. Mandelstam: *Analytic properties of transition amplitudes in perturbation theory*, Phys. Rev. **115** (1959), 1741–1751.

[MB+85] C. Mahaux, P. F. Bortignon, R. A. Broglia, and C. H. Dasso: *Dynamics of the shell model*, Phys. Rept. **120** (1985), 1–274.

[MBC00] M. Mangin-Brinet and J. Carbonell: *Solutions of the Wick-Cutkosky model in the light front dynamics*, Phys. Lett. **B474** (2000), 237–244, (nucl-th/9912050).

[MF+00] S. Moszkowski, S. Fleck, A. Krikeb, L. Theußl, J.-M. Richard, and K. Varga: *Binding three or four bosons without bound subsystems*, Phys. Rev. **A62** (2000), 032504, (nucl-th/0003026).

[MG84] A. Manohar and H. Georgi: *Chiral quarks and the nonrelativistic quark model*, Nucl. Phys. **B234** (1984), 189–212.

[MHE87] R. Machleidt, K. Holinde, and C. Elster: *The Bonn meson-exchange model for the nucleon-nucleon interaction*, Phys. Rept. **149** (1987), 1–89.

[Mic69] L. Micu: *Decay rates of meson resonances in a quark model*, Nucl. Phys. **B10** (1969), 521–526.

[Mit99] A. N. Mitra: *3d-4d interlinkage of qqq wave functions under 3d support for pairwise Bethe-Salpeter kernels*, Int. J. Mod. Phys. **A14** (1999), 4781.

[MM84] A. N. Mitra and A. Mittal: *Bethe-Salpeter qqq dynamics: Electromagnetic properties of baryons*, Phys. Rev. **D29** (1984), 1399–1407.

[Mos69] M. Moshinsky: *The Harmonic Oscillator in Modern Physics: From Atoms to Quarks*, Gordon and Breach, 1969.

[MP78] W. Marciano and H. Pagels: *Quantum Chromodynamics*, Phys. Rept. **36** (1978), 137–276.

[MP91] G. B. Mainland and L. A. Parson: *Derivation of the coordinate system that separates the Bethe-Salpeter equation for the Wick-Cutkosky model*, J. Math. Phys. **32** (1991), 1072–1075.

[MP00] E. Moulin and N. Ploquin: *Effets d'une interaction non locale sur la spectroscopie d'un système à deux corps*, Stage Maîtrise, Institut des Sciences Nucléaires, Grenoble, 2000.

[MR67] A. Mitra and M. Ross: *Meson-baryon couplings in a quark model*, Phys. Rev. **158** (1967), 1630–1638.

[MS65] K. T. Mahanthappa and E.C.G. Sudarshan: $SU(6) \otimes O(3)$ *structure of strongly interacting particles*, Phys. Rev. Lett. **14** (1965), 163–166.

[MS92] D. M. Manley and E. M. Saleski: *Multichannel resonance parametrization of πN scattering amplitudes*, Phys. Rev. **D45** (1992), 4002–4033.

[MS95] G. B. Mainland and J. R. Spence: *Numerical solutions to the partially separated, equal mass, Wick-Cutkosky model*, Few Body Syst. **19** (1995), 109–120.

[Mut87] T. Muta: *Foundations of Quantum Chromodynamics*, World Scientific, 1987.

[MZB95] N. C. Mukhopadhyay, J.-F. Zhang, and M. Benmerrouche: *Extraction of the ratio of the N*(1535) electromagnetic helicity amplitudes from eta photoproduction off neutrons and protons*, Phys. Lett. **B364** (1995), 1–7, (hep-ph/9510307).

[Nak65a] N. Nakanishi: *Normalization condition and normal and abnormal solutions of the Bethe-Salpeter equation*, Phys. Rev. **138** (1965), B1182–B1192, [Erratum: Phys. Rev. **139** (1965) B1].

[Nak65b] N. Nakanishi: *Normalization condition and normal and abnormal solutions of the Bethe-Salpeter equation. II*, Phys. Rev. **139** (1965), B1401–B1406.

[Nak69] N. Nakanishi: *A general survey of the theory of the Bethe-Salpeter equation*, Prog. Theor. Phys. Suppl. **43** (1969), 1–81.

[Nak88] N. Nakanishi: *Review of the Wick-Cutkosky model*, Prog. Theor. Phys. Suppl. **95** (1988), 1–24.

[NG83] A. R. Neghabian and W. Glöckle: *Derivation of the external field in the Dirac equation based on quantum electrodynamics*, Can. J. Phys. **61** (1983), 85–92.

[Nic00] A. Nicolet: *Etude de largeurs de désintegration de résonances baryoniques*, Stage Maîtrise, Institut des Sciences Nucléaires, Grenoble, 2000.

[Nic01] A. Nicolet: *Désintegrations fortes, Etude d'une relation entre le modèle $^3P_0$ et un modèle plus microscopique*, Stage DEA, Institut des Sciences Nucléaires, Grenoble, 2001.

[NJL61a] Y. Nambu and G. Jona-Lasinio: *Dynamical model of elementary particles based on an analogy with superconductivity. I*, Phys. Rev. **122** (1961), 345–358.

[NJL61b] Y. Nambu and G. Jona-Lasinio: *Dynamical model of elementary particles based on an analogy with superconductivity. II*, Phys. Rev. **124** (1961), 246–254.

[Nod88] M.-T. Noda: *Bibliography of the Bethe-Salpeter equation*, Prog. Theor. Phys. Suppl. **95** (1988), 78–111.

[NT96a] T. Nieuwenhuis and J. A. Tjon: *Nonperturbative study of generalized ladder graphs in a $\phi^2\chi$ theory*, Phys. Rev. Lett. **77** (1996), 814–817, (hep-ph/9606403).

[NT96b] T. Nieuwenhuis and J. A. Tjon: *O(4) expansion of the ladder Bethe-Salpeter equation*, Few Body Syst. **21** (1996), 167–185, (nucl-th/9607041).

[Oet00] M. Oettel: *Baryons as relativistic bound states of quark and diquark*, Dissertation, Eberhard-Karls-Universität, Tübingen, 2000, (nucl-th/0012067).

[Ôku54] S. Ôkubo: *Diagonalization of Hamiltonian and Tamm-Dancoff equation*, Prog. Theor. Phys. **12** (1954), 603–622.

[PA96] D. R. Phillips and I. R. Afnan: *Solving the four-dimensional $NN-\pi NN$ equations for scalars below the meson-production threshold*, Phys. Rev. **C54** (1996), 1542–1560, (nucl-th/9605004).

[Pag75] H. Pagels: *Departures from chiral symmetry*, Phys. Rept. **16** (1975), 219–311.

[PKP00] Z. Papp, A. Krassnigg, and W. Plessas: *Faddeev approach to confined three-quark problems*, Phys. Rev. **C62** (2000), 044004, (nucl-th/0002006).

[PP96] Z. Papp and W. Plessas: *Coulomb-Sturmian separable expansion approach: Three-body Faddeev calculations for Coulomb-like interactions*, Phys. Rev. **C54** (1996), 50–56, (nucl-th/9604027).

[PS64] F. G. Perey and D. S. Saxon: *The local energy approximation to nonlocality and finite range effects*, Phys. Lett. **10** (1964), 107–109.

[PS+97] S. Pepin, Fl. Stancu, M. Genovese, and J.-M. Richard: *Tetraquarks with colour-blind forces in chiral quark models*, Phys. Lett. **B393** (1997), 119–123, (hep-ph/9609348).

[PS98] S. Pepin and Fl. Stancu: *Heavy hexaquarks in a chiral constituent quark model*, Phys. Rev. **D57** (1998), 4475–4478, (hep-ph/9710528).

[PT98] V. Pascalutsa and J. A. Tjon: *Relativistic covariance of quasipotential equations*, Phys. Lett. **B435** (1998), 245–250, (nucl-th/9711005).

[PW96] D. R. Phillips and S. J. Wallace: *Relativistic bound-state equations in three dimensions*, Phys. Rev. **C54** (1996), 507–522, (nucl-th/9603008).

[PW98] D. R. Phillips and S. J. Wallace: *A covariant gauge-invariant three-dimensional description of relativistic bound-states*, Few Body Syst. **24** (1998), 175–191, (nucl-th/9708027).

[Rah99] F. Rahoui: *Recherche et normalisation des solutions anormales de l'équation de Bethe-Salpeter*, Stage Maîtrise, Institut des Sciences Nucléaires, Grenoble, 1999.

[RB99] D. O. Riska and G. E. Brown: *Two-pion exchange interaction between constituent quarks*, Nucl. Phys. **A653** (1999), 251–273, (hep-ph/9902319).

[RGG75] A. De Rújula, H. Georgi, and S. L. Glashow: *Hadron masses in a gauge theory*, Phys. Rev. **D12** (1975), 147–162.

[Rip97] G. Ripka: *Quarks Bound by Chiral Fields*, Clarendon Press, 1997.

[Ris96] D. O. Riska: *Nucleon models*, Adv. Nucl. Phys. **22** (1996), 1–36.

[RS80] P. Ring and P. Schuck: *The Nuclear Many-Body Problem*, Springer Verlag, 1980.

[RSB92] W. Roberts and B. Silvestre-Brac: *General method of calculation of any hadronic decay in the $^3P_0$ model*, Few Body Syst. **11** (1992), 171–193.

[RSB98] W. Roberts and B. Silvestre-Brac: *Meson decays in a quark model*, Phys. Rev. **D57** (1998), 1694–1702, (hep-ph/9708235).

[RT88] G. Rupp and J. A. Tjon: *Bethe-Salpeter calculation of three-nucleon observables with rank-one separable potentials*, Phys. Rev. **C37** (1988), 1729–1738.

[RT90] G. Rupp and J. A. Tjon: *Relativistic contributions to the deuteron electromagnetic form factors*, Phys. Rev. **C41** (1990), 472–483.

[RT92] G. Rupp and J. A. Tjon: *Bethe-Salpeter calculation of three-nucleon observables with multi-rank separable interactions*, Phys. Rev. **C45** (1992), 2133–2142.

[S+95] G. Sterman et al.: *Handbook of perturbative QCD*, Rev. Mod. Phys. **67** (1995), 157–248.

[Sal] A. Salam: *Weak and electromagnetic interactions*, In: Elementary Particle Theory, Proceedings of The Nobel Symposium, (1968).

[Sal52] E. E. Salpeter: *Mass corrections to the fine structure of hydrogen like atoms*, Phys. Rev. **87** (1952), 328–342.

[SB51] E. E. Salpeter and H. A. Bethe: *A relativistic equation for bound state problems*, Phys. Rev. **84** (1951), 1232–1242.

[SBB+84] B. Silvestre-Brac, A. Bilal, C. Gignoux, and P. Schuck: *On the validity of various approximations for the Bethe-Salpeter equation and their WKB quantization*, Phys. Rev. **D29** (1984), 2275–2281.

[Sch51a] J. Schwinger: *On the Green's functions of quantized fields. 1*, Proc. Nat. Acad. Sci. **37** (1951), 452–455.

[Sch51b] J. Schwinger: *On the Green's functions of quantized fields. 2*, Proc. Nat. Acad. Sci. **37** (1951), 455–459.

[Sch53] J. Schwinger: *The theory of quantized fields. II*, Phys. Rev. **91** (1953), 713–728.

[Sch62] S. S. Schweber: *The Bethe-Salpeter equation in nonrelativistic quantum mechanics*, Ann. Phys. **20** (1962), 61–77.

[Sch65] C. Schwartz: *Solution of a Bethe-Salpeter equation*, Phys. Rev. **137** (1965), 717–719.

[Sch68] C. Schwartz: *Generalized Bethe-Salpeter equation for coupled two- and three-body amplitudes*, in: Three-Particle Scattering in Quantum Mechanics (J. Gillespie and J. Nuttal, eds.), W.A. Benjamin, 1968, pp. 147–194.

[Set76] N. Setô: *Asymptotic behavior of the eigenvalues in the Wick-Cutkosky model for large principal quantum number*, Prog. Theor. Phys. **56** (1976), 919–925.

[Set77] N. Setô: *Reflection symmetry of the eigenvalues in the Wick-Cutkosky model*, Prog. Theor. Phys. **57** (1977), 1403–1408.

[Set80] N. Setô: *Suppression of abnormal solutions below a critical coupling strength in a spinor-type Bethe-Salpeter equation*, Prog. Theor. Phys. **64** (1980), 1026–1037.

[Set88] N. Setô: *Review of the spinor-spinor Bethe-Salpeter equation: Spectral properties in the massless ladder model*, Prog. Theor. Phys. Suppl. **95** (1988), 25–45.

[SF+00] J. H. O. Sales, T. Frederico, B. V. Carlson, and P. U. Sauer: *Light-front Bethe-Salpeter equation*, Phys. Rev. **C61** (2000), 044003, (nucl-th/9909029).

[Sil98] Z. K. Silagadze: *Wick-Cutkosky model: An introduction*, hep-ph/9803307.

[Sin72] S. Singh: *Form factors in the Bethe-Salpeter model*, Phys. Rev. **D6** (1972), 1648–16541.

[SK99] K. Shimizu and M. Koyama: *H-particle in a chiral quark model*, Nucl. Phys. **A646** (1999), 211–230.

[SÔ60] M. Sugawara and S. Ôkubo: *Two-nucleon potential from pion field theory with pseudoscalar coupling*, Phys. Rev. **117** (1960), 605–610.

[SPG97] Fl. Stancu, S. Pepin, and L. Ya. Glozman: *Nucleon-nucleon interaction in a chiral constituent quark model*, Phys. Rev. **C56** (1997), 2779–2788, (nucl-th/9705030).

[SPG98] Fl. Stancu, S. Pepin, and L. Ya. Glozman: *How the "H particle" unravels the quark dynamics*, Phys. Rev. **D57** (1998), 4393–4396, (hep-ph/9707356).

[SS85] R. Sartor and Fl. Stancu: *Hyperfine splitting in a realistic basis for baryons*, Phys. Rev. **D31** (1985), 128–136.

[SS86] R. Sartor and Fl. Stancu: *Strong decay of hadrons in a semirelativistic quark model*, Phys. Rev. **D34** (1986), 3405–3413.

[SS88] Fl. Stancu and P. Stassart: *Pion decay of baryons in a flux-tube quark model*, Phys. Rev. **D38** (1988), 233–237.

[SS89] Fl. Stancu and P. Stassart: *Role of the pion size and flux tube extension in a baryon decay model*, Phys. Rev. **D39** (1989), 343–346.

[SS90a] Fl. Stancu and P. Stassart: *Improved description of the Roper resonance in a constituent quark model*, Phys. Rev. **D41** (1990), 916–919.

[SS90b] P. Stassart and Fl. Stancu: *$N + \rho$ decay of baryons in a flux-tube-breaking mechanism*, Phys. Rev. **D42** (1990), 1521–1526.

[SS91] Fl. Stancu and P. Stassart: *Negative parity nonstrange baryons*, Phys. Lett. **B269** (1991), 243–246.

[SS93] Fl. Stancu and P. Stassart: *$N + \omega$ decay of baryons in a flux-tube-breaking mechanism*, Phys. Rev. **D47** (1993), 2140–2142.

[SS95] P. Stassart and Fl. Stancu: *$\Delta\pi$ decay of baryons in a flux-tube-breaking mechanism*, Z. Phys. **A351** (1995), 77–82.

[SS97a] P. Stassart and Fl. Stancu: *Positive parity nonstrange baryons beyond 2 GeV*, Z. Phys. **A359** (1997), 321–325.

[SS97b] P. Stassart and Fl. Stancu: *The spectrum of non-strange baryons: Unsettled issues*, in: Quark confinement and the hadron spectrum II (N. Brambilla and G. M. Prosperi, eds.), World Scientific, 1997.

[SS+99] S. Simula, B. Saghai, N. C. Mukhopadhyay, and V. D. Burkert (eds.): *N^* physics and nonperturbative quantum chromodynamics. Proceedings of the joint ECT*/JLAB workshop, Trento, 1998*, Few Body Syst. Suppl. **11** (1999).

[SS+00] P. Stassart, Fl. Stancu, J.-M. Richard, and L. Theußl: *On the scalar meson exchange in the baryon spectra*, J. Phys. **G26** (2000), 397–403, (nucl-th/9905015).

[ST93] Yu. A. Simonov and J. A. Tjon: *The Feynman-Schwinger representation for the relativistic two-particle amplitude in field theory*, Ann. Phys. **228** (1993), 1–18.

[Sta96] Fl. Stancu: *Group Theory in Subnuclear Physics*, Clarendon Press, 1996.

[Sta98] Fl. Stancu: *Positive parity pentaquarks in a Goldstone boson exchange model*, Phys. Rev. **D58** (1998), 111501, (hep-ph/9803442).

[Sta99] Fl. Stancu: *Multiquark states in a Goldstone boson exchange model*, Few Body Syst. Suppl. **11** (1999), 33–36, (hep-ph/9808491).

[ŞTG99] Ç. Şavklı, J. A. Tjon, and F. Gross: *Feynman-Schwinger representation approach to nonperturbative physics*, Phys. Rev. **C60** (1999), 055210, (hep-ph/9906211).

[Sut75] L. G. Suttorp: *Exact solutions of the spinor Bethe-Salpeter equation for tightly bound states*, Nuovo Cim. **A29** (1975), 225–255.

[Sut78] L. G. Suttorp: *Numerical solution of the spinor Bethe-Salpeter equation and the Goldstein problem*, Ann. Phys. **113** (1978), 257–276.

[SV98] Y. Suzuki and K. Varga: *Stochastic Variational Approach to Quantum-Mechanical Few-Body Problems*, Springer Verlag, 1998.

[SW65] T. Shibuya and C. E. Wulfman: *Molecular orbitals in momentum space*, Proc. Roy. Soc. Ser. **A 286** (1965), 376–389.

[SXM92] F. Sammarruca, D. P. Xu, and R. Machleidt: *Relativistic corrections to the triton bindig energy*, Phys. Rev. **C46** (1992), 1636–1641, (nucl-th/9210011).

[Tal68] J. D. Talman: *Special Functions*, W.A. Benjamin, 1968.

[Tay66] J.G. Taylor: *Relativistic three-particle equations. I.*, Phys. Rev. **150** (1966), 1321–1330.

[Tay72] J. R. Taylor: *Scattering Theory*, Wiley & Sons, 1972.

[TD+99] L. Theußl, B. Desplanques, B. Silvestre-Brac, and K. Varga: *Describing the nucleon electromagnetic form factors at high momentum transfers*, Few Body Syst. Suppl. **10** (1999), 403–406.

[TD01] L. Theußl and B. Desplanques: *Crossed-boson exchange contribution and Bethe-Salpeter equation*, Few Body Syst. **30** (2001), 5–19, (nucl-th/9908007).

[The97] L. Theußl: *Strong decays of baryon resonances in a chiral constituent quark model*, Diplomarbeit, Karl-Franzens Universität, Graz, 1997.

[Tho81] A. W. Thomas: *Low-energy pion scattering in the cloudy-bag model*, J. Phys. **G7** (1981), L283–L286.

[Tho98] T. Thonhauser: *Meson spectra in a chiral constituent quark model*, Diplomarbeit, Karl-Franzens Universität, Graz, 1998.

[tHV79] G. 't Hooft and M. Veltman: *Scalar one-loop integrals*, Nucl. Phys. **B153** (1979), 365–401.

[TL80] A. W. Thomas and R. H. Landau: *Pion - deuteron and pion - nucleus scattering: A review*, Phys. Rept. **58** (1980), 121–212.

[Tod71] I. T. Todorov: *Quasipotential equation corresponding to the relativistic Eikonal approximation*, Phys. Rev. **D3** (1971), 2351–2356.

[TW+00] L. Theußl, R. F. Wagenbrunn, B. Desplanques, and W. Plessas: *Hadronic decays of N and Δ resonances in a chiral quark model*, nucl-th/0010099.

[TW01] L. Theußl and R. F. Wagenbrunn: *On the fourth P_{11} resonance predicted by the constituent quark model*, nucl-th/0104024.

[VDL00] T. P. Vrana, S. A. Dytman, and T. S. H. Lee: *Baryon resonance extraction from π N data using a unitary multichannel model*, Phys. Rept. **328** (2000), 181–236, (nucl-th/9910012).

[VFF95] A. Valcarce, A. Faessler, and F. Fernandez: *Influence of the d wave quintuplet nucleon delta channel on the s wave singlet nucleon-nucleon phase shift in a quark model*, Phys. Lett. **B345** (1995), 367–371.

[vFT86] E. van Faassen and J. A. Tjon: *Relativistic three-body approach to NN scattering at intermediate energies*, Phys. Rev. **C33** (1986), 2105–2120.

[VG+00] A. Valcarce, P. Gonzalez, F. Fernandez, and V. Vento: *Comment on "Effective Q-Q interactions in constituent quark models"*, Phys. Rev. **C61** (2000), 019803.

[VMK88] D. A. Varshalovich, A. N. Moskalev, and V. K. Khersonskii: *Quantum Theory of Angular Momentum*, World Scientific, 1988.

[vRW67] R. van Royen and V. F. Weisskopf: *Hadron decay processes and the quark model*, Nuovo Cim. **A50** (1967), 617–645.

[VS95] K. Varga and Y. Suzuki: *Precise solution of few-body problems with the stochastic variational method on a correlated Gaussian basis*, Phys. Rev. **C52** (1995), 2885–2905, (nucl-th/9508023).

[Wag98] R. F. Wagenbrunn: *Chiral constituent quark model for light and strange baryons*, Dissertation, Karl-Franzens Universität, Graz, 1998.

[Wat66] G. N. Watson: *A Treatise on the Theory of Bessel Functions*, Cambridge University Press, 1966.

[WB+01] R. F. Wagenbrunn, S. Boffi, W. Klink, W. Plessas, and M. Radici: *Covariant nucleon electromagnetic form factors from the Goldstone-boson-exchange quark model*, Phys. Lett. **B511** (2001), 33–39, (nucl-th/0010048).

[Wei67] S. Weinberg: *A model of leptons*, Phys. Rev. Lett. **19** (1967), 1264–1266.

[Wei79] S. Weinberg: *Phenomenological lagrangians*, Physica **A96** (1979), 327–340.

[WG+00a] R. F. Wagenbrunn, L. Ya. Glozman, W. Plessas, and K. Varga: *Extended Goldstone-boson-exchange constituent quark model*, Nucl. Phys. **A663** (2000), 703–706.

[WG+00b] R. F. Wagenbrunn, L. Ya. Glozman, W. Plessas, and K. Varga: *Extension of the GBE chiral constituent quark model*, Nucl. Phys. **A666** (2000), 29–32.

[Wic54] G. C. Wick: *Properties of Bethe-Salpeter wave functions*, Phys. Rev. **96** (1954), 1124–1134.

[Wil74] K. G. Wilson: *Confinement of quarks*, Phys. Rev. **D10** (1974), 2445–2459.

[Wor99] R. Workman: *Pole versus Breit-Wigner resonance description of the orbitally excited baryons*, Phys. Rev. **C59** (1999), 3441–3443, (nucl-th/9811056).

[WP+99] R. F. Wagenbrunn, W. Plessas, L. Ya. Glozman, and K. Varga: *Goldstone boson exchange dynamics in the constituent quark model for baryons*, Few Body Syst. Suppl. **10** (1999), 387–390.

[WR+00] R. F. Wagenbrunn, M. Radici, S. Boffi, and P. Demetriou: *Nucleon magnetic moments in an extended chiral constituent quark model*, Eur. Phys. J. **A8** (2000), 385–388, (hep-ph/0002110).

[Wul71] C. E. Wulfman: *Dynamical groups in atomic and molecular physics*, in: Group Theory and its Applications (E. M. Loebl, ed.), Academic Press, 1971, pp. 145–197.

[YO+73] A. Le Yaouanc, L. Oliver, O. Pène, and J.-C. Raynal: *"Naive" quark-pair-creation model of strong-interaction vertices*, Phys. Rev. **D8** (1973), 2223–2234.

[YO+74] A. Le Yaouanc, L. Oliver, O. Pene, and J.-C. Raynal: *Naive quark pair creation model and baryon decays*, Phys. Rev. **D9** (1974), 1415–1419.

[YO+75] A. Le Yaouanc, L. Oliver, O. Pene, and J.-C. Raynal: *Resonant partial-wave amplitudes in $\pi N \to \pi\pi N$ according to the naive quark-pair-creation model*, Phys. Rev. **D11** (1975), 1272–1286.

[YO+88] A. Le Yaouanc, L. Oliver, O. Pène, and J.-C. Raynal: *Hadron Transitions in the Quark Model*, Gordon and Breach, 1988.

[zLM69] E. zur Linden and H. Mitter: *Bound-state solutions of the Bethe-Salpeter equation in momentum space*, Nuovo Cim. **61B** (1969), 389–402.

[ZT82] M. J. Zuilhof and J. A. Tjon: *One loop diagrams in nucleon-nucleon scattering*, Phys. Rev. **C26** (1982), 1277–1291.

[Zwe64] G. Zweig: *An SU(3) model for strong interaction symmetry and its breaking*, CERN-TH-412.

Appendix A

Notations and Conventions

A.1 Dirac matrices and spinors

We use the Lorentz metric $g_{\mu\nu} = \mathrm{diag}(1,-1,-1,-1)$. For the Dirac matrices we use:

$$\gamma^0 = \begin{pmatrix} 1 & 0 \\ 0 & -1 \end{pmatrix}, \qquad \gamma^i = \begin{pmatrix} 0 & \sigma^i \\ \sigma^i & 0 \end{pmatrix}, \qquad \gamma^5 = \gamma_5 = \begin{pmatrix} 0 & 1 \\ 1 & 0 \end{pmatrix}, \qquad \sigma_{\mu\nu} = \frac{i}{2}\left[\gamma_\mu, \gamma_\nu\right], \quad \text{(A.1-1)}$$

where σ^i are the Pauli matrices:

$$\sigma^1 = \begin{pmatrix} 0 & 1 \\ 1 & 0 \end{pmatrix}, \qquad \sigma^2 = \begin{pmatrix} 0 & -i \\ i & 0 \end{pmatrix}, \qquad \sigma^3 = \begin{pmatrix} 1 & 0 \\ 0 & -1 \end{pmatrix}. \quad \text{(A.1-2)}$$

$$\sigma^i = \sigma_i, \qquad [\sigma_i, \sigma_j] = 2\,i\,\epsilon_{ijk}\,\sigma_k, \qquad \{\sigma_i, \sigma_j\} = 2\,\delta_{ij}, \qquad \sigma_i\,\sigma_j = \delta_{ij} + i\,\epsilon_{ijk}\,\sigma_k. \quad \text{(A.1-3)}$$

The spinors u and v correspond to positive- and negative-energy solutions of the Dirac equation. For free spinors,

$$(\not{p} - m)\,u_s(p) = (\not{p} + m)\,v_s(p) = 0, \quad \text{(A.1-4)}$$

where $\not{p} = \gamma_\mu p^\mu$, and summation over repeated indices is understood. The explicit form of the spinors is then given by

$$u_s(p) = \left(\frac{E+m}{2m}\right)^{1/2} \begin{pmatrix} \chi_s \\ \frac{\vec{\sigma}\cdot\vec{p}}{E+m}\chi_s \end{pmatrix}, \qquad \text{and} \qquad v_s(p) = \left(\frac{E+m}{2m}\right)^{1/2} \begin{pmatrix} \frac{\vec{\sigma}\cdot\vec{p}}{E+m}\chi_s \\ \chi_s \end{pmatrix}, \quad \text{(A.1-5)}$$

where χ_s are Pauli spinors. The Dirac spinors are normalized according to

$$\bar{u}_s(p)u_s(p) = 1, \qquad \bar{v}_s(p)v_s(p) = -1. \quad \text{(A.1-6)}$$

Appendix B

The Stochastic Variational Method

We discuss rather briefly in this section the numerical method that was employed almost exclusively throughout this work. The stochastic variational method has turned out to be a very economic and performing method, whether it was used to obtain three-body wave functions of baryon resonances in the first part of this work, or for the solution of the four-dimensional, relativistic two-body problem in the chapters dealing with the Bethe-Salpeter equation. A general discussion of the method may be found in ref. [SV98], applications to baryon spectroscopy are detailed in particular in refs. [Wag98, The97].

B.1 Principles of the Method

The basic starting point of the method is the Rayleigh-Ritz variational principle. Let H denote the Hamiltonian of a quantum system and $E[\Psi]$ the average value of its energy:

$$E[\Psi] = \frac{\langle \Psi | H | \Psi \rangle}{\langle \Psi \mid \Psi \rangle}, \tag{B.1-1}$$

Any state vector for which this average value, considered as a functional of the vectors of state-vector space, is stationary, is an eigenvector of the discrete spectrum of H, and conversely. The corresponding eigenvalue is the stationary value of the functional $E[\Psi]$. The Rayleigh-Ritz variational principle then states that whatever may be the dynamical state of the system, the average value of its energy is equal to or greater than the energy of the ground state:

$$E[\Psi] \geq E_0. \tag{B.1-2}$$

The variational principle therefore gives systematic upper bounds on the energy levels of the system. In searching for an optimal upper bound for the ground-state energy, a convenient ansatz for a trial wave function is the linear combination of some well-chosen basis states ψ_i:

$$\Psi = \sum_{i-1}^{N-1} c_i \, \psi_i. \tag{B.1-3}$$

The theorem of Hyllerass-Undheim then tells us, that by adding a N^{th} state in the expansion of eq. (B.1-3), the energy will automatically approach the exact result and give a new, improved upper bound for the ground state energy. Furthermore, the same is true for each excited state.

In a normal variational calculation, one fixes the number of terms in the expansion to a small value und determines the variational parameters by an exact minimization of the energy. This has the advantage of giving an optimized value for a given number of terms, but the minimization procedure becomes rather time consuming when the number of terms increases. In the stochastic approach, one does not minimize the energy in a rigorous way at each step, but rather adds additional terms, relying on a rapid convergence of the expansion. If the basis functions are chosen such that matrix elements can be calculated analytically, the numerical procedure reduces to that of the diagonalization of large matrices.

This is what has been done throughout this work, the basis functions have been chosen of Gaussian type, so that a large class of matrix elements can be determined analytically. Even though Gaussian functions do not in general reproduce the correct asymptotic behaviour of realistic wave functions (for instance at spatial infinity), this shortcoming is easily compensated by the principal possibility of adding a large number of terms in the expansion.

The variational principle tells us that we approach the exact eigen-values systematically from above. In order to estimate the error at a given number of terms in the expansion, it would be useful therefore to have simultaneously lower bounds on the binding energy. Unfortunately, these ones are much harder to obtain [JF+01], in practice we therefore estimate the error only by the rate of change in the energy when adding a certain number of terms in the wave function.

B.2 Variational Calculation

In this section we collect some basic formulas that are necessary to obtain the three-quark wave functions of baryonic resonances that were discussed in the first part of this work.

The general wave function of a baryonic state with total angular momentum J and isospin T is given in the form:

$$\Psi_{JM_JTM_T}(123) = \sum_{j=1}^{N} \sum_{\alpha} C_{\alpha j} \varphi_{\alpha j}(123) \tag{B.2-1}$$

with expansion coefficients $C_{\alpha j}$ and trial wave functions $\varphi_{\alpha j}(123)$ that are constructed to be fully symmetric under exchange of any two particles:

$$\varphi_{\alpha j}(123) = \varphi_{\alpha j}(1,23) + \varphi_{\alpha j}(2,31) + \varphi_{\alpha j}(3,12). \tag{B.2-2}$$

Here, $\varphi_{\alpha j}(k,pq)$ represents the specific wave function in a Jacobi channel k (to be defined below) and is parameterized in terms of correlated Gaussians [VS95] of the form:

$$\varphi_{\alpha j}(k,pq) = x_k^{2\nu+\lambda}\, y_k^{2n+l}\, e^{-\beta_j x_k^2 - \delta_j y_k^2 + \gamma_j \vec{x}_j \cdot \vec{y}_j} \times \mathcal{F}_{\alpha_0}^{JM_JTM_T}(k,pq). \tag{B.2-3}$$

Here α_0 denotes the set of quantum numbers λ, l, L, S, s, t, where λ is the relative orbital angular momentum in the subsystem of particles p and q, l is the same in the subsystem of particle k, l is the total orbital angular momentum, S is the total spin and s and t are the subsystem spin and isospin of the pair (pq), respectively. The variational parameters β_j, δ_j and γ_j are chosen stochastically in the SVM, and $\alpha = (n, \nu, \alpha_0)$ where $n, \nu \geq 0$. Finally, the angular-spin-isospin part $\mathcal{F}$ is given by:

$$\mathcal{F}_{\alpha_0}^{JM_JTM_T}(k,pq) = \left[\mathcal{Y}_{\lambda l}^{L}(\hat{x}_k, \hat{y}_k) \otimes \left[\chi_{\frac{1}{2}}(k) \otimes \chi_s(pq)\right]_S\right]_{JM_J} \times \left[\eta_{\frac{1}{2}}(k) \otimes \eta_t(pq)\right]_{TM_T} \tag{B.2-4}$$

where

$$\chi_s(pq) = \left[\chi_{\frac{1}{2}}(p) \otimes \chi_{\frac{1}{2}}(q)\right]_{sm} \quad , \quad \eta_t(pq) = \left[\eta_{\frac{1}{2}}(p) \otimes \eta_{\frac{1}{2}}(q)\right]_{tm} \tag{B.2-5}$$

and

$$\mathcal{Y}_{\lambda l}^{LM}(\hat{x}_k, \hat{y}_k) = \left[Y_\lambda(\hat{x}_k) \otimes Y_l(\hat{y}_k)\right]_{LM}. \tag{B.2-6}$$

For an equal-mass three-body system the Jacobi coordinates in Jacobi system (k,pq) are defined by

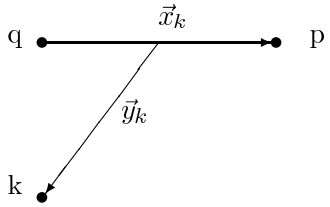

$$\begin{aligned} \vec{x}_k &= \vec{r}_p - \vec{r}_q \\ \vec{y}_k &= \vec{r}_k - \frac{\vec{r}_p + \vec{r}_q}{2} \\ \vec{R} &= \frac{1}{3}\left(\vec{r}_k + \vec{r}_p + \vec{r}_q\right) \end{aligned} \tag{B.2-7}$$

Any single-particle operator is in general given by a sum over components that act on one particle only: $\hat{O} = \hat{O}_{(1)} + \hat{O}_{(2)} + \hat{O}_{(3)}$. By making use of the total symmetry of the wave function, eq. (B.2-2), the matrix elements of this operator can be reduced to the matrix elements of just one of its components:

$$\left\langle \varphi_{\alpha j}(123) \middle| \hat{O} \middle| \varphi_{\alpha' j'}(123) \right\rangle = 3 \left\langle \varphi_{\alpha j}(123) \middle| \hat{O}_{(3)} \middle| \varphi_{\alpha' j'}(123) \right\rangle. \tag{B.2-8}$$

In order to evaluate matrix elements of operators with wave functions like eq. (B.2-2), one therefore encounters states in different Jacobi systems:

$$\langle k|p|q\rangle = \left\langle \varphi_{\alpha j}(k,pq)\middle|\hat{O}_{(p)}\middle|\varphi_{\alpha' j'}(q,kp)\right\rangle . \tag{B.2-9}$$

Therefore, one needs to transform both the bra and ket states from Jacobi systems k and q, respectively, to p. This can be accomplished by use of transformation matrices that are given in ref. [VS95]:

$$\begin{pmatrix} \vec{x}_k \\ \vec{y}_k \end{pmatrix} = A^{kq} \begin{pmatrix} \vec{x}_q \\ \vec{y}_q \end{pmatrix} . \tag{B.2-10}$$

Thereby the transformation of the exponential part of the correlated Gaussian basis is trivial. The rest of the spatial wave function is transformed using the methods outlined in ref. [Glö83]:

$$\begin{aligned} x_k^{2\nu_k+\lambda_k}\, y_k^{2n_k+l_k}\, \mathcal{Y}^{LM}_{\lambda_k l_k}(\hat{x}_k,\hat{y}_k) = \\ \sum B^{\nu\lambda\nu'\lambda' n l n' l' \kappa\kappa'}_{\nu_k\lambda_k n_k l_k L}(kq) x_q^{2\nu+\lambda+2n+l}\, y_q^{2\nu'+\lambda'+2n'+l'}\, \mathcal{Y}^{LM}_{\kappa\kappa'}(\hat{x}_q,\hat{y}_q), \end{aligned} \tag{B.2-11}$$

where the sum is over all new indices and the expansion coefficients are given by

$$\begin{aligned} B^{\nu\lambda\nu'\lambda' n l n' l' \kappa\kappa'}_{\nu_k\lambda_k n_k l_k L}(kq) = D^{\nu\lambda\nu'\lambda'}_{\nu_k\lambda_k}\, D^{nln'l'}_{n_k l_k} \\ \times \left(A^{kq}_{11}\right)^{2\nu+\lambda} \left(A^{kq}_{12}\right)^{2\nu'+\lambda'} \left(A^{kq}_{21}\right)^{2n+l} \left(A^{kq}_{22}\right)^{2n'+l'} E^{\lambda\lambda'\lambda_k l l' l_k L}_{\kappa\kappa'}, \end{aligned} \tag{B.2-12}$$

with

$$D^{n_1 l_1 n_2 l_2}_{NL} = \frac{B_{n_1 l_1} B_{n_2 l_2}}{B_{NL}} \frac{(2N+L)!}{(2n_1+l_1)!\,(2n_2+l_2)!} C^{L}_{l_1 l_2} \tag{B.2-13}$$

and

$$B_{nl} = \frac{4\pi\,(2n+l)!}{2^n n!\,(2n+2l+1)!!}, \qquad C^{\lambda}_{ll'} = \frac{\hat{l}\hat{l}'}{\sqrt{4\pi}\hat{\lambda}} C^{\lambda 0}_{l0l'0}. \tag{B.2-14}$$

Here the $C^{\lambda 0}_{l0l'0}$ are standard Clebsch-Gordan coefficients, $\hat{l} = \sqrt{2l+1}$, and

$$E^{l_1 l_2 l_1' l_2' l' L}_{\lambda\lambda'} = \hat{l}\hat{l}'\hat{\lambda}\hat{\lambda}' \begin{Bmatrix} l_1 & l_2 & l \\ l_1' & l_2' & l' \\ \lambda & \lambda' & L \end{Bmatrix} C^{\lambda}_{l_1 l_1'}\, C^{\lambda'}_{l_2 l_2'}, \tag{B.2-15}$$

where the quantity in brackets is the 9j - symbol. The spin part of the wave function transforms as (see ref. [VMK88])

$$\begin{aligned} \left[\chi_{\frac{1}{2}}(k)\chi_s(pq)\right]_{SM_S} &= (-1)^s \sum_{s'} \hat{s}\hat{s}' \begin{Bmatrix} \frac{1}{2} & \frac{1}{2} & s \\ \frac{1}{2} & S & s' \end{Bmatrix} \left[\chi_{\frac{1}{2}}(p)\chi_{s'}(qk)\right]_{SM_S} \\ &= \sum_{s'} (-1)^{s'} \hat{s}\hat{s}' \begin{Bmatrix} \frac{1}{2} & \frac{1}{2} & s \\ \frac{1}{2} & S & s' \end{Bmatrix} \left[\chi_{\frac{1}{2}}(q)\chi_{s'}(kp)\right]_{SM_S} . \end{aligned} \tag{B.2-16}$$

Matrix elements of various operators may then be calculated between basis states in one Jacobi channel only. Formulas for various relevant operators, in particular non- and semi-relativistic kinetic energy, spin-isospin dependent potentials and spin-orbit and tensor operators, may be found in ref. [Wag98]. The same work gives a detailed analysis of the convergence in terms of the number of basis functions in the stochastic expansion, as well as more sophisticated optimization procedures.

Appendix C

Useful Formulas

This Appendix contains a collection of formulas and relations that were used during this work but did not find their place in the main part.

C.1 Baryon Wave Functions

We shall specify in some detail here the construction of baryon wave functions that were used in the first part of this work. This is of course a standard procedure that may be found in many textbooks, see for instance refs. [FS86, Bha88, YO$^+$88]. For books on group theory applied to physical problems see the books by Barut and Raczka [BR86] and Stancu [Sta96].

To build up wave functions of definite symmetry one uses the representations of the group of permutations of 3 objects. Besides the symmetric and the antisymmetric one-dimensional representations, there is the so called mixed-symmetric representation of dimension 2, whose basis vectors will be denoted by e' and e''. One chooses e' antisymmetric and e'' symmetric with respect to the exchange of particles 1 and 2, and their relative sign is fixed by specifying their transformation properties under the exchange $1 \leftrightarrow 3$:

$$\begin{array}{rcl} e' & \rightarrow & \frac{1}{2}e' - \frac{\sqrt{3}}{2}e'' \\ e'' & \rightarrow & -\frac{\sqrt{3}}{2}e' - \frac{1}{2}e''. \end{array} \qquad \text{(C.1-1)}$$

One has to combine the various degrees of freedom (spin, flavor, space and color) to an antisymmetric total wave function. For the combination of two degrees of freedom one can work out the following rules:

$$\begin{array}{ll} S \otimes S = S: & g^s = e^s f^s \\ S \otimes A = A: & g^a = e^s f^a \\ S \otimes M = M: & g' = e^s f', \quad g'' = e^s f'' \\ A \otimes A = S: & g^s = e^a f^a \\ M \otimes M = S \oplus A \oplus M: & g^s = \frac{1}{\sqrt{2}}(e'f' + e''f'') \\ & g^a = \frac{1}{\sqrt{2}}(e'f'' - e''f') \\ & g' = \frac{1}{\sqrt{2}}(e'f'' + e''f'), \quad g'' = \frac{1}{\sqrt{2}}(e'f' - e''f''). \end{array} \qquad \text{(C.1-2)}$$

The link between SU(N) and the permutations is that the tensors of given symmetry, here S, A, M' or M'', form an irreducible representation of SU(N). The following table gives the dimensions of these representations for N=2, 3 and 6.

$$\begin{array}{rcl} SU(2) & : & \mathbf{2} \otimes \mathbf{2} \otimes \mathbf{2} = \mathbf{4}_S \oplus \mathbf{2}_{M'} \oplus \mathbf{2}_{M''} \\ SU(3) & : & \mathbf{3} \otimes \mathbf{3} \otimes \mathbf{3} = \mathbf{10}_S \oplus \mathbf{8}_{M'} \oplus \mathbf{8}_{M''} \oplus \mathbf{1}_A \\ SU(6) & : & \mathbf{6} \otimes \mathbf{6} \otimes \mathbf{6} = \mathbf{56}_S \oplus \mathbf{70}_{M'} \oplus \mathbf{70}_{M''} \oplus \mathbf{20}_A \end{array} \qquad \text{(C.1-3)}$$

Spin

The SU(2) spin wave functions will be denoted by χ; χ^S has a spin $S=\frac{3}{2}$, χ' and χ'' have a spin $S=\frac{1}{2}$. Explicitly one has

$$\begin{aligned}
\chi^S(S_z=+\frac{3}{2}) &= \uparrow\uparrow\uparrow &&= \left[\left[\frac{1}{2},\frac{1}{2}\right]_1,\frac{1}{2}\right]_{\frac{3}{2}},\\
\chi'(S_z=+\frac{1}{2}) &= \tfrac{1}{\sqrt{2}}(\uparrow\downarrow\uparrow-\downarrow\uparrow\uparrow) &&= \left[\left[\frac{1}{2},\frac{1}{2}\right]_0,\frac{1}{2}\right]_{\frac{1}{2}},\\
\chi''(S_z=+\frac{1}{2}) &= \tfrac{1}{\sqrt{6}}(2\uparrow\uparrow\downarrow-\downarrow\uparrow\uparrow-\uparrow\downarrow\uparrow) &&= \left[\left[\frac{1}{2},\frac{1}{2}\right]_1,\frac{1}{2}\right]_{\frac{1}{2}},
\end{aligned} \tag{C.1-4}$$

where the second form gives the standard coupling in terms of Clebsch-Gordan coefficients.

Flavor

The SU(3) flavor wave functions will be denoted by φ: φ^S corresponds to the decuplet, φ' and φ'' correspond to the octet and φ^A to the singlet of SU(3).

- Decuplet

	φ^S(to be symmetrized)
$\Delta^{++},\Delta^{+},\Delta^{0},\Delta^{-}$	uuu,uud,udd,ddd
$\Sigma^{+},\Sigma^{0},\Sigma^{-}$	uus,uds,dds
Ξ^{0},Ξ^{-}	uss,dss
Ω^{-}	sss

(C.1-5)

- Octet

	φ'	φ''
p	$\frac{1}{\sqrt{2}}(udu-duu)$	$\frac{1}{\sqrt{6}}(2uud-duu-udu)$
n	$\frac{1}{\sqrt{2}}(udd-dud)$	$\frac{1}{\sqrt{6}}(-2ddu+dud+udd)$
Σ^{+}	$\frac{1}{\sqrt{2}}(suu-usu)$	$\frac{1}{\sqrt{6}}(-2uus+suu+usu)$
Σ^{0}	$\frac{1}{2}(sud+sdu-usd-dsu)$	$\frac{1}{2\sqrt{3}}(sdu+sud+usd+dsu-2uds-2dsu)$
Σ^{-}	$\frac{1}{\sqrt{2}}(sdd-dsd)$	$\frac{1}{\sqrt{6}}(-2dds+dsd+sdd)$
Λ	$\frac{1}{2\sqrt{3}}(usd+sdu-sud-dsu-2dus+2uds)$	$\frac{1}{2}(sud+usd-sdu-dsu)$
Ξ^{0}	$\frac{1}{\sqrt{2}}(sus-uss)$	$\frac{1}{\sqrt{6}}(2ssu-sus-uss)$
Ξ^{-}	$\frac{1}{\sqrt{2}}(sds-dss)$	$\frac{1}{\sqrt{6}}(2ssd-sds-dss)$

(C.1-6)

- Singlet

$$\varphi^A = \frac{1}{\sqrt{6}}(uds+dsu+sud-dus-usd-sdu) \tag{C.1-7}$$

If we are only dealing with non-strange baryons (N's and Δ's) we can forget about the SU(3) structure of the flavor symmetry and restrict ourselves to the smaller SU(2) of 2 flavors (u and d). This symmetry is in fact valid to a better degree of approximation, since the mass difference between the u and d quarks is much smaller than the difference between those masses and the s quark. In this case, the flavor wave functions may be written in complete analogy with eqs. C.1-4, where $\uparrow\equiv u$, $\downarrow\equiv d$ and S_z would denote the isospin projection (charge state).

Spin - Flavor

By combining the spin and flavor wave functions one gets those of SU(6), the fundamental representations of which will be formed by non-relativistic Pauli spinors, $u\uparrow$, $u\downarrow$, $d\uparrow$, $d\downarrow$, $s\uparrow$, $s\downarrow$, where the arrows represent spin up and down along some quantization axis. Their decomposition under spin - SU(3) goes as follows:

- Symmetric

$$\begin{array}{lcl} \left|\mathbf{56}, S=\frac{1}{2}, \mathbf{8}\right\rangle & = & \frac{1}{\sqrt{2}}(\varphi'\chi' + \varphi''\chi'') \\ \left|\mathbf{56}, S=\frac{3}{2}, \mathbf{10}\right\rangle & = & \varphi^s\chi^s \end{array} \tag{C.1-8}$$

- Mixed symmetric

$$\begin{array}{lcllcl} \left|\mathbf{70}, S=\frac{1}{2}, \mathbf{8}\right\rangle' & = & \frac{1}{\sqrt{2}}(\varphi'\chi'' + \varphi''\chi') & \left|\mathbf{70}, S=\frac{1}{2}, \mathbf{8}\right\rangle'' & = & \frac{1}{\sqrt{2}}(\varphi'\chi' - \varphi''\chi'') \\ \left|\mathbf{70}, S=\frac{3}{2}, \mathbf{8}\right\rangle' & = & \varphi'\chi^s & \left|\mathbf{70}, S=\frac{3}{2}, \mathbf{8}\right\rangle'' & = & \varphi''\chi^s \\ \left|\mathbf{70}, S=\frac{1}{2}, \mathbf{10}\right\rangle' & = & \varphi^s\chi' & \left|\mathbf{70}, S=\frac{1}{2}, \mathbf{10}\right\rangle'' & = & \varphi^s\chi'' \\ \left|\mathbf{70}, S=\frac{1}{2}, \mathbf{1}\right\rangle' & = & \varphi^a\chi'' & \left|\mathbf{70}, S=\frac{1}{2}, \mathbf{1}\right\rangle'' & = & -\varphi^a\chi' \end{array} \tag{C.1-9}$$

- Antisymmetric

$$\begin{array}{lcl} \left|\mathbf{20}, S=\frac{1}{2}, \mathbf{8}\right\rangle & = & \frac{1}{\sqrt{2}}(\varphi'\chi'' - \varphi''\chi') \\ \left|\mathbf{20}, S=\frac{3}{2}, \mathbf{1}\right\rangle & = & \varphi^a\chi^s \end{array} \tag{C.1-10}$$

Space

The spatial wave functions will be denoted by ψ. The levels and their symmetries depend on the potential that is used in the Schrödinger equation, but quite generally, the ground state level is symmetric with $L^P = 0^+$, and the next level is of mixed symmetry with $L^P = 1^-$. We give in the following the harmonic oscillator (HO) wave functions [Mos69], which are useful, because they allow for an analytic solution and they may be used as a first approximation to more realistic wave functions. In the HO model the Hamiltonian reads (for the equal mass case):

$$H = \sum_{i=1}^{3} \frac{(\vec{p}_i)^2}{2m} + \sum_{i<j} \frac{1}{6} m\omega^2 \, (\vec{r}_i - \vec{r}_j)^2 + 3V_0. \tag{C.1-11}$$

We define the Jacobi coordinates in analogy with eq. (B.2-7) where we just put now $\vec{x}_3 = \vec{r}_{12}$ and $\vec{\rho} = \vec{y}_3$, so that expressing the Hamiltonian in these coordinates yields:

$$H = \frac{\vec{P}^{\,2}}{6m} + \left(\frac{\vec{p}_{12}^{\,2}}{2m_{12}} + \frac{1}{2} m_{12}\, \omega^2\, \vec{r}_{12}^{\,2} \right) + \left(\frac{\vec{p}_{\rho}^{\,2}}{2m_{\rho}} + \frac{1}{2} m_{\rho}\, \omega^2\, \vec{\rho}^{\,2} \right) + 3V_0, \tag{C.1-12}$$

where $m_{12} = m/2$, $m_\rho = (2/3)m$, and $\vec{P}$ is the c.m. momentum. We see that the Hamiltonian separates into the sum of two three-dimensional oscillators. The corresponding Schrödinger equation is therefore solved by the ansatz

$$\Psi(\vec{r}_{12}, \vec{\rho}) = e^{i\vec{P}\cdot\vec{R}}\, \phi(\vec{r}_{12})\, \phi(\vec{\rho}). \tag{C.1-13}$$

Thus the solution is factorized into a part which describes the free c.m. motion and a part responsible for the internal motion of the quarks inside the baryon. Now the two components $\phi(\vec{r}_{12})$ and $\phi(\vec{\rho})$ each fulfil the ordinary three-dimensional harmonic-oscillator Schrödinger equation, the solution of which can be written down analytically:

$$\phi_{nlm}(\vec{\rho}) = \frac{A_{nl}}{(\frac{3}{2}b^2)^{3/4}} \left(\sqrt{\frac{2}{3}} \frac{\rho}{b} \right)^l L_n^{l+1/2}\!\left(\frac{2\rho^2}{3b^2}\right) exp\left(-\frac{\rho^2}{3b^2} \right) Y_l^m(\hat{\rho}), \tag{C.1-14}$$

$$\phi_{nlm}(\vec{r}_{12}) = \frac{A_{nl}}{(2b^2)^{3/4}} \left(\frac{r_{12}}{\sqrt{2}b} \right)^l L_n^{l+1/2}\!\left(\frac{r_{12}^2}{2b^2}\right) exp\left(-\frac{r_{12}^2}{4b^2} \right) Y_l^m(\hat{r}_{12}). \tag{C.1-15}$$

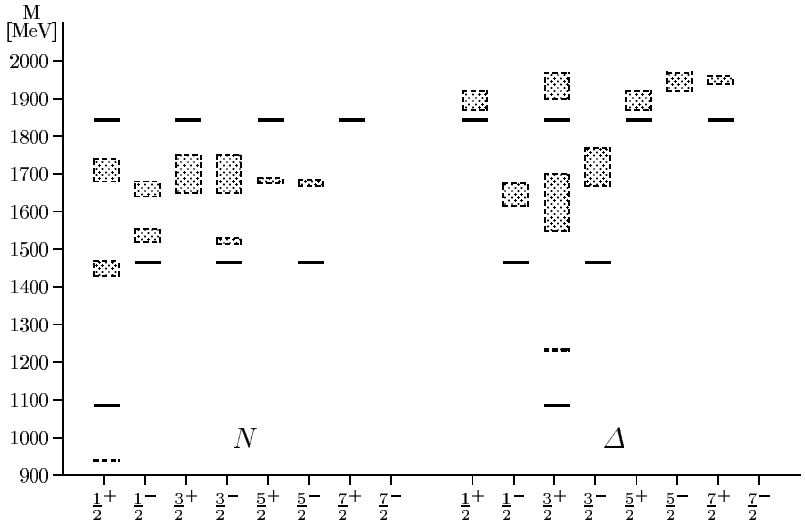

Figure C.1: Energy spectrum of the harmonic oscillator model for $\hbar\omega = 379$ MeV and $V_0 = -17$ MeV.

Here A_{nl} is a normalization constant and b is the harmonic-oscillator spring constant:

$$A_{nl} = \frac{1}{\pi^{1/4}}\sqrt{\frac{n!\,2^{n+l+2}}{(2n+2l+1)!!}} \quad ; \qquad b = \sqrt{\frac{1}{m\omega}}. \tag{C.1-16}$$

The $L_n^{l+1/2}$ are associated Legendre polynomials and $\hat{r}_{12}$ and $\hat{\rho}$ denote the angular parts of $\vec{r}_{12}$ and $\vec{\rho}$, respectively.

The energy eigenvalues of $\phi_{nlm}(\vec{\rho})$ and $\phi_{nlm}(\vec{r}_{12})$ are given by $\epsilon_\rho = \hbar\omega(2n_\rho + l_\rho + \frac{3}{2})$ and $\epsilon_{12} = \hbar\omega(2n_{12} + l_{12} + \frac{3}{2})$, respectively. The energy eigenvalues of the whole Hamiltonian (C.1-12) are therefore:

$$E = \hbar\omega(N+3) + 3V_0, \qquad \text{with} \qquad N = 2n_\rho + l_\rho + 2n_{12} + l_{12}. \tag{C.1-17}$$

We then have the following spatial wave functions up to the $N = 2$ harmonic oscillator band:

a. N = 0

$$|0(00)[3]0(111)\rangle = \phi_{000}(\vec{r}_{12})\,\phi_{000}(\vec{\rho}) = \psi_0$$

b. N = 1

$$|1(10)[21]1(112)\rangle = \phi_{000}(\vec{r}_{12})\,\phi_{01M}(\vec{\rho}) = \psi''$$
$$|1(10)[21]1(121)\rangle = \phi_{01M}(\vec{r}_{12})\,\phi_{000}(\vec{\rho}) = \psi'$$

c. N = 2

$$|2(20)[3]0(111)\rangle = \tfrac{1}{\sqrt{2}}\phi_{100}(\vec{r}_{12})\,\phi_{000}(\vec{\rho}) + \tfrac{1}{\sqrt{2}}\phi_{000}(\vec{r}_{12})\,\phi_{100}(\vec{\rho}) = \psi^s(0^+)$$
$$|2(20)[3]2(111)\rangle = \tfrac{1}{\sqrt{2}}\phi_{02M}(\vec{r}_{12})\,\phi_{000}(\vec{\rho}) + \tfrac{1}{\sqrt{2}}\phi_{000}(\vec{r}_{12})\,\phi_{02M}(\vec{\rho}) = \psi^s(2^+)$$
$$|2(20)[21]0(112)\rangle = \tfrac{1}{\sqrt{2}}\phi_{000}(\vec{r}_{12})\,\phi_{100}(\vec{\rho}) - \tfrac{1}{\sqrt{2}}\phi_{100}(\vec{r}_{12})\,\phi_{000}(\vec{\rho}) = \psi''(0^+)$$
$$|2(20)[21]0(121)\rangle = -\textstyle\sum_{m_1,m_2} C^{00}_{1m_1 1m_2}\phi_{01m_1}(\vec{r}_{12})\,\phi_{01m_2}(\vec{\rho}) = \psi'(0^+)$$
$$|2(20)[21]2(112)\rangle = \tfrac{1}{\sqrt{2}}\phi_{000}(\vec{r}_{12})\,\phi_{02M}(\vec{\rho}) - \tfrac{1}{\sqrt{2}}\phi_{02M}(\vec{r}_{12})\,\phi_{000}(\vec{\rho}) = \psi''(2^+)$$
$$|2(20)[21]2(121)\rangle = -\textstyle\sum_{m_1,m_2} C^{2M}_{1m_1 1m_2}\phi_{01m_1}(\vec{r}_{12})\,\phi_{01m_2}(\vec{\rho}) = \psi'(2^+)$$
$$|2(01)[111]1(123)\rangle = \textstyle\sum_{m_1,m_2} C^{1M}_{1m_1 1m_2}\phi_{01m_1}(\vec{r}_{12})\,\phi_{01m_2}(\vec{\rho}) = \psi^a(1^+)$$

Spin - Flavor - Space

We now combine the SU(6) spin-flavor part with the space part to get a symmetric total wave-function (the color part, which ensures the total antisymmetry of the wave function, will be omitted). Combining the **56** of SU(6) with the spatial wave function $L^P = 0^+$, one gets the low-lying baryons:

$$\begin{aligned} \mathbf{8}, J = \tfrac{1}{2}: &\quad \tfrac{1}{\sqrt{2}}(\phi'\chi' + \phi''\chi'')\psi_0, \\ \mathbf{10}, J = \tfrac{3}{2}: &\quad \phi^s\chi^s\psi_0. \end{aligned} \tag{C.1-18}$$

Combining the **70** of SU(6) with the spatial wave function $L^P = 1^-$, one gets the wave functions of negative-parity baryons:

$$\begin{aligned} \mathbf{8}, J = \tfrac{1}{2}, \tfrac{3}{2}: &\quad \tfrac{1}{2}\left[(\phi'\chi'' + \phi''\chi')\psi' + (\phi'\chi' - \phi''\chi'')\psi''\right]_J, \\ \mathbf{8}, J = \tfrac{1}{2}, \tfrac{3}{2}, \tfrac{5}{2}: &\quad \tfrac{1}{\sqrt{2}}\left[\phi'\chi^s\psi' + \phi''\chi^s\psi''\right]_J, \\ \mathbf{10}, J = \tfrac{1}{2}, \tfrac{3}{2}: &\quad \tfrac{1}{\sqrt{2}}\left[\phi^s\chi'\psi' + \phi^s\chi''\psi''\right]_J, \\ \mathbf{1}, J = \tfrac{1}{2}, \tfrac{3}{2}: &\quad \tfrac{1}{\sqrt{2}}\left[\phi^a\chi''\psi' - \phi^a\chi'\psi''\right]_J, \end{aligned} \tag{C.1-19}$$

where the index J under the bracket means that the spatial and spin wave functions are coupled by Clebsch-Gordan coefficients to get a total angular momentum J.

Finally we write the wave functions for the $N = 2$ level, which have the same SU(3) and J^P quantum numbers as the low-lying baryons, and may therefore mix with their wave functions when SU(6) - breaking effects are taken into account. For the octet, $J^P = \frac{1}{2}^+$ there are 4 wave functions:

$$\begin{aligned} \mathbf{56}, S = \tfrac{1}{2}, L = 0: &\quad \tfrac{1}{\sqrt{2}}(\phi'\chi' + \phi''\chi'')\psi^s(0^+), \\ \mathbf{70}, S = \tfrac{1}{2}, L = 0: &\quad \tfrac{1}{2}\left[(\phi'\chi'' + \phi''\chi')\psi'(0^+) + (\phi'\chi' - \phi''\chi'')\psi''(0^+)\right], \\ \mathbf{70}, S = \tfrac{3}{2}, L = 2: &\quad \tfrac{1}{\sqrt{2}}\left[\phi'\chi^s\psi'(2^+) + \phi''\chi^s\psi''(2^+)\right]_{\frac{1}{2}}, \\ \mathbf{20}, S = \tfrac{1}{2}, L = 1: &\quad \tfrac{1}{\sqrt{2}}\left[(\phi'\chi'' - \phi''\chi')\psi^a(1^+)\right]_{\frac{1}{2}}. \end{aligned} \tag{C.1-20}$$

For the decuplet, $J^P = \frac{3}{2}^+$ there are 3 wave functions:

$$\begin{aligned} \mathbf{56}, S = \tfrac{3}{2}, L = 0 &\quad \phi^s\chi^s\psi^s(0^+), \\ \mathbf{56}, S = \tfrac{3}{2}, L = 2 &\quad \left[\phi^s\chi^s\psi^s(2^+)\right]_{\frac{3}{2}}, \\ \mathbf{70}, S = \tfrac{1}{2}, L = 2 &\quad \tfrac{1}{\sqrt{2}}\left[\phi^s\chi'\psi'(2^+) + \phi^s\chi''\psi''(2^+)\right]_{\frac{3}{2}}. \end{aligned} \tag{C.1-21}$$

The construction of the relevant wave functions in the TISM scheme has been explicitly given in ref. [GK94], see also ref. [The97].

C.2 Transition Matrix Elements for Decay Models

This section contains some analytic results for matrix elements of operators responsible for the strong decays of baryon resonances. These ones include in particular the elementary emission model and the $^3P_0$ quark-pair creation model, discussed in chapter 3.

Spatial parts

In table C.1, matrix elements are collected for the lowest baryonic resonances of the following operators:

$$\hat{A} = 3\tau^- \, e^{-i\vec{q}\cdot\vec{r}} \, \vec{\sigma}\cdot\vec{q}, \qquad \hat{C} = \sqrt{3}\, e^{-i\vec{q}\cdot\vec{r}} \, \vec{\sigma}\cdot\vec{q}, \tag{C.2-1}$$

which are essentially the operators of the direct term for decays into $N\pi^+$ and $N\eta$ in the EEM, respectively, and

$$\hat{B} = 3\tau^- \, e^{-i\vec{q}\cdot\vec{r}} \, \vec{\sigma}\cdot\vec{p}, \qquad \hat{D} = \sqrt{3}\, e^{-i\vec{q}\cdot\vec{r}} \, \vec{\sigma}\cdot\vec{p}, \tag{C.2-2}$$

which corresponds to the recoil term in the above sense. Table C.2 contains the necessary integrals for computing these matrix elements.

Table C.1: Matrix elements of $\hat{A}$, $\hat{B}$, $\hat{C}$ and $\hat{D}$ as defined in eqs. (C.2-1) and (C.2-2) for $N^* \to N\pi$ and $N^* \to N\eta$ amplitudes of the lowest N and Δ resonances. The integrals I_{nl} and J^{μ}_{nlm} are given in table C.2 for the EEM and in table C.3 for the $^3P_0$.

N^*	$\left\langle N_{939}\middle\vert\hat{A}\middle\vert N^*\right\rangle$	$\left\langle N_{939}\middle\vert\hat{B}\middle\vert N^*\right\rangle$	$\left\langle N_{939}\middle\vert\hat{C}\middle\vert N^*\right\rangle$	$\left\langle N_{939}\middle\vert\hat{D}\middle\vert N^*\right\rangle$
N_{1440}	$\frac{5}{3}qI_{10}$	$i\frac{5}{3}J^0_{100}$		
N_{1710}	$\frac{2\sqrt{2}}{3}qI_{10}$	$i\frac{2\sqrt{2}}{3}J^0_{100}$	$\sqrt{\frac{2}{3}}qI_{10}$	$i\sqrt{\frac{2}{3}}J^0_{100}$
N_{1535}	$-\frac{4}{3\sqrt{3}}qI_{01}$	$-i\frac{4}{3\sqrt{3}}J^0_{010}+i\frac{8}{3\sqrt{3}}J^-_{011}$	$-\frac{\sqrt{2}}{3}qI_{01}$	$-i\frac{\sqrt{2}}{3}J^0_{010}+i\frac{2\sqrt{2}}{3}J^-_{011}$
N_{1650}	$-\frac{2}{3\sqrt{3}}qI_{01}$	$-i\frac{2}{3\sqrt{3}}J^0_{010}+i\frac{4}{3\sqrt{3}}J^-_{011}$	$\frac{\sqrt{2}}{3}qI_{01}$	$i\frac{\sqrt{2}}{3}J^0_{010}-i\frac{2\sqrt{2}}{3}J^-_{011}$
N_{1720}	$-\frac{\sqrt{10}}{3}qI_{02}$	$-i\frac{\sqrt{10}}{3}J^0_{020}+i\sqrt{\frac{10}{3}}J^-_{021}$	$-\frac{1}{\sqrt{15}}qI_{02}$	$-i\frac{1}{\sqrt{15}}J^0_{020}+i\frac{1}{\sqrt{5}}J^-_{021}$
N_{1520}	$\frac{4}{3}\sqrt{\frac{2}{3}}qI_{01}$	$i\frac{4}{3}\sqrt{\frac{2}{3}}J^0_{010}+i\frac{4}{3}\sqrt{\frac{2}{3}}J^-_{011}$	$\frac{2}{3}qI_{01}$	$i\frac{2}{3}J^0_{010}+i\frac{2}{3}J^-_{011}$
N_{1700}	$-\frac{2}{3\sqrt{15}}qI_{01}$	$-i\frac{2}{3\sqrt{15}}J^0_{010}-i\frac{2}{3\sqrt{15}}J^-_{011}$	$\frac{1}{3}\sqrt{\frac{2}{5}}qI_{01}$	$i\frac{1}{3}\sqrt{\frac{2}{5}}J^0_{010}+i\frac{1}{3}\sqrt{\frac{2}{5}}J^-_{011}$
N_{1680}	$\sqrt{\frac{5}{3}}qI_{02}$	$i\sqrt{\frac{5}{3}}J^0_{020}+i\frac{2}{3}\sqrt{5}J^-_{021}$	$\frac{1}{\sqrt{10}}qI_{02}$	$i\frac{1}{\sqrt{10}}J^0_{020}+i\sqrt{\frac{2}{15}}J^-_{021}$
N_{1675}	$\frac{2}{3}\sqrt{\frac{3}{5}}qI_{01}$	$i\frac{2}{\sqrt{15}}J^0_{010}+i\frac{2}{\sqrt{15}}J^-_{011}$	$-\sqrt{\frac{2}{5}}qI_{01}$	$-i\sqrt{\frac{2}{5}}J^0_{010}-i\sqrt{\frac{2}{5}}J^-_{011}$
Δ_{1620}			$\frac{1}{3}qI_{01}$	$i\frac{1}{3}J^0_{010}-i\frac{2}{3}J^-_{011}$
Δ_{1232}			$-\frac{4}{3}\sqrt{3}qI_{00}$	$-i\frac{4}{3}\sqrt{3}J^0_{100}$
Δ_{1600}			$-\frac{2}{3}\sqrt{6}qI_{10}$	$-i\frac{2}{3}\sqrt{6}J^0_{100}$
Δ_{1700}			$-\frac{\sqrt{2}}{3}qI_{01}$	$-i\frac{\sqrt{2}}{3}J^0_{010}-i\frac{\sqrt{2}}{3}J^-_{011}$

Spin-isospin parts

The matrix elements of the spin-part of the wave functions are calculated in the following way [VMK88]:

$$\langle S'_{12}:S'M'_S|\sigma_\mu|S_{12}:SM_S\rangle = (-1)^{\frac{3}{2}+S'+S_{12}}\sqrt{6}\,\hat{S}\,C^{S'M'_S}_{SM_S1\mu}\left\{\begin{array}{ccc}\frac{1}{2} & S_{12} & S\\ S' & 1 & \frac{1}{2}\end{array}\right\}\delta_{S_{12}S'_{12}}, \qquad \text{(C.2-3)}$$

where $\hat{S}=\sqrt{2S+1}$ and σ_μ are the spherical components of the Pauli spin matrices. The matrix elements of the isospin operator are completely analogous.

Table C.2: Integrals in the matrix elements of the EEM. The I_{nl} and J^{μ}_{nlm} in the lower part of the table are obtained from $I_{nlm}(\vec{q})$ and $J^{\mu}_{nlm}(\vec{q})$ by choosing $\vec{q}$ in the z - direction.

$$I_{nlm}(\vec{q}) := \int d\vec{\rho}\, \phi^*_{000}(\vec{\rho})\, e^{i\frac{2}{3}\vec{q}\cdot\vec{\rho}}\, \phi_{nlm}(\vec{\rho})$$
$$J^{\mu}_{nlm}(\vec{q}) := \int d\vec{\rho}\, \phi^*_{000}(\vec{\rho})\, e^{i\frac{2}{3}\vec{q}\cdot\vec{\rho}}\, \nabla_{\mu}(\vec{\rho})\, \phi_{nlm}(\vec{\rho})$$

$$I_{nlm}(\vec{q}) = i^l \sqrt{4\pi} \sqrt{\frac{2^{n+l}}{n!\,(2n+2l+1)!!}} \left(\frac{bq}{\sqrt{6}}\right)^{2n+l} e^{-\frac{b^2q^2}{6}}\, Y^m_l(\hat{q})$$
$$J^{\mu}_{nlm}(\vec{q}) = -i\, \left(\tfrac{2}{3}\, q_{\mu} + \tfrac{1}{b^2}\nabla_{\mu}(\vec{q})\right) I_{nlm}(\vec{q})$$

$$I_{00} = e^{-\frac{b^2q^2}{6}} \qquad I_{01} = i\tfrac{bq}{\sqrt{3}} I_{00}$$
$$I_{10} = \tfrac{b^2q^2}{3\sqrt{6}} I_{00} \qquad I_{02} = -\tfrac{b^2q^2}{3\sqrt{3}} I_{00}$$
$$J^0_{000} = -\tfrac{i}{3} q I_{00} \qquad J^0_{010} = \tfrac{1}{b\sqrt{3}}(1 + \tfrac{b^2q^2}{3}) I_{00}$$
$$J^-_{011} = -\tfrac{1}{b\sqrt{3}} I_{00} \qquad J^0_{100} = -i\tfrac{2}{3\sqrt{6}} q (1 + \tfrac{b^2q^2}{6}) I_{00}$$
$$J^0_{020} = i\tfrac{2}{3\sqrt{3}} q (1 + \tfrac{b^2q^2}{6}) I_{00} \qquad J^-_{021} = -i\tfrac{1}{3} q I_{00}$$
$$I_{nl} = \delta_{m0} I_{nl0}(\vec{q} \parallel \vec{z}) \qquad J^{\mu}_{nlm} = J^{-\mu}_{nl-m} = \delta_{-m\mu} J^{-m}_{nlm}$$

Table C.3: Integrals in the matrix elements of the $^3P_0$. The I_{nl} and J^{μ}_{nlm} in the central part of the table are obtained from $I_{nlm}(\vec{q})$ and $J^{\mu}_{nlm}(\vec{q})$ by choosing $\vec{q}$ in the z - direction.

$$I_{nlm}(\vec{q}) := \int d\vec{p}_{\rho}\, \phi^*_{000}(\vec{p_{\rho}} + \tfrac{2}{3}\vec{q})\, \psi^*_M(\vec{p_{\rho}} + \tfrac{\vec{q}}{2})\, \phi_{nlm}(\vec{p}_{\rho})$$
$$J^{\mu}_{nlm}(\vec{q}) := \int d\vec{p}_{\rho}\, \phi^*_{000}(\vec{p}_{\rho} + \tfrac{2}{3}\vec{q})\, \psi^*_M(\vec{p_{\rho}} + \tfrac{\vec{q}}{2})\, \nabla_{\mu}(\vec{p}_{\rho})\, \phi_{nlm}(\vec{p}_{\rho})$$

$$I_{nlm}(\vec{q}) = B\, i^{l+2n}\, A_{nl}\, L_n^{l+\frac{1}{2}}[\tfrac{3b^2W^2q^2}{4Va^2}]\, (-\sqrt{\tfrac{3}{2}}\tfrac{bW}{2V}q)^l\, (\tfrac{a^2}{2V})^n\, Y^m_l(\hat{q})$$
$$J^{\mu}_{nlm}(\vec{q}) = (-1)^{\mu+1}\, \tfrac{1}{W}\, [2Uq_{\mu} + \nabla_{\mu}(\vec{q})]\, I_{nlm}(\vec{q})$$

$$I_{00} = B\pi^{-\frac{3}{4}} \qquad I_{10} = -\sqrt{\tfrac{3}{2}}(1 - \tfrac{b^2W^2q^2}{2Va^2})\tfrac{a^2}{2V} I_{00}$$
$$I_{01} = -i\sqrt{3}\tfrac{W}{2V} bq I_{00} \qquad I_{02} = -[\sqrt{3}(\tfrac{bW}{2V}q)^2] I_{00}$$
$$J^0_{000} = -\tfrac{W}{2V} q I_{00} \qquad J^0_{010} = [i\sqrt{3}\tfrac{b}{2V}(1 + \tfrac{W^2}{2V}q^2)] I_{00}$$
$$J^-_{011} = i\sqrt{\tfrac{3}{4}}\tfrac{b}{V} I_{00} \qquad J^0_{100} = -\sqrt{\tfrac{3}{2}}\tfrac{Wa^2}{2V^2} q[\tfrac{b^2}{a^2} - \tfrac{1}{2} + \tfrac{b^2W^2q^2}{4Va^2}] I_{00}$$
$$J^0_{020} = \sqrt{\tfrac{3}{4}}\tfrac{b^2W}{V^2} q[1 + q^2\tfrac{W^2}{4V}] I_{00} \qquad J^-_{021} = \tfrac{3}{4}\tfrac{W}{V^2} b^2 q I_{00}$$
$$I_{nl} = \delta_{m0} I_{nl0}(\vec{q} \parallel \vec{z}) \qquad J^{\mu}_{nlm} = J^{-\mu}_{nl-m} = \delta_{-m\mu} J^{-m}_{nlm}$$

$$B = A_{00} e^{-(U - \frac{W^2}{4V})q^2} (\tfrac{a^2}{\pi})^{\frac{3}{4}} (\tfrac{\pi}{2}) (\tfrac{3b^2}{2V})^{\frac{3}{2}}$$
$$U = \tfrac{b^2}{3} + \tfrac{a^2}{8} \qquad W = b^2 + \tfrac{a^2}{2} \qquad V = \tfrac{3b^2}{2} + \tfrac{a^2}{2}$$

C.3 Useful Integrals

We give here a more or less arbitrary and certainly incomplete collection of formulas and relations that were used during the work.

For the calculation of the spectral function for the contribution of the crossed double-box in section 5.4.3, the following formulas were used:

$$\iint_{-1}^{1} \frac{dx\,dy}{(x+\epsilon)(y+\epsilon')} \frac{\Theta\left(1-x^2-y^2-z^2+2xyz\right)}{\sqrt{1-x^2-y^2-z^2+2xyz}} = \frac{\pi}{\sqrt{c}} \log\left(\frac{\epsilon\epsilon'-z+\sqrt{c}}{\epsilon\epsilon'-z-\sqrt{c}}\right), \tag{C.3-1}$$

with

$$c = \epsilon^2+\epsilon'^2+z^2-1-2\epsilon\epsilon' z. \tag{C.3-2}$$

Furthermore,

$$\int_{-\infty}^{\infty} \frac{dp_0}{\left[p_0^2-2iAp_0k_0+\vec{p}^{\,2}-B\right]^{2n+2}} = \frac{(4n+1)!!}{2^{2n+1}(2n+1)!} \frac{\pi}{\left(\vec{p}^{\,2}+A^2k^2-B\right)^{2n+3/2}}, \tag{C.3-3}$$

$$\int_0^{\infty} \left(\frac{p}{p^2+D}\right)^{2n} \frac{dp}{(p^2+D)^{3/2}} = \frac{(2n)!}{(4n+1)!!} \frac{1}{D^{n+1}}. \tag{C.3-4}$$

Numerous times, for the calculation of multi-dimensional integrals, like for instance the ones giving the normalization of the Bethe-Salpeter amplitude in the Wick-Cutkosky model, see eq.(5.3-38), we used the Feynman transformation:

$$\frac{1}{A^\alpha B^\beta} = \frac{\Gamma(\alpha+\beta)}{\Gamma(\alpha)\,\Gamma(\beta)} \int_0^1 \frac{x^{\alpha-1}(1-x)^{\beta-1}}{[Ax+B(1-x)]^{\alpha+\beta}}\,dx. \tag{C.3-5}$$

For the numerical solution of the Wick-Cutkosky model we encountered the integrals in eqs. (5.3-23) and (5.3-24). In eq. (5.3-23), with the explicit form eq. (5.3-20) for G, one only encounters simple Gaussian integrals, that can be done analytically:

$$\int_{-\infty}^{\infty} d\rho_0 \int_0^{\infty} d\rho_s\, \rho_0^{2i} \rho_s^{2j} e^{-\alpha\rho_0^2-\beta\rho_s^2} = \frac{(2i-1)!!}{2^i\alpha^i} \frac{(2j-1)!!}{2^{j+1}\beta^j} \frac{\pi}{\sqrt{\alpha\beta}}. \tag{C.3-6}$$

The integrals of eq. (5.3-24) on the other hand have to be solved numerically. By use of a Laplace - transformation one can however express them in form of one-dimensional integrals only:

$$\begin{aligned}
&\int_{-\infty}^{\infty} d\rho_0 \int_0^{\infty} d\rho_s \frac{\rho_0^{2l'}\rho_s^{2(l+1)} e^{-\alpha\rho_0^2-\beta\rho_s^2}}{[(\rho_0^2+\rho_s^2+1-\epsilon^2)^2+4\rho_0^2\epsilon^2]} = \\
&\quad \frac{(2l+1)!!}{2^{l+3}} \frac{\sqrt{\pi}}{\epsilon} \int_0^{\infty} dt \frac{e^{-(1-\epsilon^2)t}}{(\beta+t)^{l+3/2}} \int_{-\infty}^{\infty} \rho_0^{2l'-1} \sin(2\epsilon t\rho_0)\, e^{-(\alpha+t)\rho_0^2}\, d\rho_0 = \\
&\quad \frac{\pi(2l'-1)!!(2l+1)!!}{2^{l+l'+2}} \int_0^{\infty} dt \frac{t\,e^{-(1-\epsilon^2)t}}{(\beta+t)^{l+3/2}} \frac{e^{-\frac{\epsilon^2t^2}{\alpha+t}}}{(\alpha+t)^{l'+1/2}}\, {}_1F_1\left(1-l';\frac{3}{2};\frac{\epsilon^2t^2}{\alpha+t}\right).
\end{aligned} \tag{C.3-7}$$

Here ${}_1F_1$ denotes the confluent hyper-geometric function. The remaining integral can easily be done numerically.

When calculating matrix elements of operators in hadronic decay models of baryonic resonances, one generally encounters integrals of the form

$$\begin{aligned}
&\iint_0^{\infty} dx\,dy\, x^{2k_1+j+2}\, y^{2k_2+j+l+2}\, e^{-ux^2-vy^2}\, i_j(wxy)\, j_l(qy) = \\
&\qquad \frac{\pi}{2} \frac{q^l\, w^j\, k_1!\, e^{-\frac{q^2}{4a}}}{2^{j+l+3}\, u^{k_1+j+3/2}} \sum_{i=0}^{k_1} \frac{n!}{i!} \frac{\left(\frac{w^2}{4u}\right)^i}{a^{n+l+3/2}} \begin{pmatrix} k_1+j+1/2 \\ k_1-i \end{pmatrix} L_n^{l+1/2}\left(\frac{q^2}{4a}\right),
\end{aligned} \tag{C.3-8}$$

where $n = k_2+j+i$ and $a = v-\frac{w^2}{4u}$, see ref. [GR80]. The spherical and modified spherical Bessel functions $j_l(qy)$ and $i_j(wxy)$ stem from the expansion of the exponentials $e^{i\vec{q}\cdot\vec{r}}$ and $e^{w\vec{x}\cdot\vec{y}}$, respectively.

The Box Diagram

We give here the analytic result for the box diagram of fig. 6.2a, in the case where the factors m/e and terms like $E-e-e'$ in the denominator of eq. (6.2-7) are neglected. It is not what was actually used in the calculations presented in this work but it turned out to be quite useful for numerical tests. The (energy-independent) expression for $V^{(2a)}(\vec{p},\vec{p}\,')$ then takes the form

$$V^{(2a)}(\vec{p},\vec{p}\,') = -\frac{1}{2}\int \frac{d\vec{q}}{(2\pi)^3}\,\frac{m}{e}\left(\frac{g^4\,(O_1\,O_2)\,(O_1\,O_2)}{\omega\omega'\,(\omega+\omega')}\;\frac{1}{\omega\omega'}\right)\frac{m}{e'}, \tag{C.3-9}$$

with the definitions $\omega=\sqrt{\mu^2+(\vec{p}-\vec{q}\,)^2}$, $\omega'=\sqrt{\mu^2+(\vec{p}\,'-\vec{q}\,)^2}$, $e=\sqrt{m^2+\vec{p}^{\,2}}$ and $e'=\sqrt{m^2+\vec{p}\,'^2}$. If one defines the integral I by

$$V^{(2a)}(\vec{p},\vec{p}\,') =: \frac{1}{2}\frac{m^2}{ee'}\frac{g^4}{(2\pi)^3}(O_1\,O_2)\,(O_1\,O_2)\,I, \tag{C.3-10}$$

then one finds that

$$\begin{aligned} I &= \int \frac{d\vec{q}}{[\mu^2+(\vec{p}-\vec{q}\,)^2]\,[\mu^2+(\vec{p}\,'-\vec{q}\,)^2]\left[\sqrt{\mu^2+(\vec{p}-\vec{q}\,)^2}+\sqrt{\mu^2+(\vec{p}\,'-\vec{q}\,)^2}\right]} \\ &= \frac{2\pi}{k}\int_0^\infty \frac{q\;dq}{(\mu^2+q^2)^{\frac{3}{2}}}\log\frac{\sqrt{\mu^2+(k+q)^2}\left[\sqrt{\mu^2+q^2}+\sqrt{\mu^2+(k-q)^2}\right]}{\sqrt{\mu^2+(k-q)^2}\left[\sqrt{\mu^2+q^2}+\sqrt{\mu^2+(k+q)^2}\right]}, \end{aligned} \tag{C.3-11}$$

where $k=|\vec{k}|=|\vec{p}-\vec{p}\,'|$. From this form one derives the following analytic properties of the integral I:

$$\begin{aligned} I &= \frac{2\pi}{3\mu^2} && \text{if} && \vec{k}=0, \\ I &= \frac{2\pi}{k^2}\,4\log 2 && \text{if} && \mu=0, \\ I &\to \frac{2\pi}{k^2}\,4\log 2 && \text{for} && k\to\infty. \end{aligned} \tag{C.3-12}$$

Integrating by parts, one finds the following expression for I:

$$I=\frac{2\pi}{k\sqrt{k^2+4\mu^2}}\left\{\frac{2}{\sqrt{1-c}}\log\frac{1+\sqrt{1-c}}{1-\sqrt{1-c}}-4\sqrt{\frac{c}{1-c}}\arctan\sqrt{\frac{1-c}{c}}+2\log c\right\}, \tag{C.3-13}$$

where the factor c is given by

$$c=\frac{\sqrt{k^2+4\mu^2}-k}{\sqrt{k^2+4\mu^2}+k}. \tag{C.3-14}$$

A careful analysis reveals that the expression of eq. (C.3-13) satisfies the conditions of eqs. (C.3-12), because of a cancellation of divergences in single terms.

Appendix D

O(4) Spherical Harmonics

This Appendix contains a collection of useful relations concerning the orthogonal group in four dimensions [Tal68]. Specific informations for applications related to the present work may be found in refs. [BI66a, BI66b, KMW76], in particular for works related to the Bethe-Salpeter equation, see refs. [DS64, Dom67, BB70, KSZ70], for a recent application, see ref. [NT96b].

D.1 General relations

Let us start by defining spherical coordinates in four dimensions:

$$\begin{aligned} p_0 &= p\cos\chi \\ p_1 &= p\sin\chi\sin\theta\sin\phi \\ p_2 &= p\sin\chi\sin\theta\cos\phi \\ p_3 &= p\sin\chi\cos\theta, \end{aligned} \tag{D.1-1}$$

$$\begin{aligned} d^4p &= p^3\,dp\,d\hat{p} \\ d\hat{p} &= \sin^2\chi\,d\chi\,\sin\theta\,d\theta\,d\phi. \end{aligned} \tag{D.1-2}$$

Let L^2 and $\mathcal{L}^2$ be the angular parts of the three- and four-dimensional Laplacian, respectively. Thus,

$$L^2 = -\frac{1}{\sin\theta}\frac{\partial}{\partial\theta}\left(\sin\theta\frac{\partial}{\partial\theta}\right) - \frac{1}{\sin^2\theta}\frac{\partial^2}{\partial\phi^2}, \tag{D.1-3}$$

$$\mathcal{L}^2 = -\frac{1}{\sin^2\chi}\frac{\partial}{\partial\chi}\left(\sin^2\chi\frac{\partial}{\partial\chi}\right) + \frac{1}{\sin^2\chi}L^2, \tag{D.1-4}$$

$$\Box = \nabla^2 + \frac{\partial^2}{\partial p_0^2} = \frac{\partial^2}{\partial p^2} + \frac{3}{p}\frac{\partial}{\partial p} - \frac{1}{p^2}\mathcal{L}^2. \tag{D.1-5}$$

Their eigen-values and eigen-functions are:

$$L^2 Y_l^m(\theta,\phi) = l(l+1)Y_l^m(\theta,\phi), \tag{D.1-6}$$

$$\mathcal{L}^2\,|nlm\rangle = n(n+2)\,|nlm\rangle\,. \tag{D.1-7}$$

The four-dimensional spherical harmonics are given in terms of Gegenbauer polynomials C_n^l:

$$|nlm\rangle\,(\chi,\theta,\phi) = \sqrt{\frac{2^{2l+1}(n+1)(n-l)!(l!)^2}{\pi(n+l+1)!}}\;(\sin\chi)^l\;C_{n-l}^{l+1}\,(\cos\chi)\;Y_{lm}(\theta,\phi)\;. \tag{D.1-8}$$

They form a complete, orthonormal (with respect to the angular integration measure of eq. (D.1-2)) set of functions on the unit sphere in four dimensions.

Let us first note the representation of the exponential function:

$$e^{\pm q\cdot r} = 4\pi^2 \sum_{klm} (\pm 1)^k \frac{I_{k+1}(qr)}{qr} \, |klm\rangle^*_{(\hat{q})} \, |klm\rangle_{(\hat{r})} \,. \tag{D.1-9}$$

This allows one to determine the expansion formula

$$\begin{aligned} &|\, a+b\,|^{2k+n} \, |nlm\rangle_{\widehat{(a+b)}} = \\ &\quad \sum B^{nk}_{n_1 k_1 n_2 k_2} \sum C^{nlm}_{n_1 l_1 m_1 n_2 l_2 m_2} a^{2k_1+n_1} b^{2k_2+n_2} \, |n_1 l_1 m_1\rangle_{(\hat{a})} \, |n_2 l_2 m_2\rangle_{(\hat{b})} \,, \end{aligned} \tag{D.1-10}$$

where the sum is over all new indices with the restriction $2k_1 + n_1 + 2k_2 + n_2 = 2k + n$, and the factors B are given by

$$B^{nk}_{n_1 k_1 n_2 k_2} = 2\pi^2 \frac{k!\,(k+n+1)!}{k_1!\,(k_1+n_1+1)!\,k_2!\,(k_2+n_2+1)!}. \tag{D.1-11}$$

The coefficients C are defined by the expansion formula

$$|n_1 l_1 m_1\rangle_{(\hat{p})} \;\; |n_2 l_2 m_2\rangle_{(\hat{p})} = \sum_{nlm} C^{nlm}_{n_1 l_1 m_1 n_2 l_2 m_2} \, |nlm\rangle_{(\hat{p})} \,, \tag{D.1-12}$$

and so are given by

$$C^{nlm}_{n_1 l_1 m_1 n_2 l_2 m_2} = \int d\hat{p} \, |nlm\rangle^*_{\hat{p}} \, |n_1 l_1 m_1\rangle_{(\hat{p})} \;\; |n_2 l_2 m_2\rangle_{(\hat{p})} \,. \tag{D.1-13}$$

From refs. [Wul71, SW65, Bie61] we get an explicit expression for these coefficients:

$$\begin{aligned} &C^{nlm}_{n_1 l_1 m_1 n_2 l_2 m_2} = \\ &\quad \frac{(-1)^{(l_1+l_2-l)/2}}{\sqrt{2\pi^2}} \sqrt{(n_1+1)(n_2+1)(n+1)} \, \hat{l}_1 \hat{l}_2 \, C^{lm}_{l_1 m_1 l_2 m_2} \begin{Bmatrix} \frac{n_1}{2} & \frac{n_2}{2} & \frac{n}{2} \\ \frac{n_1}{2} & \frac{n_2}{2} & \frac{n}{2} \\ l_1 & l_2 & l \end{Bmatrix}, \end{aligned} \tag{D.1-14}$$

where the symbols on the right hand side denote standard SU(2) Clebsch-Gordan coefficients and 9j symbols, and $\hat{l} = \sqrt{2l+1}$. As a special case we note

$$C^{000}_{n_1 l_1 m_1 n_2 l_2 m_2} = \delta_{n_1 n_2} \, \delta_{l_1 l_2} \, \delta_{m_1 - m_2} \, \frac{(-1)^{m_1}}{\sqrt{2\pi^2}}. \tag{D.1-15}$$

It is possible to obtain an expression for

$$S^{nn'}_{n_1 n_2} = \sum_{l_1 m_1 l_2 m_2} C^{nlm}_{n_1 l_1 m_1 n_2 l_2 m_2} C^{n'l'm'}_{n_1 l_1 m_1 n_2 l_2 m_2} = \frac{1}{2\pi^2} \frac{(n_1+1)(n_2+1)}{n+1} I^n_{n_1 n_2} \delta_{nn'} \, \delta_{ll'} \, \delta_{mm'}. \tag{D.1-16}$$

Here $I^n_{n_1 n_2}$ is given by

$$I^n_{n_1 n_2} = \frac{2}{\pi} \int_{-1}^{1} C^1_n(x) C^1_{n_1}(x) C^1_{n_2}(x) (1-x^2)^{1/2} dx = \delta_{n, n_1+n_2}, \tag{D.1-17}$$

a result that is valid for $n_1 + n_2 \leq n$. To obtain eq. (D.1-17) we have used the Theorem of Hecke [Mai86]. It states the following.

Let Θ be the angle between two four-vectors p and q. The angular integral over the product of any function of $\cos\Theta$ with a spherical harmonic function of $\hat{q}$ is proportional to a spherical harmonic function of $\hat{p}$ with the same quantum numbers:

$$\int d\hat{q} \; F(\cos\Theta) \;\; |nlm\rangle_{(\hat{q})} = \Lambda_n \;\; |nlm\rangle_{(\hat{p})} \,. \tag{D.1-18}$$

The proportionality factor is given by

$$\Lambda_n = \frac{4\pi}{n+1} \int_{-1}^{1} F(x) \; C^1_n(x) \; (1-x^2)^{1/2} \; dx, \tag{D.1-19}$$

where the function F is the same as in eq. (D.1-18).

Finally we note the expansion of the four-dimensional δ-function:

$$\delta^4(p-q) = \frac{\delta(p-q)}{q^3} \sum_{klm} |klm\rangle^*_{(\hat{p})} \, |klm\rangle_{(\hat{q})} \,. \tag{D.1-20}$$

List of Figures

List of Tables

Glossary

The page-number gives either the page of first occurrence or the page of definition.

χPT Chiral perturbation theory, page 16

$^3P_0$ The QPCM with $^3P_0$ quantum numbers, page 61

B.S. Bethe-Salpeter, page 138

BCN The model of Bhaduri, Cohler and Nogami, page 28

BSA Bethe-Salpeter amplitude, page 92

BSE Bethe-Salpeter equation, page 96

BSLT The Blankenbecler-Sugar, Logunov-Tavkhelidze equation, page 121

CMS Center of mass system, page 19

CQM Constituent Quark Model, page 14

d.o.f. Degree of freedom, page 31

EEM Elementary emission model, page 48

ET The equal-time equation, page 121

GBE Goldstone-boson exchange, page 30

HH Hyperspherical harmonics expansion method, page 72

HO Harmonic oscillator, page 189

IK The Isgur-Karl model, page 26

M$^3P_0$ The modified $^3P_0$, page 63

NR Non-relativistic, page 28

O(4) The orthogonal group in four dimensions, page 100

OGE One Gluon Exchange, page 24

OPE Operator product expansion, page 13

OZI Okubo-Zweig-Iizuka rule, page 62

PCAC Partial conservation of the axial current, page 16

PDG Particle Data Group, page 21

PQCD Perturbative QCD, page 13

PWA Partial wave analysis, page 21

QCD Quantum Chromodynamics, page 12

QED Quantum Electrodynamics, page 12

QPCM Quark-pair creation model, page 61

SBχS Spontaneous breaking of chiral symmetry, page 32

SR Semi-relativistic, page 28

SU(3)$_f$ The SU(3) flavor group, page 18

SU(3)$_c$ The SU(3) color group, page 12

SVM Stochastic variational method, page 42

TISM Translationally invariant shell model, page 23

TOPT Time-ordered perturbation theory, page 132

WCM Wick-Cutkosky model, page 101

Index

The page-number gives either the page of first occurrence or the page of definition.

RESUME en français

Dans la première partie de ce travail, nous avons traité de quelques sujets qui sont pertinents dans le domaine de la physique des résonances nucléoniques dans le cadre des différents modèles des quarks constituants. Dans ce contexte, nous avons concentré nos recherches sur la description théorique des désintégrations π et η des résonances N et Δ. Les résultats obtenus montrent la nécessité d'une description plus microscopique de la dynamique responsable à la fois pour la liaison des quarks dans les baryons et la désintégration de ceux-ci. Dans la seconde partie de notre étude nous avons contribué à une recherche sur le rôle de l'échange de deux bosons croisés dans l'équation de Bethe-Salpeter, aussi bien qu'à l'étude de différentes approches tri-dimensionelles, qui proviennent de l'équation de Bethe-Salpeter dans une réduction non relativiste, en particulier une équation avec une interaction dépendant de l'énergie. Il est montré qu'une telle équation reproduit bien certaines propriétés de l'équation de Bethe-Salpeter et, en particulier, qu'il émerge aussi des solutions anormales dans une telle approche.

TITRE en anglais

Selected Topics on the Description of Strongly Interacting Systems

RESUME en anglais

In the first part of this work we have dealt with some issues that are relevant in the area of nucleonic resonances within different constituent quark models. In this context we have concentrated on the theoretical description of π and η decays for N and Δ resonances. The results obtained point to the necessity of a more microscopic description of the dynamics which is at the same time responsible for the binding of quarks inside baryons and the decay of the latter ones. In the second part we have contributed to the study of crossed two-boson exchanges in the Bethe-Salpeter equation as well as to the investigation of different three-dimensional approaches that follow from the Bethe-Salpeter equation in a certain non-relativistic reduction scheme. These one include in particular an equation whose interaction depends on the total energy of the system. It was shown that such an equation is able to account for a certain number of properties of the Bethe-Salpeter equation, in particular, that there also arise abnormal solutions in such an approach.

DISCIPLINE

Physique Nucléaire Théorique

MOTS-CLES

Modèles de quarks constituants	Etats liés relativistes
Spectroscopie baryonique	Diagrammes croisés
Désintégrations fortes	Interactions effectives

INTITULE ET ADRESSE DU LABORATOIRE

Institut des Sciences Nucléaires. 53, av. des Martyrs. 38026 Grenoble Cedex.